

---

**Hydraulic Calcium Silicate Cements with Incorporations:  
Modification of Physical, Chemical, and Biological Properties  
across Diverse Environmental Conditions**

---

Thesis for the Degree of Philosophiae Doctor by  
Andreas Koutroulis



Department of Endodontics  
Institute of Clinical Dentistry  
Faculty of Dentistry  
University of Oslo  
Norway  
January 2024

© **Andreas Koutroulis, 2024**

*Series of dissertations submitted to the  
Faculty of Dentistry, University of Oslo*

ISBN 978-82-8327-093-8

All rights reserved. No part of this publication may be  
reproduced or transmitted, in any form or by any means, without permission.

Cover: UiO.

Print production: Graphic center, University of Oslo.

*“The impediment to action advances action.  
What stands in the way becomes the way”*

Marcus Aurelius (121 – 180 AD)



# Table of Contents

<b>Preface</b> .....	9
<b>Summary</b> .....	11
<b>List of Publications</b> .....	13
<b>Abbreviations</b> .....	15
<b>1. Introduction</b> .....	17
1.1 Apical periodontitis .....	17
1.1.1 Infection control .....	20
1.2 Root filling materials .....	22
1.2.1 Materials for endodontic surgery .....	23
1.2.1.1 From historical to currently used materials .....	24
Amalgam .....	24
Glass ionomer cements .....	25
Resin systems .....	25
Zinc oxide/eugenol-based cements .....	26
1.2.1.2 Hydraulic calcium silicate cements .....	27
Portland cement .....	28
Type 1 HCSCs - Mineral trioxide aggregate .....	28
Types 4 and 5 HCSCs .....	32
Representative type 4 HCSC .....	32
Representative type 5 HCSC .....	34
1.2.1.3 Interactions with the clinical environment .....	36
Interactions with microorganisms .....	36
Interactions with dentin .....	38
Interactions with tissue fluids and blood in general ...	38
1.3 Exploring enhanced antibacterial properties with nanoparticles .....	40
1.3.1 Silver nanoparticles in dentistry .....	40
1.3.1.1 Silver ions and silver nanoparticles in endodontics .....	42

1.4	The use of bioactive glass as an alternative approach to modify HCSCs .....	44
1.4.1	Mechanism of biological activity .....	45
1.4.2	Applications of BG in endodontics .....	46
1.4.2.1	Experimental materials with inclusion of BG in HCSCs ...	50
1.5	Current status of HCSCs for endodontic surgery and gaps in knowledge .....	50
<b>2.</b>	<b>Aims and Objectives .....</b>	<b>53</b>
<b>3.</b>	<b>Methodological Aspects .....</b>	<b>55</b>
3.1	Material selection .....	55
3.1.1	Basic experimental formulation .....	55
3.1.2	Silver nanoparticle-containing cements .....	56
3.1.3	Bioactive glass-containing cements .....	57
3.1.4	Commercial HCSCs .....	58
3.1.5	IRM .....	59
3.2	Assessment of environmental conditions .....	59
3.2.1	The effect of immersion medium ( <b>Studies I &amp; II</b> ) .....	59
3.2.2	The effect of aging period ( <b>Studies I, II &amp; III</b> ) .....	61
3.2.3	Interaction with dentin ( <b>Study III</b> ) .....	63
3.3	Antibacterial evaluation ( <b>Studies I, II &amp; III</b> ) .....	64
3.3.1	Selection of bacteria .....	64
3.3.2	Assessment of bacterial adhesion ( <b>Study I</b> ) .....	65
3.3.3	Leachate antibacterial activity ( <b>Study II</b> ) .....	67
3.3.4	Antibacterial activity in contact with dentin ( <b>Study III</b> ) .....	68
3.3.4.1	Independent assessment of dentin and material surfaces .....	68
3.3.4.2	Biofilm assay upon the dentin/material interface .....	70
3.4	Cytotoxicity assessment ( <b>Study II</b> ) .....	72
3.5	Analysis of surface characteristics ( <b>Study I</b> ) .....	72
3.5.1	Qualitative and quantitative analysis of surface structure .....	73
3.5.2	Wettability .....	75
3.5.3	Microhardness .....	76

---

3.6	Leachate characteristics ( <b>Study II</b> ) .....	76
3.6.1	Alkalinity .....	76
3.6.2	Calcium release .....	77
3.7	Characterization of cement bulk ( <b>Study II</b> ) and dentin/material interface ( <b>Study III</b> ) .....	77
3.8	Statistical considerations .....	79
<b>4.</b>	<b>Main Results</b> .....	<b>81</b>
4.1	Surface characteristics and bacterial adhesion .....	81
4.2	Chemical properties and indirect contact antibacterial activity .....	82
4.3	Antibacterial activity in contact with dentin .....	83
<b>5.</b>	<b>Discussion</b> .....	<b>85</b>
5.1	The effect of incorporations on properties of HCSCs .....	85
5.1.1	SNP additions .....	85
5.1.2	Replacement of HCSC with BG .....	87
5.1.3	Outcomes from assessing the commercial HCSCs .....	88
5.2	The effect of environmental conditions .....	89
5.2.1	Aging period .....	90
5.2.2	Immersion medium .....	91
5.2.3	Dentin .....	94
<b>6.</b>	<b>Conclusions</b> .....	<b>95</b>
<b>7.</b>	<b>Future Perspectives</b> .....	<b>97</b>
	<b>Bibliography</b> .....	<b>101</b>
	<b>Published Studies</b> .....	<b>133</b>
	I .....	135
	II .....	177
	III .....	201





## Preface

This thesis is submitted in partial fulfilment of the requirements for the degree of Philosophiae Doctor at the Department of Endodontics, Institute of Clinical Dentistry, Faculty of Dentistry, University of Oslo. The experimental work was carried out at the Nordic Institute of Dental Materials (NIOM). The studies were financially supported by University of Oslo, NIOM and UNIFOR.

First of all I am immensely grateful to my main supervisor, Associate Professor Pia Titterud Sunde, for providing me with the opportunity to embark on the journey of doctoral studies. Thank you, Pia, for your constant trust and support, your kind approach, and for giving me the space to implement my ideas and develop myself as a researcher over these years. You have always been a source of motivation for me when the setbacks would come. I would also like to thank my secondary supervisor Dr Håkon Valen, my first mentor in the microbiology lab. Håkon, I truly admire your unique scientific perspective. My gratitude goes also to my co-supervisor Professor Josette Camilleri for the invaluable knowledge and expertise she generously offered. In addition, I am truly thankful to Professor emeritus Dag Ørstavik. I am humble by the enlightening scientific discussions we have shared. Thank you for being a constant inspiration.

It would not be an exaggeration to say that NIOM has been a second home for me these past 4.5 years. I feel privileged to have worked here and to be a part of their team. My heartfelt thanks go to each and everyone to NIOM, for creating a warm environment filled with positivity, offering help and support whenever needed.

To my colleague and dearest friend Vasilis. I am grateful for undertaking this academic journey with you. Your support in the lab, and more importantly, outside of it, is invaluable.

To my friends in Norway and Greece. Thank you for reminding me the importance of the work-life balance. You have been the fuel to move forward on challenging days.

Finally, to my family - my parents Petros and Chrysoula, and my siblings Kostas and Eleftheria - for the unconditional love and support. I always carry you with me.

Andreas Koutroulis, January 2024



## Summary

Hydraulic calcium silicate cements (HCSCs) find application in various clinical procedures within the field of endodontics. Although initially introduced for endodontic surgery, certain aspects of their use in these applications have not been thoroughly explored. Moreover, considering the interactions of these materials with the surrounding environment, it becomes crucial to understand how these might influence their properties. It is possible that specific modifications of the HCSC composition could improve some target biological properties, provided that changes do not compromise any of their current characteristics.

This thesis delves into the impact of material modifications on the physical, chemical and biological properties, including antibacterial activity and cytotoxicity, of HCSCs. It also explores the influence of environmental conditions, namely the immersion medium, aging period, and the role of the dentin substrate in this context. The primary aim was to evaluate the effect of incorporating silver nanoparticles or bioactive glass into a basic experimental formulation, which comprised 80% w/w tricalcium silicate cement and 20% w/w zirconium oxide radiopacifier, with the rationale to enhance its biological properties. Commercial materials were also assessed for comparison purposes. An additional aim was to investigate the effect of environmental factors on the material properties.

In **Study I**, the surface characteristics alongside the bacterial adhesion of endodontic cements were assessed. Incorporation of silver nanoparticles (0.5, 1, 2 mg/ml) or bioactive glass (10, 20% w/w) increased the surface roughness of the experimental HCSCs over time but had no impact on the antibacterial effect. Immersion of all tested HCSCs to a serum-containing environment triggered surface reactions compared to immersion in water, but this did not affect the bacterial adhesion. While the physical parameters measured did not appear to be related to the degree of bacterial adhesion in experimental HCSCs, the commercial HCSC Biodentine (Septodont, Saint Maur-des-Fosses, France) displayed improved physical properties but compromised antibacterial efficacy, with significant bacterial adhesion from day one compared to the experimental HCSCs.

**Study II** tested leachates from the cements. The results showed that both modifications of HCSCs and different environmental conditions significantly influenced the

leaching properties of the materials. More specifically, immersing the materials in fetal bovine serum resulted in reduced alkalinity, decreased bactericidal properties, and lower cytotoxicity of both experimental and commercial HCSCs compared to water immersion. The 20% bioactive glass-containing cement and Biodentine exhibited overall lower alkalinity, calcium release, and antibacterial activity than the basic experimental HCSC formulation. Mixing the experimental HCSC with a 2 mg/ml silver nanoparticle solution enhanced the antibacterial efficacy of water leachates but had no such effect in the serum leachates.

In **Study III**, the antibacterial characteristics of the dentin/material interface and dentin surfaces exposed to the test materials were examined. All tested HCSCs conferred antibacterial activity onto the adjacent dentin. However, this effect was lower for the experimental HCSC with inclusion of 40% w/w bioactive glass and for Biodentine compared to the basic experimental formulation. Conversely, a 2 mg/ml silver nanoparticle solution increased the antibacterial potential of the basic experimental formulation in an assay with a longer interaction period (three-day bacterial exposure instead of one-day).

Taken together, findings of the current thesis suggest that modifications of the composition of HCSCs led to notable changes in their physical and chemical properties, which subsequently impacted their biological activity. The addition of 2 mg/ml silver nanoparticles did not compromise the physico-chemical characteristics of the cement but only led to a modest improvement in antibacterial properties. Incorporation of 20% bioactive glass into tricalcium silicate cement reduced the calcium hydroxide release, thereby compromising the indirect contact antibacterial efficacy of the cement in both the immersion medium and dentin surfaces, with an even greater impact at 40% incorporation for the conferred effect in dentin. Biodentine displayed enhanced physical properties and lower cytotoxicity, but weaker antibacterial efficacy compared to the basic experimental formulation. These differences are attributed to the chemical additives in the manufacturing of Biodentine. Lastly, the immersion medium and aging period had a notable influence on HCSCs. These factors should be thus carefully assessed in the context of the cements' clinical application. Aging of materials in a clinically relevant medium had a detrimental effect on their leachate antibacterial properties, while achieving long-lasting antimicrobial activity remains a distant goal.

## List of Publications

- Study I** Koutroulis, A., Valen, H., Ørstavik, D., Kapralos, V., Camilleri, J. & Sunde, P. T. Surface characteristics and bacterial adhesion of endodontic cements. *Clin. Oral Investig.* **26**, 6995–7009 (2022). <https://doi.org/10.1007/s00784-022-04655-y>.
- Study II** Koutroulis, A., Valen, H., Ørstavik, D., Kapralos, V., Camilleri, J. & Sunde, P. T. Effect of exposure conditions on chemical properties of materials for surgical endodontic procedures. *Eur. J. Oral Sci.* **131**, e12943 (2023). <https://doi.org/10.1111/eos.12943>.
- Study III** Koutroulis, A., Valen, H., Ørstavik, D., Kapralos, V., Camilleri, J. & Sunde, P. T. Antibacterial activity of hydraulic calcium silicate cements in contact with dentin- an ex vivo study. *J. Funct. Biomater.* **14**, 511 (2023). <https://doi.org/10.3390/jfb14100511>.



## Abbreviations

<b>BG</b>	Bioactive glass
<b>CFU</b>	Colony forming unit
<b>CLSM</b>	Confocal laser scanning microscopy
<b>EBA</b>	Ethoxy benzoic acid
<b>EDX</b>	Energy dispersive x-ray
<b>EPS</b>	Extracellular polymeric matrix
<b>FBS</b>	Fetal bovine serum
<b>GIC</b>	Glass ionomer cement
<b>HCSC</b>	Hydraulic calcium silicate-based cement
<b>HBSS</b>	Hank's balanced salt solution
<b>IRM</b>	Intermediate restorative material
<b>ISO</b>	International Organization for Standardization
<b>MTA</b>	Mineral trioxide aggregate
<b>MTT</b>	3-(4,5 dimethylthiazolyl-2-yl)-2,5-diphenyl tetrazolium bromide
<b>NP</b>	Nanoparticle
<b>Ra</b>	Arithmetic roughness
<b>RRM</b>	Root repair material
<b>ROS</b>	Reactive oxygen species
<b>SEM</b>	Scanning electron microscopy
<b>SNP</b>	Silver nanoparticle
<b>Super EBA</b>	Super ethoxy benzoic acid
<b>Water</b>	Ultrapure water
<b>ZOE</b>	Zinc oxide/eugenol





# 1. Introduction

The tooth structure comprises external layers of hard mineralized tissues (enamel, cementum, dentin) that surround a soft vascularized and innervated connective tissue, the dental pulp<sup>1</sup>. The tooth root is positioned within a fibrous joint, the periodontium. The periodontium encompasses the supporting and investing tissues of the tooth<sup>2</sup>. Blood supply to the pulp primarily comes from end arteries passing from the periodontium through the tooth root's apical foramina<sup>3</sup>. A local inflammatory reaction can be triggered in the dental pulp by external irritation, much like any other human tissue. However, due to its encasement in a rigid area with limited adaptability, this inflammation can also lead to irreversible events<sup>4</sup>.

Endodontics (from the Greek words endo-, meaning "within", and odont-, meaning "tooth"<sup>5</sup>) is concerned with the biology and pathology of the dental pulp and the associated periradicular tissues<sup>6</sup>. In the clinical field, this branch of dentistry mainly focuses on the treatment of the root canal system and the application of root filling materials to adequately seal the root canal space from the periradicular tissues<sup>7</sup>. The ultimate aim behind all clinical procedures in endodontic treatment is to cure and/or prevent apical periodontitis<sup>7</sup>.

## 1.1 Apical periodontitis

Apical periodontitis is the inflammation of the apical periodontium of endodontic origin<sup>6</sup>. As the dental pulp and the periodontium have a direct communication, primarily through the apical foramina, apical periodontitis is most often caused by a pulpal infection<sup>8</sup>. Pulpal infection may be induced by bacteria from dental caries, trauma, iatrogenic procedures, or periodontal disease. The sequence of events begins with oral bacteria contaminating the root canal system and consequently, the infection reaches the periradicular tissues, inducing an inflammatory reaction<sup>9</sup> (**Figure 1**).

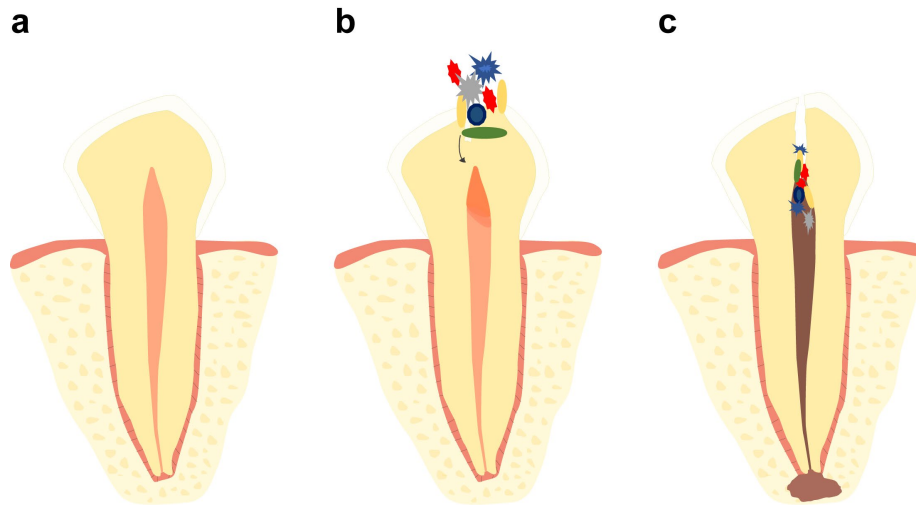


**Figure 1** Schematic representation of the stages of apical periodontitis. (a) Healthy tooth in the periodontium. (b) Bacteria invasion to the dentinal tissues causes pulpal inflammation. (c) The pulp is infected, and the infection has proceeded further causing inflammation of the periradicular tissues, where a lesion is formed.

Microorganisms, and mainly bacteria, are the etiological factor of apical periodontitis<sup>9</sup>. Since Babylonian times, the speculation of a tooth-worm being responsible for tooth-aches was prevalent<sup>10</sup>. The tooth-worm theory carried on for hundreds of years, with its relation to dental caries being further strengthened in the mid-1600s by claims of observations of worms coming out from carious teeth<sup>11</sup>. In the 17<sup>th</sup> century, the “*father of modern microscopy*” Antony van Leeuwenhoek, was the first to observe bacteria in a necrotic root canal and described it as a “*soft matter... that seemed to be alive*”<sup>12</sup>. Even though his work did not invalidate the belief in the worm-theory, it did raise doubts about its credibility<sup>11</sup>. It was only until 1894 that the causal relationship between bacteria and apical periodontitis was first suggested by Miller<sup>13</sup>. Confirmation came initially in 1965 through the classic histological study of Kakehashi et al., who observed that the artificial exposure of dental pulps to the oral cavity in conventional and germ-free rats led to different sequels: while the first group developed pulp necrosis and apical periodontitis, the pulps of the germ-free rats remained vital and dentin-like tissue was formed to cover the exposure area instead<sup>14</sup>. The necessity of the bacterial factor for the development of the disease was further validated by two subsequent landmark studies. In 1976, Sundqvist used

anaerobic culturing techniques to identify bacteria from necrotic pulps of teeth after trauma<sup>15</sup>. Bacterial cultures were acquired only from teeth with radiographic signs of apical periodontitis<sup>15</sup>. In 1981, Möller et al. demonstrated radiographically and histologically the development of apical periodontitis in devitalized teeth of monkeys, only in the presence of a preceding pulpal infection<sup>16</sup>.

Since the establishment of the microbial causation on the endodontic infections, more than 450 bacterial species have been identified in relevant studies<sup>17</sup>, the majority of which remain uncultivated and/or uncharacterized<sup>18</sup>. Another milestone within the field is the demonstration of the strong association of apical periodontitis with biofilms<sup>19</sup>. Biofilms are multicellular microbial communities of cells that are attached to a substrate and enmeshed in a self-produced extracellular polymeric matrix<sup>20</sup> (**Figure 2**). When organized in such communities, bacteria exhibit a different phenotype than their planktonic forms, and demonstrate increased resistance characteristics. Particularly for endodontic infections, the multispecies nature of the biofilm contributes to its virulence and resistance<sup>21</sup>.

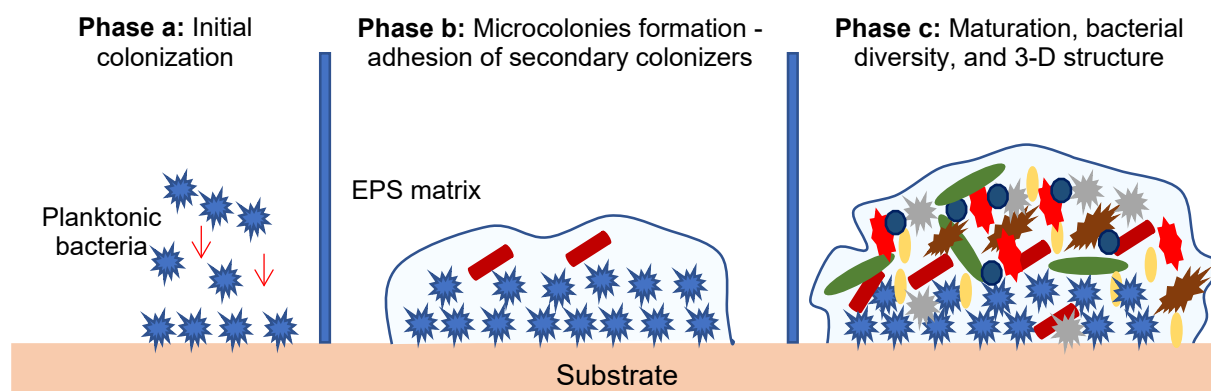


**Figure 2** Schematic representation of the three basic stages of biofilm formation and development. EPS: extracellular polymeric matrix.

Evidence of high interindividual bacterial diversity in endodontic infections<sup>22-24</sup> indicates the role of bacterial community as the main unit of pathogenicity in apical periodontitis, rather than the presence of a specific bacterial species or a group of them<sup>25</sup>. It was additionally shown that the bacterial composition in the infected root canal system

varies significantly in the apical portion compared to the coronal part<sup>26-28</sup>. In the context of the localization of the microorganisms in endodontic infections, a categorization between intraradicular and extraradicular infections has been suggested: in the former, microorganisms have colonized the root canal system, while in the latter, these have expanded further into the periradicular tissues<sup>29</sup>.

### 1.1.1 Infection control

The cause-and-effect relationship between bacteria and pulpal or periapical diseases underscores the common goal of clinical endodontics: treating and/or preventing microbial contamination<sup>30</sup>. Nonsurgical root canal treatment entails mechanical instrumentation, irrigation, optional inter-appointment medication, and finally a root canal filling<sup>31,32</sup>. These steps aim to substantially reduce or, when possible, eliminate the microbial irritants and establish a tight seal within the root canal system (**Figure 3**).

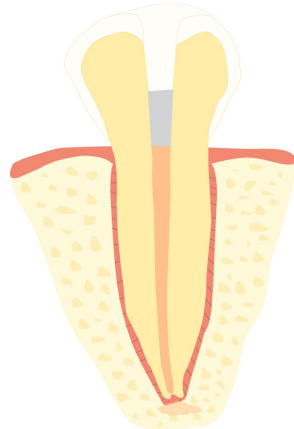


**Figure 3** Schematic drawing of the tooth in **Figure 1** after nonsurgical root canal treatment. The root filling materials provide a tight seal from the periradicular tissues. A coronal restoration is also placed. The apical lesion resolves towards healing of the region.

In practice, the current procedure can achieve disinfection but not sterilization of the root canal system. A critical microbial elimination threshold therefore exists<sup>33</sup>, which is compatible with periradicular tissue healing<sup>34</sup>. A recent meta-analysis of clinical studies

assessing the outcome of primary non-surgical root canal treatment in teeth with apical periodontitis found that periapical health was evident in 74% of cases<sup>35</sup>.

On the other side, under certain conditions, apical periodontitis might persist, emerge, or recur after treatment<sup>18</sup>. The main causes for post-treatment apical periodontitis are:

- Root canal contamination during treatment due to a breach of the aseptic protocol or leakage through the coronal restoration after treatment<sup>34</sup>.
- Bacterial persistence, particularly in the apical portion of the root canal system<sup>34,36</sup> in anatomic complexities that the instruments and antimicrobial substances cannot reach.
- Extraradicular infections<sup>36</sup>. Though rare (2 - 4%), the presence of biofilm in the periradicular area, which may be independent from the intraradicular microbiota and is yet to be fully understood<sup>37</sup>, cannot be successfully managed by nonsurgical root canal treatment.

These conditions may require retreatment, either by revision of the root canal treatment or through surgical endodontic procedures. Nonsurgical root canal retreatment shares the same focus as the initial approach<sup>32</sup>, but an additional challenge is the removal of the filling material, which may as well serve as a substrate for biofilm formation at the interface with the root canal walls<sup>38</sup>. Complete periapical healing is achieved in 69% of the cases, approximately 5% lower than the primary treatment<sup>35</sup>.

In cases where nonsurgical root canal retreatment fails or is not indicated - such as in cases of inaccessible apical anatomy, extrusion of filling materials, suspicion of cyst, root fracture or root perforation - surgical endodontics might be implemented<sup>32,39</sup> (**Figure 4**). Surgical intervention includes procedures aiming to eliminate the infection by means of apical curettage, periradicular surgery, crown and root resection, or tooth extraction with replantation<sup>40</sup>. Procedures that involve root-end resection or perforation repair, have as a final step the application of a root filling material as a tight, permanent seal within the root canal system, following a similar rationale as in nonsurgical root canal treatment<sup>41</sup>.

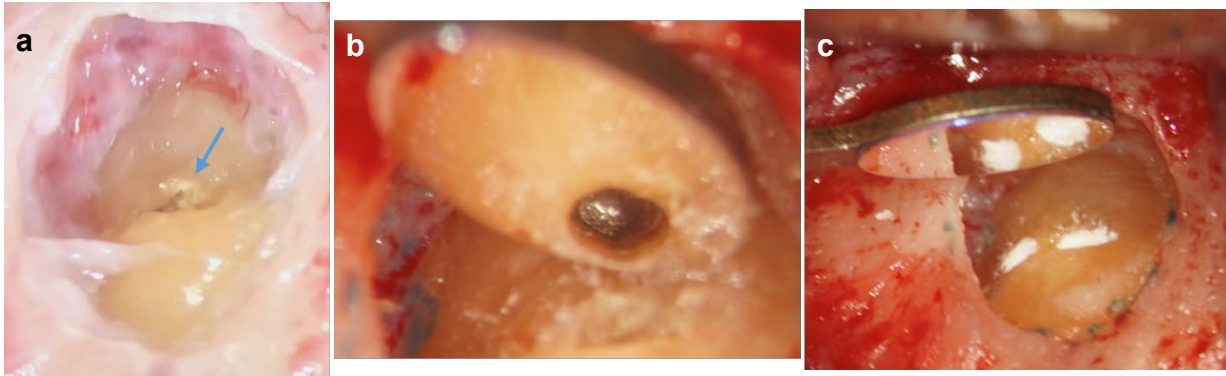


**Figure 4** Surgical treatment of a right maxillary central incisor with challenging anatomy and a metal post, making nonsurgical root canal retreatment non-indicated. (a) After removal of the apical lesion and initial bone cavity refinement, bacterial biofilm was localized (arrow) at the buccal portal of exit of the root canal system (b) Micro-mirror view of the metal post inside the root canal system after retrograde root preparation. (c) The root canal exit portals were sealed with retrograde filling material. Courtesy Dr Thanos Fasoulas, Amsterdam, Netherlands.

## 1.2 Root filling materials

Historically, a plethora of different materials have been used for root-filing. The list of the utilized materials until 50 years ago includes amalgam, asbestos, balsam, bamboo, copper, cotton, gold, indium, ivory, lead, paper, paraffin, pitch, rosin, rubber, spunk, thistles, wax, and wood<sup>42</sup>. Back in 1958, Grossman pointed out: “*I doubt very much whether there is any hollow cavity in the body that has been plugged with as many different materials as the root canal of a tooth*”<sup>43</sup>. He vividly likened the root canal to “*the attic of the dental household*”<sup>43</sup>. In addition, Grossman had suggested a list of requirements for the ideal root filling material<sup>42</sup>, many of which are still relevant to this day<sup>44</sup>.

In principle, sealing the root canal system from the periradicular tissues aims to prevent bacterial invasion and infection following the completion of endodontic treatment<sup>32</sup>. Root filling materials may achieve that by means of physical integrity and excellent adaptation to the dentin walls and/or by exerting antimicrobial activity<sup>41</sup>.

In nonsurgical root canal treatment, an inert core material (gutta-percha) is used in combination with an endodontic sealer. The former acts as a piston for the latter, which in turn fills the voids between gutta-percha and dentin, and thus determines the functional characteristics of the root filling<sup>45</sup>. In surgical approaches and perforation repair, a single endodontic material is used<sup>46</sup>.

### **1.2.1 Materials for endodontic surgery**

The exposed material surface in contact with the periradicular tissues in conventional root filling procedures of mature teeth with closed apices is relatively small as this occurs mainly through the apical foramina and any lateral canals. In contrast, in clinical procedures entailing endodontic surgery, perforation repair or treatment of immature teeth with open apices, the contact area with the subsequent tissues may be considerably larger<sup>41</sup> (**Figure 5**). The clinical environment to which the root-end filling and perforation repair materials are exposed to is inherently humid due to blood and other tissue fluids. In addition, the materials typically meet an inflamed tissue that has been formed in response to the preceding infection<sup>47</sup>. These materials therefore have a complex role towards blocking the pathways of communication of the root canal system with the periradicular area in a dynamic environment. Furthermore, it is deemed beneficial if they can facilitate healing of the periradicular tissues<sup>48</sup>. Materials are placed in direct contact with dentin and the periradicular tissues but interactions with the subsequent tissues may not be limited in direct contact, as leachable material elements can reach further beyond the application field<sup>41</sup>. The physical and chemical characteristics of the material will therefore define their biological profile.

The term “materials for endodontic surgery” will be used inclusively to refer both to root-end filling materials and those used for perforation repair. It is recognized that repair of coronal perforations in certain cases might be also performed through the root canal instead of surgically<sup>46</sup>, and thus a non-differentiating inclusion of perforation repair materials under the term “surgery” is not strictly accurate. However, it will be used further in terms of convenience. The term “*extra-radicular materials*” has been previously used in

the same context<sup>49</sup> but might also lack accuracy as it implies that materials are located outside of the root.

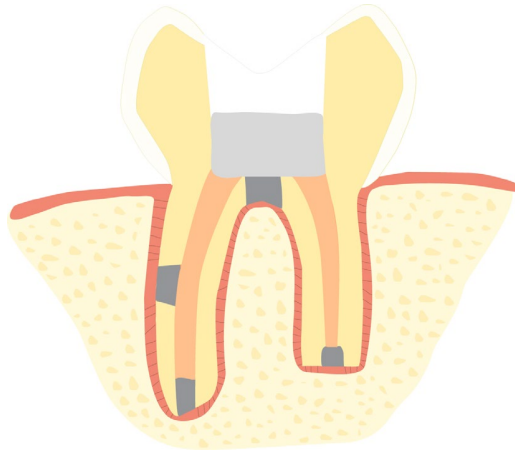


**Figure 5** Schematic representation of application of a root filling material for perforation repair, root-end surgery, or treatment of open apex on a tooth. The contact area of the root filling material with the subsequent tissues is considerably larger than in conventional root filling procedures.

Similar to conventional root filling, a variety of materials with different chemical compositions has been used for endodontic surgery. These include gold foil and leaf, gutta-percha (both cold and injectable), teflon, titanium screws, amalgam, silver points, zinc oxide/calcium sulfate cements, polycarboxylate cement, polyvinyl resin, poly-HEMA, resin-based sealers, various zinc oxide/eugenol-based cements, glass ionomer cement, composite resin, and, most recently, hydraulic calcium silicate cements<sup>50-52</sup>.

### 1.2.1.1 From historical to currently used materials

#### Amalgam

Silver amalgam was for many years the most vastly applied material for endodontic surgery<sup>53-55</sup> with reports of use even until recently<sup>56</sup>, mainly due to its ease of manipulation, absence of resorption and adequate radiopacity<sup>57</sup>. Today, several drawbacks have been



reported, with the most significant being: cytocompatibility concerns<sup>58</sup> associated with mercury release<sup>59</sup>; corrosion<sup>60</sup> and tissue staining due to silver salts<sup>61,62</sup>. Its use has been also associated with poor prognosis<sup>63,64</sup>.

## Glass ionomer cements

Glass ionomer cements (GICs) are mainly used as restorative cements due to their adhesion to dentin via ionic exchange and a caries-inhibitory potential through fluoride release<sup>65</sup>. The application of GICs in root-end filling does not need a mechanical cavity preparation but the dentin smear layer should be removed to enable adhesion<sup>46</sup>. In terms of their clinical performance, a systematic review resulted that GIC and amalgam were equally the least effective materials for root-end filling<sup>66</sup>.

Modifications of GICs with resin components have been introduced that improve the working and setting time but significantly reduce the fluoride release<sup>46,67</sup>. The materials are dual cure: light-activation in addition to the acid-base reaction take place. Similar with conventional GICs, their use in endodontic surgery today is not popular.

## Resin systems

Dentin bonding agents, along with the use of resin composites have found application in endodontic surgery. Adjusted from restorative dentistry to the specific surgical field, resin systems still require good control of humidity during application<sup>68,69</sup>. For root-end surgery, a conservative cavity with a concave shape is prepared, followed by etching of the dentin surfaces<sup>70</sup>. Similar to resin-modified GICs, the main advantages of the resin systems are bonding to dentin and sealing of exposed dentinal tubules<sup>69</sup>. The best-known material in this category is RetroPlast (RetroPlast Trading, Roervig, Denmark).

The release of unreacted monomers by the resin systems has been associated with cytotoxicity<sup>46</sup>. Studies of dentin bonding agents found a suppression in the normal macrophage function and an initial cytotoxic behavior<sup>71-73</sup>. But studies on RetroPlast demonstrated contradictory findings with either a proliferative effect in contact with fibroblasts<sup>74</sup> or inhibition of the cell growth of fibroblasts and macrophages<sup>75</sup> and poor

fibroblast attachment upon the material<sup>76</sup>. When implanted into the dorsal connective tissue of rats, resin systems induced a moderate to severe inflammation that declined within a three-month observation period<sup>77</sup>. In terms of the antibacterial effect, this has been shown to vary among different commercial materials, depending on the inclusion of antibacterial monomers or fluoride in their composition<sup>78</sup>.

Although several clinical studies have reported good outcomes from the application of resin systems with the accompanied preparation technique<sup>68,79-81</sup>, a meta-analysis found that the resin-system technique had a lower weighted pool success rate compared to the contemporary root-end surgery with non-resin cement<sup>82</sup>. This was mainly attributed to bonding failure due to the humid application field<sup>82</sup>. However, the effect of different materials was not assessed in the meta-analysis, and the outcomes seem to have been mainly influenced by one<sup>83</sup> of the three included studies using the resin-system technique.

### Zinc oxide/eugenol-based cements

Zinc oxide/eugenol (ZOE) cements have been used in endodontic surgery for several decades<sup>84,85</sup>. These cements constitute chelates of zinc with eugenol (salt zinc eugenolate) in a weak bond<sup>41</sup>, and have, today, two main modified representatives: Super EBA (Bosworth, Skokie, IL, USA) and Intermediate restorative material (IRM; Dentsply Sirona, Charlotte, NC, USA). In Super EBA, eugenol is partly substituted by ethoxy benzoic acid (EBA; 68%) in the liquid component, while fumed silica and, later on, aluminium oxide (34%), along with natural resin (6%) are added in its powder formulation<sup>86</sup>. IRM contains polymethacrylate (20%) within its powder composition, along with the addition of acetic acid (1%) to the liquid component<sup>40,46</sup>. The adaptation of ZOE-based cements to dentin is achieved with purely mechanical means.

The biological reactivity of the ZOE-based cements is attributed to eugenol release by progressive hydrolysis of the material surface<sup>87,88</sup>, which might even increase over time<sup>78</sup>. The cytotoxicity evaluation of Super EBA and IRM has yielded contradictory results compared to amalgam<sup>89-92</sup>. Some in vitro studies reported cytotoxic effects of Super EBA on gingival fibroblasts and periodontal ligament cells<sup>93-96</sup>, as well as in undiluted extracts

against cancer cells<sup>97</sup>. Similarly, IRM exhibited the highest cytotoxicity on fibroblasts<sup>75,98,99</sup> and osteoblasts<sup>91</sup> among some contemporary materials used in endodontic surgery.

In studies on monkeys, Super EBA and IRM induced a mild inflammatory response in the periradicular area<sup>100-102</sup>. Although one clinical study found no evidence of hard tissue formation within five weeks of application of IRM to healthy resected dog teeth<sup>103</sup>, a later study demonstrated that IRM induces long-term healing after six months when used as a retrograde material in infected dog teeth<sup>104</sup>.

Only few studies have assessed the antibacterial properties of super EBA and IRM with particular reference to their application in endodontic surgery. In direct contact tests against planktonic bacteria, IRM exhibits varying antibacterial activity against *Enterococcus faecalis*. One study reported potent antibacterial behavior in freshly set samples, lasting up to one day<sup>105</sup>. Another study found this effect extended to three-day set samples and included resistance against *Staphylococcus aureus* and *Pseudomonas aeruginosa* as well<sup>78</sup>. Interestingly, a moderate yet sustained antibacterial effect has been also reported, lasting even after 18 weeks of material storage in water<sup>106</sup>. In a dentin infection model with *E. faecalis*, IRM showed antibacterial efficacy, which was reduced between one and seven days<sup>107</sup>. Additionally, an assessment of minimum bactericidal concentration deemed IRM's efficacy acceptable against *E. faecalis*, *S. aureus* and *Streptococcus mutans*<sup>108</sup>.

Several human clinical studies have demonstrated that the ZOE-based cements exhibit acceptable success rates as materials for endodontic surgery<sup>109-113</sup>, with follow-up evaluations performed up to two years for IRM<sup>114</sup> and up to four years for Super EBA<sup>115,116</sup>. Thus, IRM and Super EBA continue to be recommended for use in endodontic surgery<sup>117</sup>.

### 1.2.1.2 Hydraulic calcium silicate cements

Hydraulic calcium silicate cements (HCSCs) are used today in various endodontic procedures<sup>46,118,119</sup>. The term “hydraulic” is derived from the Greek word hydra, meaning “water”, and is used to denote that water is the reactant for setting of these materials<sup>120</sup>. “Calcium silicate” is used to indicate the materials’ basic chemical composition, with their

primary constituent being tricalcium silicate<sup>121</sup>. To be classified as a HCSC, the hydration reaction must be the primary reaction that occurs<sup>121</sup>, leading to the formation of calcium silicate hydrate and calcium hydroxide. While several other terms have been assigned to this material category, the current one appears to be the most appropriate for adequately specifying their chemistry and main attributes<sup>121</sup>.

An abundance of clinically used HCSCs is available today. These may be classified on two levels: 1) based on their composition, and particularly on the main components that can modify their hydration (**Table 1**); 2) based on the endodontic procedure they are indicated for (i.e. “*intra-coronal, intra-radicular, extra-radicular*”)<sup>49</sup>.

## Portland cement

The first reported use of a HCSC in dentistry was Portland cement as a root canal filling material in 1878<sup>122</sup>. Invented in 1824, Portland cement is commonly used in the construction industry as a binder for concrete. To manufacture it, limestone and shale are crushed and heated in a kiln<sup>123</sup>, resulting in a powder composed of tricalcium silicate (45 - 70%), dicalcium silicate (5 - 30%) tricalcium aluminate (<10%), calcium aluminoferrite (<10%), and trace oxides (≈0.5%) from raw materials. Calcium sulfate is added in the final step<sup>124,125</sup>. When mixed with water, the following reactions occur:

- Tricalcium aluminate dissolves and reacts with calcium and sulfate ions. Ettringite (a calcium aluminate sulfate) is formed and precipitates upon the cement surface.
- The hydration reaction of (tri-, di-) calcium silicates produces amorphous calcium silicate hydrate and calcium hydroxide.

## Type 1 HCSCs - Mineral trioxide aggregate

More than a century after the first published use of a HCSC to fill root canals, Torabinejad patented a new material for “*tooth filling*” under the name Mineral trioxide aggregate (MTA)<sup>126</sup>. MTA is a blend of Portland cement (80%) with bismuth oxide radiopacifier (20%)<sup>125</sup>. In practice, MTA shares the properties of Portland cement and incorporates bismuth oxide

to provide radiopacity. After a series of in vitro investigations<sup>90,127,128</sup>, animal studies<sup>129-132</sup> and clinical applications in patients<sup>133</sup>, MTA was commercialized as ProRoot MTA (Dentsply, Tulsa Dental, Johnson City, TN, USA) in 1998.

**Table 1** Classification of commercially available hydraulic calcium silicate cements based on cement type, presence of additives and water component (i.e liquid vehicle)<sup>49</sup>.

Type	Cement	Additives	Liquid vehicle	Representative material
1	Portland cement	–	✓	ProRoot MTA (Dentsply)
2	Portland cement	✓	✓	NeoMTA Plus (Avalon Biomed)
3	Portland cement	✓	–	Bio-C repair (Angelus)
4	Tricalcium/dicalcium silicate	✓	✓	Biodentine (Septodont)
5	Tricalcium/dicalcium silicate	✓	–	TotalFill (FKG Dentaire)

ProRoot MTA is a type 1 HCSC. A white version (tooth-colored ProRoot MTA) became available a few years later with a significantly lower concentration of iron<sup>134</sup>, in an effort to address concerns about the induction of tooth discoloration. Soon, other companies began to launch their own “MTA”s, with first being Angelus (Londrina, Brazil) in 2001. Today, as the initial patents for the material have expired, several commercial products have the term MTA in their name. Despite some adjustments from the initial composition in some of the most recent products and occasional confusions created by the commercial

exploitation of “MTA” as a trade name, the term corresponds to mixtures of Portland cement-like materials with a chemical compound as radiopacifier (type 1 or 2 HCSCs)<sup>46</sup>. In the current overview, the term MTA is used to refer both to the ProRoot and Angelus versions. Type 3 materials could be considered as MTA-like, since they are Portland cement-based HCSCs but with the main difference being that they are not mixed with any liquid vehicle (**Table 1**) and their hydration relies solely in the reaction with the environmental fluids<sup>46</sup>.

The MTA powder is hand spatulated with distilled water at a 0.33 water/powder ratio<sup>135</sup>. The mixture has a grainy consistency, which can make its application challenging<sup>124</sup>. The setting process can extend for several hours as the initial stages of the reaction of Portland cement have a complex sequence of procedures<sup>124</sup>. The exclusion of calcium sulfate from the cement can accelerate the reaction<sup>136,137</sup>. Following material hydration, the cement structure consists of a matrix of amorphous calcium silicate hydrate interspersed with non-hydrated cement particles and bismuth oxide particles<sup>138</sup>. Calcium hydroxide leaches out and interacts with the local environment<sup>139</sup>, substantially raising the pH<sup>127,140,141</sup>. Bismuth oxide was found not to remain inert; it interferes with the hydration of tricalcium silicate<sup>138</sup>, leaches out from the cement<sup>139</sup> causing tooth discoloration<sup>142</sup> and has been shown to be cytotoxic<sup>143,144</sup>. Recently, it has been replaced by other radiopacifiers in some formulations, namely calcium tungstate in MTA Angelus<sup>145</sup>.

The biological properties of MTA have been extensively assessed using various methods, from cellular studies to research involving animals and humans. Overall, it appears that the material is cytocompatible<sup>95-97,99,146-155</sup>. Fresh specimens might induce an initial cytotoxic effect, but this is followed by cell recovery<sup>75,92,98,156</sup>, or even enhancement of cell growth in aged samples<sup>94,150</sup>. However, cumulative material leaching in vitro from one to 42 days resulted in a decrease in cell survival<sup>157</sup>. The absence of cytotoxicity of MTA is further supported by the enhancement of cellular attachment on its surface with osteoblasts<sup>91,158-160</sup>, bone marrow mesenchymal stem cells and periodontal ligament stem cells<sup>161</sup>. Additionally, it appears that MTA enhances the secretion of biochemical markers associated with new bone formation<sup>150,153,162,163</sup> and modulates the secretion of inflammatory mediators, contributing to the resolution of inflammation and tissue repair<sup>151,158-160</sup>.

Tissue reactions have been histologically assessed following subcutaneous or intraosseous implantation of MTA in animals. Studies indicate an inflammatory reaction of varying severity during the initial days of implantation, which typically subsides over time<sup>164-175</sup>, and may as well be accompanied by tissue repair and healing<sup>176</sup>. Notably, when dentin blocks filled with MTA were implanted in the dorsal tissue of rats, mineral deposition in the material/dentin interface occurred<sup>177</sup>. This apatite precipitation upon the material surface coincides with the initial inflammatory phase<sup>178</sup> and suggests that MTA promotes a beneficial proinflammatory and pro-wound environment<sup>177,178</sup>. Moreover, the use of MTA as root-end filling material induced soft and hard tissue formation in the periapical tissues of both healthy and infected dog teeth<sup>103,104,179,180</sup>. In cases of perforations treated with MTA, an initial inflammatory response was observed after one week, which subsided at one month<sup>181</sup>, while other studies observed healing with hard tissue-like formation after three<sup>182,183</sup> or four<sup>184-186</sup> months.

The antimicrobial potential of MTA, as in all HCSCs, stems mainly from the alkaline-induced environment<sup>187,188</sup>. Its antimicrobial effect is strong in fresh samples and appears to decrease in aged specimens<sup>78,189-192</sup>. However, two studies demonstrated that MTA exhibited stable antibacterial behavior between 30 min and 24 hours of set samples in direct contact with planktonic *E. faecalis*<sup>193</sup> or between 24 hours and seven days of set samples in a dentin infection model against biofilms of the same species<sup>107</sup>. The presence of dentin substrate in the latter study was hypothesized to enhance its effect<sup>107</sup>. Overall, the antibacterial effect seems to depend on the bacterial species being tested<sup>78</sup>, with susceptibility varying also among different strains<sup>193</sup>. Another study reported “acceptable” values of minimum bactericidal effect against *S. aureus*, *E. faecalis* and *S. mutans*, yet the results were not compared to any control or were not assessed statistically<sup>108</sup>. Against multispecies biofilms, MTA failed to show any potent activity<sup>194</sup>. The somewhat contradictory nature of data from different studies can be attributed to varying assessment methods, including direct contact tests and dentin infection models<sup>194,195</sup>. In a laboratory study using conditions relevant to endodontic surgery, exposure to blood was found to neutralize MTA’s antibacterial activity<sup>191</sup>.

In human clinical studies, the use of MTA for root-end filling has demonstrated similar success rates to IRM<sup>111,114</sup> and super EBA<sup>113,116</sup>. Utilizing microsurgical techniques in

conjunction with MTA-application yields high success rates<sup>196-199</sup>. The clinical success of MTA for perforation repair has been very little investigated<sup>200</sup>, but, as explained above, the conditions are practically the same.

### Types 4 and 5 HCSCs

As Portland cement is manufactured by naturally occurring raw materials, concerns have been raised about the presence of trace metal elements in MTA<sup>201,202</sup>, most importantly aluminum ions, which have been found to leach into peripheral organs<sup>203,204</sup> and have even been associated with the induction of oxidative stress in the brain<sup>205</sup>. These considerations led to the replacement of Portland cement by pure calcium silicates manufactured using laboratory-grade materials<sup>206,207</sup> (types 4 and 5 HCSCs). The difference between the types 4 and 5 HCSCs is the absence of a liquid component in the latter, which use a water-free vehicle to suspend the powder instead<sup>46,208</sup>. The inclusion of additives in the calcium silicate phase of the materials as well as in the liquid component of type 4 HCSCs is carried out mainly to improve issues with the handling characteristics and long setting time of MTA. Two representative and well-researched materials from these categories are Biodentine (Septodont, Saint Maur-des-Fosses, France) and TotalFill BC (FKG Dentaire, La Chaux-de-Fonds, Switzerland) formulations (**Table 1**).

#### Representative type 4 HCSC

Biodentine, classified as a type 4 HCSC, was originally introduced as a dentin replacement material, but it is also indicated for endodontic surgery<sup>209</sup> and commonly used for perforation repair<sup>117</sup>. The powder phase of the material consists of tri- and di- calcium silicate (80%), calcium carbonate (15%), iron oxide (<1%) and zirconium oxide (5%)<sup>207</sup>. Calcium carbonate acts as an accelerator of the hydration reaction<sup>210</sup>. The material exhibits lower radiopacity than MTA<sup>207</sup>, which can be attributed to the relatively low amount of zirconium oxide radiopacifier. The liquid component includes water, calcium chloride as a setting accelerator and a water-soluble polymer to enhance workability and reduce the water/powder ratio<sup>207,211</sup>. The material powder is supplied in a capsule and is mixed with



the recommended powder/liquid ratio in a triturator. Biodentine has a setting time of approximately 12 minutes<sup>209</sup>, which is considerably lower than MTA<sup>210</sup>, while it also presents enhanced mechanical properties compared to MTA<sup>211</sup>.

Given that MTA preceded types 4 and 5 HCSCs by several years, it routinely serves as a reference material for evaluating the biocompatibility of newer formulations. These comparisons have provided varying results. Biodentine's 24-hour extracts had a negligible cytotoxic effect on primary human osteoblast, similar to MTA<sup>157</sup>. Furthermore, while the cumulative 42-day extract of MTA induced cytotoxicity, Biodentine's effect was not significantly altered in that period<sup>157</sup>. No cytotoxicity was induced in human periodontal ligament cells by three-day extracts of Biodentine, which reported values similar to MTA<sup>212</sup>. On the contrary, other studies found that neat 24-hour extracts of Biodentine induced cytotoxicity in apical papilla cells<sup>152</sup>, murine mesenchymal stem cells<sup>162</sup> and osteoblasts<sup>213</sup>, whereas eluates of MTA or MTA-like materials performed better<sup>162,213</sup> or even did not affect cell viability at all<sup>152</sup>. In a wound healing assay, MTA allowed for unhindered cellular migration and proliferation, in contrast to Biodentine, but both cements showed adequate cell attachment upon their surfaces<sup>152</sup>. Direct exposure to a fibroblast cell line showed overall similar values of cell viability for Biodentine and MTA compared to the control, with significantly more cells adhering to the Biodentine surface than MTA<sup>214</sup>. In regard to the osteogenic potential, Biodentine stimulated differentiation of murine mesenchymal stem cells similar to MTA<sup>162</sup> as well as enhanced the mineralization activity in osteoblasts<sup>213,215,216</sup>. In an ex vivo model assessing the regeneration of bone defects in mice, Biodentine eluates had a slightly lower potential compared to MTA<sup>153</sup>. In another study, Biodentine was as effective as MTA in suppressing inflammatory markers<sup>216</sup>.

Subcutaneous implantation of Biodentine in rats induced a moderate inflammation at seven days, which subsided by 14 days<sup>166</sup>. In a dog periradicular surgery model, both MTA and Biodentine induced periradicular healing<sup>212</sup>. Furthermore, Biodentine and MTA promoted similar healing responses when used to treat furcation perforations in rats, with reduction in inflammation from 14 to 21 days and decreased bone resorption<sup>217</sup>. At 60 days, both materials led to narrowed periodontal spaces, reduced numbers of immune cells and osteoclasts, and increased densities of osteoblasts, fibroblasts, and collagen<sup>218</sup>. In dog models with artificially induced furcation perforations, Biodentine and MTA showed

overall similar outcomes: one study reported comparable hard tissue formation for both materials but noted a lower degree of inflammation induced by Biodentine<sup>186</sup>, whereas other studies found that MTA exhibited a better mineralization potential<sup>185</sup> and resulted in smaller proportions of inflammatory scores<sup>181</sup>.

The evaluation of the antimicrobial activity of Biodentine has yielded reports of varying efficiency against different bacterial species and in comparison to MTA<sup>219-222</sup>. Several studies have used cariogenic bacteria, which might not be relevant in the context of endodontic surgery, but they do provide information on the material's overall antibacterial potential. Using a direct contact test, Biodentine and MTA exhibited similar antibacterial efficiency against *E. faecalis*, with the effect decreasing when samples aged<sup>189</sup>. In another study, incubation of Biodentine with a planktonic *E. faecalis* culture yielded bacterial growth after 24 hours exposure<sup>223</sup>. In studies with cariogenic bacteria, fresh Biodentine was highly effective against a planktonic polymicrobial *Streptococcus* suspension upon direct contact, but the effect decreased with longer exposure, allowing eventually biofilm formation upon its surface<sup>224</sup>. The material leachate had no effect on the same suspension<sup>225</sup>. Biodentine exhibited antibacterial activity against *S. mutans* both in direct contact<sup>226</sup> and leachate assays<sup>227</sup>, as well as a moderate effect against *Lactobacillus casei*<sup>227</sup>. However, it had no impact on a multispecies biofilm in a dentin model<sup>194</sup>.

Human clinical studies on the use of Biodentine in endodontic surgery are limited, possibly because it is primarily used for perforation repair rather than root-end surgery<sup>117</sup>. Its clinical potential for root-end filling has been suggested in case reports<sup>228,229</sup>. In a clinical case trial with artificially induced perforations in teeth scheduled for extraction and assessed histologically after three months, Biodentine showed comparable biocompatibility to MTA, but the latter showed more formation of cementum-like tissue<sup>230</sup>.

### Representative type 5 HCSC

The term “root repair material” abbreviated as “RRM” will be utilized consistently throughout the remainder of this document to refer to a group of materials that are marketed under various commercial names, such as TotalFill (FKG Dentaire, La Chaux-de-Fonds, Switzerland), Endosequence (Brasseler, Savannah GA, USA), and iRoot

(Veriodent, Vancouver, Canada), possibly due to regional licensing issues. These “*premixed*” materials (type 5 HCSCs) do not contain a liquid component and undergo thus, hydration in the presence of environmental fluids, similar to type 3 HCSCs (**Table 1**). A range of materials with different consistencies is available, which were specifically introduced for root repair. These include RRM paste, RRM putty, and RRM fast set putty. The composition of these formulations is rather similar, as it is also denoted by the fact that they have the same safety data sheet<sup>231</sup>.

The manufacturer reports a composition of tricalcium silicate (30 - 36%), dicalcium silicate (9 - 13%), calcium sulfate (3 - 8%) and radiopacifiers zirconium oxide (15 - 18%) and tantalum pentoxide (12 - 15%)<sup>231</sup>. Additionally, the materials contain a calcium phosphate phase, which, although not explicitly mentioned in the safety data sheet, is documented in the “*Instructions for use*” file for Endosequence BC RRM<sup>232</sup>. The presence of two radiopacifiers renders the materials particularly radiopaque<sup>233</sup>. As regards their setting times, one study reported an initial setting time of 62 min for the RRM paste and 18 min for the RRM fast set putty<sup>234</sup>. Another study found initial setting times of two hours for the RRM paste and 22.5 hours for the RRM putty<sup>233</sup>. These variations can be attributed to differences in testing conditions, including immersion in water in the first study and exposure to 95% humidity in the second<sup>233</sup>.

In terms of biological properties, exposure of an osteoblast cell line to RRM putty resulted in higher numbers of viable cells and lower rates of apoptosis compared to MTA and RRM paste, which were also cytocompatible<sup>235</sup>. The seven-day extracts of MTA and RRM putty had a similar effect on cell viability of human gingival fibroblasts, but the two-day RRM putty extracts were more cytotoxic<sup>96</sup>. Similar cell viability values (>90%), were also obtained with 24-hour leachates on dermal fibroblasts, although the putty scored lower values than the negative control<sup>147</sup>. Another study found that the two- and seven-day extracts of RRM putty and RRM paste had similar cell viability values to MTA, except for the two-day RRM paste, which was more cytotoxic compared to MTA<sup>99</sup>. All three materials promoted cell attachment<sup>99,161,235</sup>. RRM putty exhibited potent osteogenic behavior with increased expression of osteoblastic genes, mineralization activity and acceptable cell viability in both an osteoblast cell line and rat mesenchymal stem cells, but in the case of the latter, MTA had an overall superior effect<sup>154,163</sup>.

Comparison of healing outcomes between RRM paste and MTA in root-end surgeries on dog teeth with apical periodontitis showed no significant difference in the inflammatory infiltration and cortical plate healing six months after the operation, but the RRM had more favorable tissue healing adjacent to the resected root-end surface<sup>180</sup>. In artificially induced perforations in rat teeth, after an initial inflammatory response at one week, the RRM putty induced complete cortical plate healing at one month, whereas in 50% of the Biodentine cases, the periodontal ligament had still necrotic areas infiltrated by inflammatory cells<sup>236</sup>.

The RRM paste and putty have demonstrated comparable antimicrobial efficacy to MTA in a direct contact test against *E. faecalis* and *Candida albicans*: fresh and one-day set samples reduced the microbial colonies, although this effect diminished in the seven-day aged samples<sup>192</sup>. In another study, all three materials remained equally antibacterial after seven days against different *E. faecalis* strains<sup>193</sup>. When assessed against cariogenic bacteria, Biodentine and RRM formulations have shown similar efficacy<sup>226,227</sup>.

Human clinical studies on the use of RRM putty in endodontic microsurgery have reported similarly favorable outcomes as those observed with MTA in terms of clinical and radiographic examination for at least one year of follow-up<sup>197-199</sup>.

### 1.2.1.3 Interactions with the clinical environment

HCSCs are identified as reactive materials<sup>237</sup>: once the calcium hydroxide is released, it dissolves into calcium and hydroxyl ions, which may induce changes in the local microenvironment. At the same time, the environment affects the material properties as well<sup>237</sup>. These may vary depending on the specific clinical application field as different interactions occur with various subsequent tissues<sup>121</sup>. For endodontic surgery, interactions include dentin, blood and tissue fluids in general<sup>46</sup>, as well as possibly persisting or newly established microorganisms<sup>238</sup>.

### Interactions with microorganisms

The antimicrobial efficacy of the HCSCs primarily arises from their alkalization potential<sup>187,188</sup>. Against bacteria, three distinguished alkalinity-related mechanisms exist:

- Degradation of the bacterial phospholipid bilayer, resulting in the lysis of the bacterial cytoplasmic membrane via lipid peroxidation<sup>239</sup>.
- Direct damage to bacterial protein structure by breakdown of their ionic bonds<sup>239</sup>.
- Inhibition of bacterial DNA replication<sup>239,240</sup>.

The release of calcium hydroxide in the biological environment suggests that HCSCs exert their antibacterial effect through both direct and indirect contact. To date, there is a lack of standardized models for the investigation of the antimicrobial properties of HCSCs, but there seems to be evidence of limited and/or diminishing long-term antimicrobial capacity<sup>121</sup>. Absence of adequate antibacterial activity may result to biofilm formation by persisting or newly established bacteria between the filling material and the root canal walls leading to post-treatment apical periodontitis<sup>38</sup> even following endodontic surgery<sup>238</sup> (**Figure 6**). Dentinal and material surfaces may serve as footholds in this process for bacteria to attach and multiply<sup>241</sup>.

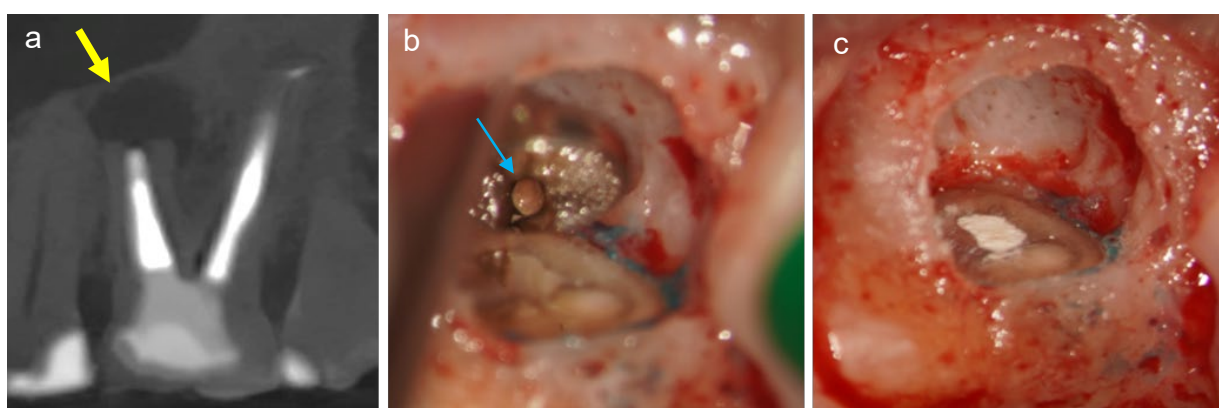


**Figure 6** Retreatment of root-end surgery of the mesiobuccal root of a maxillary left molar. (a) Preoperative sagittal view of cone-beam computed tomography showing periapical lesion on the mesial root (arrow). (b) During the removal of the root-end filling material, a dark area at the dentin/material interface (arrow) was observed, indicative of discoloration and possible biofilm presence (micro-mirror view). (c) After root-end cavity preparation, RRM fast set putty was placed. Courtesy Dr Thanos Fasoulas, Amsterdam, Netherlands.

## Interactions with dentin

Hydroxyl ions induce a highly caustic effect in the local microenvironment. In contact with dentin, this can result in the degradation of collagen components within the dentin matrix and the release of proteins from its structure, which can stimulate dental reactionary processes in cases of vital pulp therapy<sup>242</sup>. This interaction of the HCSCs with dentin, referred to as “*caustic etching*”<sup>243</sup>, leads to ionic precipitation from the cement and the formation of a zone rich in calcium and phosphorus at their interface<sup>244-247</sup>. A study demonstrated that this zone further infiltrated the intertubular dentin and formed an independent dentin layer adjacent to the HCSC, known as the “*mineral infiltration zone*”<sup>243</sup>. At the same time, these interactions do not seem to affect the highly mineralized peritubular dentin<sup>243</sup>. Interestingly, a subsequent study did not observe any ultrastructural or chemical changes on the dentin surface that could support the outcomes of an independent interfacial layer, except for a calcium phosphate gap-filling property at the interface<sup>248</sup>; another study did not conclude on the presence of such layer at the interface, as their findings appeared to depend on the observation technique<sup>249</sup>.

The role of dentin in the antimicrobial activity of the HCSCs is also intricate. From one aspect, dentin has a buffering capacity<sup>250,251</sup> that may hinder the antibacterial effect<sup>252,253</sup>. Conversely, other studies have found an enhancement of the antibacterial effect of endodontic materials in contact with dentin<sup>107,254</sup>. Dentin, through its complex anatomy, may be the recipient of the ions released from the adjacent materials and promote further cement dissolution particularly in the presence of an aqueous suspension, facilitating thus the antibacterial effect within the microenvironment via constant ionic release<sup>255</sup>.

## Interactions with blood and tissue fluids in general

The effect of HCSCs in the host tissues was discussed in the previous sections for each cement type independently with regard to their effect on cell viability, modulation of inflammation, osteogenic potential and overall induction of healing. As a general mechanism described in pulp capping, the initial release of calcium hydroxide from these cements induces a necrotic layer in nearby cells<sup>256</sup> through physico-chemical alterations

in the intracellular substance that lead to the rupture of glycoproteins and protein denaturation<sup>257</sup>. An inflammatory reaction in the tissues below that layer is also triggered. The release of biochemical markers recruits immune cells to the area, which clear the necrotic zone, along with stem cells that differentiate and induce tissue repair and regeneration<sup>258, 259</sup>. In addition, calcium ions may induce the secretion of mineralization-related genes and contribute to the formation of an intermediate zone below the zone of necrosis, consisting of calcium salts and calcium-protein complexes<sup>257</sup>.

The local microenvironment can in turn induce changes in the material characteristics<sup>237</sup>. Calcium released from the materials can react with free phosphates in the tissue fluids to form calcium phosphates, a phenomenon commonly referred to as “*bioactivity*” in the literature<sup>260-262</sup>. The nucleation and crystallization of the precipitated calcium phosphate towards carbonated apatite are regarded as the first necessary steps towards bonding to bone tissue<sup>263</sup>. The osteogenic potential of HCSCs has been in fact suggested to primarily result from the formation of this apatite layer upon the material surface<sup>245</sup>. However, the transformation of the initially formed amorphous calcium phosphate to apatite is not consistently documented<sup>246</sup>, possibly due to differences in the chemical composition of the in vitro immersion media. Additionally, the availability of free phosphates in the tissue is not abundant<sup>46</sup>. Therefore, the over simplified in vitro models assessing the apatite forming ability of HCSCs in phosphate-containing media cannot be indicative of the interactions within the living tissues<sup>264</sup>.

Instead, the cements’ chemical reactivity can be compromised due to the consumption of the released calcium hydroxide through its reaction with the carbon dioxide in the tissue fluid environment<sup>265</sup>. Inert calcium carbonate<sup>266</sup> can be therefore formed. The calcium carbonate precipitates onto the material surface and may block the pore channels throughout which calcium is leached<sup>267</sup>. Surface porosities can also become obstructed by tissue fluid proteins that adsorb onto the material surface, retarding the hydration reaction and resulting in cement expansion<sup>268</sup>. In MTA, blood and human serum exposure have been found to impair its surface characteristics and mechanical properties<sup>269-271</sup>, as well as its color stability<sup>272,273</sup>. The reduction of available hydroxyl ions in the environment can negatively affect the antibacterial properties of the cements, as demonstrated by the neutralization potential of blood in MTA<sup>191</sup>.

## 1.3 Exploring enhanced antibacterial properties with nanoparticles

In addition to the conflicting outcomes from laboratory studies, the moderating effect of the clinical environment on the antibacterial efficacy of HCSCs renders the enhancement of such properties worth exploring. The inclusion of antibacterial agents into HCSCs is a common approach. Recently, there has been growing attention towards incorporating nanoparticles due to a series of beneficial characteristics<sup>274</sup>.

Nanoparticles have dimensions that range between 1 and 100 nm. Their ultra-small size, increased surface area in proportion to their mass and volume, as well as their high charge density, are the main characteristics that enhance their chemical reactivity in comparison to their bulk form<sup>274,275</sup>. Nanoparticles can be categorized according to their shape (spheres, tubes, rods, etc.), their occurrence (natural or synthetic), and their chemistry (organic or inorganic)<sup>274</sup>. Moreover, the functionalization of nanoparticles using a core as a carrier of molecules or proteins provides further possibilities<sup>276,277</sup>. The specific physico-chemical characteristics of each form influence their antibacterial properties<sup>278</sup>.

### 1.3.1 *Silver nanoparticles in dentistry*

Silver is a relatively unreactive element and the least soluble in aqueous solutions from the Group 11 of the periodic table. This is explained by its electron configuration  $[\text{Kr}]4d^{10}5s^1$ . Specifically, the filled 4d orbital does not shield effectively the outer “s” shell from a strong nucleus attraction, rendering thus the element stable<sup>279</sup>. In the dental field, silver was historically used in dental amalgams in the 19<sup>th</sup> century, but amalgam has been gradually replaced by resin composites<sup>280</sup>. Lately, the progress achieved in nanoscience has enabled the enhancement of the antibacterial activity of silver and its usage in antimicrobial mechanisms. Inclusion of silver nanoparticles (SNPs) in dental materials has gathered significant research interest<sup>278,281</sup>.

Silver ions are found in bonds usually with sulfur, nitrogen, or oxygen. Their antibacterial effectiveness primarily arises from these bonds. SNPs have demonstrated



greater antibacterial potential than free silver ions, likely due to their reactive nature at the nanoscale<sup>282</sup>. Even though the antibacterial mechanisms of SNPs are still not fully understood, it seems that they mainly exert their antibacterial effects through the action of silver ions<sup>283</sup>. This is further facilitated by the nanoparticles' penetration of the bacterial cell wall and membrane and their ability to oxidize within the cells releasing silver ions<sup>284</sup>.

Specifically, interactions with sulfhydryl groups and nitrogen atoms in proteins and nucleic acids can significantly disrupt bacterial cell functionality at various stages of the cell's life cycle<sup>285</sup>. Silver ions adhere to the bacterial cell wall and the cytoplasmic membrane through electrostatic attraction<sup>286</sup> and affinity for sulfur proteins, impairing their permeability and even leading to their disruption<sup>286,287</sup>. Similarly, they can bind to bacterial DNA and disrupt its replication, as well as interact with the ribosome and inhibit protein synthesis<sup>288</sup>. Additionally, the high catalytic potential of SNPs generates reactive oxygen species that can damage bacterial protein function and destroy DNA<sup>289,290</sup> (**Figure 7**). While SNPs are effective against both aerobic and anaerobic bacteria, including Gram-negative and Gram-positive ones<sup>291,292</sup>, concerns exist about the concentration threshold above which cytotoxic events can be induced in osteoblasts<sup>291,293,294</sup>.

Another interesting aspect of incorporating SNPs in dental materials is to determine whether their antibacterial effect is solely induced through leaching or via direct contact with the modified material surface<sup>295</sup>. In a recent study, SNPs were shown to possess both a direct bactericidal effect as well as acting dispersed in the culture medium<sup>296</sup>. Studies from various disciplines have examined the effect on surface characteristics following the incorporation of SNPs. While this modification can result in a rougher surface profile, potentially increasing bacterial adhesion, it remains to be further elucidated whether this effect can be counteracted by the bactericidal effect of silver nanoparticles<sup>297</sup>.

SNPs have been applied in various dental disciplines, including prosthodontics, restorative dentistry, implantology, periodontics, orthodontics and endodontics<sup>278</sup>. They have been incorporated into acrylic resins used in dentures due to their antifungal properties, which can inhibit *C. albicans*-associated stomatitis, as well as their ability to deter bacterial adherence and colonization<sup>298-303</sup>. Similarly, SNPs have been utilized in resin composites<sup>304-306</sup> and dentin bonding systems<sup>296,297,307-311</sup> to prevent secondary

carries. Overall, the antibacterial effectiveness is concentration-dependent<sup>309</sup> and might be further enhanced with the addition of other antibacterial agents<sup>307,312</sup>. Incorporating SNP formulations into GICs improved their antibacterial effect, but also left their mechanical characteristics unaffected<sup>313</sup>, or even enhanced them in specific concentrations<sup>314-316</sup>. Moreover, SNP-coated orthodontic brackets demonstrated improved bacterial inhibition<sup>317</sup>. In implantology, coating titanium surfaces with SNPs has been explored alone<sup>291,294</sup> or in combination with nano-hydroxyapatite<sup>292,318,319</sup> to achieve a balance between bacterial inhibition and desirable biocompatibility.

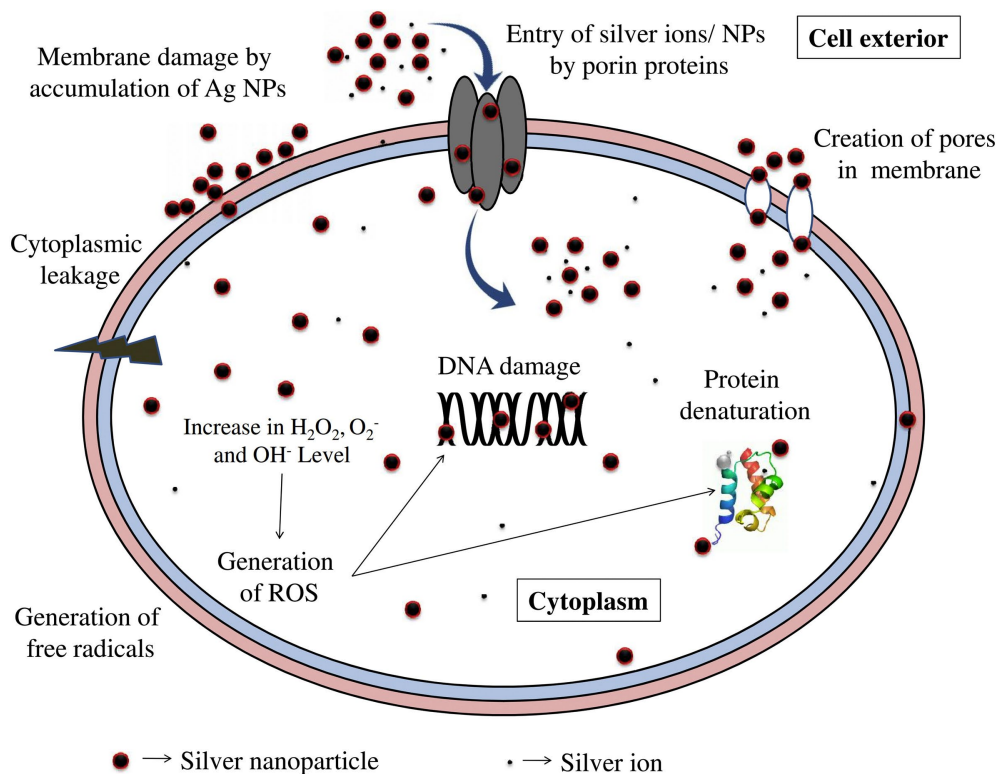


**Figure 7** Antibacterial mechanisms of silver nanoparticles. [Reproduced with permission from Pareek et al. 2018<sup>283</sup>]. NPs: nanoparticles; ROS: Reactive oxygen species.

### 1.3.1.1 Silver ions and silver nanoparticles in endodontics

In endodontics, the combination of the ability of SNPs to penetrate dentinal tubules<sup>320</sup> and the antibacterial activity of free silver ions against bacteria associated with endodontic

infections, such as *E. faecalis*<sup>321</sup>, has gathered interest in their use for root canal disinfection strategies. Incorporation of silver has been mainly explored in irrigation solutions, inter-appointment medicaments, and endodontic sealers. In terms of the efficacy of disinfecting the root canal, it appears that SNP-containing medicaments are more efficient than irrigation solutions<sup>322</sup>, due to their prolonged application period<sup>323</sup>. Notably, mixing calcium hydroxide powder with a SNP solution instead of saline enhanced its antibacterial effectiveness against *E. faecalis*<sup>323-325</sup>. SNPs have also demonstrated their antimicrobial efficacy when considered as medicaments in regenerative endodontic procedures<sup>326</sup>. Furthermore, the incorporation of SNPs in the molecular structure of mesoporous calcium silicate nanoparticles showed antibacterial potential as an intracanal disinfectant agent and relatively low cytotoxicity<sup>320</sup>.

Regarding their use as an irrigation solution, SNPs have exhibited potent antimicrobial efficacy, although they were found less effective than conventional solutions like 2.5% or 2% NaOCl<sup>322,327,328</sup>, with one exception reporting equal efficiency<sup>329</sup>. Comparisons with a lower NaOCl concentration (1%) yielded conflicting results<sup>327,330</sup>. However, it is important to consider the differences in chemical characteristics due to varied synthesis procedures for SNPs, as well as substantial variations in tested SNP concentrations and differences in methodology across all these studies. Furthermore, experimental irrigation solutions have demonstrated that coating SNPs with silica can enhance their long-term antimicrobial potential<sup>331</sup>. Compared to 2% chlorhexidine, different SNP solutions have shown an equal<sup>328,332</sup> or stronger antibacterial effect<sup>327</sup>. One study reported reduced potential at the five-minute application period but no significant difference at longer ones (15, 30 min)<sup>328</sup>. The combination of SNPs with chlorhexidine<sup>333</sup> and ethylene diamine tetraacetic acid<sup>334</sup> has been also investigated in experimental solutions showing enhanced and prolonged antibacterial properties<sup>333,334</sup>.

While there are currently no commercially available endodontic sealers containing SNPs, the use of micro-silver is reported in the Guttaflow 2 and Guttaflow Bioseal (Coltène/Whaledent, Altstätten, Switzerland). Detailed characterization of the materials that could provide information on the concentration and particle size of micro-silver is not available, while the Guttaflow 2 does not exhibit any discernible antimicrobial property<sup>335</sup>. In experimental formulations, the addition of silver in conjunction with calcium aluminate

has been assessed in a resin-modified MTA-based sealer, MTA Fillapex (Angelus, Londrina, Brazil). Interestingly, no leaching of silver ions was observed, while the surface modification of the material to a rougher profile resulted in higher bacterial adhesion<sup>336</sup>.

The incorporation of SNPs has been investigated in both commercial<sup>337-341</sup> and experimental endodontic sealers<sup>342-344</sup>, with experimental sealers mainly being resin-based and occasionally incorporating other nanoparticles as well, such as zinc oxide<sup>342</sup> or calcium phosphate<sup>344</sup>. These studies explored different concentrations aiming to optimize the antibacterial efficacy while preserving their physical properties.

Few studies have investigated the effect of incorporation of SNPs in HCSCs, by mainly testing MTA<sup>345-352</sup>, while one of them explored an experimental material with 70% Portland cement and 30% zirconium oxide<sup>352</sup>. Apart from some independent primary screening of antibacterial effectiveness or cytocompatibility in these studies, two of them additionally assessed radiopacity<sup>351,352</sup>, while one assessed the compressive strength, solubility and pH showing favorable results towards incorporation of SNPs<sup>352</sup>.

## **1.4 The use of bioactive glass as an alternative approach to modify HCSCs**

Adopting an alternative strategy, incorporating compounds with effective adaptation to dentin while promoting favorable ionic release for antimicrobial efficacy and periodontal tissue healing could enhance the overall biological profile of HCSCs for endodontic surgery. Bioactive glass (BG) could be considered a potential candidate for this purpose.

Bioactive glasses are calcium sodium phosphosilicates and represent the first materials introduced in medicine that could bond to the host tissue<sup>353</sup>. They were initially developed in 1969 by Dr Hench at the University of Florida as part of a project funded by the US Army, aimed at creating orthopedic implant materials capable of integrating with human tissues<sup>353</sup>. The original composition, known as BG 45S5, comprises 45% silicon dioxide, 24.5% calcium oxide, 24.5% sodium oxide and 6% diphosphorus pentoxide<sup>353</sup>. Since then, various types of BG have been formulated, differing primarily in glass structure, composition, manufacturing process, and particle size<sup>354</sup>.

### 1.4.1 Mechanism of biological activity

Bioactive glass consists of a silicon oxide matrix, which is disrupted by calcium and sodium ions. When exposed to an aqueous environment, bioactive glass dissolves<sup>355</sup>, resulting in a dose-dependent increase in pH<sup>356, 357</sup>. The solubility of the material is closely related to the degree of interconnectivity between the elements in its structure (i.e., network connectivity), affecting the release of sodium and calcium ions<sup>358</sup>.

When bioactive glass interacts with the phosphate-containing bone tissue, it forms a carbonated apatite layer on its surface. This layer establishes a chemical bond with the collagen fibrils of the bone<sup>353</sup>. Initially, exposure to an aqueous environment causes a rapid release of  $\text{Na}^+$  and  $\text{Ca}^{2+}$  in exchange for  $\text{H}^+$ , leading to a pH increase and disruption of the Si-O-Si network. This process finally results in the condensation and re-polymerization of a Si-O<sub>2</sub>-rich layer (**Figure 8 a, b**). The migration of  $\text{Ca}^{2+}$  and  $\text{PO}_4^{3-}$  on the BG surface leads to the formation of an initial amorphous calcium phosphate layer, which later crystallizes in the presence of  $\text{CO}_3^-$ ,  $\text{OH}^-$  and  $\text{F}^-$ . This structure provides a substrate for the adsorption of growth factors and the attachment, proliferation, and differentiation of osteoprogenitor cells<sup>353</sup> (**Figure 8c**). Consequently, a chemical bond forms with the surrounding bone tissue as it becomes incorporated into the developing collagen-apatite matrix and glycoproteins<sup>359</sup> (**Figure 8d**).

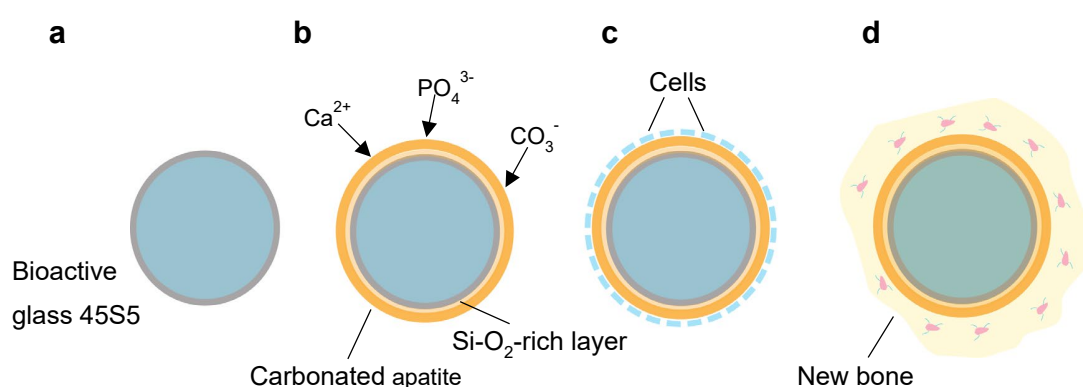


**Figure 8** Reaction stages of (a) bioactive glass 45S5. (b) Precipitation of ions upon the silica-rich layer leads to the formation of carbonated apatite. (c) Colonization of the surface by bone-forming cells. (d) Crystallization of the bone-like matrix towards bone formation.

According to another approach, BG can be viewed as an inorganic matrix of oxygen that is interrupted by silicon atoms<sup>360</sup>. Its reactivity is thus believed to be contingent on the crosslink connections between silicon atoms and oxygen within the polymer network<sup>360</sup>.

The antibacterial efficacy of BGs is dose-dependent<sup>356</sup>, while it appears to be significantly influenced by the specific BG-composition<sup>354,361</sup>. The main antibacterial factor associated with BG is its alkalization potential<sup>361</sup>. The dissolution products of BG can penetrate the cell membrane, leading to an increase in intracellular pH, ultimately resulting in bacterial death. While the mechanism regarding the pH increase and bacterial contact-killing is well-established, some studies have suggested that an increase in osmotic pressure, stemming from the ionic release of BG<sup>274,362</sup>, may also contribute to its antibacterial activity. However, the antibacterial role of osmolarity in BGs has been questioned by other studies<sup>361,363</sup>.

Similar with the HCSCs, there is evidence of a decline in the antibacterial activity due to the buffering effect of body fluids on the alkalization potential<sup>364,365</sup>. However, studies have demonstrated an increased antibacterial potential of BG when it comes into contact with dentin and bone powder, possibly due to the elevated silica release triggered by these substrates in conjunction with elevated pH levels<sup>366-368</sup>.

### 1.4.2 Applications of BG in endodontics

Today, BGs serve as bone grafts and regeneration materials in medicine. In dentistry, they are used for implant coatings and dentin hypersensitivity treatment<sup>369</sup>. In restorative dentistry, they have been investigated for use in resin composites<sup>370</sup>, bonding agents<sup>371</sup>, as well as GICs<sup>372,373</sup> in order to enhance mineralization and inhibit collagen degradation<sup>374</sup>. Formation of mineral tags in the dentin/material interface has also been demonstrated to increase micro-mechanical properties and reduce permeability<sup>375,376</sup>.

In endodontics, BGs were initially explored as intracanal medicaments, with their antibacterial capacity mainly assessed against *E. faecalis*<sup>377-380</sup> and, to a lesser extent, other bacteria<sup>368</sup> or fungi<sup>381</sup>. Controversial findings exist regarding the efficacy of BGs against *E. faecalis*, especially in comparison to calcium hydroxide pastes<sup>368,378-380</sup>. These

discrepancies may be attributed to variations in methodological protocols, strain susceptibility, and BG composition<sup>380</sup>. Additionally, BG showed a lower inhibition effect compared to 1% and 2% chlorhexidine medicaments<sup>379,382</sup>. In terms of biocompatibility, subcutaneous implantation in rats' tissues revealed a mild inflammation in the host tissues within 30 days that was similar to the negative control group, and superior mineralization induction compared to a calcium hydroxide paste<sup>380</sup>. Furthermore, dentin treatment with BG resulted in enhanced microhardness compared to calcium hydroxide medicaments, showing good potential for longer-term applications such as apexification and regenerative procedures<sup>383</sup>.

BG fillers were included in Resilon™, a thermoplastic polymer material introduced in 2004 as an alternative to gutta-percha for root canal filling<sup>384,385</sup>. This system included a methacrylate in order to create a “*monoblock*” structure with Resilon™, resin sealer, bonding agent, and dentin<sup>386</sup>. Despite initial positive evidence from ex vivo and animal studies<sup>387-389</sup>, Resilon™ was withdrawn from the market in 2014<sup>390</sup>. A retrospective analysis revealed a 5.7 times higher failure rate associated with its use<sup>390</sup>. Limited information is available on the exact concentration and role of BG in the polymer matrix.

Following the concept of introducing a filling material that could create a “*monoblock*” with the surrounding dentin in the root canal system, an experimental material was developed and later commercialized as Bio-Gutta (Smartodont llc, Zurich, Switzerland)<sup>391-393</sup>. Bio-Gutta comprises a mixture of trans-1.4-polyisoprene, zinc oxide, nanometric BG 45S5 particles and softener<sup>391</sup>. The rationale behind this material is to substitute certain components of the conventional gutta-percha while incorporating BG as a reactive component, aiming for improved adaptation with the dentinal wall even without the need for an endodontic sealer. After initial in vitro bioactivity testing, the formation of calcium phosphate deposits was observed upon the material surface<sup>391,393</sup>. Interestingly, the hydroxyapatite crystals formed more rapidly and to a greater extent compared to a similar experimental material containing polycaprolactone as a composite, even though the BG nanoparticles being embedded in the polyisoprene matrix<sup>391</sup>. Another noteworthy aspect of this material is the reported increase in mass loss, which was positively correlated to the amount of BG-incorporation, possibly due to the ion leaching. The mass loss is supposedly compensated by the hydroxyapatite formation<sup>391</sup>. During an eight-day

evaluation period, the material exhibited a progressively increasing self-adherence within root canals, surpassing the performance of conventional gutta-percha<sup>393</sup>. These findings are attributed to the hydrophilicity of BG, which leads to particle expansion and improved material adaptation to canal walls<sup>393</sup>.

BG is also included in commercial endodontic sealers and experimental formulations. One such product is Guttaflow Bioseal, which comprises gutta-percha powder, polydimethylsiloxane, platinum catalyst, zirconium dioxide, silver, coloring and bioactive glass-ceramic. Scanning electron microscopy revealed that BG particles are within the size range of 20-40  $\mu\text{m}$ , both in its bulk composition and on its surface<sup>394</sup>. Studies have generally demonstrated acceptable cytocompatibility scores<sup>395-397</sup> and its potential to induce cementoblastic differentiation in vitro<sup>397</sup>. Its biocompatibility was further confirmed through subcutaneous implantation experiments in rats, showing an acceptable degree of inflammation, which gradually decreased over a 30-day evaluation period<sup>398</sup>. In terms of the antibacterial potential of Guttaflow Bioseal, one study reported negligible efficacy one day after immersion in phosphate buffered saline that, however, increased significantly over time after seven and particularly at 28 days aged samples<sup>399</sup>. The immersion medium could have possibly facilitated surface reactions of the material over time. In another study, the antibacterial effect of Guttaflow Bioseal within infected dentinal tubules was found to be similar to some HCSC sealers<sup>400</sup>. Inconsistent bacterial killing effects were observed across various biofilms for material exposures ranging from six days to long-term periods (30, 60 days)<sup>400</sup>.

Another BG-containing formulation is NISHIKA Canal Sealer BG (Nippon Shika Yakuhin, Yamaguchi, Japan)<sup>401</sup>, a two-paste system. One paste contains fatty acid, bismuth subcarbonate and silicon dioxide, while the other paste consists of magnesium oxide, purified water, calcium silicate glass, silicon dioxide, and other components<sup>402</sup>. A similar BG-containing pulp capping material (NSY-222-S) has been tested but not launched by the company. The main apparent difference is the substitution of magnesium oxide with calcium oxide in the second paste<sup>402</sup>. Formation of hydroxyapatite crystals have been reported upon the surface of NISHIKA following immersion in a simulated body fluid<sup>403</sup>. Additionally, the cement did not impair the in vitro assessed cell viability or even enhanced it<sup>403</sup>, while it was also found to induce an osteogenic potential<sup>404</sup>. In fact,



NISHIKA and NSY-222-S demonstrated overall similar levels of cytocompatibility when compared to MTA, and they reported better values than calcium hydroxide<sup>402</sup>. Additionally, these materials showed the potential for reparative dentin formation following direct pulp capping in rat teeth<sup>402</sup>. On the other hand, fresh NISHIKA samples appear to have a cytotoxic potential<sup>405</sup>. Recently, another calcium silicate glass from the same company, NSY-224, was tested with the addition of BG-based powder in different consistencies aiming to develop a root-end filling material<sup>406</sup>. The 60% BG-addition induced mild inflammation in mouse tissue upon subcutaneous inflammation, while presenting favorable physico-chemical characteristics and in vitro cytocompatibility values similar to MTA<sup>406</sup>.

Other experimental formulations incorporating BG materials have also been investigated<sup>407</sup>, demonstrating their apatite-forming ability along with favorable physical characteristics<sup>408</sup>, but also a relatively high weight loss that renders further research<sup>409</sup>. The incorporation of different types of BG into an epoxy resin-based commercial sealer, for instance, resulted in varying degrees of enhancement in antibacterial effectiveness in vitro, depending on the specific BG formulations tested<sup>410</sup>. Meanwhile, their application in infected dog teeth showed successful healing induction, with no significant differences compared to the control material<sup>410</sup>.

The osteogenic potential of BG led to investigation for its use in forming a dentin-like bridge over the exposed pulp. Various BG formulations have been explored in this regard in vitro<sup>411</sup> and in animal studies<sup>412,413</sup>, yielding findings that support further investigation toward their use as pulp capping agents. Following pulpotomies in rat teeth with BG, acute inflammation was evident at two weeks, which subsided within four weeks<sup>414</sup>. MTA exhibited better overall performance in reducing inflammation and promoting dentine-like bridge formation<sup>414</sup>. Conversely, in another rat study, BG demonstrated similar results to MTA in terms of dentin-like formation and inflammation reduction<sup>415</sup>. These findings align with those of a human clinical study<sup>416</sup>.

In some in vitro studies, micro- and nano- sized BG particles were investigated for their impact on human dental pulp cells, particularly in terms of mineralization potential and odontogenic protein expression. The results demonstrated odontogenic differentiation

and dentin formation, especially in the nanoparticle group, possibly due to its larger surface area and greater number of bonding sites, exhibiting a faster and more substantial release of ions<sup>417,418</sup>. Another study investigated different BG-compositions and correlated their ionic release to cellular responses towards the most desirable odontogenic effect<sup>419</sup>.

#### 1.4.2.1 Experimental materials with inclusion of BG in HCSCs

Few studies have explored the incorporation of BG in HCSCs. In Biodentine, BG, whether alone<sup>420</sup> or in formulations containing strontium or fluoride<sup>421</sup>, demonstrated accelerated in vitro apatite formation<sup>420</sup>. Furthermore, the addition of BG nanoparticles improved certain physical properties of Biodentine<sup>422</sup>. However, in an experimental Portland cement-based cement, the inclusion of BG 45S5 at 10%, 20%, and 30% increased the material's solubility<sup>423</sup>. In another study, the incorporation of a phosphate-free BG, similar to BG 45S5, into MTA resulted in an overall unaltered tissue response in rat connective tissue upon subcutaneous implantation<sup>424</sup>. Addition of 20% Biosilicate, which is another BG formulation, to an experimental HCSC resulted in complete killing of planktonic *E. faecalis* in a direct contact test, in contrast to the unmodified cement, while it did not compromise the cement's impact on cell viability or its physico-chemical properties<sup>425</sup>. An experimental HCSC sealer containing different concentrations of BG nanoparticles was also tested recently in vitro, showing an enhanced osteogenic profile, while maintaining the antibacterial efficacy of the HCSC<sup>426</sup>.

### 1.5 Current status of HCSCs for endodontic surgery and gaps in knowledge

While hydraulic calcium silicate cements were originally developed for applications in endodontic surgery, there is still relatively sparse scientific data on their testing with the rationale for use in such procedures, especially within the context of the evaluation of their antibacterial properties. Assessment of HCSCs for their use for pulp protection or regenerative endodontic procedures is, to this day, predominant<sup>121</sup>.

Modifications to the composition of HCSCs could potentially enhance specific material properties. Silver nanoparticles and bioactive glass show promise in improving the antibacterial activity of HCSCs throughout different mechanisms<sup>274</sup>. While SNPs inherently act as antibacterial agents, BG could both contribute to the antibacterial efficacy of HCSCs while also promoting a more balanced biological profile due to their established osteogenic properties<sup>353</sup>. At the same time, it is crucial that such modifications do not compromise the existing beneficial characteristics of HCSCs. Therefore, a comprehensive evaluation of the changes in the material's physico-chemical profile and biological activity is necessary if these modifications are to be explored. Understanding the connections between the physical (e.g., surface) and chemical (e.g., leachate) properties of these materials and their biological reactivity is also important. In addition, valuable insights into the combined effect of modifications of HCSCs on their physico-chemical characteristics and associated antibacterial properties can be gained by studying commercially available types 4 and 5 HCSCs in comparison to a conventional radiopacified HCSC that includes no chemical additives in its synthesis.

Furthermore, the interactive nature of HCSCs, which depends on the specific procedure they are used for, is often disregarded in laboratory studies, while evidence suggests that the clinical environment could potentially decrease their antibacterial efficacy. Despite the inherent limitations of *in vitro* investigations in accurately representing the clinical scenario, adjusting certain experimental parameters could still allow for more clinically relevant extrapolation of results. Testing of HCSCs could thus be conducted in light of their interactions with the specific clinical environment they are placed in. In the case of endodontic surgery, as outlined in Section 1.2.1.3, these interactions include tissue fluids from the periradicular region, dentin and possibly persisting microorganisms.



## 2. Aims and Objectives

The main aim of the thesis was to assess the effect of incorporation of bioactive glass and silver nanoparticles on the antibacterial properties and cytotoxicity of experimental hydraulic calcium silicate cements, along with associated changes in physico-chemical characteristics. Additionally, the effect of environmental factors on their properties was monitored in relation to this aspect.

### Hypotheses

The overall null hypotheses were that modifications of the composition of HCSCs and variations in environmental conditions would not exert any influence on the physical, chemical, and biological properties (antibacterial effect and cytotoxicity) of the cements, and that cements will not contribute to any antibacterial potential on dentin.

### Specific objectives

- Examine the surface characteristics alongside bacterial adhesion of experimental HCSCs with or without the incorporation of SNPs or BG and commercial materials (**Study I**), as well as their leaching properties in conjunction with the indirect contact antibacterial effect (**Study II**).
- Assess the role of environmental conditions (immersion medium and aging period) on the physical characteristics (**Study I**), chemical properties (**Study II**), and associated antibacterial effect and cytotoxicity (**Studies I & II**) of HCSCs.
- Evaluate the antibacterial properties of the experimental HCSCs and commercial materials in contact with dentin (**Study III**).



## 3. Methodological Aspects

The following section provides insights into the material selection and the rationale for the methods used. A detailed description on the materials and methods is presented in the three published studies. Herein, the selection of the test materials and the methods used are critically discussed in light of their suitability for addressing the research aims set.

### 3.1 Material selection

#### 3.1.1 *Basic experimental formulation*

A basic experimental formulation (TZ-base) was consistently used throughout all three studies, comprising:

- 80% w/w tricalcium silicate cement (CAS No: 12168–85-3, American Elements, Los Angeles, CA, USA) (**Figure 9a**);
- 20% w/w zirconium oxide (ZO; Koch-Light Laboratories, Colnbrook, Bucks, UK).

The cementitious phase of types 4 and 5 HCSCs consists of pure tricalcium and dicalcium silicates<sup>49</sup>. At the same time, in the current basic experimental formulation, no additives were introduced that could potentially alter the material properties, such as setting accelerators, modifiers of the hydration reaction, antibacterial agents or other fillers. This approach therefore assisted not only in identifying the effect of incorporation of SNPs and BG in the experimental cements but also assessing the role of additives in the properties of the commercial materials that were screened in parallel.

Zirconium oxide was included in the formulation, serving as a radiopacifier. Due to its successful application in other commercial dental materials<sup>427</sup>, it was initially proposed as a substitute for bismuth oxide in MTA, yielding adequate results<sup>428,429</sup>. A later study confirmed no adverse effects on the material's physical properties<sup>430</sup>. It is a cytocompatible filler agent<sup>431</sup> that is used in several commercial HCSCs either on its own<sup>209</sup> or in combination with other radiopacifiers<sup>231</sup>. Compliance with the radiopacity specifications

outlined in the International Organization for Standardization (ISO) 6876:2012<sup>432</sup> for the specific concentration used here (20% w/w) was evaluated.

### 3.1.2 *Silver nanoparticle-containing cements*

Silver nanoparticles were considered as candidates for improving the antibacterial properties of HCSCs due to their bactericidal effect and evidence of their potential to penetrate dentinal tubules, which are properties that could fit well in materials for endodontic surgery<sup>320</sup>. Initially (**Studies I & II**), three different SNP concentrations were tested as additions to the HCSC (0.5, 1, 2 mg/ml SNP: TZ-Ag0.5, TZ-Ag1, TZ-Ag2 respectively). The material with the lowest SNP-concentration was excluded from **Study III** due to its non-significant effect on the antibacterial properties of the cements in the first two studies (**Table 2**).

SNPs were added in the material through the liquid vehicle. This method enabled the adequate dispersion of potentially agglomerated particles prior to their inclusion in the cement. Silver nanopowder (CAS No: 7440-22-4, <100 nm particle size, Merck KGaA, Darmstadt, Germany) (**Figure 9b**) was dispersed into ultrapure water (water; Elix Essential 5 UV Water Purification System, Merck KGaA, Darmstadt, Germany) according to the NANOGENOTOX dispersion protocol<sup>433</sup> with slight modifications. Notably, the protocol recommends the dispersion of nanoparticles in 1% w/v bovine serum albumin water. The use of bovine serum albumin as a dispersant in the water solution was deemed unnecessary, as the SNP formulation used here already contains polyvinylpyrrolidone, a synthetic polymer that serves this role<sup>434</sup>. Additionally, mixing the HCSC with a serum-containing medium could potentially introduce changes in their hydration reaction, which would require further investigation, but this falls beyond the scope of the thesis.

The selection of the SNP-concentrations used in the current studies was also guided by the dispersion protocol<sup>433</sup>. The initially dispersed solution was adjusted to 2 mg/ml SNPs to facilitate further dilution into two rounded lower concentrations (1 and 0.5 mg/ml). All experimental cements were mixed at a 0.35 liquid/powder ratio, and thus the amount of SNPs in the three cements per 1 g of HCSC powder was 0.175, 0.35 and 0.7 mg for



TZ-Ag0.5, TZ-Ag1, and TZ-Ag2 respectively. While varying SNP concentrations have been implemented in HCSCs in the literature<sup>347,352</sup>, it is important to note that SNP reactivity depends on the specific physico-chemical characteristics of each formulation<sup>293</sup>, rendering direct comparisons between different concentrations unfeasible.

**Table 2** Presentation of test materials per study. BG: Bioactive glass; HCSC: hydraulic calcium silicate cement; IRM: Intermediate restorative material; RRM: Root repair material; SNP: Silver nanoparticle; TZ-base: basic experimental formulation; ZOE: Zinc oxide/eugenol.

Study	Experimental HCSCs			Commercial HCSCs	ZOE-based	
	TZ-base	SNPs addition	BG-replacement	Biodentine	RRM putty	IRM
I	✓	0.5, 1, 2 mg/ml	10, 20%	✓	–	✓
II	✓	0.5, 1, 2 mg/ml	10, 20%	✓	–	✓
III	✓	1, 2 mg/ml	20, 40%	✓	✓	✓

### 3.1.3 Bioactive glass-containing cements

The beneficial properties of bioactive glass (BG), including its antibacterial potential combined with the apatite-forming ability and good adaptation to hard tissues would seem advantageous for materials used in endodontic surgery. Herein, we investigated potential alterations in the physico-chemical profile of the cements and any associated changes in their antibacterial properties and cytotoxicity upon incorporation of BG into the HCSCs. BG 45S5 micro-particles (Cas No: 65997–17-3, 10 µm particle size, Mo-Sci Corporation, Rolla, MO, USA) (**Figure 9c**) were incorporated into the material formulation by replacing a portion of the tricalcium silicate cement by weight. In **Studies I & II**, the effect of 10%

and 20% BG-replacement in the cement (TZ-bg10, TZ-bg20 respectively) was explored. These concentrations were selected based on previous research in the field, which showed potential enhancement of antibacterial efficacy with 20% BG incorporation, albeit using a different type of BG (Biosilicate)<sup>425</sup>. Consequently, in **Study III**, TZ-bg10 was not included in the investigation as it did not significantly alter the previously studied characteristics. Properties of the experimental HCSC with 40% BG-replacement (TZ-bg40) were therefore screened to further explore the pattern of the impact of BG-replacement in tricalcium silicate cement (**Table 2**).

The original synthesis BG 45S5 (**Figure 9c**) was used here. These compounds are well-characterized and have demonstrated a superior chemical profile compared to other BG formulations<sup>407</sup>. Furthermore, they share similar characteristics with BG particles that have been previously integrated into a commercial endodontic sealer<sup>394,397</sup>.

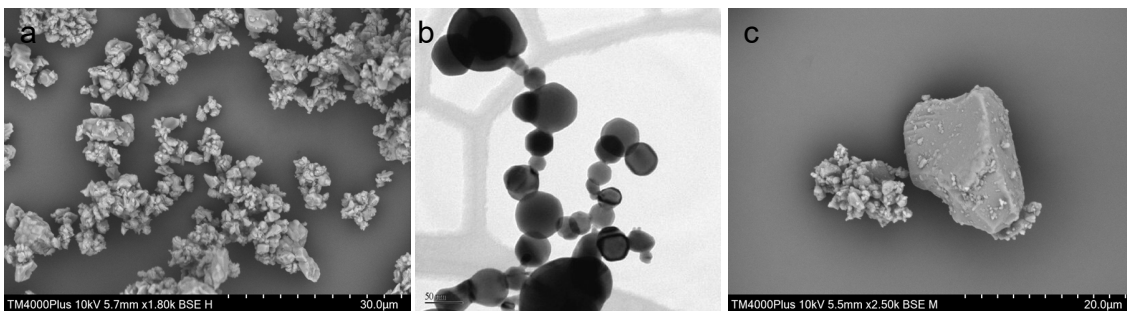


**Figure 9** Presentation of compounds used in the experimental formulations. (a) Scanning electron microscope image of tricalcium silicate cement powder. (b) Transmission electron microscope image of silver nanoparticles (reproduced with permission from Merck KGaA, Darmstadt, Germany). (c) Scanning electron microscope image of bioactive glass 45S5.

### 3.1.4 Commercial HCSCs

Biodentine was used as a commercial control material in all studies (**Table 2**), due to its chemical resemblance with the basic experimental formulation (TZ-base), while being an extensively researched cement<sup>435</sup>. Biodentine shares a similar calcium silicate concentration as TZ-base (80%), although it contains a substantially lower amount of

zirconium oxide (5%)<sup>207</sup>. In addition to serving as a control material, comparing Biodentine and TZ-base provided insights into how additives during the synthesis of Biodentine might influence its physico-chemical characteristics and antibacterial properties.

The RRM putty was additionally included in **Study III**, as a representative material of the type 5 HCSCs (**Table 2**). As previously pointed out, the antibacterial testing of these materials with the rationale of use in endodontic surgery is rather limited<sup>121</sup>.

At the same time, including a commercial MTA cement in our studies would have been relevant, but this material category has fewer chemical similarities with the experimental cements than types 4 and 5 HCSCs. MTA consists of a Portland cement phase instead of pure calcium silicates, while it contains bismuth oxide<sup>125</sup> (or calcium tungstate in some recent versions<sup>145</sup>) as a radiopacifier, rather than zirconium oxide.

### 3.1.5 *IRM*

The use of IRM in all studies served as a control material (**Table 2**) in order to better explore the effect of environmental conditions on materials of different chemical composition and same clinical use. IRM is an extensively studied cement that is widely utilized in endodontic surgery, with a success rate comparable to that of MTA<sup>111,114</sup>.

## 3.2 **Assessment of environmental conditions**

An overview of the different variables assessed in each study is provided in **Table 3**.

### 3.2.1 *The effect of immersion medium (Studies I & II)*

To evaluate the potential influence of the environment on the properties of HCSCs, the materials were immersed to either water or fetal bovine serum (FBS; F7524, Merck KGaA, Darmstadt, Germany) before testing. Water is vastly used as an immersion medium for HCSC assessment<sup>187</sup> as it offers easily standardized conditions. However, cement aging in a state devoid of any organic or inorganic substances does not accurately replicate the

complexity of the clinical environment<sup>436</sup>. Simulated body fluid solutions and other commercial media, such as Hank’s balanced salt solution, have been utilized as more physiologically relevant than water<sup>437</sup>, due to their ionic composition resembling that of the human serum<sup>438</sup>. These media lack the protein components, and implement additional buffering agents. Additionally, their carbonate content is not controlled<sup>264</sup>. The use of a protein-rich medium here (i.e. FBS) was intended to better simulate the interactions that occur between the cements and host tissue fluids<sup>439</sup>. FBS is frequently used in in vitro studies because of its similar biochemical composition to human serum, containing mainly proteins, amino acids, inorganic salts, carbohydrates, hormones, vitamins, growth factors and lipids, while it also exhibits buffering capacity<sup>440</sup>. It was used here instead of other clinically relevant fluids for ease of procurement.

Antibacterial properties following contact with clinically relevant fluids have not been thoroughly explored. A previous study evaluated the antibacterial activity of MTA when exposed to blood and heparin in a direct contact assay or a dentin infection model<sup>191</sup>. Nonetheless, no studies are available for other HCSCs or concerning the antibacterial properties of their leachate when exposed to a serum-containing environment.

**Table 3** Overview of the parameters investigated per study. HCSC; Hydraulic calcium silicate cement.

Study	<i>Parameters assessed</i>			
	<i>Incorporations in HCSCs</i>	<i>Immersion medium</i>	<i>Aging period</i>	<i>Dentin models</i>
I	✓	✓	✓	-
II	✓	✓	✓	-
III	✓	-	✓	✓

### 3.2.2 *The effect of aging period (Studies I, II & III)*

Cements were assessed at various time intervals to monitor potential changes in their properties as the hydration reaction progressed, until the HCSCs reached their maximum physical attributes at the 28-day mark<sup>124</sup>. Material samples were primarily evaluated after one- and 28- day aging periods, as the emphasis was on comparing the physico-chemical characteristics and biological properties between fresh and aged specimens. In **Studies I & II**, materials were also tested at seven days as an intermediate period. In the case of leachate chemical characterization (**Study II**), samples were additionally assessed in some occasions at 14 and 21 days (**Table 4**). This approach enabled tracking of potential plateaus in calcium hydroxide release and the impact of the refreshment of the immersion medium on leaching by preventing solution buffering.

In **Studies I & II**, materials were allowed to set for 24 hours in a humid environment prior immersion to the aging medium (**Figure 10a**), as this facilitated their handling and is commonly performed in similar investigations<sup>226,441</sup>. In **Study II**, biological assays were also conducted using the extract medium collected immediately after material placement, mimicking a more clinically relevant scenario, as by-product release began as soon as the materials were compacted onto the cell culture inserts (**Figure 10b**). At the same time, the surface area/volume ratio was kept the same between the two extraction methods, allowing for comparisons of results.

In **Study II**, an additional parameter concerning specimen aging was introduced, by either replenishing the medium weekly or maintaining the same medium throughout the 28-day period (**Table 4**). Laboratory aging conditions inherently have limitations in replicating the clinical situation. In clinical settings, continuous leachate renewal occurs through blood circulation and tissue fluid drainage; assessing, therefore, cement extracts in a closed environment could potentially lead to an overestimation of their impact<sup>121</sup>. Taking another approach, the periodic in vitro extract-refreshment conditions also do not replicate the clinical scenario accurately, as constant blood supply provides a continuous renewal of tissue fluids<sup>442</sup>. Consequently, the complexity of in vivo conditions suggests that results obtained from laboratory studies, such as the present one on long-term leachate properties, can only be extrapolated within the context of the specific testing

conditions used. The implementation of the two different protocols for leachate refreshment, or lack thereof, aimed to underscore this discrepancy.

**Table 4** Presentation of sample aging conditions per assay in **Studies I & II**.

Study	Tests Performed	Material aging conditions prior testing		
		Weekly medium change	No medium change	Cell culture insert system
<b>Surfaces</b> <b>(Study I)</b>	<i>Analysis of surface characteristics</i> (material photography, surface roughness, microscopy, wettability, microhardness)	7, 28 days	1 day	–
	<i>Bacterial adhesion</i>			
<b>Leachates</b> <b>(Study II)</b>	<i>Chemical characterization</i> (pH, Ca <sup>2+</sup> release)	7, 14, 21, 28 days	1, 7, 28 days	–
	<i>Biological assays</i> (antibacterial, cytotoxicity)	7, 28 days	1, 7, 28 days	24 hours
	<i>Cement bulk characterization</i> (microscopy)	–	28 days	–

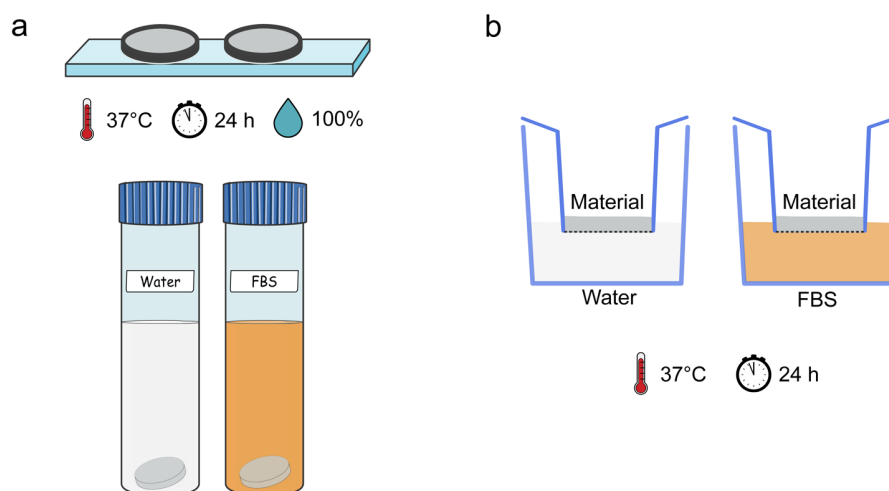


**Figure 10** Schematic representation of (a) main sample preparation for **Studies I & II**, and (b) the additional leachate preparation method for **Study II** during the first 24 hours immediately after material placement. The figure was partially generated by using pictures from Servier Medical Art, provided by Servier, licensed under a Creative Commons Attribution 3.0 unported license. FBS: Fetal bovine serum; Water: Ultrapure water.

In **Study III**, the dentin segments were evaluated 24 hours after material placement or following a 28-day aging period in Hank's balanced salt solution (HBSS; H6648, Merck KGaA, Darmstadt, Germany) before testing. Immersing the dentin segments in HBSS for fresh specimens was not considered necessary as the aim was to assess their antibacterial activity at an early time point. For the 28-day specimens, HBSS was used to prevent any interaction between the material surface and atmospheric carbon dioxide, which could potentially introduce artifacts in material characteristics<sup>443</sup>. Additionally, HBSS was preferred here because its inorganic ionic composition resembles that of human blood plasma, making it relevant for such investigations<sup>444</sup>, while also maintaining a controlled environment to ensure reproducible assessment of cement properties.

### 3.2.3 Interaction with dentin (**Study III**)

In **Study III**, ex vivo models were implemented to provide deeper insights into the antibacterial characteristics of the dentin/material interface. This investigation was

prompted by the conflicting results in the literature regarding the impact of dentin on the antibacterial characteristics of root filling materials and the lack of *ex vivo* models to assess antibacterial properties, as discussed in Section 1.2.1.3. Unlike the approach used in the first two studies, where the effect of environmental conditions was assessed by exposing the cements to two different media, **Study III** took a different perspective. Instead of assessing materials after contact or without contact with dentin, we primarily examined the interactions with dentin by independently testing dentin and material surfaces that have previously been in contact, as well as the intact dentin/material interfaces. The results across the different assays and evaluation periods were combined to comprehensively evaluate the material/dentin interactions and assess whether an antibacterial effect would be conferred on the dentin substrate.

### **3.3 Antibacterial evaluation (Studies I, II & III)**

Dentinal and material surfaces may serve as substrates for initial bacterial attachment and further biofilm formation, causing apical periodontitis<sup>241</sup>. The materials play a crucial role in preventing bacteria from accessing nutrients that can enable them to proliferate and cause infection. Their morphological characteristics and leachable components define their antibacterial profile<sup>445</sup>.

The investigations of the antibacterial properties of the materials were designed in order to assess the activity of the respective surfaces (**Study I**) and leachates (**Study II**), and the interaction with dentin (**Study III**).

#### **3.3.1 Selection of bacteria**

*Enterococcus faecalis*, a Gram-positive bacterium, was consistently examined in all studies. Its selection was based on its relevance, as it is commonly isolated from failed endodontic cases<sup>446-448</sup>, although it is no longer regarded as the primary pathogenic species in post-treatment apical periodontitis<sup>449</sup>. Furthermore, it exhibits rapid growth and is quite resilient in laboratory conditions<sup>450</sup>. These characteristics render it the most



extensively researched bacterium in endodontic literature<sup>449</sup>, and its use here additionally allowed for potential comparisons with other studies.

The strain of *E. faecalis* that was used in the current studies (OG1RF) was kindly provided as a gift<sup>451</sup> and is in fact not relevant to refractory endodontic cases *per se*. However, it has been utilized in previous endodontic research and compared to other clinically relevant strains<sup>452,453</sup>. The use of the specific strain was favored because it expresses the green-fluorescent protein as a result of a genetic modification, which enabled us minimize excessive sample manipulation and potential staining interference during the imaging process in **Study I** with fluorescence. To maintain consistency, the same strain was used in all studies.

Antibacterial investigations in **Studies II & III** were further complemented by the inclusion of *Pseudomonas aeruginosa*, a Gram-negative bacterium that has also been isolated from persistent endodontic infections<sup>448</sup>. The parallel testing of bacterial species with differing Gram staining characteristics provided better insights into the antibacterial potential of the test materials due to potential variations in susceptibility between them.

The use of monospecies bacterial models for antibacterial testing is an undisputed limitation, as it does not mimic the complexity and resilience of multispecies biofilms that are isolated from the root canal system<sup>17</sup>. However, using simplified models for initial antibacterial screening offers advantages, such as ease of cultivation, broad applicability, and better reproducibility<sup>449</sup>, while providing insights for more complex subsequent testing.

### 3.3.2 Assessment of bacterial adhesion (**Study I**)

Potential alterations in the surface characteristics of HCSCs, resulting from the modifications of their composition or environmental interactions may impact the bacterial adherence and the subsequent biofilm formation<sup>224</sup>. A fluorescent assay was therefore implemented to assess the bacterial adhesion of *E. faecalis*, after exposing the samples to the bacterial inoculum for one hour (**Figure 11**). Bacterial adhesion is an early process in biofilm formation<sup>454</sup>, and thus a relatively short incubation period was selected here as in a similar study<sup>455</sup>. Images acquired from the microscope were processed using a

suitable software (ImageJ; US National Institute of Health, Bethesda, MD, USA), and after applying a noise threshold, the counts in each image were correlated with bacterial cells.

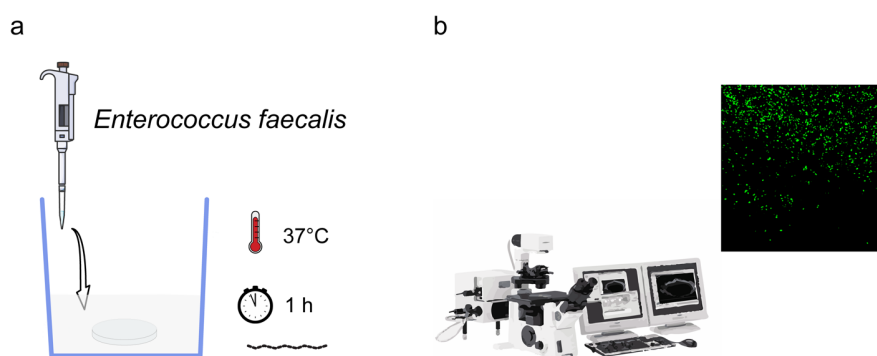


**Figure 11** Schematic representation of the bacterial adhesion assay (**Study I**). (a) Samples were incubated for one hour with the bacterium inoculum. (b) Bacterial adhesion was consequently observed with fluorescent microscopy. **Figure 11a** was partially generated by using a picture from Servier Medical Art, provided by Servier, licensed under a Creative Commons Attribution 3.0 unported license.

In the current assay, both direct bactericidal activity and anti-adherence surface characteristics may coexist. Extending the incubation periods of cements prior testing in our investigation allowed us to distinguish these two roles more clearly, as the bactericidal effect might diminish over time. Preliminary experiments were additionally conducted in order to compare the results obtained from the fluorescent assay with cultural data under the exact same sample exposure conditions. Specifically, after the one hour exposure to the bacterial inoculum, samples were immersed in phosphate buffered saline and bacterial survival was assessed using the Miles and Misra method by counting colony forming units (CFUs) on agar plates<sup>456</sup>. The fluorescent assay produced reliable, reproducible and similar results with the cultural data so we continued using it.

Our study could have benefited by complementing this assay with measurements of adhesion forces to obtain a more comprehensive characterization profile of the adhesion properties. Therefore, it serves as an initial assessment that warrants further research. An

advantage of the current technique was the use of the confocal microscope alongside a fluorescent *E. faecalis* strain as this prevented sample disturbance, which could have occurred if SEM had been selected for observations.

### 3.3.3 Leachate antibacterial activity (*Study II*)

Despite the acknowledged role of leaching in the antimicrobial properties of HCSCs<sup>225</sup>, there is scarce scientific literature on the antibacterial activity of these materials through indirect contact, particularly in the context of their use in endodontic surgery. Here, their antibacterial potential was assessed against two-day monospecies biofilms, for a 24-hour exposure period (**Figure 12**). Biofilms were grown upon membrane filters (MF-Millipore, 0.45  $\mu\text{m}$  pore, Merck KGaA, Darmstadt, Germany) that received a two  $\mu\text{l}$  bacterial inoculum and were incubated upon tryptic soy broth agar plates<sup>457</sup>. A main advantage of this technique is that biofilm membranes could be readily retrieved from the test-leachate and further processed for bacterial survival with culturing methods.

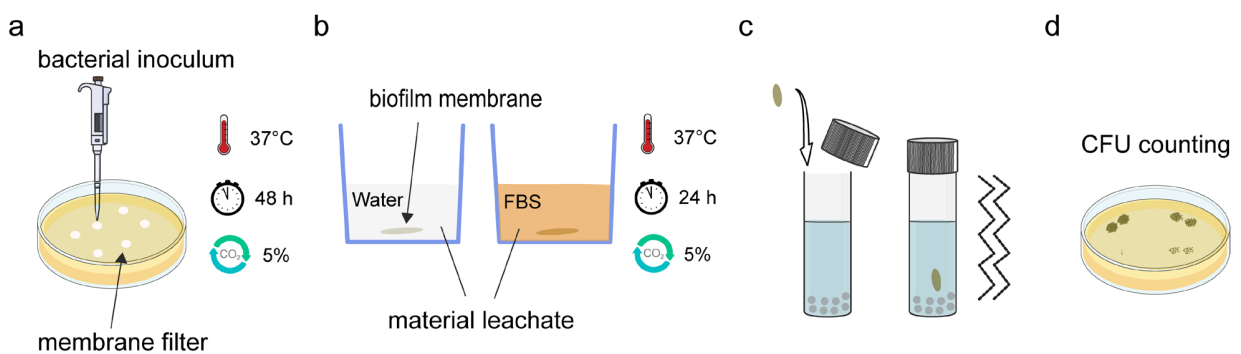


**Figure 12** Schematic representation of the antibacterial investigation of material leachates. (a) Development of monospecies biofilms upon membrane filters. (b) Exposure of biofilm membranes to material leachates. (c) Membranes are retrieved and immersed in phosphate buffer saline for bacterial culturing. (d) Bacterial survival assessment by colony forming units calculations. The figure was partially generated by using pictures from Servier Medical Art, provided by Servier, licensed under a Creative Commons Attribution 3.0 unported license. CFU: Colony forming unit.

The subsequent calculation of CFUs is a widely used and easily applicable method<sup>449</sup>. Its main limitation, as used here is its inability to detect bacteria being in a state of low metabolic activity, occasionally leading to false negative results<sup>449</sup>. However, this “*viable but nonculturable*” state for bacteria usually results from prolonged stress exposure over several days<sup>458</sup>, so it might hardly come into play here. Therefore, this method is undoubtedly superior to other indirect contact techniques that assess the turbidity or the optical density of bacterial solutions, as it allows for precise calculations of the surviving bacteria following the test-period<sup>459</sup>.

### **3.3.4 Antibacterial activity in contact with dentin (Study III)**

Two distinct tests were used to assess the antibacterial properties of the dentin/material interface. The limited utilization of ex vivo models for studying the antibacterial properties of materials in endodontic surgery is evident in the literature, with only two studies examining Biodentine with a dentin substrate<sup>194,460</sup>, and no current studies available for RRM putty. At the same time, the antibacterial effect of Biodentine has mainly been evaluated using the agar diffusion assay<sup>219-222</sup>. This method relies on measuring zones of bacterial inhibition on agar medium and is no longer considered to accurately reflect their true antimicrobial efficacy as the results are affected by the materials’ diffusion ability<sup>461</sup>.

#### **3.3.4.1 Independent assessment of dentin and material surfaces**

A split tooth model, initially developed to study the residual antibacterial effect of irrigation solutions and sealers<sup>462</sup>, was used here for the independent assessment of the antibacterial efficacy of the material and the dentin surfaces of the interface. This was achieved by initially cutting the root segments longitudinally, reassembling them to apply the material, and later separating them after the specified aging periods. As a result, one material-free dentin segment and another dentin segment containing the material bulk were acquired (**Figure 13**). The reproducibility of the model was further assessed here to confirm the absence of complete dentin coverage by the test-material on the material-free dentin segment. Scanning electron microscopy (SEM) / Energy dispersive x-ray (EDX)

observations of the split segments revealed occasional cement particles on the dentin surface, with some penetrating inside the dentinal tubules. Overall, consistent separation of the material bulk from the material-free dentin segment was observed, in line with the findings of the study that introduced this protocol<sup>462</sup>. Subsequent experiments were therefore conducted.

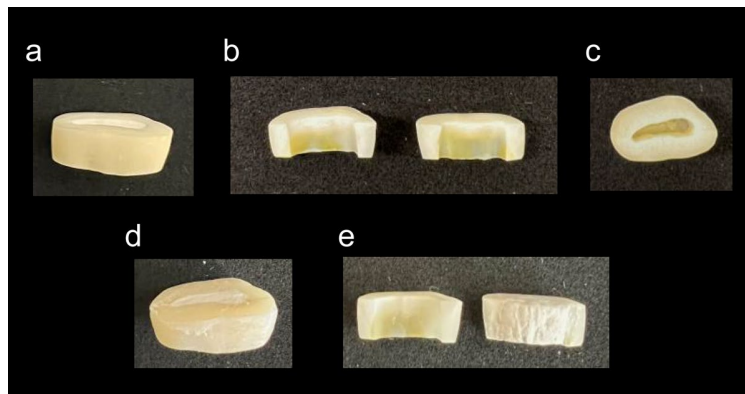


**Figure 13** Photographic presentation of the root segment preparation for the independent antibacterial assessment of material and dentin surfaces, according to a previously introduced protocol<sup>462</sup>. A schematic representation of the complete assay is available in **Study III**. (a) Root segment (3 mm length) after canal space preparation. (b) Longitudinal split of the root segment. (c) Reassembly of the two parts of the root segment with plastic membrane. (d) Material application inside the clamped segment. (d) After the specified aging period (24 hours after material placement or an additional 28-day aging period), the two parts of the root segment were carefully separated for independent testing.

Unlike other *ex vivo* models where dentin is used as substrate for biofilm cultivation<sup>463-465</sup>, the dentin and material surfaces in this model were tested against previously established three-day monospecies biofilms grown on membrane filters (biofilm membranes), as presented in Section 3.3.3 (**Figure 12a**). Even though this approach may lack clinical relevance, it enabled the investigation of the indirect contact antibacterial potential of the test materials on dentin.

Another aspect of this protocol not relevant to the clinical situation is the treatment of the dentin surfaces with 17% ethylene diamine tetraacetic acid before material application. This practice lacks clinical documentation in endodontic surgery<sup>46</sup>. Nevertheless, this procedure was crucial for standardizing the dentin substrate by ensuring the presence of open tubules instead of the inconsistent smear layer. Additionally, it facilitated the observation and visualization of material remnants on the dentin structure and enabled a more effective interaction with the dentin substrate.

#### 3.3.4.2 Biofilm assay upon the dentin/material interface

The antibacterial properties of the intact dentin/material interface were consequently assessed with a biofilm growth assay. Bacterial establishment and further proliferation after treatment at this area could potentially provide pathways towards reinfection<sup>466</sup>. Such aspects have been explored for endodontic sealers<sup>467,468</sup> but not for materials for endodontic surgery.

In this model, the dentin/material interface was exposed to previously established one-day mature biofilm membranes in the presence of culture medium for three days (**Figure 14**). The biofilm membranes for this assay were prepared similarly to the previous assays (Section 3.3.3, **Figure 12a**), with differences in shape and dimensions (one mm thick rectangular membranes instead of two or three mm circular ones) and the incubation period (24 h for this assay). The use of the one-day biofilm membranes positioned along the dentin/material interface facilitated the localization of the investigation area. In addition, observations on bacteria-free samples enabled better sample orientation and threshold optimization.

After three days of incubation of the samples in the growth medium, the membrane biofilms were carefully removed and biofilms upon the dentin/material interface were stained and imaged with confocal laser scanning microscopy (CLSM; Olympus FluoView FV1200, Olympus, Tokyo, Japan). The multiple two-dimensional images captured by the laser scanning feature at different sample depths can be reconstructed to a three-dimensional biofilm representation<sup>469</sup>. The imaging technique relies on fluorescent labeling of specimens to generate images. In the current biofilm assay, samples were

stained with a bacterial viability kit (LIVE/DEAD BacLight Bacterial Viability Kit; Invitrogen, Eugene, OR, USA) before observation in order to assess bacterial survival based on their membrane integrity. The kit contains two stains, SYTO 9 and propidium iodide. SYTO 9 is a green fluorescent stain that can penetrate and therefore label both live and dead microorganisms; propidium iodide is a red fluorescent stain that labels only cells with a damaged membrane, therefore designated as injured or dead cells. The quantification of the differently stained bacteria captured in the set of images with the CLSM is consequently conducted with an appropriate software. This technique is vastly applied in the literature because it is rapid, non-invasive, and offers quantitative results in combination to observing biofilm architecture<sup>449</sup>.

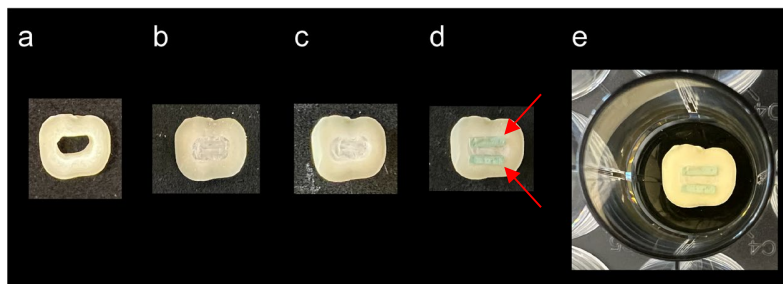


**Figure 14** Photographic presentation of the biofilm assay at the dentin/material interface. A schematic representation of this assay is also available in **Study III**. (a) Root segment (1.5 mm thick) after enlargement of the canal space. (b) Test-material compacted inside the canal space. (c) After the specified aging periods (24 hours after material placement or an additional 28-day aging period), the sample was carefully ground, and (d) one-day biofilm membranes were positioned along the dentin/material interface of the sample (arrows), with the biofilm surface in direct contact with the sample. (e) The sample was incubated in tryptic soy broth and transferred to a new well with fresh medium daily for a total period of three days.

Despite the above-mentioned advantages of CLSM, there are limitations in comparison to conventional culturing methods. Bacterial viability measurements are indirect as they rely on membrane integrity for dye penetration, which can lead to misinterpretations. For instance, SYTO 9 may not readily penetrate Gram-negative

bacteria, potentially underestimating live bacterial populations<sup>470,471</sup>. Additionally, no clear differentiation can be made between dead bacteria and injured or bacteria under stress<sup>472</sup>. Viable bacteria might also be misinterpreted as dead or injured due to membrane permeability to propidium iodide during cell division or cell wall synthesis<sup>473</sup>.

### **3.4 Cytotoxicity assessment (Study II)**

Modifications aimed at enhancing the antibacterial profile of HCSCs should not compromise the materials' effect on host tissue cells, but rather, maintain or improve it. Herein, a cytotoxicity assessment was conducted. Indirect methods were used, because SEM imaging of cells upon HCSCs surfaces requires procedures that can significantly alter the materials' microstructure and thus impacts the results<sup>143,474</sup>. Cytotoxicity was screened with the 3-(4,5 dimethylthiazolyl-2-yl)-2,5-diphenyl tetrazolium bromide (MTT) assay, which is commonly used for preliminary assessments due to its availability and ease of use<sup>475</sup>. The assay relies on measurements of color intensity of formazan, a compound generated through the metabolic conversion of mitochondrial dehydrogenase by the cell cultures. The blue-violet formazan is solubilized and quantified with photospectrometry. With this technique, the cell metabolic activity as expressed by the optical density of the produced formazan is assessed, and further correlated to the cell viability<sup>476</sup>. The L929 cells that were tested in the thesis are recommended by the ISO specifications<sup>476</sup>, due to their ease of cultivation and the reproducibility they offer.

A limitation of the method is that it may underestimate the cytotoxic potential of the test materials since it can only detect it at the stage of apoptosis, when a substantial reduction in cell mitochondrial activity indicates cell death. Any possible earlier cellular damage might therefore remain undetected<sup>477</sup>. Another issue is that some of the formazan may be lost during the technical procedures of the test<sup>475</sup>.

### **3.5 Analysis of surface characteristics (Study I)**

In **Study I**, evaluation of cements' surface characteristics was conducted to explore potential changes following modifications of the composition of HCSCs or across different



aging conditions (**Tables 3, 4**). Results were then linked to their antibacterial characteristics.

### ***3.5.1 Qualitative and quantitative analysis of surface structure***

Quantitative tests involved measurements (surface roughness, wettability, microhardness), while qualitative assays served for identification (material photography, observation of micrographs, energy dispersive x-ray analysis).

Visual assessments were made to detect any potential color variations from the cement modifications and environmental conditions, and photographs of specimens were captured. While a quantitative analysis of color stability using a spectrophotometer could have provided more objective data, it was not considered necessary for this investigation, as the primary focus of research for the test materials is their use in endodontic surgery. Discoloration potential may not be as a significant concern in these applications compared to coronal placements. Therefore, these assessments were mainly conducted as part of the surface analysis of the cements, from a macroscopic to a microscopic perspective.

Scanning electron microscopy (SEM; TM4000Plus II, Hitachi, Tokyo, Japan) was used to assess the surface topography of materials with both quantitative and qualitative approaches. SEM utilizes a focused high-energy electron beam, which produces various signals upon scanning the surface of a solid sample. These signals provide information on the specimens' morphology, composition, and even crystalline structure, and assist in the construction of a two-dimensional image with a wide range of spatial resolutions and magnifications<sup>478</sup>.

The surface roughness of the substrate can impact bacterial adhesion<sup>479</sup>. Even though optical profilometry is a commonly used technique for quantitative assessment of surface topography, in our study, the presence of light scattering from the HCSC surfaces interfered with data acquisition, making it not feasible to collect reproducible data. Thus, in the current investigation, the average arithmetic roughness (Ra) values in each observation field were obtained with a quad-type backscatter electron detector at 200× magnification. With the use of a software (MountainsMap 8; Digital Surf, Besançon,

France), these four images were stereoscopically reconstructed in a 3D model (**Figure 15**).

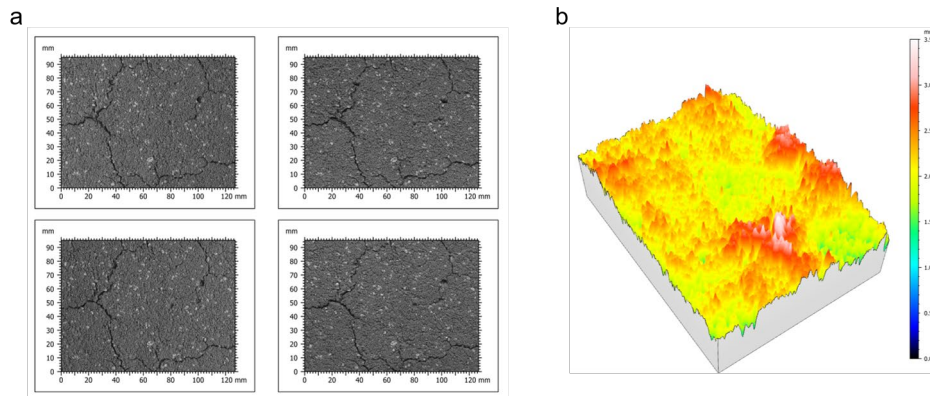


**Figure 15** (a) The four images obtained under the scanning electron microscope were (b) stereoscopically reconstructed in a 3D model.

The program was calibrated using a reference material (TZ-base) with a consistent artificially induced angle ( $30^\circ$ ). The Ra values for each test material were consequently obtained. These Ra values are associated with the Gaussian filter that was applied to reduce the high-frequency noise and enhance the surface feature visualization. Consequently, they may not be suitable for direct comparisons with Ra values of similar materials in other studies.

Material surfaces were characterized by capturing SEM images using a combined back-scattered electron and secondary electron signal detector (mixed signal). This approach facilitated additional morphological assessments and the identification of different chemical phase distributions on the surface microstructure. Energy dispersive x-ray (EDX) analysis complemented these assessments by indicating changes in elemental composition on the material surface. Additionally, the possibility of conducting X-ray diffraction analysis to gather information about the crystallographic structure of the material surfaces could have been explored.

In addition, an attempt was made to assess surface porosity using computed tomography. However, this approach encountered several technical challenges that

rendered the results non-reproducible. Initially, we utilized a low-resolution nanotomograph (SKYSCAN 2211, Bruker, Billerica, MA, USA) but it was found that the scattering of the cements did not allow for adequate pore identification (**Figure 16**).

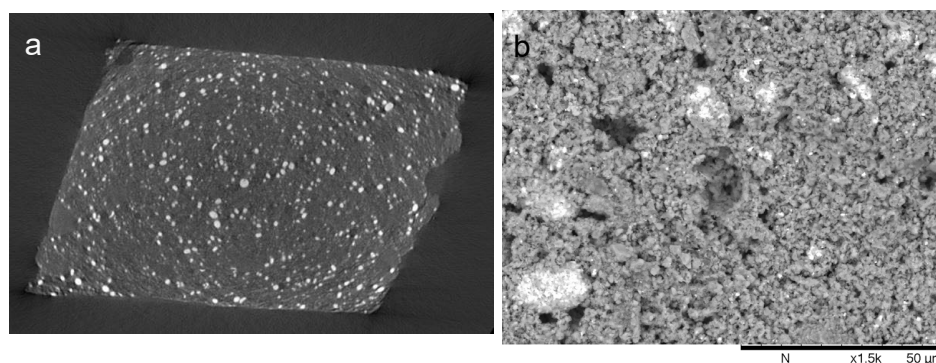


**Figure 16** (a) Slice acquired with the nanotomograph for the basic experimental formulation (TZ-base). (b) Scanning electron micrograph of the same sample, revealing a heavier pore distribution that was not depicted in the former.

We then proceeded with higher resolution settings. Pores below the micrometer-range resolution threshold that was set could thus not be detected. A further limitation was that no clear differentiation could be established between air bubbles entrapped in the cement core during material compaction and true pores, which led to significant result variations. Consequently, the results obtained from this method were considered not reliable for investigation of porosity.

### 3.5.2 *Wettability*

Contact angle measurements (NRL 100–10, ramohart, Mountain Lakes, NJ, USA) were conducted using a 10  $\mu$ l water droplet on the material surfaces to evaluate their wettability. Low contact angles indicate high wettability (surface free energy)<sup>480</sup> and are in fact associated with higher bacterial adhesion<sup>481</sup>. Surfaces with contact angle values below 90° are considered hydrophilic<sup>482</sup>. A limitation in the current test was the inability to differentiate between potential absorption of the liquid droplet by the cement surface and

complete wetting, as such differentiation would have required volume measurements of the droplet over time. To ensure reproducibility, all measurements were conducted at a standard time point (30 sec) after placing the drop.

### 3.5.3 *Microhardness*

An indentation test (100 g load for 15 sec dwelling time; Duramin-40 A1, Struers, Rotherham, UK) was used to assess the surface microhardness of test materials. The obtained values not only indicate the hardness of the material surface but also provide information about the setting process and how different setting conditions impact the material's strength<sup>475</sup>.

## 3.6 **Leachate characteristics (Study II)**

The interaction of HCSCs with the environment occurs not only through direct contact with their material surface but also via the release of hydration by-products, particularly calcium hydroxide<sup>227</sup>. Therefore, the leachate characteristics of HCSCs are of particular interest. In **Study II**, indirect assays were chosen to assess leaching characteristics and were subsequently correlated with their biological profile.

### 3.6.1 *Alkalinity*

Alkalinity measurements were conducted using a pH meter (Sension+ PH3; Hach, Loveland, CO, USA) that was calibrated with three buffer solutions before each use. While material alkalinity can provide an indication of hydroxyl release, HCSC leachates tend to reach saturation due to their high alkalinity potential, which may reduce the sensitivity in depicting differences among cements, particularly in the cumulative leaching models<sup>227</sup>.

### 3.6.2 *Calcium release*

Complementing the leachate chemical analysis with calcium release assessments provided clearer insights into the hydroxyl release as well and the hydration reaction overall. Tests were carried out using a calcium ion-selective electrode connected to a laboratory meter (ION450; Radiometer analytical, Hach, Loveland, CO, USA). Data acquisition is based on the voltage difference between a reference electrode and a calcium ion-selective membrane. The voltage change is proportional to the concentration of calcium ions in the measured solution. Four standard solutions were used for calibration. Although this method is vastly utilized in similar research studies<sup>233,483,484</sup> and was chosen here due to its availability, it is acknowledged that techniques such as inductively-coupled plasma spectrometry might have yielded potentially more precise measurements<sup>485</sup>. At the same time, conducting inductively-coupled plasma spectrometry with pure FBS as the extract medium might have been problematic due to the need for massive dilutions to reduce the background elements before analysis.

## 3.7 **Characterization of cement bulk (Study II) and dentin/material interface (Study III)**

SEM and EDX were also employed for sample characterization in **Studies II & III**. In **Study II**, SEM images of polished specimens were acquired in back-scattered mode to identify the arrangement of different chemical phases within the bulk of each material<sup>475</sup>. The generated image contrast is the result of reflected electrons (back-scattered) from the various atoms on the material's surface<sup>486</sup>. The distribution of hydration products, non-hydrated particles, radiopacifiers and potentially other filler compounds within the bulk of each material could be assessed. Their elemental composition was assessed through EDX analysis in different areas of the sample. Similar with the characterization of the material surfaces (**Study I**), complementary X-ray diffraction analysis could have added insights on the mineral phases of the samples.

In **Study III**, we characterized the dentin/material interface in polished specimens using SEM, EDX, and elemental mapping to enhance our understanding of the

interactions taking place in this region. It is important to note that sample dehydration, a necessary step before SEM observation, and sample-induced shrinkage due to the constant vacuum environment during observation, can both influence the adaptability of root-filling materials to dentin and may create artificial marginal gaps in the observations<sup>249,487</sup>. This technique is therefore not indicated in gap assessments<sup>478</sup>. However, material detachment from the dentin surface does not appear to affect the elemental distribution in the two surfaces<sup>248</sup>. Despite being a potentially destructive method, the SEM observation technique was deemed more reliable compared to confocal laser scanning microscopy (CLSM). The latter method requires the incorporation of fluorescent dyes into the test materials for proper sample observation and has been shown to induce artifacts at the interface<sup>249</sup>, due to the passive diffusion of the dyes into the dentinal tubules<sup>478</sup>. Additionally, SEM has substantially higher resolution than CLSM.

The elemental mapping in **Study III** provided valuable insights into the migration of certain elements, although it cannot depict the migration of those present in both substrates, such as calcium. Additionally, there can be overlaps in the detection of elements with closely positioned peaks in the X-ray spectrum, as observed with zirconium and phosphorus in this study. A more comprehensive evaluation could have been achieved by integrating high-resolution field emission-gun electron probe microanalysis due to its superior spatial resolutions, and even complementing it with a technique capable of detecting molecular composition rather than just elemental content, such as micro-Raman spectroscopy<sup>248</sup>. Furthermore, metallographic polishing of the material/dentin interfaces entails the risk of transferring smear debris into previously unoccupied areas of the sample, such as voids or open tubule spaces, potentially creating artifacts in the evaluation<sup>248</sup>. To mitigate this risk, excessive grinding of the specimens was avoided. Additionally, specimens were regularly cleaned and inspected at each step, and the polishing process utilized a diamond suspension (DP-1  $\mu\text{m}$ ; Struers, Rotherham, UK), which also assisted in reducing the risk of transferring smear debris.

### 3.8 Statistical considerations

In **Studies I & III**, normally distributed data were processed using analysis of variance and Bonferroni posthoc tests. When the normality assumptions were violated, data transformation was attempted. If the data remained severely skewed, Kruskal–Wallis tests adjusted by the Bonferroni correction were performed. In **Study II**, the impact of the independent variables was evaluated using regression analyses. Sample size calculations were conducted *a priori* for **Studies II & III**, but not for **Study I**, where experiments were ensured to be conducted at a minimum of triplicate.

The variations in the statistical models and sample size across the three different studies might have introduced some inconsistencies in the investigation, potentially carrying a risk of bias in the overall outcome. However, it is important to note that all the statistical models implemented in each assay effectively addressed the primary research questions of their respective studies.





## 4. Main Results

Here, the main findings of the three studies are presented. A detailed description of the results can be found in the published papers.

### 4.1 Surface characteristics and bacterial adhesion

The main results of **Study I** were:

- The SNP- and BG- containing experimental cements increased the surface roughness of the basic experimental formulation (TZ-base) after 28 days, without any differences in their wettability or microhardness.
- Biodentine exhibited smoother surface characteristics, and significantly higher microhardness than the experimental HCSCs. It had a similar wettability pattern to the experimental cements but did not demonstrate complete wetting like them.
- The immersion of materials in FBS led to a gradual precipitation on the surfaces of all HCSCs and altered their microstructure. At 28 days, a rougher surface morphology compared to the water-immersed HCSCs was evident, with complete surface coverage by compounds rich in oxygen, calcium, and phosphorus, or carbon. The hydrophilicity of all HCSCs was initially moderated (day one), but it gradually returned to its initial state over time. The microhardness of experimental HCSCs remained unchanged. For Biodentine, it significantly increased in FBS after 28 days but decreased when immersed in water for the same aging period.
- The immersion medium did not affect the bacterial adhesion profile of the experimental and commercial HCSCs.
- Experimental HCSCs at one- and seven- day aging displayed minimal bacterial adhesion, whereas Biodentine and IRM had substantial adherence from day one. At 28 days, all materials showed bacterial adherence, but TZ-bg20 water-immersed samples had significantly lower *E. faecalis* counts than the positive control.

## 4.2 Chemical properties and indirect contact antibacterial activity

The main results of **Study II** were:

- The leachates from both the experimental and commercial HCSCs exhibited increased alkalinity, calcium release, antibacterial efficacy, and cell cytotoxicity over time. These properties decreased when the immersion medium was refreshed.
- Immersion in FBS reduced the alkalinity, bactericidal activity, and cytotoxicity of HCSCs compared to the water immersion.
- The effect of immersion medium on calcium leaching varied. In the weekly medium refreshment model, FBS consistently reduced the calcium release compared to water leachates. In the cumulative leaching model, however, the experimental HCSCs leached more calcium ions in FBS than in water, whereas Biodentine displayed the opposite pattern.
- Biodentine and TZ-bg20 exhibited overall reduced alkalinity, calcium release, and antibacterial activity in comparison to TZ-base. Additionally, Biodentine demonstrated lower cytotoxicity than TZ-base.
- The SNP-containing experimental formulations had overall similar antibacterial effectiveness to TZ-base. However, in water leachates against *E. faecalis*, the experimental cement mixed with a 2 mg/ml SNP solution (TZ-Ag2) displayed the highest bacterial reduction, except for the 0–24 hour leaching period, where no changes were observed.

### 4.3 Antibacterial activity in contact with dentin

The primary findings of **Study III** are summarized below:

- The dentin surfaces that were exposed to test-materials for one day and the one-day material surfaces exhibited antibacterial behavior.
- Dentin surfaces exposed to the experimental HCSC with 40% BG (TZ-bg40), Biodentine, or IRM, demonstrated overall reduced antibacterial effect compared to the dentin surfaces of the other tested samples.
- TZ-Ag2 exhibited the strongest antibacterial capacity in the biofilm growth assay upon intact dentin/material interfaces.
- In the biofilm growth assay, a significantly smaller percentage of dead/injured bacteria was observed in the 28-day samples compared to the one-day ones.
- Microscopic observations of the interfacial characteristics of the tested HCSCs (both experimental and commercial ones) revealed similar characteristics.



## 5. Discussion

The current chapter discusses the outcome of the hypotheses that were tested, reflecting on the existing literature.

### 5.1 The effect of incorporations on properties of HCSCs

Results from the tested experimental formulations that incorporated silver nanoparticles or bioactive glass, and the parallel screening of commercial HCSCs with additives in their synthesis, in comparison to the basic experimental formulation (TZ-base), suggest that changes in the HCSC composition affected certain physico-chemical properties and their biological activity (antibacterial activity and cytotoxicity). The null hypothesis was therefore rejected. Specific changes on cements' properties per incorporation or commercial formulation are discussed below.

#### 5.1.1 *SNP additions*

The only alteration in the physico-chemical properties of HCSCs that were investigated following the incorporation of SNPs was the rougher surface profile at 28 days compared to TZ-base. Since the amount of tricalcium silicate cement was not changed in the modified cements, it seems that SNPs did not disrupt the hydration reaction.

The combination of results from the direct contact antibacterial assays suggests that mixing the experimental HCSC with a 2 mg/ml SNP solution enhanced their antibacterial profile only under longer exposure periods. Notably, in the bacterial adhesion assay (one-hour exposure period; **Study I**) or the split tooth model (24-hour contact time; **Study III**), no changes in the antibacterial effect of the cements were observed. However, in the biofilm growth assay upon the intact dentin/material interfaces (three-day exposure period; **Study III**), TZ-Ag2 exhibited increased antibacterial effect than the basic experimental formulation. These findings align with a previous study that demonstrated the potent

antibacterial effect of a SNP gel as an intracanal medicament, in contrast to the inadequate efficacy of 2-minute irrigation with a higher concentration SNP solution<sup>322</sup>.

Water leachates of TZ-Ag2 demonstrated overall the highest antibacterial efficacy against *E. faecalis*, but no such improvement was observed against *P. aeruginosa* (**Study II**). A possible explanation might be that *P. aeruginosa* was in general more susceptible than *E. faecalis* in the specific model used, especially at seven-day leachates, where the increased effect of TZ-Ag2 was most noticeable. Interestingly, in **Study III**, the enhanced antibacterial performance of TZ-Ag2 was primarily evident against *P. aeruginosa*. This aligns with reports that Gram-negative bacteria are more susceptible to SNPs due to the thinner layer of peptidoglycan in their cell wall<sup>286</sup>.

Overall, in the current investigations, while the SNP additions did not appear to have a negative impact on the physico-chemical characteristics of the HCSC, the enhancement in antibacterial properties that they conferred appears to be moderate. A previous study showed improved antibacterial activity of a SNP-modified MTA, but their testing was conducted only two days after setting<sup>352</sup>. In the direct contact studies conducted here at a similar early time-point (one day), the basic experimental formulation also exhibited antibacterial properties, rendering it difficult to discern any differentiation. Furthermore, elemental mapping confirmed the release of SNPs into neighboring dentin; however, this did not appear to enhance the antibacterial effect of the dentin surface at the 24-hour contact period with the monospecies biofilms (**Study III**).

The possibility that higher SNP concentrations or formulations with other characteristics and possibly higher reactivity could have yielded a more robust antimicrobial effect should be considered. At the same time, determining the ideal concentration for SNPs should also involve a comprehensive assessment of their impact on host tissue cells to maintain the overall positive biological equilibrium of the cements. While the cytotoxicity studies conducted here were preliminary, they revealed no changes in the HCSC's cytotoxic profile at the SNP concentrations used.

### 5.1.2 Replacement of HCSC with BG

Similar to SNPs, BG-replacement increased the surface roughness of test materials, particularly at 20% incorporation. The combination of findings from **Studies I & III** suggest that the direct contact antibacterial effect was not significantly altered for concentrations of 10% or 20% of BG-replacement. Yet, TZ-bg20 was the only material at 28 days that marked significantly lower *E. faecalis* adhesion than the positive control. These results are in relative accordance with previous research that demonstrated the enhancement of the direct antibacterial activity in an experimental HCSC when incorporating 20% of another BG formulation, Biosilicate<sup>425</sup>. However, in the latter study, materials were only tested after one day of setting. Therefore, no comparisons can be made on the long-term antibacterial properties. In our experiments, it was only in **Study III** that the cement with 40% BG had diminished antibacterial efficacy in direct-contact experiments.

Besides the relatively minor modification in surface characteristics of TZ-bg10 and TZ-bg20, the main alterations resulting from the BG incorporation were observed in the chemical properties of the cements. Notably, it appears that the hydration profile of the BG-modified HCSCs was changed. A more gradual release of calcium ions was found, which, on the whole, remained at a lower level compared to the basic experimental formulation. A possible explanation to this might be that calcium from the BG particles may not become readily available in the surrounding environment and could instead become deposited within the cement matrix, as a recent study suggested<sup>426</sup>. As a result, the indirect contact antibacterial activity of the BG-modified cements decreased, both when assessed in the materials' extracts (**Study II**), and with regard to the cements' conferred effect on the dentin surfaces (**Study III**). Thus, although the primary mechanism of the antibacterial activity of BG is alkaline-related<sup>274</sup>, akin to HCSCs<sup>187</sup>, it could not fully compensate for the antibacterial activity lost when tricalcium silicate was replaced.

Considering the above, the beneficial attributes of BG could be further examined as supplementary components within the cementitious phase of HCSC, without substituting any portion of tricalcium silicate cement. At the same time, a more comprehensive assessment of the impact on host tissue cells is crucial, running in parallel with the evaluation of antibacterial effectiveness. This approach could help identify a potential

equilibrium between sufficient antibacterial activity and the modulation of inflammation towards healing procedures.

### 5.1.3 Outcomes from assessing the commercial HCSCs

Biodentine was consistently examined in all studies providing thus a comprehensive assessment of its physico-chemical profile and biological properties compared to the experimental cements. RRM putty was only assessed in **Study III**, offering limited extrapolation of the role of additives in its composition.

Biodentine exhibited overall substantial differences in some of its surface and chemical characteristics in comparison to the basic experimental formulation (TZ-base), which were indicative of the additives present in the commercial material. Notably, Biodentine consistently demonstrated smoother surface morphology, which can be attributed to the incorporation of a water-soluble polymer that minimizes cement flocculation<sup>488</sup>. Additionally, the higher microhardness values of Biodentine compared to the experimental cements are a result of the reduction in the powder/liquid ratio<sup>207,211</sup>. Interestingly, Biodentine's microhardness decreased with extended incubation in water, likely due to ongoing dissolution. In water leachates, minor differences in the chemical profile were observed between the experimental HCSC and Biodentine. The most notable distinction was the sharp reduction of calcium release in the latter upon medium change, indicating an accelerated hydration reaction due to the inclusion of calcium carbonate<sup>210</sup>.

In terms of its biological properties, Biodentine displayed a different bacterial adhesion pattern compared to TZ-base with marked bacterial presence on its surface, even at the one-day immersed samples (**Study I**). Against the three-day established biofilms, even though no statistically significant differences were observed between Biodentine and the experimental cements, the values for bacterial survival for Biodentine appeared higher (**Study III**). Taken together, Biodentine exhibited moderate effectiveness against *E. faecalis*, which aligns with results from a direct contact test of a previous study<sup>223</sup>. In the context of its indirect contact antibacterial activity, Biodentine demonstrated an overall lower effect than the experimental HCSCs. In contrast to TZ-base, the bactericidal effect



of dentin surfaces in contact with either RRM putty or Biodentine decreased from one to 28 days. This reduction may be linked to the faster hydration reaction of the commercial HCSCs when compared to TZ-base. As the biggest part of the hydration process is completed, the amount of the released calcium hydroxide is expected to decrease significantly<sup>489</sup>. While accelerated hydration reaction is a known characteristic for Biodentine as it was discussed above, it is worth noting that RRM's hydration relies on its exposure to an aqueous environment<sup>46,208</sup> and may be influenced by the water availability in it. Therefore, the speed of this reaction may vary under different water conditions both in laboratory studies, as well as in the clinical setting. At the same time, the putty version tested here is reported to have a faster reaction rate than the paste form<sup>233</sup>, possibly due to differences in particle size<sup>117</sup>. Overall, the antibacterial properties of Biodentine and RRM formulations have been found equivalent against cariogenic bacteria<sup>226,227</sup>.

Furthermore, the cytotoxicity values differed significantly between the experimental cements and Biodentine, with the latter displaying a less aggressive profile, especially in one-day leachates. Similar findings have been reported previously<sup>227</sup>. The initial cytotoxicity observed in cell cultures exposed to HCSCs is attributed to the increased alkalinity caused by hydroxyl ion diffusion<sup>490</sup>. Despite both Biodentine and experimental cements producing similarly high pH values in their water leachates, variations in cytotoxicity levels, combined with pH measurements in FBS, suggest the following:

- The cytotoxicity threshold related to alkalinity<sup>491</sup> is relatively high.
- Leachates from experimental HCSCs are likely saturated with calcium hydroxide and have a higher alkalization potential than Biodentine, resulting in higher cytotoxicity.

## **5.2 The effect of environmental conditions**

The environmental conditions (immersion medium and aging period) significantly affected the properties of the test materials. Furthermore, the test cements contributed to an antibacterial effect in the dentin surface after contact and separation from it. Thus, the null hypotheses that changes in environmental conditions would not alter the properties of the

materials and that dentin exposed to the test materials would not exhibit any antibacterial potential were both rejected. These different aspects are discussed individually below.

### 5.2.1 *Aging period*

Long-lasting antibacterial properties are desirable for materials for endodontic surgery in order to minimize the risk of infection following the completion of endodontic treatment. In practice, achieving this goal is a challenging task<sup>128</sup>. Moreover, considerations related to physical integrity are important, as a continuous antibacterial effect may indicate the ongoing release of chemical compounds from the material's bulk<sup>41</sup>. The results of the current studies suggest that the aging period affected the chemical properties of the HCSCs. When compiling all the results from the antibacterial experiments, none of the studied materials maintained consistently potent antibacterial behavior after 28 days of aging. Even the SNP additions, which were found not to impair the hydration profile of HCSCs, did not yield any significant antibacterial enhancement after extended aging periods at the current concentrations.

In the leachates assessments (**Study II**), the weekly medium replenishment model provided a more accurate representation of the respective evaluation period. In contrast, not changing the medium resulted in a cumulative effect from the point of immersion rather than providing a true measurement of the leachate's properties at the point of evaluation. Interestingly, in the weekly medium change model, the 28-day HCSC water leachates (from both the experimental cements and Biodentine) exhibited no antibacterial efficacy, despite their relatively high pH values (>11.5). Similar to the alkalinity-related cytotoxicity threshold, it can be speculated that adequate antibacterial efficacy in terms of alkalization requires relatively high values. Sustained alkalization in the application field *per se* may therefore not be a sufficient factor for a lasting long-term antibacterial effect.

Furthermore, at the same evaluation period (28-day leachates upon medium change), the cytotoxicity of experimental HCSCs was lower in comparison to the seven-day leachates. However, the leachates' viability score remained still below the ISO-recommended 70% cytocompatibility threshold<sup>476</sup>. The behavior of Biodentine is

particularly noteworthy at that period, since it showed the lowest viability values among the HCSCs, whereas maintaining a non-cytotoxic behavior at one-day leachates (relative MTT activity > 70%). Given the similarities in the pH values of HCSCs at the early time-point and based on our previous assumptions regarding leachate saturation, it appears that pH measurements lack the sensitivity to distinguish the differences in leachate reactivity here as well. Thus, the differences in the cytotoxic profile between the one- and 28- day leachates (upon medium change) necessitate an explanation that goes beyond the measured alkalinity. Notably, the results can be considered in conjunction with findings of **Study I**, which revealed a decrease in the microhardness of Biodentine after prolonged immersion to water. The weekly medium change appears to have impacted the physical integrity of Biodentine, possibly by promoting increased leaching, as it does not allow solution buffering. In the experimental formulations, especially TZ-base, minor fluctuations in hardness values, mainly between seven and 28 days, may have a similar explanation, though they may not be as distinguishable due to the overall lower microhardness values.

The varying impact of aging period on materials in relationship to their chemical composition is also evident in the behavior of the ZOE-based IRM. Notably, IRM displayed a relatively more stable yet inferior antibacterial profile over time compared to HCSCs. These findings align with a study that found steady yet modest antibacterial performance of IRM between fresh and 18 weeks aged samples against *E. faecalis* in direct contact tests, alongside a gradual release of eugenol during extended evaluation periods<sup>106</sup>. This gradual release of eugenol occurs as the cement undergoes hydrolysis in an aqueous environment<sup>87,88</sup>, providing the explanation for the material's antibacterial profile.

### 5.2.2 Immersion medium

The immersion of HCSCs into FBS induced significant changes in both their surface characteristics and leaching properties. Even though exposure to FBS altered the surface structure of all studied HCSCs (**Study I**), the bacterial adhesion pattern remained the same. Material surfaces gradually accumulated products of the reaction between calcium hydroxide and serum components, resulting in a layer primarily composed of calcium carbonate, and an amount of calcium phosphate, as indicated by SEM images and EDX

analysis. This layer slightly reduced the HCSCs' hydrophilicity, particularly in the short-term immersion (one and seven days), while it enhanced the surface microhardness of Biodentine over longer periods, contrasting with its behavior in water as described earlier. Changes in the hydration process upon exposure to serum-containing environments have been previously displayed both *in vitro*<sup>191,265,271,273</sup> and *in vivo*<sup>265,273</sup>.

In contrast to the behavior of HCSCs, no environment-induced structural surface changes were evident in IRM; however, EDX analysis revealed an elemental modification of the material surface from the adsorption of FBS components. The surface microhardness of IRM experienced an increase when exposed to FBS, likely due to a shift in the balance between dissolution and adsorption of the serum components. Interestingly, immersion of IRM in FBS resulted in greater wettability and reduced *E. faecalis* adhesion. The surface roughness of IRM remained constant in both water and FBS, suggesting that mainly chemical changes on the material surface contributed to the decreased bacterial adhesion. Enhanced hydrophilicity has previously been associated with reduced biofilm formation on resin composites<sup>492</sup>, indicating the need for further investigation into the hydrophilic properties of materials used in endodontic surgical procedures. At the same time, it is important to note that the bacterial adhesion is defined by the hydrophilic properties of both interacting surfaces (bacterial and material ones)<sup>493</sup>.

As regards the effect of FBS in material extracts (**Study II**), it consistently diminished the antibacterial effect. Assessments of the chemical profile of HCSCs revealed a deterioration in their alkalization potential in FBS, and a different calcium leaching behavior between the experimental cements and Biodentine. Notably, in the cumulative leaching model, the experimental HCSCs released a higher amount of calcium ions into FBS compared to water. Previous studies have shown evidence of increased *in vivo* elemental leaching of MTA in contact with blood<sup>273</sup> or in a 10% serum-supplemented physiologic solution compared to the neat physiologic solution<sup>436</sup>. In contrast, Biodentine exhibited a lower overall release of calcium ions in FBS compared to water in the cumulative model. Similarly, a decrease in Biodentine leaching has been found in a bicarbonate solution when compared to deionized water<sup>494</sup>, but this trend was not observed in a 10% serum-supplemented physiologic solution when compared to the neat solution<sup>436</sup>. These variations may be attributed to differences in the immersion media.

The carbon dioxide that is present in the tissues can promote the reaction of the leached calcium through carbonation<sup>495</sup>. This leads to the formation of calcium carbonate, which precipitates on the cement surface, and as a consequence blocks the capillary pores through which calcium is released<sup>267,268</sup>. The latter situation may be particularly pertinent when explaining the decrease of calcium leaching observed with Biodentine in FBS, as findings from experimental HCSCs indicate that calcium may not be entirely consumed through carbonation. The hydration of Biodentine is less susceptible to environmental conditions<sup>496</sup>, possibly due to the accelerated reaction that takes place in it, which leads to the formation of a higher percentage of amorphous phase<sup>497</sup>, thereby enhancing its stability. This is further supported by the significant decrease in the amount of calcium ions observed upon refreshment of the extract medium.

The reduction in calcium hydroxide leaching from Biodentine compared to experimental HCSCs in FBS is further supported by its reduced antibacterial activity. The increased bacterial adhesion observed in **Study I** for Biodentine in contrast to the experimental cements may have a similar explanation. It additionally reflects the diverse leaching behavior of the HCSCs in an acidic environment (i.e the bacterial inoculum), which Biodentine can withstand well<sup>498</sup>.

The neutralization of the leachate antibacterial activity by FBS can be attributed to its buffering capacity, as it contains proteins that act as weak acids<sup>499</sup>. A corresponding decrease to leachate alkalinity was followed by the deterioration of the antibacterial effect. In addition, serum components may create more favorable conditions for bacterial survival acting as nutrients for them. More importantly, evidence from the plateau of reactivity observed in the cumulative leachate model at seven days, and even the decline in antibacterial efficacy for the BG-containing cements and Biodentine, indicates the consistent buffering effect of FBS, even in static conditions.

Furthermore, the addition of SNPs did not enhance the antibacterial properties of HCSCs in FBS leachates. At the same time, the antibacterial efficacy of IRM was also compromised in FBS. Hence, it appears that the serum environment can not only diminish the alkalinity-mediated bactericidal impact of HCSCs but also decreases the antibacterial potential of other released components.

### 5.2.3 *Dentin*

In the split-tooth model, upon one-day application, all tested cements imparted antibacterial activity to the dentin surfaces that they were in contact with (**Study III**). SEM and EDX observations confirmed the complete separation of the material and dentin surfaces, with occasional cement particles found on dentin surfaces or penetrating inside dentinal tubules. The materials altered the elemental composition of the adjacent dentin surfaces, as demonstrated by spectroscopic scans. The combination of these findings with the results from the antibacterial evaluation confirmed that the conferred antibacterial effect is a result of material leaching in the adjacent dentin tissue. Therefore, despite the buffering effect of dentin, it can still facilitate the antibacterial effect within the microenvironment. Dentin's buffering capacity had a greater impact over time on the commercial HCSCs, potentially due to the earlier completion of hydroxyl ion diffusion as discussed in Section 5.1.3, and on the BG-containing cements due to the overall decreased calcium hydroxide release profile that was discussed in Section 5.1.2. Findings on the BG-containing cements do not necessarily contradict studies reporting an enhanced antibacterial effect of BG in contact with mineralized tissues (i.e dentin powder or bone)<sup>366-368</sup>. This enhancement is attributed to increased BG dissolution, and thus elevated silica and pH levels<sup>366-368</sup>. However, this effect might be less potent than that of the replaced tricalcium silicate cement.

Furthermore, the potential of BG to induce dentin remineralization<sup>500</sup> could be further investigated in conjunction with its antibacterial characteristics. While the examination of that aspect was beyond the scope of the current study, it is worth noting that, as mentioned above, there was no consistent pattern of dentinal tubule coverage from any of the HCSCs, including the BG-containing cements. The characterization of the interfaces did not reveal any particular distinctions among the HCSCs, apart from the migration of SNPs to dentin, or the presence of the BG particles in the bulk of the respective BG-containing materials. Previous investigations of the dentin/HCSC interfacial characteristics have yielded somewhat contradictory results<sup>243,248,249</sup> as it was pointed out in Section 1.2.1.3, with findings being influenced by the evaluation methods that are used.

## 6. Conclusions

The following conclusions can be extracted:

- Incorporation of 2 mg/ml silver nanoparticles into an experimental HCSC resulted in a modest improvement of the antibacterial effect. Although it did not enhance the inhibition of bacterial adherence, it improved the bactericidal effect in water leachates, but not in a serum-containing environment. Additionally, it increased the antibacterial potential for longer interaction periods.
- Replacement of tricalcium silicate cement by bioactive glass in the HCSC reduced the calcium hydroxide release, which subsequently compromised the indirect contact antibacterial efficacy of the cement. It diminished, also, the antibacterial effect of dentin surfaces exposed to TZ-bg20 and, to a greater extent, to TZ-bg40.
- Differences in the surface characteristics of experimental HCSCs, resulting from the inclusion of SNPs and BG, did not influence their bacterial adhesion pattern.
- The inclusion of additives in the manufacturing of commercial HCSCs resulted in notable changes in their physico-chemical properties and biological activity.
- Exposure of HCSCs to FBS induced surface changes but did not affect the bacterial adhesion.
- Environmental conditions, i.e immersion medium and aging period, significantly affected the materials' leaching properties.
- Aging of HCSCs in FBS had a detrimental effect on their antibacterial properties compared to aging in water.
- Dentin surfaces had a residual antibacterial effect after a one-day application of both experimental and commercial HCSCs on them.
- Assessing the clinical properties of HCSCs in a laboratory setting warrants consideration of the environmental conditions. Laboratory studies should thus include experimental parameters that offer a more accurate clinical representation.





## 7. Future Perspectives

The use of hydraulic calcium silicate cements in a variety of endodontic procedures<sup>46,118,119</sup> has been established for three decades. The first cement, MTA, introduced for endodontic surgical applications, has undergone extensive laboratory and clinical research, which has enhanced our understanding in the basic chemistry of this material. At the same time, the influx of numerous commercial HCSCs into the dental field has introduced several modified compositions that often lack comprehensive research and evidence prior to clinical application or even full manufacturer documentation. The chemistry in the recent types of HCSCs differs, e.g., by the amount of the calcium silicates<sup>501</sup>, which leads to distinct hydration characteristics<sup>121</sup>.

Thus, on one side, we have a solid understanding of the cements' hydration reaction behavior, enabling us to focus on improving existing formulations' limitations. On the other side, we must contend with the new materials claiming distinctions from previous market formulations, often with limited supporting evidence. All the while, the lack of standardized models specifically designed for HCSCs, renders the direct comparisons of results from laboratory studies difficult<sup>121</sup>.

The replacement of the Portland cement with tricalcium silicate cement and the substitution of bismuth oxide with inert radiopacifiers in MTA have been supported by substantial laboratory and clinical evidence in materials that have been in use for over a decade now<sup>502</sup>. However, despite the advances in material development, especially since the introduction of HCSCs, the significance of the currently available materials on clinical outcome remains unclear<sup>83,503</sup>. This also raises the question of whether materials like IRM, which has several decades of clinical application but lacks the biological interaction of HCSCs, will/should eventually be replaced.

As a basic principle, enhancement of target properties of HCSCs is desirable, provided that such modifications do not compromise the already established beneficial material characteristics. While being theoretically an ideal scenario, achieving all desired properties simultaneously is not practically feasible<sup>120</sup>. What can be accomplished is a shift in the balance, favoring specific material characteristics over others, on the condition

that any undesired changes are minor and deemed acceptable. In the case of HCSCs, it is prudent to conclude that it is the hydration reaction that shall not be negatively affected by any potential alterations.

The modifications of the experimental HCSC by incorporation of silver nanoparticles or bioactive glass in the current thesis, aimed to enhance our understanding of the interplay between the physico-chemical characteristics of the materials and their biological activity. The overarching aim was to enhance the biological properties of the test cements, with particular focus in the antibacterial properties and screening of cytocompatibility. The inclusion of Biodentine, a thoroughly researched commercial HCSC that contains chemical additives, provided additional insights into this perspective. Moreover, we focused on the impact of the local microenvironment, due to the evidence indicating variations in the HCSCs' behavior under different clinical applications.

The current thesis provides insights into the specific roles of the compounds examined in conjunction with tricalcium silicate cement. Additionally, our findings offer a broader understanding of the interplay between changes in physico-chemical attributes and their associated antibacterial effects.

In light of the above, the following aspects warrant further investigation:

- Assessment of the effect of bioactive glass as additions to the HCSC, without removing an amount of the tricalcium silicate cement. As previously noted, the incorporation of BG in these formulations, with its ionic release profile, could potentially complement the material rather than contemplating for the loss of reactivity due to the decrease in the amount of tricalcium silicate cement.
- Investigation of the inflammatory potential of HCSCs alongside their antibacterial effect. The direct interaction of materials for endodontic surgery with the periodontal ligament and possibly the alveolar bone gives prominence to the importance of biocompatibility behavior. Notably, chronic inflammation with accompanied tissue destruction is usually prevalent in the endodontic surgical field. Modulation of inflammation and potential stimulation of the immune system towards healing are valuable attributes in that perspective. These properties should be thoroughly assessed in conjunction with the

antibacterial potential to explore the balance between immunomodulation and adequate antibacterial profile.

- Exploring various formulations of silver nanoparticles in HCSCs within the same study design is warranted to determine whether the modest effect observed in the current study is due to the potential inefficacy of the existing formulation or other factors.
- A thorough physico-chemical characterization, cytocompatibility screening and assessment with complex antibacterial models should be conducted once an experimental formulation seems to provide initial positive evidence of antibacterial enhancement.
- Development of standardized protocols specific to HCSCs and their clinical applications. Currently, ISO tests are available for endodontic sealers, but not for materials for endodontic surgical procedures. Furthermore, due to their chemical uniqueness in terms of the reactive nature of calcium hydroxide, testing of HCSCs with the available ISO standards might not be relevant<sup>436</sup>. In addition to the criticism directed at ISO standards for utilizing oversimplified models<sup>120</sup>, the development of assays that can facilitate a consistent characterization of the physico-chemical attributes of HCSCs and other relevant properties, while considering clinical perspectives, particularly the endodontic surgical setting, is crucial. These assays are necessary for a more comprehensive evaluation of existing research data, avoiding redundant studies with only minor model variations, and focusing on further improvements in current formulations. In addition, the implementation of more stringent criteria in the safety data sheets of commercial materials, providing a detailed report of their constituents, accompanied by comprehensive testing before market approval, can contribute to this direction.



## Bibliography

1. Haug, S. R., Kim, S. & Heyeraas, K. J. Structure and function of the pulp–dentin complex. In *Ingle's Endodontics*, 7<sup>th</sup> edn (eds Rotstein, I. & Ingle, J. I.) 59-84 (PMPH, 2019).
2. Nanci, A. Periodontium. In *Ten Cate's Oral Histology*, 9<sup>th</sup> edn (ed Nanci, A.) 205-232 (Mosby, 2013).
3. Bergreen, E., Bletsa, A. & Heyeraas, K. J. Circulation in normal and inflamed dental pulp. *Endod. Top.* **17**, 2-11 (2007).
4. Tjäderhane, L. & Paju, S. Dentin-pulp and periodontal anatomy and physiology. In *Essential Endodontology*, 3<sup>rd</sup> edn (ed Ørstavik, D.) 11-58 (Wiley-Blackwell-Blackwell, 2019).
5. Merriam-Webster.com Dictionary – Endodontics. <https://www.merriam-webster.com/dictionary/endodontics> (6 December 2023).
6. American Association of Endodontists. Glossary of endodontic terms, 10<sup>th</sup> edn (2020). At <https://www.aae.org/specialty/clinical-resources/glossary-endodontic-terms/> (6 December 2023).
7. Ørstavik, D. Apical periodontitis: microbial infection and host responses. In *Essential Endodontology*, 3<sup>rd</sup> edn (ed Ørstavik, D.) 1-10 (Wiley-Blackwell, 2019).
8. Nair, P. N. Pathogenesis of apical periodontitis and the causes of endodontic failures. *Crit. Rev. Oral Biol. Med.* **15**, 348-381 (2004).
9. Siqueira, J. F., Jr & Rôças, I. N. Endodontic infections and the etiology of apical periodontitis – an overview. In *Treatment of Endodontic Infections*, 2<sup>nd</sup> edn (eds Siqueira, J. F., Jr & Rôças, I. N.) 5-16 (Quintessence Publishing, 2022).
10. Cruse, W. P. & Bellizzi, R. A historic review of endodontics, 1689-1963, part 1. *J. Endod.* **6**, 495-499 (1980).
11. Ring, M. E. Anton van Leeuwenhoek and the tooth-worm. *J. Am. Dent. Assoc.* **83**, 999-1001 (1971).
12. Dobel, C. Antony van Leeuwenhoek and his “Little Animals” (Harcourt, 1932).
13. Miller, W. D. An introduction to the study of the bacterio-pathology of the dental pulp. *Dent. Cosmos* **36**, 505-528 (1894).
14. Kakehashi, S., Stanley, H. R. & Fitzgerald, R. J. The effects of surgical exposures of dental pulps in germ-free and conventional laboratory rats. *Oral Surg. Oral Med. Oral Pathol.* **20**, 340-349 (1965).
15. Sundqvist, G. Bacteriological studies of necrotic dental pulps (University of Umea, 1976).
16. Möller, A. J., Fabricius, L., Dahlén, G., Ohman, A. E. & Heyden, G. Influence on periapical tissues of indigenous oral bacteria and necrotic pulp tissue in monkeys. *Scand. J. Dent. Res.* **89**, 475-484 (1981).
17. Siqueira, J. F., Jr. & Rôças, I. N. Diversity of endodontic microbiota revisited. *J. Dent. Res.* **88**, 969-981 (2009).

18. Siqueira, J. F., Jr. & Rôças, I. N. Present status and future directions: Microbiology of endodontic infections. *Int. Endod. J.* **55**, 512-530 (2022).
19. Siqueira, J. F., Jr. & Rôças, I. N. Exploiting molecular methods to explore endodontic infections: part 2--redefining the endodontic microbiota. *J. Endod.* **31**, 488-498 (2005).
20. Donlan, R. M. & Costerton, J. W. Biofilms: survival mechanisms of clinically relevant microorganisms. *Clin. Microbiol. Rev.* **15**, 167-193 (2002).
21. Burmølle, M., Ren, D., Bjarnsholt, T. & Sørensen, S. J. Interactions in multispecies biofilms: do they actually matter? *Trends Microbiol.* **22**, 84-91 (2014).
22. Li, L. et al. Analyzing endodontic infections by deep coverage pyrosequencing. *J. Dent. Res.* **89**, 980-984 (2010).
23. Machado de Oliveira, J. C. et al. Bacterial community profiles of endodontic abscesses from Brazilian and USA subjects as compared by denaturing gradient gel electrophoresis analysis. *Oral Microbiol. Immunol.* **22**, 14-18 (2007).
24. Rôças, I. N., Siqueira, J. F., Jr., Aboim, M. C. & Rosado, A. S. Denaturing gradient gel electrophoresis analysis of bacterial communities associated with failed endodontic treatment. *Oral Surg. Oral Med. Oral Pathol.* **98**, 741-749 (2004).
25. Siqueira, J. F., Jr. & Rôças, I. N. Community as the unit of pathogenicity: an emerging concept as to the microbial pathogenesis of apical periodontitis. *Oral Surg. Oral Med. Oral Pathol.* **107**, 870-878 (2009).
26. Siqueira, J. F., Jr., Alves, F. R. & Rôças, I. N. Pyrosequencing analysis of the apical root canal microbiota. *J. Endod.* **37**, 1499-1503 (2011).
27. Ozok, A. R. et al. Ecology of the microbiome of the infected root canal system: a comparison between apical and coronal root segments. *Int. Endod. J.* **45**, 530-541 (2012).
28. Rôças, I. N., Alves, F. R., Santos, A. L., Rosado, A. S. & Siqueira, J. F., Jr. Apical root canal microbiota as determined by reverse-capture checkerboard analysis of cryogenically ground root samples from teeth with apical periodontitis. *J. Endod.* **36**, 1617-1621 (2010).
29. Siqueira, J. F., Jr. Endodontic infections: concepts, paradigms, and perspectives. *Oral Surg. Oral Med. Oral Pathol.* **94**, 281-293 (2002).
30. Peters, O. A., Peters, C. I. & Basrani, B. Cleaning and shaping of the root canal system. In *Cohen's Pathways of the Pulp*, 12<sup>th</sup> edn (eds Berman, L. H. & Hargreaves, K. M.) 456-536 (Elsevier, 2020).
31. American Association of Endodontists. Guide to clinical endodontics, 6<sup>th</sup> edn (2019). At <https://www.aae.org/specialty/download/guide-to-clinical-endodontics/> (6 December 2023).
32. European Society of Endodontology. Quality guidelines for endodontic treatment: consensus report of the European Society of Endodontology. *Int Endod. J.* **39**, 921-930 (2006).
33. Zandi, H. et al. Outcome of endodontic retreatment using 2 root canal irrigants and influence of infection on healing as determined by a molecular method: a randomized clinical trial. *J. Endod.* **45**, 1089-1098.e5 (2019).

34. Siqueira, J. F., Jr. & Rôças, I. N. Clinical implications and microbiology of bacterial persistence after treatment procedures. *J. Endod.* **34**, 1291-1301.e3 (2008).
35. Gulabivala, K. & Ng, Y. L. Factors that affect the outcomes of root canal treatment and retreatment—a reframing of the principles. *Int. Endod. J.* **56**, 82-115 (2023).
36. Siqueira, J. F., Jr. Aetiology of root canal treatment failure: why well-treated teeth can fail. *Int. Endod. J.* **34**, 1-10 (2001).
37. Siqueira, J. F., Jr. Periapical actinomycosis and infection with *Propionibacterium propionicum*. *Endod. Top.* **6**, 78-95 (2003).
38. Ricucci, D., Siqueira, J. F., Jr., Bate, A. L. & Pitt Ford, T. R. Histologic investigation of root canal-treated teeth with apical periodontitis: a retrospective study from twenty-four patients. *J. Endod.* **35**, 493-502 (2009).
39. Duncan, H. F. et al. Treatment of pulpal and apical disease: the European Society of Endodontology (ESE) S3-level clinical practice guideline. *Int. Endod. J.* **56**, 238-295 (2023).
40. Setzer, F. C. & Karabucak, B. Surgical endodontics. In *Essential Endodontology*, 3<sup>rd</sup> edn (ed Ørstavik, D.) 345-385 (Wiley-Blackwell, 2019).
41. Ørstavik, D. Endodontic filling materials. *Endod. Top.* **31**, 53-67 (2014).
42. Grossman, L. I. *Endodontic practice*, 7th edn (Lea & Febiger Co, 1970).
43. Grossman, L. I. Some observations in root canal filling materials. In *Transactions of the Second International Conference on Endodontics* (ed Grossman, L. I.) (University of Pennsylvania, 1958).
44. Trope, M., Bunes, A. & Debelian, G. Root filling materials and techniques: bioceramics a new hope? *Endod. Top.* **32**, 86-96 (2015).
45. Ørstavik, D. Endodontic treatment of apical periodontitis. In *Essential Endodontology*, 3<sup>rd</sup> edn (ed Ørstavik, D.) 313-344 (Wiley-Blackwell, 2019).
46. Camilleri, J. & Pertl, C. Root-end filling and perforation repair materials and techniques. In *Endodontic Materials in Clinical Practice* (ed Camilleri, J.) 219-261 (Wiley-Blackwell, 2021).
47. Braz-Silva, P. H. et al. Inflammatory profile of chronic apical periodontitis: a literature review. *Acta Odontol. Scand.* **77**, 173-180 (2019).
48. Ørstavik, D. Obturation of root canals. In *Endodontic Prognosis: Clinical Guide for Optimal Treatment Outcome* (eds Chugal, N. & Lin, L. M.) 141-159 (Springer, 2017).
49. Camilleri, J. Classification of hydraulic cements used in dentistry. *Front. Dent. Med.* **1** (2020).
50. Johnson, B. R. Considerations in the selection of a root-end filling material. *Oral Surg. Oral Med. Oral Pathol. Oral Radiol. Endod.* **87**, 398-404 (1999).
51. Gutmann, J. L. & Harrison J. H. *Surgical Endodontics*. (Blackwell Scientific Publications, 1991).
52. Torabinejad, M. & Pitt Ford, T. R. Root end filling materials: a review. *Endod. Dent. Traumatol.* **12**, 161-178 (1996).
53. Block, R. M. & Bushell, A. retrograde amalgam procedures for mandibular posterior teeth. *J. Endod.* **8**, 107-112 (1982).

54. Friedman, S. Retrograde approaches in endodontic therapy. *Endod. Dent. Traumatol.* **7**, 97-107 (1991).
55. ElDeeb, M. E., ElDeeb, M., Tabibi, A. & Jensen, J. R. An evaluation of the use of amalgam, cavit, and calcium hydroxide in the repair of furcation perforations. *J. Endod.* **8**, 459-466 (1982).
56. Bronkhorst, M. A., Bergé, S. J., Van Damme, P. A., Borstlap, W. A. & Merckx, M. A. [Use of root-end filling materials in a surgical apical endodontic treatment in the Netherlands]. *Ned. Tijdschr. Tandheelkd.* **115**, 423-427 (2008).
57. Bodrumlu, E. Biocompatibility of retrograde root filling materials: a review. *Aust. Endod. J.* **34**, 30-35 (2008).
58. Tronstad, L. & Wennberg, A. In vitro assessment of the toxicity of filling materials. *Int. Endod. J.* **13**, 131-138 (1980).
59. Eley, B. M. & Cox, S. W. The release, absorption and possible health effects of mercury from dental amalgam: a review of recent findings. *Br. Dent. J.* **175**, 355-362 (1993).
60. Ravnholt, G. Corrosion current and pH rise around titanium coupled to dental alloys. *Scand. J. Dent. Res.* **96**, 466-472 (1988).
61. Harrison, J. D., Rowley, P. S. & Peters, P. D. Amalgam tattoos: light and electron microscopy and electron-probe micro-analysis. *J. Pathol.* **121**, 83-92 (1977).
62. Eley, B. M. Tissue reactions to implanted dental amalgam, including assessment by energy dispersive x-ray micro-analysis. *J. Pathol.* **138**, 251-272 (1982).
63. Dorn, S. O. & Gartner, A. H. Retrograde filling materials: a retrospective success-failure study of amalgam, EBA, and IRM. *J. Endod.* **16**, 391-393 (1990).
64. Setzer, F. C., Shah, S. B., Kohli, M. R., Karabucak, B. & Kim, S. Outcome of endodontic surgery: a meta-analysis of the literature--part 1: Comparison of traditional root-end surgery and endodontic microsurgery. *J. Endod.* **36**, 1757-1765 (2010).
65. Sidhu, S. K. Glass-ionomer cement restorative materials: a sticky subject? *Aust. Dent. J.* **56**, 23-30 (2011).
66. Niederman, R. & Theodosopoulou, J. N. A systematic review of in vivo retrograde obturation materials. *Int. Endod. J.* **36**, 577-585 (2003).
67. Sidhu, S. K. & Nicholson, J. W. A review of glass-ionomer cements for clinical dentistry. *J. Funct. Biomater.* **7**, 16 (2016).
68. Rud, J., Rud, V. & Munksgaard, E. C. Retrograde root filling with dentin-bonded modified resin composite. *J. Endod.* **22**, 477-480 (1996).
69. von Arx, T., Hänni, S. & Jensen, S. S. Clinical results with two different methods of root-end preparation and filling in apical surgery: mineral trioxide aggregate and adhesive resin composite. *J. Endod.* **36**, 1122-1129 (2010).
70. Rud, J., Munksgaard, E. C., Andreasen, J. O., Rud, V. & Asmussen, E. Retrograde root filling with composite and a dentin-bonding agent. 1. *Endod. Dent. Traumatol.* **7**, 118-125 (1991).
71. Rakich, D. R., Wataha, J. C., Lefebvre, C. A. & Weller, R. N. Effects of dentin bonding agents on macrophage mitochondrial activity. *J. Endod.* **24**, 528-533 (1998).



- 
- 72 Rakich, D. R., Wataha, J. C., Lefebvre, C. A. & Weller, R. N. Effect of dentin bonding agents on the secretion of inflammatory mediators from macrophages. *J. Endod.* **25**, 114-117 (1999).
- 73 Vahid, A., Hadjati, J., Kermanshah, H. & Ghabraei, S. Effects of cured dentin bonding materials on human monocyte viability. *Oral Surg. Oral Med. Oral Pathol Oral Radiol. Endod.* **98**, 619-621 (2004).
- 74 Al-Sa'eed, O. R., Al-Hiyasat, A. S. & Darmani, H. The effects of six root-end filling materials and their leachable components on cell viability. *J. Endod.* **34**, 1410-1414 (2008).
- 75 Haglund, R. et al. Effects of root-end filling materials on fibroblasts and macrophages in vitro. *Oral Surg. Oral Med. Oral Pathol. Oral Radiol. Endod.* **95**, 739-745 (2003).
- 76 Al-Hiyasat, A. S., Al-Sa'Eed, O. R. & Darmani, H. Quality of cellular attachment to various root-end filling materials. *J. Appl. Oral Sci.* **20**, 82-88 (2012).
- 77 Ozbas, H., Yaltirik, M., Bilgic, B. & Issever, H. Reactions of connective tissue to compomers, composite and amalgam root-end filling materials. *Int. Endod. J.* **36**, 281-287 (2003).
- 78 Eldeniz, A. U., Hadimli, H. H., Ataoglu, H. & Orstavik, D. Antibacterial effect of selected root-end filling materials. *J. Endod.* **32**, 345-349 (2006).
- 79 Rud, J., Rud, V. & Munksgaard, E. C. Long-term evaluation of retrograde root filling with dentin-bonded resin composite. *J. Endod.* **22**, 90-93 (1996).
- 80 Jensen, S. S. et al. A prospective, randomized, comparative clinical study of resin composite and glass ionomer cement for retrograde root filling. *Clin. Oral Investig.* **6**, 236-243 (2002).
- 81 Yazdi, P. M. et al. Dentine-bonded resin composite (Retroplast) for root-end filling: a prospective clinical and radiographic study with a mean follow-up period of 8 years. *Int. Endod. J.* **40**, 493-503 (2007).
- 82 Kohli, M. R., Berenji, H., Setzer, F. C., Lee, S. M. & Karabucak, B. Outcome of endodontic surgery: a meta-analysis of the literature-part 3: comparison of endodontic microsurgical techniques with 2 different root-end filling materials. *J. Endod.* **44**, 923-931 (2018).
- 83 von Arx, T., Jensen, S. S., Hänni, S. & Friedman, S. Five-year longitudinal assessment of the prognosis of apical microsurgery. *J. Endod.* **38**, 570-579 (2012).
- 84 Garcia, G. F. Apicoectomy experimental. *Rev. Odontol.* **25**, 145-160 (1937).
- 85 Nicholls, E. The role of surgery in endodontics. *Br. Dent. J.* **118**, 59-71 (1965).
- 86 Yaccino, J. M., Walker, W. A., 3rd, Carnes, D. L., Jr. & Schindler, W. G. Longitudinal microleakage evaluation of Super-EBA as a root-end sealing material. *J. Endod.* **25**, 552-554 (1999).
- 87 Hume, W. R. In vitro studies on the local pharmacodynamics, pharmacology and toxicology of eugenol and zinc oxide-eugenol. *Int. Endod. J.* **21**, 130-134 (1988).
- 88 Markowitz, K., Moynihan, M., Liu, M. & Kim, S. Biologic properties of eugenol and zinc oxide-eugenol. A clinically oriented review. *Oral Surg. Oral Med. Oral Pathol. Oral Radiol. Endod.* **73**, 729-737 (1992).

- 89 Zhu, Q., Safavi, K. E. & Spangberg, L. S. Cytotoxic evaluation of root-end filling materials in cultures of human osteoblast-like cells and periodontal ligament cells. *J. Endod.* **25**, 410-412 (1999).
- 90 Torabinejad, M., Hong, C. U., Pitt Ford, T. R. & Kettering, J. D. Cytotoxicity of four root end filling materials. *J. Endod.* **21**, 489-492 (1995).
- 91 Zhu, Q., Haglund, R., Safavi, K. E. & Spangberg, L. S. Adhesion of human osteoblasts on root-end filling materials. *J. Endod.* **26**, 404-406 (2000).
- 92 Keiser, K., Johnson, C. C. & Tipton, D. A. Cytotoxicity of mineral trioxide aggregate using human periodontal ligament fibroblasts. *J. Endod.* **26**, 288-291 (2000).
- 93 Balto, H. & Al-Nazhan, S. Attachment of human periodontal ligament fibroblasts to 3 different root-end filling materials: scanning electron microscope observation. *Oral Surg. Oral Med. Oral Pathol. Oral Radiol. Endod.* **95**, 222-227 (2003).
- 94 Bonson, S., Jeansonne, B. G. & Lallier, T. E. Root-end filling materials alter fibroblast differentiation. *J. Dent. Res.* **83**, 408-413 (2004).
- 95 Osorio, R. M., Hefti, A., Vertucci, F. J. & Shawley, A. L. Cytotoxicity of endodontic materials. *J. Endod.* **24**, 91-96 (1998).
- 96 Coaguila-Llerena, H., Vaisberg, A. & Velasquez-Huaman, Z. In vitro cytotoxicity evaluation of three root-end filling materials in human periodontal ligament fibroblasts. *Braz. Dent. J.* **27**, 187-191 (2016).
- 97 Huang, T. H. et al. Biocompatibility of human osteosarcoma cells to root end filling materials. *J. Biomed. Mater. Res. B Appl. Biomater.* **72**, 140-145 (2005).
- 98 Mozayeni, M. A., Milani, A. S., Marvasti, L. A. & Asgary, S. Cytotoxicity of calcium enriched mixture cement compared with mineral trioxide aggregate and intermediate restorative material. *Aust. Endod. J.* **38**, 70-75 (2012).
- 99 Ma, J., Shen, Y., Stojcic, S. & Haapasalo, M. Biocompatibility of two novel root repair materials. *J. Endod.* **37**, 793-798 (2011).
- 100 Pitt Ford, T. R., Andreasen, J. O., Dorn, S. O. & Kariyawasam, S. P. Effect of various zinc oxide materials as root-end fillings on healing after replantation. *Int. Endod. J.* **28**, 273-278 (1995).
- 101 Pitt Ford, T. R., Andreasen, J. O., Dorn, S. O. & Kariyawasam, S. P. Effect of super-EBA as a root end filling on healing after replantation. *J. Endod.* **21**, 13-15 (1995).
- 102 Pitt Ford, T. R., Andreasen, J. O., Dorn, S. O. & Kariyawasam, S. P. Effect of IRM root end fillings on healing after replantation. *J. Endod.* **20**, 381-385 (1994).
- 103 Economides, N., Pantelidou, O., Kokkas, A. & Tziafas, D. Short-term periradicular tissue response to mineral trioxide aggregate (MTA) as root-end filling material. *Int. Endod. J.* **36**, 44-48 (2003).
- 104 Tawil, P. Z. et al. Periapical microsurgery: an in vivo evaluation of endodontic root-end filling materials. *J. Endod.* **35**, 357-362 (2009).
- 105 Slutzky, H., Slutzky-Goldberg, I., Weiss, E. I. & Matalon, S. Antibacterial properties of temporary filling materials. *J. Endod.* **32**, 214-217 (2006).
- 106 Dragland, I. S., Wellendorf, H., Kopperud, H., Stenhagen, I. & Valen, H. Investigation on the antimicrobial activity of chitosan-modified zinc oxide-eugenol cement. *Biomater. Investig. Dent.* **6**, 99-106 (2019).

- 107 Prestegard, H. et al. Antibacterial activity of various root canal sealers and root-end filling materials in dentin blocks infected ex vivo with *Enterococcus faecalis*. *Acta Odontol. Scand.* **72**, 970-976 (2014).
- 108 Koçak, M. M., Koçak, S., Oktay, E. A., Kiliç, A. & Yaman, S. D. In vitro evaluation of the minimum bactericidal concentrations of different root-end filling materials. *J. Contemp. Dent. Pract.* **14**, 371-374 (2013).
- 109 Wälivaara, D., Abrahamsson, P., Fogelin, M. & Isaksson, S. Super-EBA and IRM as root-end fillings in periapical surgery with ultrasonic preparation: a prospective randomized clinical study of 206 consecutive teeth. *Oral Surg. Oral Med. Oral Pathol. Oral Radiol. Endod.* **112**, 258-263 (2011).
- 110 Wälivaara, D. A., Abrahamsson, P., Sämfors, K. A. & Isaksson, S. Periapical surgery using ultrasonic preparation and thermoplasticized gutta-percha with AH Plus sealer or IRM as retrograde root-end fillings in 160 consecutive teeth: a prospective randomized clinical study. *Oral Surg. Oral Med. Oral Pathol. Oral Radiol. Endod.* **108**, 784-79 (2009).
- 111 Lindeboom, J. A., Frenken, J. W., Kroon, F. H. & van den Akker, H. P. A comparative prospective randomized clinical study of MTA and IRM as root-end filling materials in single-rooted teeth in endodontic surgery. *Oral Surg. Oral Med. Oral Pathol. Oral Radiol. Endod.* **100**, 495-500 (2005).
- 112 Rubinstein, R. A. & Kim, S. Short-term observation of the results of endodontic surgery with the use of a surgical operation microscope and super-EBA as root-end filling material. *J. Endod.* **25**, 43-48 (1999).
- 113 Song, M. & Kim, E. A prospective randomized controlled study of mineral trioxide aggregate and super ethoxy-benzoic acid as root-end filling materials in endodontic microsurgery. *J. Endod.* **38**, 875-879 (2012).
- 114 Chong, B. S., Pitt Ford, T. R. & Hudson, M. B. A prospective clinical study of Mineral Trioxide Aggregate and IRM when used as root-end filling materials in endodontic surgery. *Int. Endod. J.* **36**, 520-526 (2003).
- 115 Rubinstein, R. A. & Kim, S. Long-term follow-up of cases considered healed one year after apical microsurgery. *J. Endod.* **28**, 378-383 (2002).
- 116 Kim, S., Song, M., Shin, S. J. & Kim, E. A randomized controlled study of Mineral Trioxide Aggregate and Super Ethoxybenzoic Acid as root-end filling materials in endodontic microsurgery: long-term outcomes. *J. Endod.* **42**, 997-1002 (2016).
- 117 Setzer, F. C. & Kratchman, S. I. Present status and future directions: Surgical endodontics. *Int. Endod. J.* **55**, 1020-1058 (2022).
- 118 American Association of Endodontists. AAE position statement on vital pulp therapy (2021). At [https://www.aae.org/wp-content/uploads/2021/05/VitalPulpTherapyPositionStatement\\_v2.pdf](https://www.aae.org/wp-content/uploads/2021/05/VitalPulpTherapyPositionStatement_v2.pdf) (9 January 2024).
- 119 Donnermeyer, D., Bürklein, S., Dammaschke, T. & Schäfer, E. Endodontic sealers based on calcium silicates: a systematic review. *Odontology* **107**, 421-436 (2019).
- 120 Darvell, B. W. Introduction. In *Endodontic Materials in Clinical Practice* (ed Camilleri, J.) 1-13 (Wiley-Blackwell, 2021).

- 121 Camilleri, J., Atmeh, A., Li, X. & Meschi, N. Present status and future directions - hydraulic materials for endodontic use. *Int. Endod. J.* **55**, 710-777 (2022).
- 122 Witte. The filling of a root canal with Portland cement. *German Q. Dent J. Central Assoc. German Dent.* **18**, 153–154 (1878).
- 123 Glasser, F. P. The burning of Portland Cement. In *Lea's Chemistry of Cement and Concrete*, 4<sup>th</sup> edn (ed Hewlett, P. C.) 195-240 (Butterworth-Heinemann, 1998).
- 124 Camilleri, J. Mineral trioxide aggregate: present and future developments. *Endod. Top.* **32**, 31-46 (2015).
- 125 De Deus, G., Camilleri, J., Primus, C. M., Duarte, M. A. H. & Bramante, C. M. Introduction to Mineral Trioxide Aggregate. In *Mineral Trioxide Aggregate in Dentistry: From Preparation to Application* (ed Josette Camilleri) 1-17 (Springer, 2014).
- 126 Torabinejad, M. & White, J. D. *Tooth Filling Material and Method of Use*. US Patent number: 5415547 (1993).
- 127 Torabinejad, M., Hong, C. U., McDonald, F. & Pitt Ford, T. R. Physical and chemical properties of a new root-end filling material. *J. Endod.* **21**, 349-353 (1995).
- 128 Torabinejad, M., Hong, C. U., Pitt Ford, T. R. & Kettering, J. D. Antibacterial effects of some root end filling materials. *J. Endod.* **21**, 403-406 (1995).
- 129 Ford, T. R., Torabinejad, M., Abedi, H. R., Bakland, L. K. & Kariyawasam, S. P. Using mineral trioxide aggregate as a pulp-capping material. *J. Am. Dent. Assoc.* **127**, 1491-1494 (1996).
- 130 Torabinejad, M., Hong, C. U., Lee, S. J., Monsef, M. & Pitt Ford, T. R. Investigation of mineral trioxide aggregate for root-end filling in dogs. *J. Endod.* **21**, 603-608 (1995).
- 131 Torabinejad, M., Hong, C. U., Pitt Ford, T. R. & Kaiyawasam, S. P. Tissue reaction to implanted super-EBA and mineral trioxide aggregate in the mandible of guinea pigs: a preliminary report. *J. Endod.* **21**, 569-571 (1995).
- 132 Ford, T. R., Torabinejad, M., McKendry, D. J., Hong, C. U. & Kariyawasam, S. P. Use of mineral trioxide aggregate for repair of furcal perforations. *Oral Surg. Oral Med. Oral Pathol. Oral Radiol. Endod.* **79**, 756-763 (1995).
- 133 Arens, D. E. & Torabinejad, M. Repair of furcal perforations with mineral trioxide aggregate: two case reports. *Oral Surg. Oral Med. Oral Pathol. Oral Radiol. Endod.* **82**, 84-88 (1996).
- 134 Asgary, S., Parirokh, M., Eghbal, M. J., Stowe, S. & Brink, F. A qualitative X-ray analysis of white and grey mineral trioxide aggregate using compositional imaging. *J. Mater. Sci. Mater. Med.* **17**, 187-191 (2006).
- 135 Torabinejad, M. & Chivian, N. Clinical applications of mineral trioxide aggregate. *J. Endod.* **25**, 197-205 (1999).
- 136 Massi, S. et al. pH, calcium ion release, and setting time of an experimental mineral trioxide aggregate-based root canal sealer. *J. Endod.* **37**, 844-846 (2011).
- 137 Hashem, A. A. & Hassanien, E. E. ProRoot MTA, MTA-Angelus and IRM used to repair large furcation perforations: sealability study. *J. Endod.* **34**, 59-61 (2008).

- 138 Camilleri, J. Hydration mechanisms of mineral trioxide aggregate. *Int. Endod. J.* **40**, 462-470 (2007).
- 139 Camilleri, J. Characterization of hydration products of mineral trioxide aggregate. *Int. Endod. J.* **41**, 408-417 (2008).
- 140 de Vasconcelos, B. C. et al. Evaluation of pH and calcium ion release of new root-end filling materials. *Oral Surg. Oral Med. Oral Pathol. Oral Radiol. Endod.* **108**, 135-139 (2009).
- 141 Chng, H. K., Islam, I., Yap, A. U., Tong, Y. W. & Koh, E. T. Properties of a new root-end filling material. *J. Endod.* **31**, 665-668 (2005).
- 142 Marciano, M. A. et al. Assessment of color stability of white mineral trioxide aggregate angelus and bismuth oxide in contact with tooth structure. *J. Endod.* **40**, 1235-1240 (2014).
- 143 Camilleri, J., Montesin, F. E., Papaioannou, S., McDonald, F. & Pitt Ford, T. R. Biocompatibility of two commercial forms of mineral trioxide aggregate. *Int. Endod. J.* **37**, 699-704 (2004).
- 144 Min, K. S. et al. The induction of heme oxygenase-1 modulates bismuth oxide-induced cytotoxicity in human dental pulp cells. *J. Endod.* **33**, 1342-1346 (2007).
- 145 Angelus Dental Products Industry. MTA Angelus (2021). At <https://angelus.ind.br/assets/uploads/2019/12/27102021-MTA-ANGELUS-Bula.pdf> (10 January 2024).
- 146 Pistorius, A., Willershausen, B. & Briseno Marroquin, B. Effect of apical root-end filling materials on gingival fibroblasts. *Int. Endod. J.* **36**, 610-615 (2003).
- 147 Damas, B. A., Wheeler, M. A., Bringas, J. S. & Hoen, M. M. Cytotoxicity comparison of mineral trioxide aggregates and EndoSequence bioceramic root repair materials. *J. Endod.* **37**, 372-375 (2011).
- 148 Samyuktha, V. et al. Cytotoxicity evaluation of root repair materials in human-cultured periodontal ligament fibroblasts. *J. Conserv. Dent.* **17**, 467-470 (2014).
- 149 Kim, E. C. et al. Evaluation of the radiopacity and cytotoxicity of Portland cements containing bismuth oxide. *Oral Surg. Oral Med. Oral Pathol. Oral Radiol. Endod.* **105**, e54-57 (2008).
- 150 Margunato, S., Tasli, P. N., Aydin, S., Karapinar Kazandag, M. & Sahin, F. In vitro evaluation of ProRoot MTA, Biodentine, and MM-MTA on human alveolar bone marrow stem cells in terms of biocompatibility and mineralization. *J. Endod.* **41**, 1646-1652 (2015).
- 151 Karygianni, L. et al. The effects of various mixing solutions on the biocompatibility of mineral trioxide aggregate. *Int. Endod. J.* **49**, 561-573 (2016).
- 152 Sequeira, D. B. et al. Effects of a new bioceramic material on human apical papilla cells. *J. Funct. Biomater.* **16**, 9 (2018).
- 153 Costa, F., Sousa Gomes, P. & Fernandes, M. H. Osteogenic and angiogenic response to calcium silicate-based endodontic sealers. *J. Endod.* **42**, 113-119 (2016).
- 154 Lee, G. W. et al. Effects of newly-developed retrograde filling material on osteoblastic differentiation in vitro. *Dent. Mater. J.* **38**, 528-533 (2019).

- 155 Lee, B. N. et al. Effects of mineral trioxide aggregate mixed with hydration accelerators on osteoblastic differentiation. *J. Endod.* **40**, 2019-2023 (2014).
- 156 Souza, N. J., Justo, G. Z., Oliveira, C. R., Haun, M. & Bincoletto, C. Cytotoxicity of materials used in perforation repair tested using the V79 fibroblast cell line and the granulocyte-macrophage progenitor cells. *Int. Endod. J.* **39**, 40-47 (2006).
- 157 Scelza, M. Z. et al. Biodentine™ is cytocompatible with human primary osteoblasts. *Braz. Oral Res.* **31**, e81 (2017).
- 158 Koh, E. T., Torabinejad, M., Pitt Ford, T. R., Brady, K. & McDonald, F. Mineral trioxide aggregate stimulates a biological response in human osteoblasts. *J. Biomed. Mater. Res.* **37**, 432-439 (1997).
- 159 Koh, E. T., McDonald, F., Pitt Ford, T. R. & Torabinejad, M. Cellular response to Mineral Trioxide Aggregate. *J. Endod.* **24**, 543-547 (1998).
- 160 Deller-Quinn, M. & Perinpanayagam, H. Osteoblast expression of cytokines is altered on MTA surfaces. *Oral Surg. Oral Med. Oral Pathol. Oral Radiol. Endod.* **108**, 302-307 (2009).
- 161 Chen, I., Salhab, I., Setzer, F. C., Kim, S. & Nah, H. D. A new calcium silicate-based bioceramic material promotes human osteo- and odontogenic stem cell proliferation and survival via the extracellular signal-regulated kinase signaling pathway. *J. Endod.* **42**, 480-486 (2016).
- 162 Lee, B. N. et al. Effects of 3 endodontic bioactive cements on osteogenic differentiation in mesenchymal stem cells. *J. Endod.* **40**, 1217-1222 (2014).
- 163 Edrees, H. Y., Abu Zeid, S. T. H., Atta, H. M. & AlQriqri, M. A. Induction of osteogenic differentiation of mesenchymal stem cells by bioceramic root repair material. *Materials (Basel)* **12**, 2311 (2019).
- 164 Cintra, L. T. et al. Evaluation of subcutaneous and alveolar implantation surgical sites in the study of the biological properties of root-end filling endodontic materials. *J. Appl. Oral Sci.* **18**, 75-82 (2010).
- 165 Aguilari, F. G., Roberti Garcia, L. F. & Panzeri Pires-de-Souza, F. C. Biocompatibility of new calcium aluminate cement (EndoBinder). *J. Endod.* **38**, 367-371 (2012).
- 166 Mori, G. G., Teixeira, L. M., de Oliveira, D. L., Jacomini, L. M. & da Silva, S. R. Biocompatibility evaluation of biodentine in subcutaneous tissue of rats. *J. Endod.* **40**, 1485-1488 (2014).
- 167 Garcia Lda, F., Huck, C., Menezes de Oliveira, L., de Souza, P. P. & de Souza Costa, C. A. Biocompatibility of new calcium aluminate cement: tissue reaction and expression of inflammatory mediators and cytokines. *J. Endod.* **40**, 2024-2029 (2014).
- 168 Gomes-Filho, J. E. et al. Influence of diabetes mellitus on tissue response to MTA and its ability to stimulate mineralization. *Dent. Traumatol.* **31**, 67-72 (2015).
- 169 Silva, G. F., Tanomaru-Filho, M., Bernardi, M. I., Guerreiro-Tanomaru, J. M. & Cerri, P. S. Niobium pentoxide as radiopacifying agent of calcium silicate-based material: evaluation of physicochemical and biological properties. *Clin. Oral Investig.* **19**, 2015-2025 (2015).

- 170 Marciano, M. A., Guimaraes, B. M., Amoroso-Silva, P., Camilleri, J. & Hungaro Duarte, M. A. Physical and chemical properties and subcutaneous implantation of mineral trioxide aggregate mixed with propylene glycol. *J. Endod.* **42**, 474-479 (2016).
- 171 da Fonseca, T. S. et al. In vivo evaluation of the inflammatory response and IL-6 immunoexpression promoted by Biodentine and MTA Angelus. *Int. Endod. J.* **49**, 145-153 (2016).
- 172 Taha, N. A., Safadi, R. A. & Alwedaie, M. S. Biocompatibility evaluation of EndoSequence root repair paste in the connective tissue of rats. *J. Endod.* **42**, 1523-1528 (2016).
- 173 Khalil, W. A. & Abunasef, S. K. Can Mineral trioxide aggregate and nanoparticulate EndoSequence root repair material produce injurious effects to rat subcutaneous tissues? *J. Endod.* **41**, 1151-1156 (2015).
- 174 Moretton, T. R., Brown, C. E., Jr., Legan, J. J. & Kafrawy, A. H. Tissue reactions after subcutaneous and intraosseous implantation of mineral trioxide aggregate and ethoxybenzoic acid cement. *J. Biomed. Mater. Res.* **52**, 528-533 (2000).
- 175 Sousa, C. J. et al. A comparative histological evaluation of the biocompatibility of materials used in apical surgery. *Int. Endod. J.* **37**, 738-748 (2004).
- 176 da Fonseca, T. S. et al. Mast cells and immunoexpression of FGF-1 and Ki-67 in rat subcutaneous tissue following the implantation of Biodentine and MTA Angelus. *Int. Endod. J.* **52**, 54-67 (2019).
- 177 Dreger, L. A. et al. Mineral trioxide aggregate and Portland cement promote biomineralization in vivo. *J. Endod.* **38**, 324-329 (2012).
- 178 Reyes-Carmona, J. F. et al. Host-mineral trioxide aggregate inflammatory molecular signaling and biomineralization ability. *J. Endod.* **36**, 1347-1353 (2010).
- 179 Wälivaara, D. et al. Periapical tissue response after use of intermediate restorative material, gutta-percha, reinforced zinc oxide cement, and mineral trioxide aggregate as retrograde root-end filling materials: a histologic study in dogs. *J. Oral Maxillofac. Surg.* **70**, 2041-2047 (2012).
- 180 Chen, I. et al. Healing after root-end microsurgery by using mineral trioxide aggregate and a new calcium silicate-based bioceramic material as root-end filling materials in dogs. *J. Endod.* **41**, 389-399 (2015).
- 181 Alazrag, M. A., Abu-Seida, A. M., El-Batouty, K. M. & El Ashry, S. H. Marginal adaptation, solubility and biocompatibility of TheraCal LC compared with MTA-angelus and biodentine as a furcation perforation repair material. *BMC Oral Health* **20**, 298 (2020).
- 182 Abboud, K. M., Abu-Seida, A. M., Hassanien, E. E. & Tawfik, H. M. Biocompatibility of NeoMTA Plus® versus MTA Angelus as delayed furcation perforation repair materials in a dog model. *BMC Oral Health* **21**, 192 (2021).
- 183 Bakhtiar, H. et al. Histologic tissue response to furcation perforation repair using mineral trioxide aggregate or dental pulp stem cells loaded onto treated dentin matrix or tricalcium phosphate. *Clin. Oral Investig.* **21**, 1579-1588 (2017).

- 184 Silva Neto, J. D. et al. Portland cement with additives in the repair of furcation perforations in dogs. *Acta Cir. Bras.* **27**, 809-814 (2012).
- 185 Silva, L. A. B. et al. Furcation perforation: periradicular tissue response to Biodentine as a repair material by histopathologic and indirect immunofluorescence analyses. *J. Endod.* **43**, 1137-1142 (2017).
- 186 Cardoso, M. et al. Biodentine for furcation perforation repair: an animal study with histological, radiographic and micro-computed tomographic assessment. *Iran. Endod. J.* **13**, 323-330 (2018).
- 187 Parirokh, M. & Torabinejad, M. Mineral trioxide aggregate: a comprehensive literature review--Part I: chemical, physical, and antibacterial properties. *J. Endod.* **36**, 16-27 (2010).
- 188 Alsalleeh, F., Chung, N. & Stephenson, L. Antifungal activity of endosequence root repair material and mineral trioxide aggregate. *J. Endod.* **40**, 1815-1819 (2014).
- 189 Koruyucu, M. et al. An assessment of antibacterial activity of three pulp capping materials on *Enterococcus faecalis* by a direct contact test: An in vitro study. *Eur. J. Dent.* **9**, 240-245 (2015).
- 190 Al-Nazhan, S. & Al-Judai, A. Evaluation of antifungal activity of mineral trioxide aggregate. *J. Endod.* **29**, 826-827 (2003).
- 191 Farrugia, C., Baca, P., Camilleri, J. & Arias Moliz, M. T. Antimicrobial activity of ProRoot MTA in contact with blood. *Sci. Rep.* **7**, 41359 (2017).
- 192 Damlar, I., Ozcan, E., Yula, E., Yalcin, M. & Celik, S. Antimicrobial effects of several calcium silicate-based root-end filling materials. *Dent. Mater. J.* **33**, 453-457 (2014).
- 193 Lovato, K. F. & Sedgley, C. M. Antibacterial activity of endosequence root repair material and proroot MTA against clinical isolates of *Enterococcus faecalis*. *J. Endod.* **37**, 1542-1546 (2011).
- 194 Jardine, A. P., Montagner, F., Quintana, R. M., Zaccara, I. M. & Kopper, P. M. P. Antimicrobial effect of bioceramic cements on multispecies microcosm biofilm: a confocal laser microscopy study. *Clin. Oral Investig.* **23**, 1367-1372 (2018).
- 195 Wang, Z. Bioceramic materials in endodontics. *Endod. Top.* **32**, 3-30 (2015).
- 196 Saunders, W. P. A prospective clinical study of periradicular surgery using mineral trioxide aggregate as a root-end filling. *J. Endod.* **34**, 660-665 (2008).
- 197 Zhou, W. et al. Comparison of Mineral trioxide aggregate and iRoot BP plus root repair material as root-end filling materials in endodontic microsurgery: a prospective randomized controlled study. *J. Endod.* **43**, 1-6 (2017).
- 198 Safi, C., Kohli, M. R., Kratchman, S. I., Setzer, F. C. & Karabucak, B. Outcome of endodontic microsurgery using Mineral trioxide aggregate or Root repair material as root-end filling material: a randomized controlled trial with cone-beam computed tomographic evaluation. *J. Endod.* **45**, 831-839 (2019).
- 199 Shinbori, N., Grama, A. M., Patel, Y., Woodmansey, K. & He, J. Clinical outcome of endodontic microsurgery that uses EndoSequence BC root repair material as the root-end filling material. *J. Endod.* **41**, 607-612 (2015).
- 200 Ghodduji, J., Sanaan, A. & Shahrami, F. Clinical and radiographic evaluation of root perforation repair using MTA. *N Y State Dent J.* **73**, 46-49 (2007).



- 
- 201 Schembri, M., Peplow, G. & Camilleri, J. Analyses of heavy metals in Mineral trioxide aggregate and Portland cement. *J. Endod.* **36**, 1210-1215 (2010).
- 202 Kum, K. Y. et al. Analysis of six heavy metals in Ortho mineral trioxide aggregate and ProRoot mineral trioxide aggregate by inductively coupled plasma-optical emission spectrometry. *Aust. Endod. J.* **39**, 126-130 (2013).
- 203 Demirkaya, K. et al. In vivo evaluation of the effects of hydraulic calcium silicate dental cements on plasma and liver aluminium levels in rats. *Eur. J Oral Sci.* **124**, 75-81 (2016).
- 204 Simsek, N., Bulut, E. T., Ahmetoğlu, F. & Alan, H. Determination of trace elements in rat organs implanted with endodontic repair materials by ICP-MS. *J. Mater. Sci. Mater. Med.* **27**, 46 (2016).
- 205 Demirkaya, K. et al. Brain aluminium accumulation and oxidative stress in the presence of calcium silicate dental cements. *Hum. Exp. Toxicol.* **36**, 1071-1080 (2017).
- 206 Camilleri, J. Characterization and hydration kinetics of tricalcium silicate cement for use as a dental biomaterial. *Dent. Mater.* **27**, 836-844 (2011).
- 207 Camilleri, J., Sorrentino, F. & Damidot, D. Investigation of the hydration and bioactivity of radiopacified tricalcium silicate cement, Biodentine and MTA Angelus. *Dent. Mater.* **29**, 580-593 (2013).
- 208 Yang, Q. & Lu, D. *Premixed biological hydraulic cement paste composition and using the same*. US Patent number: US20080299093A1 (2008).
- 209 Septodont. Biodentine – active biosilicate technology (2009). At <https://www.septodontusa.com/wp-content/uploads/2022/11/Biodentine-IFU.pdf?x92757> (10 January 2024).
- 210 Grech, L., Mallia, B. & Camilleri, J. Characterization of set Intermediate Restorative Material, Biodentine, Bioaggregate and a prototype calcium silicate cement for use as root-end filling materials. *Int. Endod. J.* **46**, 632-641 (2013).
- 211 Grech, L., Mallia, B. & Camilleri, J. Investigation of the physical properties of tricalcium silicate cement-based root-end filling materials. *Dent. Mater.* **29**, e20-28 (2013).
- 212 Tang, J. J., Shen, Z. S., Qin, W. & Lin, Z. A comparison of the sealing abilities between Biodentine and MTA as root-end filling materials and their effects on bone healing in dogs after periradicular surgery. *J. Appl. Oral Sci.* **27**, e20180693 (2019).
- 213 Gomes-Cornélio, A. L. et al. Bioactivity of MTA Plus, Biodentine and an experimental calcium silicate-based cement on human osteoblast-like cells. *Int. Endod. J.* **50**, 39-47 (2017).
- 214 Corral Nuñez, C. M., Bosomworth, H. J., Field, C., Whitworth, J. M. & Valentine, R. A. Biodentine and Mineral trioxide aggregate induce similar cellular responses in a fibroblast cell line. *J. Endod.* **40**, 406-411 (2014).
- 215 Rodrigues, E. M. et al. An assessment of the overexpression of BMP-2 in transfected human osteoblast cells stimulated by mineral trioxide aggregate and Biodentine. *Int. Endod. J.* **50**, e9-e18 (2017).

- 216 Kim, H. S., Kim, S., Ko, H., Song, M. & Kim, M. Effects of the cathepsin K inhibitor with mineral trioxide aggregate cements on osteoclastic activity. *Restor. Dent. Endod.* **44**, e17 (2019).
- 217 de Sousa Reis, M., Scarparo, R. K., Steier, L. & de Figueiredo, J. A. P. Periradicular inflammatory response, bone resorption, and cementum repair after sealing of furcation perforation with mineral trioxide aggregate (MTA Angelus™) or Biodentine™. *Clin. Oral Investig.* **23**, 4019-4027 (2019).
- 218 da Fonseca, T. S. et al. Biodentine and MTA modulate immunoinflammatory response favoring bone formation in sealing of furcation perforations in rat molars. *Clin. Oral Investig.* **23**, 1237-1252 (2019).
- 219 Poggio, C. et al. Cytocompatibility and antibacterial properties of capping materials. *ScientificWorldJournal* **2014**, 181945 (2014).
- 220 Poggio, C. et al. In vitro antibacterial activity of different pulp capping materials. *J. Clin. Exp. Dent.* **7**, e584-588 (2015).
- 221 Bhavana, V. et al. Evaluation of antibacterial and antifungal activity of new calcium-based cement (Biodentine) compared to MTA and glass ionomer cement. *J. Conserv. Dent.* **18**, 44-46 (2015).
- 222 Ozyurek, T. & Demiryurek, E. O. Comparison of the antimicrobial activity of direct pulp-capping materials: Mineral trioxide aggregate-Angelus and Biodentine. *J. Conserv. Dent.* **19**, 569-572 (2016).
- 223 Pelepenko, L. E. et al. Physicochemical, antimicrobial, and biological properties of White-MTAFlow. *Clin. Oral Investig.* **25**, 663-672 (2021).
- 224 Farrugia, C., Lung, C. Y. K., Schembri Wismayer, P., Arias-Moliz, M. T. & Camilleri, J. The relationship of surface characteristics and antimicrobial performance of pulp capping materials. *J. Endod.* **44**, 1115-1120 (2018).
- 225 Arias-Moliz, M. T., Farrugia, C., Lung, C. Y. K., Wismayer, P. S. & Camilleri, J. Antimicrobial and biological activity of leachate from light curable pulp capping materials. *J. Dent.* **64**, 45-51 (2017).
- 226 Kato, G. et al. Fast-setting calcium silicate-based pulp capping cements-integrated antibacterial, irritation and cytocompatibility assessment. *Materials (Basel)* **16**, 450 (2023).
- 227 Koutroulis, A., Kuehne, S. A., Cooper, P. R. & Camilleri, J. The role of calcium ion release on biocompatibility and antimicrobial properties of hydraulic cements. *Sci. Rep.* **9**, 19019 (2019).
- 228 Caron, G., Azérad, J., Faure, M. O., Machtou, P. & Boucher, Y. Use of a new retrograde filling material (Biodentine) for endodontic surgery: two case reports. *Int. J. Oral Sci.* **6**, 250-253 (2014).
- 229 Pawar, A. M., Kokate, S. R. & Shah, R. A. Management of a large periapical lesion using Biodentine™ as retrograde restoration with eighteen months evident follow up. *J. Conserv. Dent.* **16**, 573-575 (2013).
- 230 Tirone, F., Salzano, S., Piattelli, A., Perrotti, V. & Iezzi, G. Response of periodontium to mineral trioxide aggregate and Biodentine: a pilot histological study on humans. *Aust. Dent. J.* **63**, 231-241 (2018).

- 231 FKG Dentaire. TotalFill BC root repair material safety data sheet (2023). At [https://www.fkg.ch/sites/default/files/FKG\\_TotalFill%20BC%20RRM\\_IBC\\_Safety%20data%20sheet\\_20230815.pdf](https://www.fkg.ch/sites/default/files/FKG_TotalFill%20BC%20RRM_IBC_Safety%20data%20sheet_20230815.pdf). (10 January 2024).
- 232 Brasseler USA. Endosequence root repair material – instructions for use (2009). At [http://brasselerusadental.com/wp-content/uploads/sites/9/2015/03/B\\_3238A\\_RRM-DFU.pdf](http://brasselerusadental.com/wp-content/uploads/sites/9/2015/03/B_3238A_RRM-DFU.pdf). (10 January 2024).
- 233 Zamparini, F., Siboni, F., Prati, C., Taddei, P. & Gandolfi, M. G. Properties of calcium silicate-monobasic calcium phosphate materials for endodontics containing tantalum pentoxide and zirconium oxide. *Clin. Oral Investig.* **23**, 445-457 (2019).
- 234 Guo, Y. J. et al. Physical properties and hydration behavior of a fast-setting bioceramic endodontic material. *BMC Oral Health* **16**, 23 (2016).
- 235 Lv, F. et al. Evaluation of the in vitro biocompatibility of a new fast-setting ready-to-use root filling and repair material. *Int. Endod. J.* **50**, 540-548 (2017).
- 236 Mahmood Talabani, R., Taha Garib, B. & Masaeli, R. The response of the pulp-dentine complex, pdl, and bone to three calcium silicate-based cements: a histological study in an animal rat Model. *Bioinorg. Chem. Appl.* **13**, 9582165 (2020).
- 237 Darvell, B. W. & Smith, A. J. Inert to bioactive - A multidimensional spectrum. *Dent. Mater.* **38**, 2-6 (2022).
- 238 Hülsmann, M. & Tulus, G. Non-surgical retreatment of teeth with persisting apical periodontitis following apicoectomy: decision making, treatment strategies and problems, and case reports. *Endod. Top.* **34**, 64-89 (2016).
- 239 Siqueira, J. F., Jr. & Lopes, H. P. Mechanisms of antimicrobial activity of calcium hydroxide: a critical review. *Int. Endod. J.* **32**, 361-369 (1999).
- 240 Imlay, J. A. & Linn, S. DNA damage and oxygen radical toxicity. *Science* **240**, 1302-1309 (1988).
- 241 Wang, Z., Shen, Y. & Haapasalo, M. Dental materials with antibiofilm properties. *Dent. Mater.* **30**, e1-16 (2014).
- 242 Tomson, P. L. et al. Dissolution of bio-active dentine matrix components by mineral trioxide aggregate. *J. Dent.* **35**, 636-642 (2007).
- 243 Atmeh, A. R., Chong, E. Z., Richard, G., Festy, F. & Watson, T. F. Dentine-cement interfacial interaction: calcium silicates and polyalkenoates. *J. Dent. Res.* **91**, 454-459 (2012).
- 244 Han, L. & Okiji, T. Uptake of calcium and silicon released from calcium silicate-based endodontic materials into root canal dentine. *Int. Endod. J.* **44**, 1081-1087 (2011).
- 245 Sarkar, N. K., Caicedo, R., Ritwik, P., Moiseyeva, R. & Kawashima, I. Physicochemical basis of the biologic properties of mineral trioxide aggregate. *J. Endod.* **31**, 97-100 (2005).
- 246 Kim, J. R., Nosrat, A. & Fouad, A. F. Interfacial characteristics of Biodentine and MTA with dentine in simulated body fluid. *J. Dent.* **43**, 241-247 (2015).
- 247 Reyes-Carmona, J. F., Felipe, M. S. & Felipe, W. T. Biomineralization ability and interaction of mineral trioxide aggregate and white portland cement with dentin in a phosphate-containing fluid. *J. Endod.* **35**, 731-736 (2009).

- 248 Li, X. et al. Correlative micro-Raman/EPMA analysis of the hydraulic calcium silicate cement interface with dentin. *Clin. Oral Investig.* **20**, 1663-1673 (2016).
- 249 Hadis, M., Wang, J., Zhang, Z. J., Di Maio, A. & Camilleri, J. Interaction of hydraulic calcium silicate and glass ionomer cements with dentine. *Materialia* **9**, 100515 (2020).
- 250 Bosaid, F., Aksel, H. & Azim, A. A. Influence of acidic pH on antimicrobial activity of different calcium silicate based-endodontic sealers. *Clin. Oral Investig.* **26**, 5369-5376 (2022).
- 251 Wang, J. D. & Hume, W. R. Diffusion of hydrogen ion and hydroxyl ion from various sources through dentine. *Int. Endod. J.* **21**, 17-26 (1988).
- 252 Haapasalo, H. K., Siren, E. K., Waltimo, T. M., Orstavik, D. & Haapasalo, M. P. Inactivation of local root canal medicaments by dentine: an in vitro study. *Int. Endod. J.* **33**, 126-131 (2000).
- 253 Portenier, I. et al. Inactivation of root canal medicaments by dentine, hydroxylapatite and bovine serum albumin. *Int. Endod. J.* **34**, 184-188 (2001).
- 254 Wang, Z., Shen, Y. & Haapasalo, M. Dentin extends the antibacterial effect of endodontic sealers against *Enterococcus faecalis* biofilms. *J. Endod.* **40**, 505-508 (2014).
- 255 Du, T. et al. Combined antibacterial effect of sodium hypochlorite and root canal sealers against *Enterococcus faecalis* biofilms in dentin canals. *J. Endod.* **41**, 1294-1298 (2015).
- 256 Giraud, T., Jeanneau, C., Bergmann, M., Laurent, P. & About, I. Tricalcium silicate capping materials modulate pulp healing and inflammatory activity in vitro. *J. Endod.* **44**, 1686-1691 (2018).
- 257 Holland, R. Histochemical response of amputated pulps to calcium hydroxide. *Rev. Bras. Pesq. Med. Biol.* **4**, 83-95 (1971).
- 258 Estrela, C., Sydney, G. B., Bammann, L. L. & Felipe Junior, O. Mechanism of action of calcium and hydroxyl ions of calcium hydroxide on tissue and bacteria. *Braz. Dent. J.* **6**, 85-90 (1995).
- 259 Mohammadi, Z. & Dummer, P. M. Properties and applications of calcium hydroxide in endodontics and dental traumatology. *Int. Endod. J.* **44**, 697-730 (2011).
- 260 Tay, F. R., Pashley, D. H., Rueggeberg, F. A., Loushine, R. J. & Weller, R. N. Calcium phosphate phase transformation produced by the interaction of the portland cement component of white mineral trioxide aggregate with a phosphate-containing fluid. *J. Endod.* **33**, 1347-1351 (2007).
- 261 Bozeman, T. B., Lemon, R. R. & Eleazer, P. D. Elemental analysis of crystal precipitate from gray and white MTA. *J. Endod.* **32**, 425-428 (2006).
- 262 Han, L. & Okiji, T. Bioactivity evaluation of three calcium silicate-based endodontic materials. *Int. Endod. J.* **46**, 808-814 (2013).
- 263 Niu, L. N. et al. A review of the bioactivity of hydraulic calcium silicate cements. *J. Dent.* **42**, 517-533 (2014).
- 264 Bohner, M. & Lemaitre, J. Can bioactivity be tested in vitro with SBF solution? *Biomaterials* **30**, 2175-2179 (2009).

- 
- 265 Moinzadeh, A. T., Aznar Portoles, C., Schembri Wismayer, P. & Camilleri, J. Bioactivity potential of EndoSequence BC RRM putty. *J. Endod.* **42**, 615-621 (2016).
- 266 LeGeros, R. Z. Calcium phosphates in oral biology and medicine. *Monogr. Oral Sci.* **15**, 1-201 (1991).
- 267 Gervais, C. et al. The effects of carbonation and drying during intermittent leaching on the release of inorganic constituents from a cement-based matrix. *Cem. Concr. Res.* **34**, 119-131 (2004).
- 268 Gandolfi, M. G. et al. Setting time and expansion in different soaking media of experimental accelerated calcium-silicate cements and ProRoot MTA. *Oral Surg. Oral Med. Oral Pathol. Oral Radiol. Endod.* **108**, e39-45 (2009).
- 269 Nekoofar, M. H., Stone, D. F. & Dummer, P. M. The effect of blood contamination on the compressive strength and surface microstructure of mineral trioxide aggregate. *Int. Endod. J.* **43**, 782-791 (2010).
- 270 Nekoofar, M. H. et al. An evaluation of the effect of blood and human serum on the surface microhardness and surface microstructure of mineral trioxide aggregate. *Int. Endod. J.* **43**, 849-858 (2010).
- 271 Nekoofar, M. H., Davies, T. E., Stone, D., Basturk, F. B. & Dummer, P. M. H. Microstructure and chemical analysis of blood-contaminated mineral trioxide aggregate. *Int. Endod. J.* **44**, 1011-1018 (2011).
- 272 Guimarães, B. M. et al. Color stability, radiopacity, and chemical characteristics of white mineral trioxide aggregate associated with 2 different vehicles in contact with blood. *J. Endod.* **41**, 947-952 (2015).
- 273 Schembri Wismayer, P., Lung, C. Y., Rappa, F., Cappello, F. & Camilleri, J. Assessment of the interaction of Portland cement-based materials with blood and tissue fluids using an animal model. *Sci. Rep.* **6**, 34547 (2016).
- 274 Shrestha, A. & Kishen, A. Antibacterial nanoparticles in endodontics: a review. *J. Endod.* **42**, 1417-1426 (2016).
- 275 Allaker, R. P. The use of nanoparticles to control oral biofilm formation. *J. Dent. Res.* **89**, 1175-1186 (2010).
- 276 Veerapandian, M. & Yun, K. Functionalization of biomolecules on nanoparticles: specialized for antibacterial applications. *Appl. Microbiol. Biotechnol.* **90**, 1655-1667 (2011).
- 277 Liu, L. et al. Self-assembled cationic peptide nanoparticles as an efficient antimicrobial agent. *Nat. Nanotechnol.* **4**, 457-463 (2009).
- 278 Song, W. & Ge, S. Application of antimicrobial nanoparticles in dentistry. *Molecules* **24**, 1033 (2019).
- 279 Greenwood, N. N. & Earnshaw, A. Copper silver and gold. In *Chemistry of the Elements*, 2<sup>nd</sup> edn (eds Greenwood, N. N. & Earnshaw, A.) 1173-1200 (Butterworth-Heinemann, 1997).
- 280 Rueggeberg, F. A. From vulcanite to vinyl, a history of resins in restorative dentistry. *J. Prosthet. Dent.* **87**, 364-379 (2002).

- 281 Besinis, A., De Peralta, T., Tredwin, C. J. & Handy, R. D. Review of nanomaterials in dentistry: interactions with the oral microenvironment, clinical applications, hazards, and benefits. *ACS Nano*. **9**, 2255-2289 (2015).
- 282 Choi, O. et al. The inhibitory effects of silver nanoparticles, silver ions, and silver chloride colloids on microbial growth. *Water Res.* **42**, 3066-3074 (2008).
- 283 Pareek, V., Gupta, R. & Panwar, J. Do physico-chemical properties of silver nanoparticles decide their interaction with biological media and bactericidal action? A review. *Mater. Sci. Eng. C Mater. Biol. Appl.* **90**, 739-749 (2018).
- 284 Noronha, V. T. et al. Silver nanoparticles in dentistry. *Dent. Mater.* **33**, 1110-1126 (2017).
- 285 Bovenkamp, G. L., Zanzen, U., Krishna, K. S., Hormes, J. & Prange, A. X-ray absorption near-edge structure (XANES) spectroscopy study of the interaction of silver ions with *Staphylococcus aureus*, *Listeria monocytogenes*, and *Escherichia coli*. *Appl. Environ. Microbiol.* **79**, 6385-6390 (2013).
- 286 Abbaszadegan, A. et al. The effect of charge at the surface of silver nanoparticles on antimicrobial activity against gram-positive and gram-negative bacteria: a preliminary study. *J. Nanomater.* **2015**, 720654 (2015).
- 287 M.Raffi, F. H., T.M.Bhatti, J.I.Akhter, A.Hameed, M.M.Hasan. Antibacterial Characterization of Silver Nanoparticles against *E. Coli* ATCC-15224. *J. Mater. Sci. Technol.* **24**, 192-196 (2008).
- 288 Chaloupka, K., Malam, Y. & Seifalian, A. M. Nanosilver as a new generation of nanoparticle in biomedical applications. *Trends Biotechnol.* **28**, 580-588 (2010).
- 289 Abdal Dayem, A. et al. The role of reactive oxygen species (ROS) in the biological activities of metallic nanoparticles. *Int. J. Mol. Sci.* **18**, 120 (2017).
- 290 Afkhami, F., Forghan, P., Gutmann, J. L. & Kishen, A. Silver nanoparticles and their therapeutic applications in endodontics: a narrative review. *Pharmaceutics* **15**, 715 (2023).
- 291 Pokrowiecki, R. et al. In vitro studies of nanosilver-doped titanium implants for oral and maxillofacial surgery. *Int. J. Nanomed.* **12**, 4285-4297 (2017).
- 292 Besinis, A., Hadi, S. D., Le, H. R., Tredwin, C. & Handy, R. D. Antibacterial activity and biofilm inhibition by surface modified titanium alloy medical implants following application of silver, titanium dioxide and hydroxyapatite nanocoatings. *Nanotoxicology* **11**, 327-338 (2017).
- 293 Flores, C. Y. et al. Citrate-capped silver nanoparticles showing good bactericidal effect against both planktonic and sessile bacteria and a low cytotoxicity to osteoblastic cells. *ACS Appl. Mater. Interfaces* **5**, 3149-3159 (2013).
- 294 Jin, J., Zhang, L., Shi, M., Zhang, Y. & Wang, Q. Ti-GO-Ag nanocomposite: the effect of content level on the antimicrobial activity and cytotoxicity. *Int. J. Nanomed.* **12**, 4209-4224 (2017).
- 295 Natale, L. C. et al. Synthesis and characterization of silver phosphate/calcium phosphate mixed particles capable of silver nanoparticle formation by photoreduction. *Mater. Sci. Eng. C Mater. Biol. Appl.* **76**, 464-471 (2017).

- 
- 296 Li, F., Weir, M. D., Chen, J. & Xu, H. H. Comparison of quaternary ammonium-containing with nano-silver-containing adhesive in antibacterial properties and cytotoxicity. *Dent. Mater.* **29**, 450-461 (2013).
- 297 Ahn, S. J., Lee, S. J., Kook, J. K. & Lim, B. S. Experimental antimicrobial orthodontic adhesives using nanofillers and silver nanoparticles. *Dent. Mater.* **25**, 206-213 (2009).
- 298 De Matteis, V. et al. Silver nanoparticles addition in poly(methyl methacrylate) dental matrix: topographic and antimycotic studies. *Int. J. Mol. Sci.* **20** (2019).
- 299 Acosta-Torres, L. S., Mendieta, I., Nunez-Anita, R. E., Cajero-Juarez, M. & Castano, V. M. Cytocompatible antifungal acrylic resin containing silver nanoparticles for dentures. *Int. J. Nanomed.* **7**, 4777-4786 (2012).
- 300 Monteiro, D. R. et al. Silver distribution and release from an antimicrobial denture base resin containing silver colloidal nanoparticles. *J. Prosthodont.* **21**, 7-15 (2012).
- 301 Yu, R. Y., Zhou, Y. S., Feng, H. L. & Liu, X. Y. [Silver-ion release and particle distribution of denture base resin containing nanometer-sized silver-supported antimicrobial agent]. *Zhonghua Kou Qiang Yi Xue Za Zhi.* **43**, 54-56 (2008).
- 302 Casemiro, L. A., Gomes Martins, C. H., Pires-de-Souza Fde, C. & Panzeri, H. Antimicrobial and mechanical properties of acrylic resins with incorporated silver-zinc zeolite - part I. *Gerodontology* **25**, 187-194 (2008).
- 303 Bacali, C. et al. Flexural strength, biocompatibility, and antimicrobial activity of a polymethyl methacrylate denture resin enhanced with graphene and silver nanoparticles. *Clin. Oral Investig.* **24**, 2713-2725 (2020).
- 304 Cheng, L. et al. Antibacterial amorphous calcium phosphate nanocomposites with a quaternary ammonium dimethacrylate and silver nanoparticles. *Dent. Mater.* **28**, 561-572 (2012).
- 305 das Neves, P. B., Agnelli, J. A., Kurachi, C. & de Souza, C. W. Addition of silver nanoparticles to composite resin: effect on physical and bactericidal properties in vitro. *Braz. Dent. J.* **25**, 141-145 (2014).
- 306 Fan, C. et al. Development of an antimicrobial resin--a pilot study. *Dent. Mater.* **27**, 322-328 (2011).
- 307 Melo, M. A. et al. Novel dental adhesives containing nanoparticles of silver and amorphous calcium phosphate. *Dent. Mater.* **29**, 199-210 (2013).
- 308 Dutra-Correa, M. et al. Antibacterial effects and cytotoxicity of an adhesive containing low concentration of silver nanoparticles. *J. Dent.* **77**, 66-71 (2018).
- 309 Cheng, L. et al. Effects of antibacterial primers with quaternary ammonium and nano-silver on *Streptococcus mutans* impregnated in human dentin blocks. *Dent. Mater.* **29**, 462-472 (2013).
- 310 Cheng, L. et al. Anti-biofilm dentin primer with quaternary ammonium and silver nanoparticles. *J. Dent. Res.* **91**, 598-604 (2012).
- 311 Li, F., Weir, M. D., Fouad, A. F. & Xu, H. H. Effect of salivary pellicle on antibacterial activity of novel antibacterial dental adhesives using a dental plaque microcosm biofilm model. *Dent. Mater.* **30**, 182-191 (2014).

- 312 Zhang, K. et al. Effect of quaternary ammonium and silver nanoparticle-containing adhesives on dentin bond strength and dental plaque microcosm biofilms. *Dent. Mater.* **28**, 842-852 (2012).
- 313 El-Wassefy, N. A., El-Mahdy, R. H. & El-Kholany, N. R. The impact of silver nanoparticles integration on biofilm formation and mechanical properties of glass ionomer cement. *J. Esthet. Restor. Dent.* **30**, 146-152 (2018).
- 314 Chen, J. et al. Antibacterial and mechanical properties of reduced graphene-silver nanoparticle nanocomposite modified glass ionomer cements. *J. Dent.* **96**, 103332 (2020).
- 315 Jowkar, Z., Jowkar, M. & Shafiei, F. Mechanical and dentin bond strength properties of the nanosilver enriched glass ionomer cement. *J. Clin. Exp. Dent.* **11**, e275-e281 (2019).
- 316 Paiva, L. et al. Antibacterial properties and compressive strength of new one-step preparation silver nanoparticles in glass ionomer cements (NanoAg-GIC). *J. Dent.* **69**, 102-109 (2018).
- 317 Ramazanzadeh, B. et al. Comparison of antibacterial effects of ZnO and CuO nanoparticles coated brackets against *Streptococcus mutans*. *J. Dent. (Shiraz)* **16**, 200-205 (2015).
- 318 Gunputh, U. F. et al. Antibacterial properties of silver nanoparticles grown in situ and anchored to titanium dioxide nanotubes on titanium implant against *Staphylococcus aureus*. *Nanotoxicology* **14**, 97-110 (2020).
- 319 Salaie, R. N., Besinis, A., Le, H., Tredwin, C. & Handy, R. D. The biocompatibility of silver and nanohydroxyapatite coatings on titanium dental implants with human primary osteoblast cells. *Mater. Sci. Eng. C Mater. Biol. Appl.* **107**, 110210 (2020).
- 320 Fan, W. et al. Effects of adsorbed and templated nanosilver in mesoporous calcium-silicate nanoparticles on inhibition of bacteria colonization of dentin. *Int. J. Nanomedicine* **9**, 5217-5230 (2014).
- 321 Hiraishi, N., Yiu, C. K., King, N. M., Tagami, J. & Tay, F. R. Antimicrobial efficacy of 3.8% silver diamine fluoride and its effect on root dentin. *J. Endod.* **36**, 1026-1029 (2010).
- 322 Wu, D., Fan, W., Kishen, A., Gutmann, J. L. & Fan, B. Evaluation of the antibacterial efficacy of silver nanoparticles against *Enterococcus faecalis* biofilm. *J. Endod.* **40**, 285-290 (2014).
- 323 Balto, H., Bukhary, S., Al-Omran, O., BaHammam, A. & Al-Mutairi, B. Combined effect of a mixture of silver nanoparticles and calcium hydroxide against *Enterococcus faecalis* biofilm. *J. Endod.* **46**, 1689-1694 (2020).
- 324 Afkhami, F., Pourhashemi, S. J., Sadegh, M., Salehi, Y. & Fard, M. J. Antibiofilm efficacy of silver nanoparticles as a vehicle for calcium hydroxide medicament against *Enterococcus faecalis*. *J. Dent.* **43**, 1573-1579 (2015).
- 325 Javidi, M., Afkhami, F., Zarei, M., Ghazvini, K. & Rajabi, O. Efficacy of a combined nanoparticulate/calcium hydroxide root canal medication on elimination of *Enterococcus faecalis*. *Aust. Endod. J.* **40**, 61-65 (2014).



- 
- 326 Sadek, R. W., Moussa, S. M., El Backly, R. M. & Hammouda, A. F. Evaluation of the efficacy of three antimicrobial agents used for regenerative endodontics: an in vitro study. *Microb. Drug. Resist.* **25**, 761-771 (2019).
- 327 Ioannidis, K., Niazi, S., Mylonas, P., Mannocci, F. & Deb, S. The synthesis of nano silver-graphene oxide system and its efficacy against endodontic biofilms using a novel tooth model. *Dent. Mater.* **35**, 1614-1629 (2019).
- 328 Rodrigues, C. T. et al. Antibacterial properties of silver nanoparticles as a root canal irrigant against *Enterococcus faecalis* biofilm and infected dentinal tubules. *Int. Endod. J.* **51**, 901-911 (2018).
- 329 Afkhami, F., Akbari, S. & Chiniforush, N. *Enterococcus faecalis* elimination in root canals using silver nanoparticles, photodynamic therapy, diode laser, or laser-activated nanoparticles: an in vitro study. *J. Endod.* **43**, 279-282 (2017).
- 330 Chavez-Andrade, G. M. et al. Antimicrobial and biofilm anti-adhesion activities of silver nanoparticles and farnesol against endodontic microorganisms for possible application in root canal treatment. *Arch. Oral Biol.* **107**, 104481 (2019).
- 331 Ertem, E. et al. Core-shell silver nanoparticles in endodontic disinfection solutions enable long-term antimicrobial effect on oral biofilms. *ACS Appl. Mater. Interfaces* **9**, 34762-34772 (2017).
- 332 Halkai, K. R., Halkai, R., Mudda, J. A., Shivanna, V. & Rathod, V. Antibiofilm efficacy of biosynthesized silver nanoparticles against endodontic-periodontal pathogens: An in vitro study. *J. Conserv. Dent.* **21**, 662-666 (2018).
- 333 Zheng, T. et al. A liquid crystalline precursor incorporating chlorhexidine acetate and silver nanoparticles for root canal disinfection. *Biomater. Sci.* **6**, 596-603 (2018).
- 334 Martinez-Andrade, J. M., Avalos-Borja, M., Vilchis-Nestor, A. R., Sanchez-Vargas, L. O. & Castro-Longoria, E. Dual function of EDTA with silver nanoparticles for root canal treatment-A novel modification. *PLoS One* **13**, e0190866 (2018).
- 335 Kapralos, V., Koutroulis, A., Ørstavik, D., Sunde, P. T. & Rukke, H. V. Antibacterial activity of endodontic sealers against planktonic bacteria and bacteria in biofilms. *J. Endod.* **44**, 149-154 (2018).
- 336 Almeida, L. H. S. et al. Synthesis of silver-containing calcium aluminate particles and their effects on a MTA-based endodontic sealer. *Dent. Mater.* **34**, e214-e223 (2018).
- 337 Loyola-Rodriguez, J. P. et al. Antimicrobial activity of endodontic sealers and medications containing chitosan and silver nanoparticles against *Enterococcus faecalis*. *J. Appl. Biomater. Funct. Mater.* **17**, 2280800019851771 (2019).
- 338 Vilela Teixeira, A. B. et al. Effect of incorporation of a new antimicrobial nanomaterial on the physical-chemical properties of endodontic sealers. *J. Conserv. Dent.* **20**, 392-397 (2017).
- 339 Vilela Teixeira, A. B., de Carvalho Honorato Silva, C., Alves, O. L. & Candido Dos Reis, A. Endodontic sealers modified with silver vanadate: antibacterial, compositional, and setting time evaluation. *Biomed. Res. Int.* **2019**, 4676354 (2019).
- 340 Teixeira, A. B. V., de Castro, D. T., Schiavon, M. A. & Dos Reis, A. C. Cytotoxicity and release ions of endodontic sealers incorporated with a silver and vanadium base nanomaterial. *Odontology* **108**, 661-668 (2020).

- 341 Seung, J. et al. A modified resin sealer: physical and antibacterial properties. *J. Endod.* **44**, 1553-1557 (2018).
- 342 Chang, H. H. et al. Evaluation of carbon dioxide-Based urethane acrylate composites for sealers of root canal obturation. *Polymers (Basel)* **12**, 482 (2020).
- 343 Baras, B. H. et al. Novel endodontic sealer with dual strategies of dimethylaminohexadecyl methacrylate and nanoparticles of silver to inhibit root canal biofilms. *Dent. Mater.* **35**, 1117-1129 (2019).
- 344 Baras, B. H. et al. Novel root canal sealer with dimethylaminohexadecyl methacrylate, nano-silver and nano-calcium phosphate to kill bacteria inside root dentin and increase dentin hardness. *Dent. Mater.* **35**, 1479-1489 (2019).
- 345 Samiei, M. et al. Effect of different additives on genotoxicity of Mineral trioxide aggregate. *Iran Endod. J.* **13**, 37-41 (2018).
- 346 Samiei, M. et al. Antimicrobial efficacy of Mineral trioxide aggregate with and without silver nanoparticles. *Iran Endod. J.* **8**, 166-170 (2013).
- 347 Bahador, A., Pourakbari, B., Bolhari, B. & Hashemi, F. B. In vitro evaluation of the antimicrobial activity of nanosilver-mineral trioxide aggregate against frequent anaerobic oral pathogens by a membrane-enclosed immersion test. *Biomed. J.* **38**, 77-83 (2015).
- 348 Zand, V. et al. Tissue reaction and biocompatibility of implanted Mineral trioxide aggregate with silver nanoparticles in a rat model. *Iran Endod. J.* **11**, 13-16 (2016).
- 349 Jonaidi-Jafari, N., Izadi, M. & Javidi, P. The effects of silver nanoparticles on antimicrobial activity of ProRoot mineral trioxide aggregate (MTA) and calcium enriched mixture (CEM). *J. Clin. Exp. Dent.* **8**, e22-26 (2016).
- 350 Eskandarinezhad, M. et al. Sealing efficacy of mineral trioxide aggregate with and without nanosilver for root end filling: an in vitro bacterial leakage study. *J. Clin. Exp. Dent.* **9**, e27-e33 (2017).
- 351 Mendes, M. S. et al. Radiopacity of Mineral trioxide aggregate with and without inclusion of silver nanoparticles. *J. Contemp. Dent. Pract.* **18**, 448-451 (2017).
- 352 Vazquez-Garcia, F. et al. Effect of silver nanoparticles on physicochemical and antibacterial properties of calcium silicate cements. *Braz. Dent. J.* **27**, 508-514 (2016).
- 353 Hench, L. L. The story of Bioglass. *J. Mater. Sci. Mater. Med.* **17**, 967-978 (2006).
- 354 Skallefold, H. E., Rokaya, D., Khurshid, Z. & Zafar, M. S. Bioactive glass applications in dentistry. *Int. J. Mol. Sci.* **20**, 5960 (2019).
- 355 Shah, F. A. Fluoride-containing bioactive glasses: Glass design, structure, bioactivity, cellular interactions, and recent developments. *Mater. Sci. Eng. C Mater. Biol. Appl.* **58**, 1279-1289 (2016).
- 356 Hu, S., Chang, J., Liu, M. & Ning, C. Study on antibacterial effect of 45S5 Bioglass. *J. Mater. Sci. Mater. Med.* **20**, 281-286 (2009).
- 357 Stoor, P., Soderling, E. & Salonen, J. I. Antibacterial effects of a bioactive glass paste on oral microorganisms. *Acta Odontol. Scand.* **56**, 161-165 (1998).
- 358 Hill, R. G. & Brauer, D. S. Predicting the bioactivity of glasses using the network connectivity or split network models. *J. Non-Cryst. Solids* **357**, 3884-3887 (2011).

- 
- 359 Hench, L. L. Bioceramics. *J. Am. Ceram. Soc.* **81**, 1705-1728 (1998).
- 360 Hill, R. An alternative view of the degradation of bioglass. *J. Mater. Sci. Lett.* **15**, 1122-1125 (1996).
- 361 Begum, S., Johnson, W. E., Worthington, T. & Martin, R. A. The influence of pH and fluid dynamics on the antibacterial efficacy of 45S5 Bioglass. *Biomed. Mater.* **11**, 015006 (2016).
- 362 Munukka, E. et al. Bactericidal effects of bioactive glasses on clinically important aerobic bacteria. *J. Mater. Sci. Mater. Med.* **19**, 27-32 (2008).
- 363 Gubler, M. et al. Do bioactive glasses convey a disinfecting mechanism beyond a mere increase in pH? *Int. Endod. J.* **41**, 670-678 (2008).
- 364 Xie, Z. P. et al. In vivo study effect of particulate Bioglass in the prevention of infection in open fracture fixation. *J. Biomed. Mater. Res. B Appl. Biomater.* **90**, 195-201 (2009).
- 365 Allan, I., Newman, H. & Wilson, M. Antibacterial activity of particulate bioglass against supra- and subgingival bacteria. *Biomaterials* **22**, 1683-1687 (2001).
- 366 Zehnder, M., Waltimo, T., Sener, B. & Soderling, E. Dentin enhances the effectiveness of bioactive glass S53P4 against a strain of *Enterococcus faecalis*. *Oral. Surg. Oral Med. Oral Pathol. Oral Radiol. Endod.* **101**, 530-535 (2006).
- 367 Waltimo, T., Zehnder, M. & Soderling, E. Bone powder enhances the effectiveness of bioactive glass S53P4 against strains of *Porphyromonas gingivalis* and *Actinobacillus actinomycetemcomitans* in suspension. *Acta Odontol. Scand.* **64**, 183-186 (2006).
- 368 Zehnder, M., Soderling, E., Salonen, J. & Waltimo, T. Preliminary evaluation of bioactive glass S53P4 as an endodontic medication in vitro. *J. Endod.* **30**, 220-224 (2004).
- 369 Hench, L. Chronology of Bioactive glass development and clinical applications. *New J. Glass Ceram.* **3**, 67-73 (2013).
- 370 Sauro, S. et al. Remineralisation properties of innovative light-curable resin-based dental materials containing bioactive micro-fillers. *J. Mater. Chem. B.* **1**, 2624-2638 (2013).
- 371 Profeta, A. C. Preparation and properties of calcium-silicate filled resins for dental restoration. Part I: chemical-physical characterization and apatite-forming ability. *Acta Odontol. Scand.* **72**, 597-606 (2014).
- 372 Yli-Urpo, H., Vallittu, P. K., Narhi, T. O., Forsback, A. P. & Vakiaparta, M. Release of silica, calcium, phosphorus, and fluoride from glass ionomer cement containing bioactive glass. *J. Biomater. Appl.* **19**, 5-20 (2004).
- 373 Yli-Urpo, H., Narhi, M. & Narhi, T. Compound changes and tooth mineralization effects of glass ionomer cements containing bioactive glass (S53P4), an in vivo study. *Biomaterials* **26**, 5934-5941 (2005).
- 374 Osorio, R., Yamauti, M., Sauro, S., Watson, T. F. & Toledano, M. Zinc incorporation improves biological activity of beta-tricalcium silicate resin-based cement. *J. Endod.* **40**, 1840-1845 (2014).

- 375 Sauro, S., Osorio, R., Watson, T. F. & Toledano, M. Therapeutic effects of novel resin bonding systems containing bioactive glasses on mineral-depleted areas within the bonded-dentine interface. *J. Mater. Sci. Mater. Med.* **23**, 1521-1532 (2012).
- 376 Profeta, A. C. Preparation and properties of calcium-silicate filled resins for dental restoration. Part II: Micro-mechanical behaviour to primed mineral-depleted dentine. *Acta Odontol. Scand.* **72**, 607-617 (2014).
- 377 Waltimo, T., Brunner, T. J., Vollenweider, M., Stark, W. J. & Zehnder, M. Antimicrobial effect of nanometric bioactive glass 45S5. *J. Dent. Res.* **86**, 754-757 (2007).
- 378 Zehnder, M., Luder, H. U., Schatzle, M., Kerosuo, E. & Waltimo, T. A comparative study on the disinfection potentials of bioactive glass S53P4 and calcium hydroxide in contra-lateral human premolars ex vivo. *Int. Endod. J.* **39**, 952-958 (2006).
- 379 Atila-Pektas, B., Yurdakul, P., Gulmez, D. & Gorduysus, O. Antimicrobial effects of root canal medicaments against *Enterococcus faecalis* and *Streptococcus mutans*. *Int. Endod. J.* **46**, 413-418 (2013).
- 380 de Araújo Lopes, J. M. et al. Biocompatibility, induction of mineralization and antimicrobial activity of experimental intracanal pastes based on glass and glass-ceramic materials. *Int. Endod. J.* **53**, 1494-1505 (2020).
- 381 Correia, B. L., Gomes, A., Noites, R., Ferreira, J. M. F. & Duarte, A. S. New and efficient Bioactive glass compositions for controlling endodontic pathogens. *Nanomaterials (Basel)* **12**, 1577 (2022).
- 382 Krithikadatta, J., Indira, R. & Dorothykalyani, A. L. Disinfection of dentinal tubules with 2% chlorhexidine, 2% metronidazole, bioactive glass when compared with calcium hydroxide as intracanal medicaments. *J. Endod.* **33**, 1473-1476 (2007).
- 383 Grazziotin-Soares, R. et al. Dentin microhardness and sealer bond strength to root dentin are affected by using Bioactive glasses as intracanal medication. *Materials (Basel)* **13**, 721 (2020).
- 384 Elzubair, A., Elias, C. N., Suarez, J. C., Lopes, H. P. & Vieira, M. V. The physical characterization of a thermoplastic polymer for endodontic obturation. *J. Dent.* **34**, 784-789 (2006).
- 385 Jia, W. T. Trope, M. T. & Alpert, B. *Dental filling material*. US Patent number: US20050069836A1. (2005).
- 386 Teixeira, F. B., Teixeira, E. C., Thompson, J., Leinfelder, K. F. & Trope, M. Dentinal bonding reaches the root canal system. *J. Esthet. Restor. Dent.* **16**, 348-354 (2004).
- 387 Shipper, G., Ørstavik, D., Teixeira, F. B. & Trope, M. An evaluation of microbial leakage in roots filled with a thermoplastic synthetic polymer-based root canal filling material (Resilon). *J. Endod.* **30**, 342-347 (2004).
- 388 Shipper, G., Teixeira, F. B., Arnold, R. R. & Trope, M. Periapical inflammation after coronal microbial inoculation of dog roots filled with gutta-percha or resilon. *J. Endod.* **31**, 91-96 (2005).
- 389 Belli, S., Eraslan, O., Eskitascioglu, G. & Karbhari, V. Monoblocks in root canals: a finite elemental stress analysis study. *Int. Endod. J.* **44**, 817-826 (2011).

- 390 Barborka, B. J., Woodmansey, K. F., Glickman, G. N., Schneiderman, E. & He, J. Long-term Clinical Outcome of Teeth Obturated with Resilon. *J. Endod.* **43**, 556-560 (2017).
- 391 Mohn, D. et al. Composites made of flame-sprayed bioactive glass 45S5 and polymers: bioactivity and immediate sealing properties. *Int. Endod. J.* **43**, 1037-1046 (2010).
- 392 Belladonna, F. G. et al. Biocompatibility of a self-adhesive gutta-percha-based material in subcutaneous tissue of mice. *J. Endod.* **40**, 1869-1873 (2014).
- 393 Marending, M., Bubenhofer, S. B., Sener, B. & De-Deus, G. Primary assessment of a self-adhesive gutta-percha material. *Int. Endod. J.* **46**, 317-322 (2013).
- 394 Hoikkala, N. J. et al. Dissolution and mineralization characterization of bioactive glass ceramic containing endodontic sealer Guttaflow Bioseal. *Dent. Mater. J.* **37**, 988-994 (2018).
- 395 Collado-Gonzalez, M., Tomas-Catala, C. J., Onate-Sanchez, R. E., Moraleda, J. M. & Rodriguez-Lozano, F. J. Cytotoxicity of GuttaFlow Bioseal, GuttaFlow2, MTA Fillapex, and AH Plus on human periodontal ligament stem cells. *J. Endod.* **43**, 816-822 (2017).
- 396 Saygili, G., Saygili, S., Tuglu, I. & Davut Capar, I. In Vitro Cytotoxicity of GuttaFlow Bioseal, GuttaFlow 2, AH-Plus and MTA Fillapex. *Iran. Endod. J.* **12**, 354-359 (2017).
- 397 Rodriguez-Lozano, F. J. et al. GuttaFlow Bioseal promotes spontaneous differentiation of human periodontal ligament stem cells into cementoblast-like cells. *Dent. Mater.* **35**, 114-124 (2019).
- 398 Santos, J. M. et al. Biocompatibility of a bioceramic silicone-based sealer in subcutaneous tissue. *J. Oral Sci.* **61**, 171-177 (2019).
- 399 Ruiz-Linares, M. et al. Antibacterial and antibiofilm activity over time of GuttaFlow Bioseal and AH Plus. *Dent. Mater. J.* **38**, 701-706 (2019).
- 400 Liu, H. et al. In vitro evaluation of the antibacterial effect of four root canal sealers on dental biofilms. *Clin. Oral Investig.* **26**, 4361-4368 (2022).
- 401 Washio, A., Morotomi, T., Yoshii, S. & Kitamura, C. Bioactive glass-based endodontic sealer as a promising root canal filling material without semisolid core materials. *Materials (Basel)* **12**, 3967 (2019).
- 402 Hanada, K. et al. In vitro and in vivo effects of a novel bioactive glass-based cement used as a direct pulp capping agent. *J. Biomed. Mater. Res. B Appl. Biomater.* **107**, 161-168 (2019).
- 403 Washio, A., Nakagawa, A., Nishihara, T., Maeda, H. & Kitamura, C. Physicochemical properties of newly developed bioactive glass cement and its effects on various cells. *J. Biomed. Mater. Res. B Appl. Biomater.* **103**, 373-380 (2015).
- 404 Jo, S. B. et al. Physical properties and biofunctionalities of bioactive root canal sealers in vitro. *Nanomaterials (Basel)* **10**, 1750 (2020).
- 405 Tomokiyo, A. et al. Characterization of a clonal human periodontal ligament stem cell line exposed to methacrylate resin-, bioactive glass-, or silicon-based root canal sealers. *Odontology* **110**, 127-137 (2022).

- 406 Murata, K. et al. Physicochemical properties, cytocompatibility, and biocompatibility of a Bioactive glass based retrograde filling material. *Nanomaterials (Basel)* **11**, 1828 (2021).
- 407 Hoikkala, N. J., Siekkinen, M., Hupa, L. & Vallittu, P. K. Behaviour of different bioactive glasses incorporated in polydimethylsiloxane endodontic sealer. *Dent. Mater.* **37**, 321-327 (2021).
- 408 Huang, G., Liu, S. Y., Wu, J. L., Qiu, D. & Dong, Y. M. A novel bioactive glass-based root canal sealer in endodontics. *J. Dent. Sci.* **17**, 217-224 (2022).
- 409 Cardoso, O. S. et al. Synthesis and characterization of experimental endodontic sealers containing bioactive glasses particles of NbG or 45S5. *J. Mech. Behav. Biomed. Mater.* **125**, 104971 (2022).
- 410 Zubizarreta-Macho, Á. et al. Adding two antimicrobial glasses to an endodontic sealer to prevent bacterial root canal reinfection: an in vivo pilot study in dogs. *Antibiotics (Basel)* **10**, 1183 (2021).
- 411 Liu, J. et al. Potential of tailored amorphous multiporous calcium silicate glass for pulp capping regenerative endodontics-a preliminary assessment. *J. Dent.* **109**, 103655 (2021).
- 412 Oguntebi, B., Clark, A. & Wilson, J. Pulp capping with Bioglass and autologous demineralized dentin in miniature swine. *J. Dent. Res.* **72**, 484-489 (1993).
- 413 Oguntebi, B. R., Heaven, T., Clark, A. E. & Pink, F. E. Quantitative assessment of dentin bridge formation following pulp-capping in miniature swine. *J. Endod.* **21**, 79-82 (1995).
- 414 Salako, N. et al. Comparison of bioactive glass, mineral trioxide aggregate, ferric sulfate, and formocresol as pulpotomy agents in rat molar. *Dent. Traumatol.* **19**, 314-320 (2003).
- 415 Long, Y. et al. Evaluation of pulp response to novel Bioactive glass pulp capping materials. *J. Endod.* **43**, 1647-1650 (2017).
- 416 Haghgoo, R. & Ahmadvand, M. Evaluation of pulpal response of deciduous teeth after direct pulp capping with bioactive glass and mineral trioxide aggregate. *Contemp. Clin. Dent.* **7**, 332-335 (2016).
- 417 Wang, S. et al. Odontogenic differentiation and dentin formation of dental pulp cells under nanobioactive glass induction. *Acta Biomater.* **10**, 2792-2803 (2014).
- 418 Gong, W. et al. Ionic extraction of a novel nano-sized bioactive glass enhances differentiation and mineralization of human dental pulp cells. *J. Endod.* **40**, 83-88 (2014).
- 419 Houreh, A. B. et al. Influence of calcium and phosphorus release from bioactive glasses on viability and differentiation of dental pulp stem cells. *J. Mater. Sci.* **52**, 8928-8941 (2017).
- 420 Corral Nuñez, C., Covarrubias, C., Fernandez, E. & Oliveira, O. B. d. J. Enhanced bioactive properties of Biodentine™ modified with bioactive glass nanoparticles. *J. Appl. Oral Sci.* **25**, 177-185 (2017).
- 421 Simila, H. O., Karpukhina, N. & Hill, R. G. Bioactivity and fluoride release of strontium and fluoride modified Biodentine. *Dent. Mater.* **34**, e1-e7 (2018).

- 422 Guneser, M. B., Ozturk, T. Y., Sahin, A. N. D., Uysal, B. A. & Eldeniz, A. U. Effect of nanosized bioactive glass addition on some physical properties of biodentine. *J. Appl. Biomater. Funct. Mater.* **21**, 22808000231184059 (2023).
- 423 Flores-Ledesma, A. et al. Bioactive materials improve some physical properties of a MTA-like cement. *Mater. Sci. Eng. C Mater. Biol. Appl.* **71**, 150-155 (2017).
- 424 Mena-Álvarez, J., Rico-Romano, C., Gutiérrez-Ortega, C., Arias-Sanz, P. & Castro-Urda, J. A comparative study of biocompatibility in rat connective tissue of a new Mineral trioxide compound (Theracal) versus MTA and a bioactive G3 glass. *J. Clin. Med.* **10**, 2536 (2021).
- 425 Queiroz, M. B. et al. Development and evaluation of reparative tricalcium silicate-ZrO<sub>2</sub>-Biosilicate composites. *J. Biomed. Mater. Res. B Appl. Biomater.* **109**, 468-476 (2021).
- 426 Jung, M. K. et al. Premixed calcium silicate-based root canal sealer reinforced with bioactive glass nanoparticles to improve biological properties. *Pharmaceutics* **14**, 1903 (2022).
- 427 Tanomaru-Filho, M., Jorge, E. G., Guerreiro Tanomaru, J. M. & Gonçalves, M. Radiopacity evaluation of new root canal filling materials by digitalization of images. *J. Endod.* **33**, 249-251 (2007).
- 428 Bortoluzzi, E. A., Guerreiro-Tanomaru, J. M., Tanomaru-Filho, M. & Duarte, M. A. Radiographic effect of different radiopacifiers on a potential retrograde filling material. *Oral Surg. Oral Med. Oral Pathol. Oral Radiol. Endod.* **108**, 628-632 (2009).
- 429 Duarte, M. A. H. et al. Radiopacity of portland cement associated with different radiopacifying agents. *J. Endod.* **35**, 737-740 (2009).
- 430 Cutajar, A., Mallia, B., Abela, S. & Camilleri, J. Replacement of radiopacifier in mineral trioxide aggregate; characterization and determination of physical properties. *Dent. Mater.* **27**, 879-891 (2011).
- 431 Silva, G. F. et al. Zirconium oxide and niobium oxide used as radiopacifiers in a calcium silicate-based material stimulate fibroblast proliferation and collagen formation. *Int. Endod. J.* **50**, e95-e108 (2017).
- 432 International Standards Organization. ISO 6876. *Dentistry: Root Canal Sealing Materials* (2012).
- 433 Jensen, K.A. *The NANOGENOTOX Dispersion Protocol for NANoREG*; National Research Centre for the Working Environment: Copenhagen, Denmark (2014). At <http://safenano.re.kr/download.do?SEQ=175> (11 January 2024).
- 434 Sigma-Aldrich. Silver - nanopowder product specification. At [https://www.sigmaaldrich.com/specification-sheets/115/707/576832-BULK\\_ALDRICH.pdf](https://www.sigmaaldrich.com/specification-sheets/115/707/576832-BULK_ALDRICH.pdf) (11 January 2024)
- 435 Camilleri, J. Biodentine™ microstructure and composition. In *Biodentine™: Properties and Clinical Applications* (ed Imad About) 1-10 (Springer, 2021).
- 436 Camilleri, J., Wang, C., Kandhari, S., Heran, J. & Shelton, R. M. Methods for testing solubility of hydraulic calcium silicate cements for root-end filling. *Sci. Rep.* **12**, 7100 (2022).

- 437 Meschi, N. et al. Bioactivity potential of Portland cement in regenerative endodontic procedures: From clinic to lab. *Dent. Mater.* **35**, 1342-1350 (2019).
- 438 International Standards Organization. ISO 23317. *Implants for surgery- in vitro evaluation for apatite-forming ability of implant materials* (2014).
- 439 Tingey, M. C., Bush, P. & Levine, M. S. Analysis of mineral trioxide aggregate surface when set in the presence of fetal bovine serum. *J. Endod.* **34**, 45-49 (2008).
- 440 Yao, T. & Asayama, Y. Animal-cell culture media: History, characteristics, and current issues. *Reprod. Med. Biol.* **16**, 99-117 (2017).
- 441 Schembri-Wismayer, P. & Camilleri, J. Why biphasic? Assessment of the effect on cell proliferation and expression. *J. Endod.* **43**, 751-759 (2017).
- 442 Lakha, T., Kheur, M., Mühlemann, S., Kheur, S. & Le, B. Ultrasound and CBCT analysis of blood flow and dimensions of the lingual vascular canal: a case control study. *J. Oral Biol. Craniofac. Res.* **11**, 40-46 (2021).
- 443 Formosa, L. M., Mallia, B., Bull, T. & Camilleri, J. The microstructure and surface morphology of radiopaque tricalcium silicate cement exposed to different curing conditions. *Dent. Mater.* **28**, 584-595 (2012).
- 444 Gandolfi, M. G. et al. Kinetics of apatite formation on a calcium-silicate cement for root-end filling during ageing in physiological-like phosphate solutions. *Clin. Oral Investig.* **14**, 659-668 (2010).
- 445 Camilleri, J. et al. Standardization of antimicrobial testing of dental devices. *Dent. Mater.* **36**, e59-e73 (2020).
- 446 Pinheiro, E. T. et al. Microorganisms from canals of root-filled teeth with periapical lesions. *Int. Endod. J.* **36**, 1-11 (2003).
- 447 Rôças, I. N., Hülsmann, M. & Siqueira, J. F., Jr. Microorganisms in root canal-treated teeth from a German population. *J. Endod.* **34**, 926-931 (2008).
- 448 Rôças, I. N. & Siqueira, J. F., Jr. Characterization of microbiota of root canal-treated teeth with posttreatment disease. *J. Clin. Microbiol.* **50**, 1721-1724 (2012).
- 449 Swimberghe, R. C. D., Coenye, T., De Moor, R. J. G. & Meire, M. A. Biofilm model systems for root canal disinfection: a literature review. *Int. Endod. J.* **52**, 604-628 (2019).
- 450 Sirén, E. K., Haapasalo, M. P., Waltimo, T. M. & Ørstavik, D. In vitro antibacterial effect of calcium hydroxide combined with chlorhexidine or iodine potassium iodide on *Enterococcus faecalis*. *Eur. J. Oral Sci.* **112**, 326-331 (2004).
- 451 Nieto, C. & Espinosa, M. Construction of the mobilizable plasmid pMV158GFP, a derivative of pMV158 that carries the gene encoding the green fluorescent protein. *Plasmid.* **49**, 281-285 (2003).
- 452 Li, Y., Tong, Z. & Ling, J. Effect of the three *Enterococcus faecalis* strains on apoptosis in MC3T3 cells. *Oral Dis.* **25**, 309-318 (2019).
- 453 Kowalski, W. J. et al. *Enterococcus faecalis* adhesin, Ace, mediates attachment to particulate dentin. *J. Endod.* **32**, 634-637 (2006).
- 454 Kishen, A. & Haapasalo, M. Biofilm models and methods of biofilm assessment. *Endod. Top.* **22**, 58-78 (2010).



- 455 Xu, J. et al. Influence of Endodontic Procedure on the Adherence of *Enterococcus faecalis*. *J. Endod.* **45**, 943-949 (2019).
- 456 Miles, A. A., Misra, S. S. & Irwin, J. O. The estimation of the bactericidal power of the blood. *J. Hyg. (Lond.)* **38**, 732-749 (1938).
- 457 Kapralos, V. et al. Antimicrobial and physicochemical characterization of endodontic sealers after exposure to chlorhexidine digluconate. *Dent. Mater.* **37**, 249-263 (2021).
- 458 Oliver, J. D. The viable but nonculturable state in bacteria. *J. Microbiol.* **43**, 93-100 (2005).
- 459 Zhang, H., Shen, Y., Ruse, N. D. & Haapasalo, M. Antibacterial activity of endodontic sealers by modified direct contact test against *Enterococcus faecalis*. *J. Endod.* **35**, 1051-1055 (2009).
- 460 Marggraf, T., Ganas, P., Paris, S. & Schwendicke, F. Bacterial reduction in sealed caries lesions is strain- and material-specific. *Sci. Rep.* **8**, 3767 (2018).
- 461 The editorial board of the Journal of Endodontics. Wanted: a base of evidence. *J. Endod.* **33**, 1401-1402 (2007).
- 462 Kapralos, V. et al. The dentine-sealer interface: Modulation of antimicrobial effects by irrigation. *Int. Endod. J.* **55**, 544-560 (2022).
- 463 Ma, J., Wang, Z., Shen, Y. & Haapasalo, M. A new noninvasive model to study the effectiveness of dentin disinfection by using confocal laser scanning microscopy. *J. Endod.* **37**, 1380-1385 (2011).
- 464 Haapasalo, M. & Ørstavik, D. In vitro infection and disinfection of dentinal tubules. *J. Dent. Res.* **66**, 1375-1379 (1987).
- 465 Shabahang, S. & Torabinejad, M. Effect of MTAD on *Enterococcus faecalis*-contaminated root canals of extracted human teeth. *J. Endod.* **29**, 576-579 (2003).
- 466 Williamson, A. E., Dawson, D. V., Drake, D. R., Walton, R. E. & Rivera, E. M. Effect of root canal filling/sealer systems on apical endotoxin penetration: a coronal leakage evaluation. *J. Endod.* **31**, 599-604 (2005).
- 467 DaSilva, L., Finer, Y., Friedman, S., Basrani, B. & Kishen, A. Biofilm formation within the interface of bovine root dentin treated with conjugated chitosan and sealer containing chitosan nanoparticles. *J. Endod.* **39**, 249-253 (2013).
- 468 Del Carpio-Perochena, A., Kishen, A., Shrestha, A. & Bramante, C. M. Antibacterial properties associated with chitosan nanoparticle treatment on root dentin and 2 types of endodontic sealers. *J. Endod.* **41**, 1353-1358 (2015).
- 469 Canette, A. & Briandet, R. Microscopy: confocal laser scanning microscopy. In *Encyclopedia of Food Microbiology* (eds Batt, C. & Tortorello, M.) 676-683 (Academic Press, 2014).
- 470 Berney, M., Hammes, F., Bosshard, F., Weilenmann, H. U. & Egli, T. Assessment and interpretation of bacterial viability by using the LIVE/DEAD BacLight Kit in combination with flow cytometry. *Appl. Environ. Microbiol.* **73**, 3283-3290 (2007).
- 471 Stiefel, P., Schmidt-Emrich, S., Maniura-Weber, K. & Ren, Q. Critical aspects of using bacterial cell viability assays with the fluorophores SYTO9 and propidium iodide. *BMC Microbiol.* **15**, 36 (2015).

- 472 Tawakoli, P. N., Al-Ahmad, A., Hoth-Hannig, W., Hannig, M. & Hannig, C. Comparison of different live/dead stainings for detection and quantification of adherent microorganisms in the initial oral biofilm. *Clin. Oral Investig.* **17**, 841-850 (2013).
- 473 Shi, L. et al. Limits of propidium iodide as a cell viability indicator for environmental bacteria. *Cytometry A* **71**, 592-598 (2007).
- 474 Camilleri, J. et al. The constitution of mineral trioxide aggregate. *Dent. Mater.* **21**, 297-303 (2005).
- 475 Shen, Y., Peng, B., Yang, Y., Ma, J. & Haapasalo, M. What do different tests tell about the mechanical and biological properties of bioceramic materials? *Endod. Top.* **32**, 47-85 (2015).
- 476 International Standards Organization. ISO 10993-5. *Biological evaluation of medical devices — Part 5: Tests for in vitro cytotoxicity* (2009).
- 477 Wei, W. et al. Effects of an experimental calcium aluminosilicate cement on the viability of murine odontoblast-like cells. *J. Endod.* **38**, 936-942 (2012).
- 478 De-Deus, G. et al. A critical analysis of research methods and experimental models to study root canal fillings. *Int. Endod. J.* **55**, 384-445 (2022).
- 479 Teughels, W., Van Assche, N., Sliepen, I. & Quirynen, M. Effect of material characteristics and/or surface topography on biofilm development. *Clin. Oral Implants Res.* **17**, 68-81 (2006).
- 480 Milosevic, A. The influence of surface finish and in-vitro pellicle on contact-angle measurement and surface morphology of three commercially available composite restoratives. *J. Oral Rehabil.* **19**, 85-97 (1992).
- 481 Quirynen, M. & Bollen, C. M. The influence of surface roughness and surface-free energy on supra- and subgingival plaque formation in man. A review of the literature. *J. Clin. Periodontol.* **22**, 1-14 (1995).
- 482 Law, K.-Y. Definitions for hydrophilicity, hydrophobicity, and superhydrophobicity: getting the basics right. *J. Phys. Chem. Lett.* **5**, 686-688 (2014).
- 483 Gandolfi, M. G., Siboni, F. & Prati, C. Properties of a novel polysiloxane-guttapercha calcium silicate-bioglass-containing root canal sealer. *Dent. Mater.* **32**, e113-e126 (2016).
- 484 Siboni, F., Taddei, P., Prati, C. & Gandolfi, M. G. Properties of NeoMTA Plus and MTA Plus cements for endodontics. *Int. Endod. J.* **50**, e83-e94 (2017).
- 485 Zhao, S. et al. A preliminary investigation of metal element profiles in the serum of patients with bloodstream infections using inductively-coupled plasma mass spectrometry (ICP-MS). *Clin. Chim. Acta* **485**, 323-332 (2018).
- 486 Lloyd, G. E. Atomic number and crystallographic contrast images with the SEM: a review of backscattered electron techniques. *Mineral. Mag.* **51**, 3-19 (1987).
- 487 Torabinejad, M., Smith, P. W., Kettering, J. D. & Pitt Ford, T. R. Comparative investigation of marginal adaptation of mineral trioxide aggregate and other commonly used root-end filling materials. *J. Endod.* **21**, 295-299 (1995).
- 488 Paillere, A. M. Applications of admixtures in concrete. RILEM Report 10 (Chapman & Hall, 1995).

- 
- 489 Odler, I. Hydration, setting and hardening of Portland cement. in *Lea's Chemistry of Cement and Concrete*, 4<sup>th</sup> edn (ed Hewlett, P. C.) 241-297 (Butterworth-Heinemann, 1998).
- 490 Giraud, T. et al. Pulp capping materials modulate the balance between inflammation and regeneration. *Dent. Mater.* **35**, 24-35 (2019).
- 491 Bortoluzzi, E. A. et al. Cytotoxicity and osteogenic potential of silicate calcium cements as potential protective materials for pulpal revascularization. *Dent. Mater.* **31**, 1510-1522 (2015).
- 492 Brambilla, E. et al. Hydrophilicity of dentin bonding systems influences in vitro *Streptococcus mutans* biofilm formation. *Dent. Mater.* **30**, 926-935 (2014).
- 493 Liu, Y. et al. The influence of cell and substratum surface hydrophobicities on microbial attachment. *J. Biotechnol.* **110**, 251-256 (2004).
- 494 Atmeh, A. R. Investigating the effect of bicarbonate ion on the structure and strength of calcium silicate-based dental restorative material-Biodentine. *Clin. Oral Investig.* **24**, 4597-4606 (2020).
- 495 Morandeau, A., Thiéry, M. & Dangla, P. Investigation of the carbonation mechanism of CH and C-S-H in terms of kinetics, microstructure changes and moisture properties. *Cem. Concr. Res.* **56**, 153-170 (2014).
- 496 Ashofteh Yazdi, K. et al. Microstructure and chemical analysis of four calcium silicate-based cements in different environmental conditions. *Clin. Oral Investig.* **23**, 43-52 (2019).
- 497 Graziotin-Soares, R. et al. Crystalline phases involved in the hydration of calcium silicate-based cements: Semi-quantitative Rietveld X-ray diffraction analysis. *Aust. Endod. J.* **45**, 26-32 (2019).
- 498 Elnaghy, A. M. Influence of acidic environment on properties of biodentine and white mineral trioxide aggregate: a comparative study. *J. Endod.* **40**, 953-957 (2014).
- 499 Figge, J., Rossing, T. H. & Fencl, V. The role of serum proteins in acid-base equilibria. *J. Lab. Clin. Med.* **117**, 453-467 (1991).
- 500 Wang, Z. et al. Dentine remineralization induced by two bioactive glasses developed for air abrasion purposes. *J. Dent.* **39**, 746-756 (2011).
- 501 Cardinali, F. & Camilleri, J. A critical review of the material properties guiding the clinician's choice of root canal sealers. *Clin. Oral Investig.* **27**, 4147-4155 (2023).
- 502 About, I. *Biodentine™: Properties and Clinical Applications* (Springer, 2021).
- 503 Barone, C., Dao, T. T., Basrani, B. B., Wang, N. & Friedman, S. Treatment outcome in endodontics: the Toronto study--phases 3, 4, and 5: apical surgery. *J. Endod.* **36**, 28-35 (2010).



## **Published Studies**



I







# Surface characteristics and bacterial adhesion of endodontic cements

Andreas Koutroulis<sup>1</sup> · Håkon Valen<sup>2</sup> · Dag Ørstavik<sup>1</sup> · Vasileios Kapralos<sup>1</sup> · Josette Camilleri<sup>3</sup> · Pia Titterud Sunde<sup>1</sup>

Received: 17 March 2022 / Accepted: 23 July 2022  
© The Author(s) 2022

## Abstract

**Objectives** To investigate the effect of inclusion of silver nano-particles (SNP) or bioactive glass (BG) on the surface characteristics and bacterial adhesion of prototype tricalcium silicate (TCS)–based cements alongside two commercial cements, under different aging periods and exposure conditions.

**Materials and methods** A basic formulation of radio-opacified TCS without (TZ-base) and with additions of SNP (0.5, 1, or 2 mg/ml) or BG (10 or 20%) was used. Biodentine and intermediate restorative material (IRM) served as reference materials. Material disks were immersed in ultrapure water or fetal bovine serum (FBS) for 1, 7, or 28 days. Surface roughness ( $n=3$ ), microhardness ( $n=9$ ), and wettability ( $n=6$ ) were analyzed by standard procedures. Adhesion of *Enterococcus faecalis* was assessed by fluorescence microscopy ( $n=5$ ). Data from these assays were evaluated for normality and comparisons among groups were conducted with statistical procedures ( $p<0.05$  for significance).

**Results** The surface morphology of SNP- and BG-containing cements had higher roughness values than TZ-base after 28 days ( $p<0.05$ ). No differences in microhardness were observed among prototype cements ( $p>0.05$ ). Biodentine presented smooth surface characteristics and the highest hardness values ( $p<0.05$ ). The FBS-immersion resulted in surface reactions in prototype materials and Biodentine, depicted with scanning electron microscopy. All 1- and 7-day prototype cements showed negligible bacterial adhesion, while in Biodentine and IRM, noticeable *E. faecalis* adherence was observed from day 1 ( $p<0.05$ ).

**Conclusions** Incorporation of SNP or BG did not improve the antibacterial effect of the experimental cement; all 28-day aged materials failed to inhibit bacterial adherence. The measured physical parameters did not appear to be related to the degree of bacterial adhesion. Exposure of TCS-based cements in FBS resulted in surface reactions, which did not affect bacterial adhesion.

**Clinical relevance** Changes in the surface characteristics of prototype TCS-based cements by inclusion of SNP and BG or exposure to different environments did not affect bacterial adhesion. All experimental materials showed inferior physical properties and higher antibacterial effect than Biodentine.

**Keywords** Antibacterial compounds · Calcium silicate · Characterization · Root-end filling · Root repair

## Introduction

Root canal filling materials should provide a seal between the root canal system and the surrounding periodontal tissues [1]. The rationale is to inhibit bacterial penetration and consequent biofilm formation [2]. Materials used for apexification, perforation repair, or retrograde root filling face an additional challenge, as they have a larger contact area with underlying periodontal tissues compared to materials used for conventional root canal filling [1].

Tricalcium silicate (TCS)–based cements are materials with properties suitable for such procedures. Their main advantages are their hydraulic nature and the formation of

✉ Andreas Koutroulis  
andreas.koutroulis@odont.uio.no

<sup>1</sup> Section of Endodontics, Institute of Clinical Dentistry, Faculty of Dentistry, University of Oslo, Blindern, P.O. Box 1109, 0317 Oslo, Norway

<sup>2</sup> Nordic Institute of Dental Materials (NIOM), Oslo, Norway

<sup>3</sup> School of Dentistry, Institute of Clinical Sciences, College of Medical and Dental Sciences, University of Birmingham, Birmingham, UK

calcium hydroxide upon hydration of the calcium silicate particles [3]. Release of calcium hydroxide may stimulate healing as well as provide an antimicrobial effect [4].

Mineral trioxide aggregate (MTA) is a Portland cement (PC)-based material developed specifically as a perforation repair material and for root-end filling [5]. Since its introduction in clinical dentistry, several materials based on pure TCS have been developed. PC was later replaced because of the potential of aluminum to leach to peripheral organs [6]. In addition, the new generations of hydraulic TCS-based cements contain additives aiming to enhance materials' physico-chemical performance compared to MTA [7]. In Biodentine (Septodont, Saint Maur-des-Fosses, France), calcium carbonate and water-reducing agents are used for this purpose [8].

Antibacterial activity of endodontic materials may contribute to the eradication of bacteria that have survived the preceding disinfection procedures [9, 10]. Even in cases where root-end surgery has been performed and the area of infection has been removed, persistent bacteria may have the capacity to re-establish and cause a re-infection [11]. In TCS-based cements, the antibacterial potential stems mainly from the high alkalinity due to hydroxyl ions of the calcium hydroxide by-product [12]. However, contact with blood may neutralize the antibacterial potential of MTA [13]. Overall, it seems that interactions of hydraulic materials with the environment can modulate their physico-chemical and biological properties [14, 15]. Calcium carbonate may be formed at the expense of calcium hydroxide [16], and the reduced alkalinity may limit the material's antibacterial activity. Therefore, the surface properties as modified by interactions with the environment may play a role in the inhibition of bacterial adherence and consequent biofilm formation [17].

Taking into consideration the moderating effect of environmental conditions, introducing an antibacterial agent in TCS-based cements such as silver nano-particles (SNP) could be beneficial. SNP can penetrate the dentinal tubules [18] and limit bacterial growth by releasing free silver ions [19]. At the same time, as root-end filling and root-repair materials are usually placed in a field of chronic inflammation where tissue destruction prevails, the potential of a material to stimulate the post-treatment healing of the periodontal tissues is as important as the antibacterial effect. Inclusion of bioactive glass (BG) into TCS could contribute to the balance between these desirable properties [20]. A recent study showed that 10% addition of different types of BG to Biodentine resulted in marked apatite formation upon its surface suggesting an enhanced bioactivity potential [21]. The bioglass formulation BG 45S5 consists of silicon dioxide, calcium oxide, sodium oxide, and diphosphorus pentoxide and was the first material introduced in medicine that could induce osteogenesis and create a bond with the

host bone tissue [22]. BG 45S5 also has a moderate, pH-dependent antibacterial effect [23].

Dentinal and material surfaces may serve as footholds for bacteria to attach and multiply with biofilm formation and produce disease [24]. Modifying the chemistry of biomaterials in order to limit biofilm formation or enhance their bioactivity would seem beneficial, provided the modifications do not negatively influence essential physical properties. The main aim of the current study was to investigate the surface characteristics as well as the bacterial adhesion of prototype TCS-based cements with or without incorporation of SNP or BG 45S5. The null hypothesis studied was that incorporation of SNP or BG 45S5 in hydraulic TCS-based cements will not have any effect on the cements' surface characteristics nor in the inhibition of bacterial adhesion. An additional aim was to explore changes in the adhesion patterns in connection to surface characteristics across exposure to different environmental conditions and aging periods. For comparison, these properties were also investigated in two commercial materials, a TCS-based cement that contains modifications from the conventional synthesis of a radio-opacified TCS cement (Biodentine) and a zinc-oxide eugenol-based material (intermediate restorative material; Dentsply Sirona, Charlotte, NC, USA). Both are used in root-end filling or root repair procedures.

## Materials and methods

### Test materials

The following materials were used in the study:

- Tricalcium silicate cement (TCS; CAS No: 12168–85-3, American Elements, Los Angeles, CA, USA) with 20% weight-replacement of zirconium oxide (ZO; Koch-Light Laboratories, Colnbrook, Bucks, UK) (TZ-base).
- TZ-base with 10% or 20% replacement by weight of the TCS with bioactive glass 45S5 (BG; Cas No: 65997–17-3, 10 µm particle size, Mo-Sci Corporation, Rolla, MO, USA) (TZ-bg10, TZ-bg20 respectively).
- TZ-base with incorporation of 0.5 mg/ml, 1 mg/ml, or 2 mg/ml silver nano-particles (SNP; CAS No: 7440–22-4, < 100 nm particle size, Sigma-Aldrich, Gillingham, UK) (TZ-Ag0.5, TZ-Ag1, and TZ-Ag2 respectively), following dispersion of silver nano-powder in ultrapure water (water; Elix Essential 5 UV Water Purification System, Merck KGaA, Darmstadt, Germany).
- Biodentine (Septodont, Saint Maur-des-Fosses, France).
- Intermediate restorative material (IRM; Dentsply Sirona, Charlotte, NC, USA).

## Material preparation

### Dispersion of silver nano-particles (SNP)

The NANOGENOTOX dispersion protocol was followed with slight modifications [25]. In brief, 12 mg SNP was pre-wet in 30  $\mu$ l ethanol. Consequently, 5.97 ml water was slowly added in the solution resulting in a 2-mg/ml SNP concentration, instead of a 2.56-mg/ml concentration specified in the original protocol. The solution was then placed in an ice bath and sonicated (VCX 130, Sonics & Materials, Newtown, CT, USA). Further dilutions were prepared (1 mg/ml and 0.5 mg/ml). Sonication of SNP solution was carried out immediately before material mixing.

### Mixing and placement

Prototype materials were hand-spatulated with water or the respective SNP solutions. The liquid/powder ratio employed was 0.35 ml/g. Commercial materials were handled according to the manufacturer's instructions.

Materials were compacted inside Teflon disks (9 mm internal diameter,  $1 \pm 0.1$  mm thickness) upon glass microscope slides (Fig. 1a). They were covered with a wet gauze and allowed to set for 24 h at 37 °C. After this period, the material specimens were immersed in 4 ml water or fetal bovine serum (FBS; F7524, Merck, Darmstadt, Germany). Samples were incubated for 1, 7, or 28 days at 37 °C (Fig. 1b). Consequently, they were retrieved, vacuum desiccated, and subjected to testing, except for the ones used in the adhesion assay, which were tested immediately after the respective aging periods.

The immersion medium was replaced with fresh one every 7 days.

## Material characterization

### Evaluation of radio-opacity

Prototype materials ( $n=3$  per group) were tested in order to verify that the 20% ZO-incorporation induced adequate radio-opacity to the cements in compliance with the ISO 6876:2012 requirements [26]. Briefly, the material pellets and a 1-mm increment aluminum step wedge (1–10 mm thickness) were placed upon a photo-stimulable phosphor plate (VitaScan, Durr Dental, Bietigheim-Bissingen, Germany). Digital radiographs were acquired by a standard X-ray machine using an exposure time of 0.80 s at 10 mA, tube voltage at  $65 \pm 5$  kV, and a cathode–target film distance of 30 cm. Radiographs were consequently processed and the digital images obtained served for the interpretation of results as described by Formosa et al. [27].

## Photography

Specimens ( $n=3$ ) were photographed in a dark background to identify differences macroscopically in their color or structure after immersion in different media or from the incorporation of different components (Fig. 1c).

### Scanning electron microscopy (SEM), energy dispersive X-ray (EDX) analysis, and surface roughness assessment

The materials ( $n=3$  per group) were placed upon carbon tapes and imaged with a scanning electron microscope (TM4000Plus II, Hitachi, Tokyo, Japan). Images were obtained by combining a backscattered electron and secondary electron signal detector (mix signal). Additionally, for the surface roughness analysis, 4 backscattered images were obtained at each observation field at  $200\times$  magnification with a quad-type backscatter electron detector. Stereoscopic reconstruction in a 3D model of these images was performed with the use of a suitable software (MountainsMap; Digital Surf, Besançon, France). Eighteen surface roughness values (Ra) were consequently obtained from each 3D model following calibration of the program with an artificially induced consistent angulation upon the surface of a reference material. TZ-base was used for that purpose (Fig. 1c).

### Surface microhardness assay

Materials ( $n=9$  per group) were subjected to Vicker's microhardness testing (Duramin-40 A1, Struers, Rotherham, UK) (Fig. 1d). Values were obtained after exposing the samples to a 100-g load for 15 s of dwelling time. Three to five measurements were conducted per sample in non-overlapping planes. The Vickers hardness number (HV) was consequently automatically calculated from the program equipment using the following equation:

$$HV = 1.854(F/d^2)$$

### Wettability assessment

Contact angle measurements ( $n=6$  per group) were taken using a contact angle goniometer (NRL 100–10, ramehart, Mountain Lakes, NJ, USA). A micro-syringe was used to deliver a 10- $\mu$ l drop of water upon the material surface. The angle was determined within 30 s of placement of the drop. Two measurements were conducted per sample (Fig. 1e).

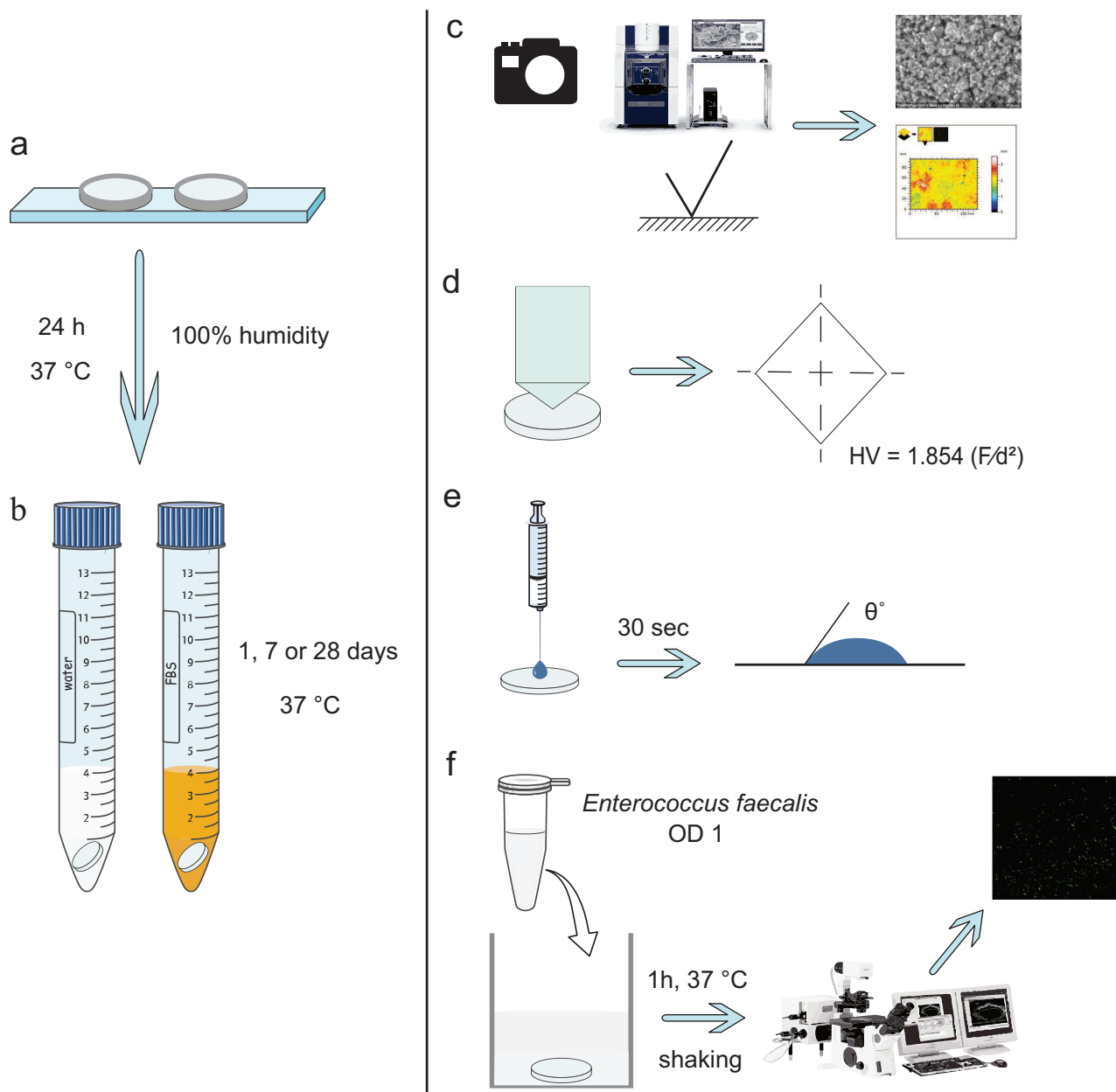


**Fig. 1** Schematic representation of the methodology. Test materials were compacted inside Teflon disks upon microscope slides (a). Consequently, they were immersed in 4 ml ultrapure water or fetal bovine serum (b). After the specified aging periods, specimens were

subjected to photography, SEM, EDX, and surface roughness analysis (c) and assessment of surface microhardness (d) and wettability (e) as well as adhesion assay (f)

### Assessment of bacterial adhesion

*Enterococcus faecalis* OG1RF, which expresses the green-fluorescent protein [28], was taken from frozen stock cultures and incubated overnight in Tryptic Soy Broth (TSB; Sigma-Aldrich, Gillingham, UK) at 37 °C with 5% CO<sub>2</sub> in a humidified atmosphere. The following day, bacterial cultures were centrifuged and suspended in phosphate buffered saline

(PBS; Fisher Scientific, Waltham, MA, USA) in order to prepare a bacterial inoculum with optical density (OD) 1.0 at 600 nm (approximately  $1 \times 10^8$  CFU/ml).

The material specimens ( $n = 5$  per group) were placed inside 48 well-plates (Thermo Fisher Scientific, Waltham, MA, USA) and exposed to 700  $\mu$ l of the *E. faecalis* inoculum for 1 h at 37 °C in a shaking incubator. Subsequently, they were carefully shaken and rinsed with sterile water

to remove loosely attached bacteria. For positive control, sterile membrane filters (MF-Millipore, 0.45 µm pore size, Merck, Darmstadt, Germany) cut to the same diameter (9 mm) as the material specimens were used. Imaging of viable *E. faecalis* cells upon the material surface was performed with a confocal laser scanning microscope (CLSM; Olympus FluoView FV1200, Olympus, Tokyo, Japan) with a 60× water immersion lens. Three images were obtained per specimen upon different areas of the material. Images (480×480 pixel size) were consequently processed with ImageJ (US National Institute of Health, Bethesda, MD, USA). Using the “find maxima” algorithm in the program and selecting a noise threshold of 12 towards a representative part of the image (1/4 of the initial size-240×240 pixel size), bacterial cells were depicted and automatically counted (Fig. 1f).

## Statistical analyses

All quantitative results were analyzed statistically, except for the radio-opacity values which were assessed qualitatively in terms of if the ISO standards [26] were fulfilled. IBM SPSS Statistics software version 27 (IBM, Armonk, NY, USA) was employed. Each set of results was assessed for normality according to the Shapiro–Wilk test. The majority of contact angle values did not follow the normal distribution and were thus analyzed with non-parametric Kruskal–Wallis test adjusted by the Bonferroni correction or Mann–Whitney *U* test. For groups with only zero values, a one sample Wilcoxon rank-sum test was used for comparisons with other groups. All other data were analyzed with ANOVA and Bonferroni post-hoc tests for multiple comparisons. Multiple comparisons for data for surface roughness, microhardness, and adhesion assays were performed among different materials for similar aging period and immersion medium or for the same materials along different aging periods and immersion medium. The significance level to all analyses was set at  $p = 0.05$ .

## Results

### Characterization

#### Radio-opacity

All prototype materials had adequate radio-opacity according to ISO 6876 [26] (Table 1). Further experiments for prototype cements were therefore conducted with the 20% ZO-replacement.

**Table 1** Mean and standard deviation of radio-opacity (mm aluminum) of prototype cements

Material	Radio-opacity (mm aluminum)
TZ-base	3.6 (0.5)
TZ-bg10	3.5 (0.3)
TZ-bg20	3.4 (0.5)
TZ-Ag0.5	3.7 (0.8)
TZ-Ag1	3.6 (0.4)
TZ-Ag2	3.4 (0.2)

### Macroscopic assessment of material surface

The color of prototype materials was not visibly affected by the incorporation of SNP (Fig. 2a). After the immersion periods in FBS, prototype cements experienced a visible yellow discoloration (Fig. 2a), while changes in Biodentine surface were evident as white depositions particularly after 28 days (Fig. 2b). No change in the color or structure of IRM was evident macroscopically (Fig. 2c).

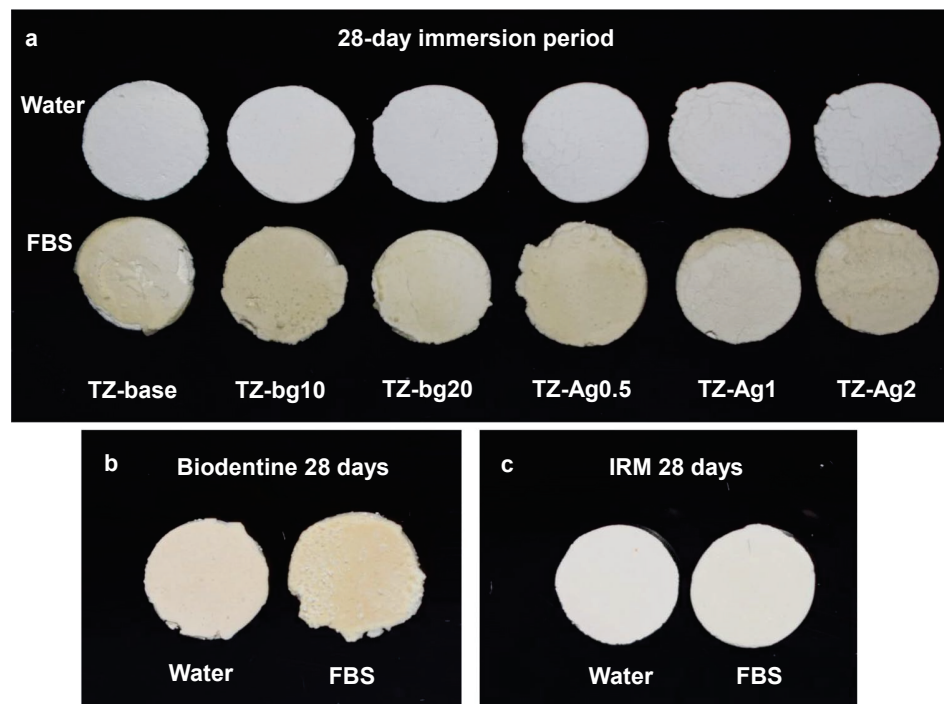
### SEM, EDX, and surface roughness

SEM images of prototype cements after immersion in water showed similar surface morphology. The material matrix appeared gradually more homogenized after 7 and 28 days (Fig. 3a, Online Resource 1). The main elements in the EDX scans were calcium, silicon, oxygen, and zirconium, while phosphate and sodium was also evident in the BG-containing materials. Silver was rarely depicted in the SNP-containing cements, mainly in the TZ-Ag2 (Fig. 3b).

For surface roughness assessments in the water-immersed materials (Table 2), all BG- and SNP-containing cements reported higher Ra values than the rest after 28 days ( $p < 0.01$ ), with TZ-bg20 having the highest Ra ( $p < 0.001$ ). The Ra values of TZ-base and TZ-Ag1 showed a significant decrease between 7 and 28 days ( $p < 0.05$ ), while those of TZ-bg20 increased between 1 and 28 ( $p < 0.05$ ). Biodentine had a smoother surface morphology than all the prototype cements in all aging periods ( $p < 0.001$ ), without fluctuations in Ra ( $p > 0.05$ ).

Immersion in FBS altered completely the surface characteristics of TCS-based cements (prototype cements and Biodentine). SEM images revealed the precipitation of organic compounds and consequent reaction with the cements' surface, which was gradually more evident for longer immersion period (Figs. 3a and 4a; Online Resources 1 and 2). The EDX analysis showed that the particles that were formed consisted mainly of calcium and oxygen as well as carbon or phosphorus. Traces of sodium, magnesium, nitrogen, and chlorine were also observed occasionally in relatively low amounts (Figs. 3b and 4b, Online Resource 1).

**Fig. 2** Indicative images of prototype materials (a), Biodentine (b), and IRM (c) after a 28-day immersion period in ultrapure water (water) or fetal bovine serum (FBS)



Consequently, a rougher surface morphology was observed in all cases for TCS-based cements upon immersion in FBS compared to the respective water ones for the same aging periods, which was statistically significant for 28 days samples ( $p < 0.05$ ), except for TZ-Ag2 ( $p > 0.05$ ). Biodentine did not report any significant difference from the prototype cements after 7 and 28 days ( $p > 0.05$ ) (Table 2).

IRM showed no alterations in Ra values for the different aging periods or immersion media ( $p > 0.05$ ) (Fig. 5a). The Ra of IRM was significantly lower than all other materials after immersion in water ( $p < 0.001$ ), except compared with Biodentine ( $p > 0.05$ ). EDX analysis showed the presence of calcium, phosphorus, and occasionally sodium and magnesium in the FBS-immersed IRM samples in addition to zinc and oxygen that were depicted in the water-immersed ones (Fig. 5b).

### Surface microhardness

Prototype materials had overall significantly lower microhardness values than Biodentine for all test conditions ( $p < 0.001$ ), as well as IRM ( $p < 0.01$ ) except for the 28-day water-immersed samples ( $p > 0.05$ ) (Table 3). Incorporation of BG or SNP did not alter the microhardness of the prototype cements for any aging period for both immersion media ( $p > 0.05$ ).

In the water-immersed materials, Biodentine reported a significant decrease in hardness values between the 1- and 28-day samples ( $p < 0.01$ ), while it increased in FBS

from the 7- to 28-day period ( $p < 0.01$ ). Hardness of Biodentine in FBS was significantly higher compared to the water-immersed samples after the 28-day immersion period ( $p < 0.001$ ).

IRM had significantly lower microhardness values than Biodentine during all tested periods ( $p < 0.001$ ). Overall, IRM had a similar pattern as Biodentine in terms of fluctuations in hardness values, reporting a significant decrease or increase in the 28-day water and FBS samples, respectively ( $p < 0.001$  for comparisons between 1- and 28-day water-immersed samples and for comparisons between 1- or 7-day FBS-immersed samples with the 28-day ones). Additionally, the 7- and 28-day FBS samples reported higher values than the respective water ones ( $p < 0.001$ ).

### Contact angle

Complete wetting was observed in all the water-immersed prototype cements (Table 4). In the FBS-immersed prototype materials, the hydrophilicity was moderated for 1-day samples ( $p < 0.05$ ) but it was gradually re-established in the 7-day samples until complete wetting was reported again after 28 days. Biodentine had a similar wettability pattern as the prototype cements, without however reporting complete wetting at any evaluation period. FBS immersion did not alter Biodentine's wettability significantly in any period ( $p > 0.05$ ). IRM had a different behavior, as the immersion in FBS resulted in relatively higher wettability, which was significantly different from the water-immersed samples

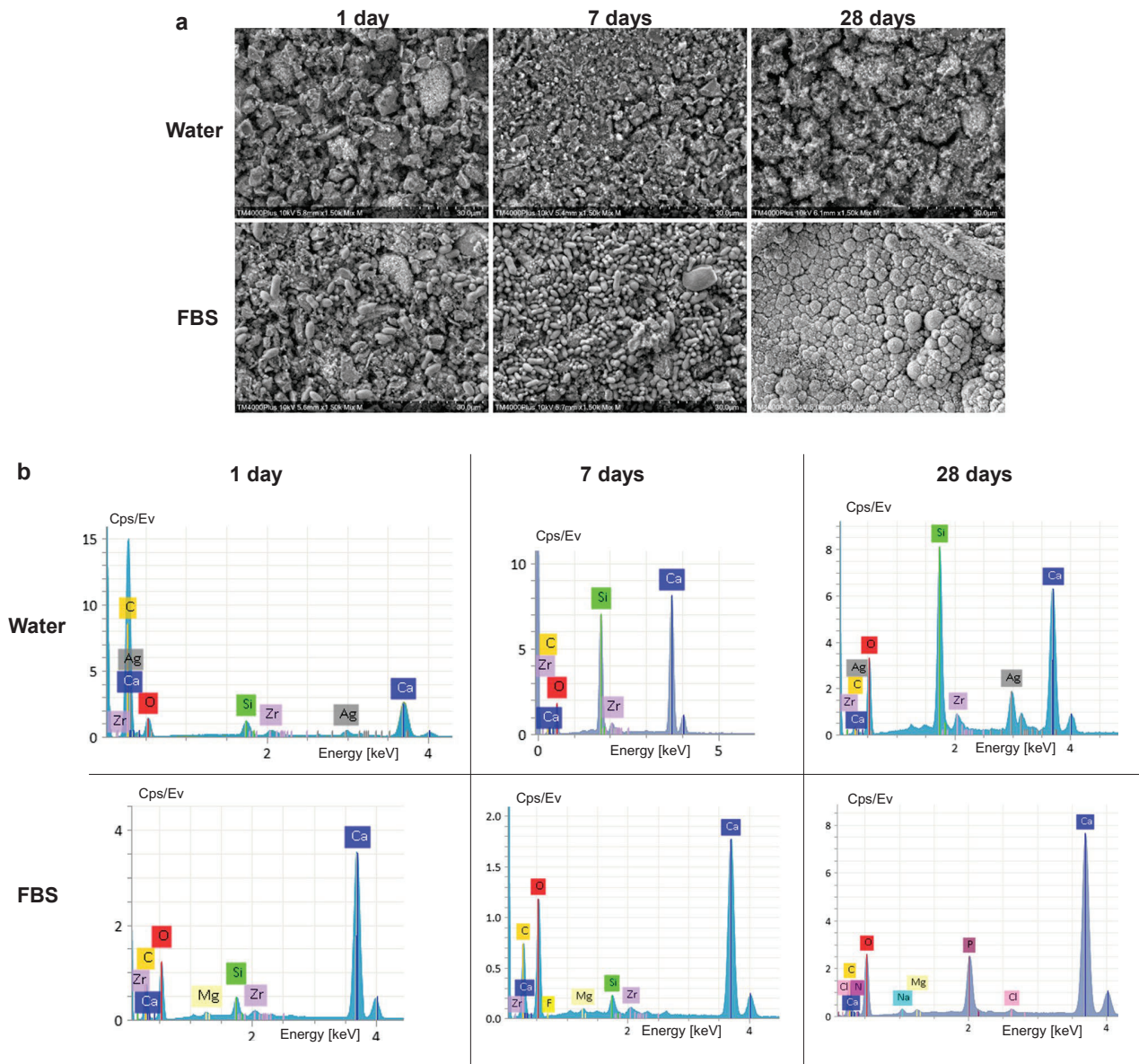


**Fig. 3** Representative scanning electron micrographs of TZ-Ag2 acquired with a mix of back-scatter and secondary electron signal detectors (1500×magnification) after exposure to ultrapure water

(water) or fetal bovine serum (FBS) for 1, 7, or 28 days (a). Representative energy-dispersive spectroscopic scans of selected spectrums (b)

after 7 days ( $p < 0.001$ ). No changes occurred throughout the immersion periods for both water- and FBS-immersed samples of IRM ( $p > 0.05$ ).

**Bacterial adhesion assay**

Prototype materials showed an overall low amount of *E. faecalis* adhesion after 1 and 7 days of aging, regardless of the immersion liquid. No significant differences were reported among them for these periods ( $p > 0.05$ ) (Fig. 6, Online Resource 3a). Additionally, significantly fewer

bacteria were observed on the surface of the prototype cements in comparison to Biodentine (Online Resource 3b) and IRM for the 1- and 7-day conditions both for water- and FBS-immersed samples ( $p < 0.001$ ). In the 28-day samples, a significant increased adhesion of the prototype cements was observed for both immersion media ( $p < 0.001$ ).

The TZ-bg20 water-immersed 28-day samples had the lowest bacterial adhesion, which was only significantly different than the positive control ( $p < 0.05$ ). No other differences were observed among prototype materials, Biodentine,

**Table 2** Mean and standard deviation of surface roughness Ra ( $\mu\text{m}$ ) for materials after immersion in water or FBS for 1, 7, or 28 days. Read horizontally, the same small superscript letter indicates no statistically significant differences between different aging periods and immersion solutions within the same material ( $p > 0.05$ ). Read vertically, the same capital letter shows non-statistically significant difference among materials for the exact same conditions of testing (aging period and immersion medium) ( $p > 0.05$ ). In 28-day water-immersed

samples, all BG- and SNP-containing cements reported higher Ra than the rest materials, with TZ-bg20 having the highest values ( $p < 0.05$ ). Water-immersed Biodentine and IRM had a smoother surface morphology than all the prototype cements in all aging periods ( $p < 0.05$ ). The 28-day FBS-immersed prototype cements had higher Ra than the respective water-exposed samples ( $p < 0.05$ ), except for TZ-Ag2 ( $p > 0.05$ )

Material	1 day		7 days		28 days	
	Water	FBS	Water	FBS	Water	FBS
<b>TZ-base</b>	0.095 (0.004) <sup>A,B-a,b</sup>	0.115 (0.006) <sup>A,B-a</sup>	0.09 (0.002) <sup>A,B-b</sup>	0.112 (0.008) <sup>A-a</sup>	0.063 (0.001) <sup>A-c</sup>	0.113 (0.022) <sup>A,B-a,b</sup>
<b>TZ-bg10</b>	0.083 (0.005) <sup>A-a</sup>	0.117 (0.016) <sup>A,B-a,b</sup>	0.104 (0.001) <sup>A-a</sup>	0.115 (0.008) <sup>A-a</sup>	0.083 (0.002) <sup>B-a</sup>	0.171 (0.056) <sup>A-b</sup>
<b>TZ-bg20</b>	0.091 (0.006) <sup>A-a</sup>	0.099 (0.006) <sup>A,C-a,b</sup>	0.1 (0.005) <sup>A,B-a,b</sup>	0.125 (0.004) <sup>A-c,d</sup>	0.109 (0.008) <sup>C-b,c</sup>	0.127 (0.004) <sup>A,B-d</sup>
<b>TZ-Ag0.5</b>	0.096 (0.001) <sup>A,B-a</sup>	0.109 (0.007) <sup>A,B-a</sup>	0.1 (0.004) <sup>A,B-a</sup>	0.125 (0.001) <sup>A-a</sup>	0.08 (0.001) <sup>B-a</sup>	0.211 (0.051) <sup>A-b</sup>
<b>TZ-Ag1</b>	0.094 (0.0001) <sup>A,B-a,b</sup>	0.123 (0.007) <sup>B-c,d</sup>	0.104 (0.004) <sup>A-a,d</sup>	0.125 (0.008) <sup>A-c,d</sup>	0.082 (0.005) <sup>B-b</sup>	0.134 (0.012) <sup>A,B-c</sup>
<b>TZ-Ag2</b>	0.106 (0.011) <sup>B-a,b</sup>	0.113 (0.001) <sup>A,B-a,b</sup>	0.087 (0.006) <sup>B-a,b</sup>	0.12 (0.002) <sup>A-a,b</sup>	0.083 (0.002) <sup>B-b</sup>	0.119 (0.026) <sup>A,B-a,b</sup>
<b>Biodentine</b>	0.038 (0.003) <sup>C-a</sup>	0.079 (0.01) <sup>C,D-a,b</sup>	0.044 (0.005) <sup>C-a</sup>	0.12 (0.024) <sup>A-a,b</sup>	0.038 (0.001) <sup>D-a</sup>	0.133 (0.061) <sup>A,B-b</sup>
<b>IRM</b>	0.036 (0.003) <sup>C-a</sup>	0.039 (0.003) <sup>D-a</sup>	0.041 (0.007) <sup>C-a</sup>	0.044 (0.01) <sup>B-a</sup>	0.03 (0.001) <sup>D-a</sup>	0.042 (0.01) <sup>B-a</sup>

and IRM for both the water- and FBS-immersed samples after 28 days ( $p > 0.05$ ).

In Biodentine, all samples allowed *E. faecalis* adhesion. However, bacterial adhesion was significantly lower than the positive control for the 1- and 7-day samples ( $p < 0.05$ ). No significant differences were reported between media for the same evaluation periods ( $p > 0.05$ ).

Bacterial adhesion was also observed in IRM, while after 28 days of aging, the water-immersed samples had significantly more bacteria compared to the FBS ones ( $p < 0.05$ ).

## Discussion

The present study assessed whether the incorporation of silver nano-particles or bioactive glass in TCS-based cements with rationale of use for root repair or root-end filling procedures could induce significant alterations in their surface characteristics and consequently modify their bacterial adhesion profile. The effect of immersion in a protein-rich solution was also investigated. Our results indicated that the additions caused an increase in surface roughness; however, this was not accompanied by changes in the adhesion patterns. The null hypothesis was therefore partially rejected. It was also shown that surface characteristics of TCS-based materials were significantly altered upon exposure to a protein-rich environment, again without affecting the bacterial adhesion patterns. Biodentine's better physical properties and smoother surface characteristics in comparison to the non-modified prototype cement were accompanied by a negligible early inhibition of bacterial adhesion.

Incorporation of BG in obturation materials has been reported to result in better adaptation to the surrounding dentin walls, probably due to the ionic exchange taking place at the interface and expansion of BG particles upon hydration [29]. BG is dissolved in contact with water leading to leaching of calcium and phosphate ions and formation of an intermediate layer rich in silicon oxide [30]. Leaching plays a significant role in the induction of healing processes [31]. A pronounced apatite-forming ability has been previously reported following BG-additions in Biodentine [21]. An antibacterial effect is also evident due to the increase in pH [23] and osmotic pressure [32]. These properties would seem beneficial in a root-repair material, and we therefore wanted to evaluate the surface modifications upon incorporation of BG compounds to TCS-based cements. We used BG 45S5 micro-particles as they appear superior in terms of their chemical profile in comparison to other BG types [33] and have similar characteristics to BG particles that have been previously incorporated in a commercial endodontic sealer [34, 35].

Similarly, silver nano-particles were considered candidates for improvement of the antibacterial properties of cements. Their antibacterial activity is attributed to the release of free silver ions that interact with sulfhydryl groups and nitrogen atoms in proteins and nucleic acids of bacterial cells and induce significant disruptions to their functionality [36]. At the same time, their nano-size enables them to penetrate into target cells and to cause cell damage by their oxidation potential [37]. Despite the well-researched potential of enhancement of the antibacterial activity of SNP-incorporation in various dental materials, such as resins [38], adhesives [39], endodontic medicaments [40], and irrigants



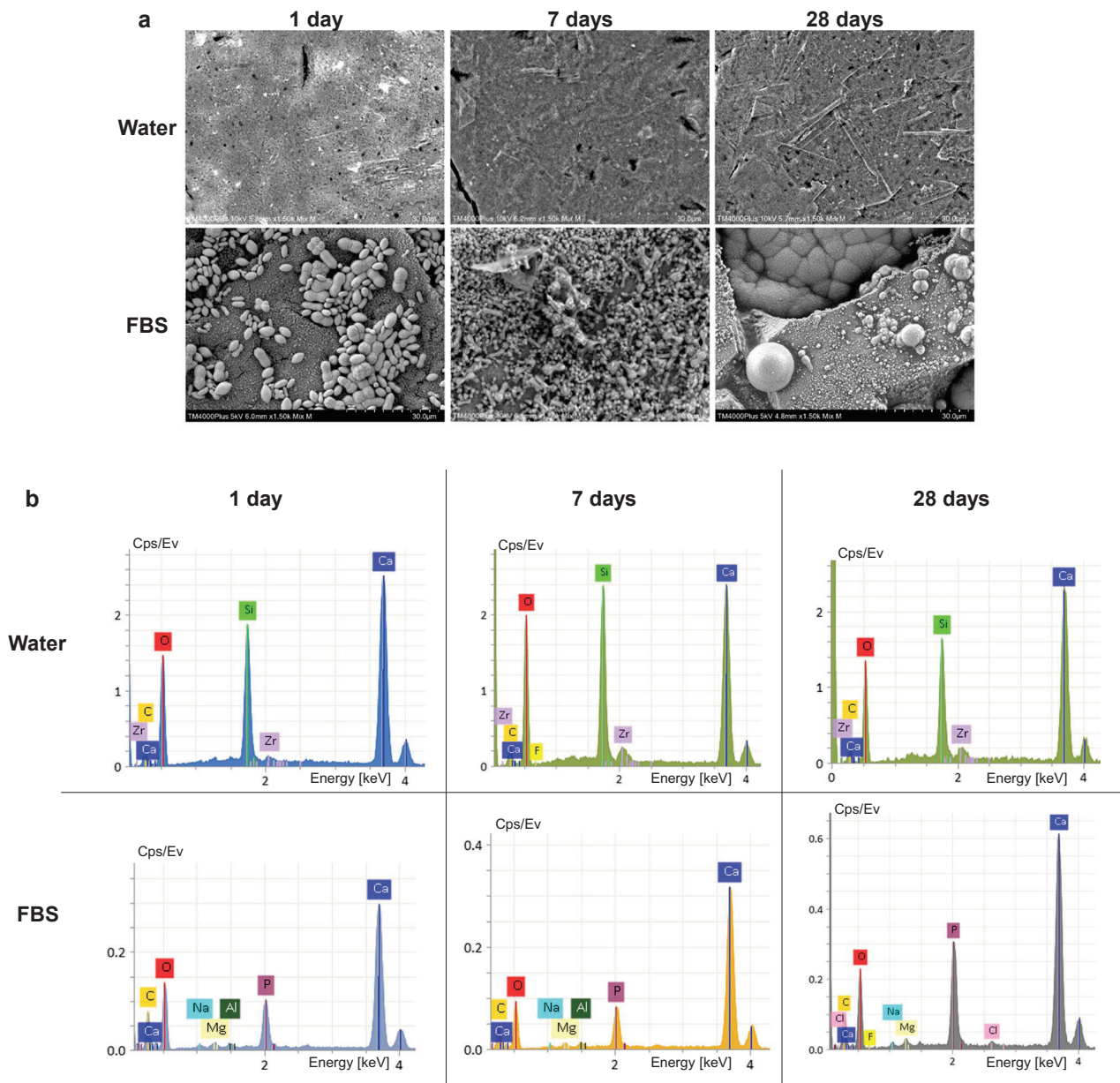


**Fig. 4** Scanning electron micrographs of Biodentine acquired with a mix of back-scatter and secondary electron signal detectors (1500×magnification) after exposure to ultrapure water (water) or fetal bovine serum (FBS) (1500×magnification) (a). Representative energy-dispersive spectroscopic scans of selected spectrums (b)

fetal bovine serum (FBS) (1500×magnification) (a). Representative energy-dispersive spectroscopic scans of selected spectrums (b)

[41, 42], there is still a controversy in the literature whether their desirable properties are derived from leaching of SNP to the immediate environment or through direct contact upon the material [43]. Furthermore, establishing an optimum concentration of silver nanoparticles for adequate antibacterial activity is challenging, as their reactivity depends on parameters that vary among the recruited compounds in the literature, namely, size, capping, and charge [44].

A commercial TCS-based cement was included in the study for comparison with the experimental formulations.

Biodentine was selected due to its chemical similarities to the prototype cements, as it consists mainly of TCS cement and has ZO as radio-opacifier, in contrast to PC-based MTA. Additionally, it contains compounds that enhance its physico-chemical profile. Calcium chloride and a water-soluble polymer are used in the liquid to reduce setting time and improve physical properties, respectively. Calcium carbonate is also added to the cement to control the hydration reaction [45]. IRM was included in the study in order to investigate the effect of environmental conditions and aging period on a

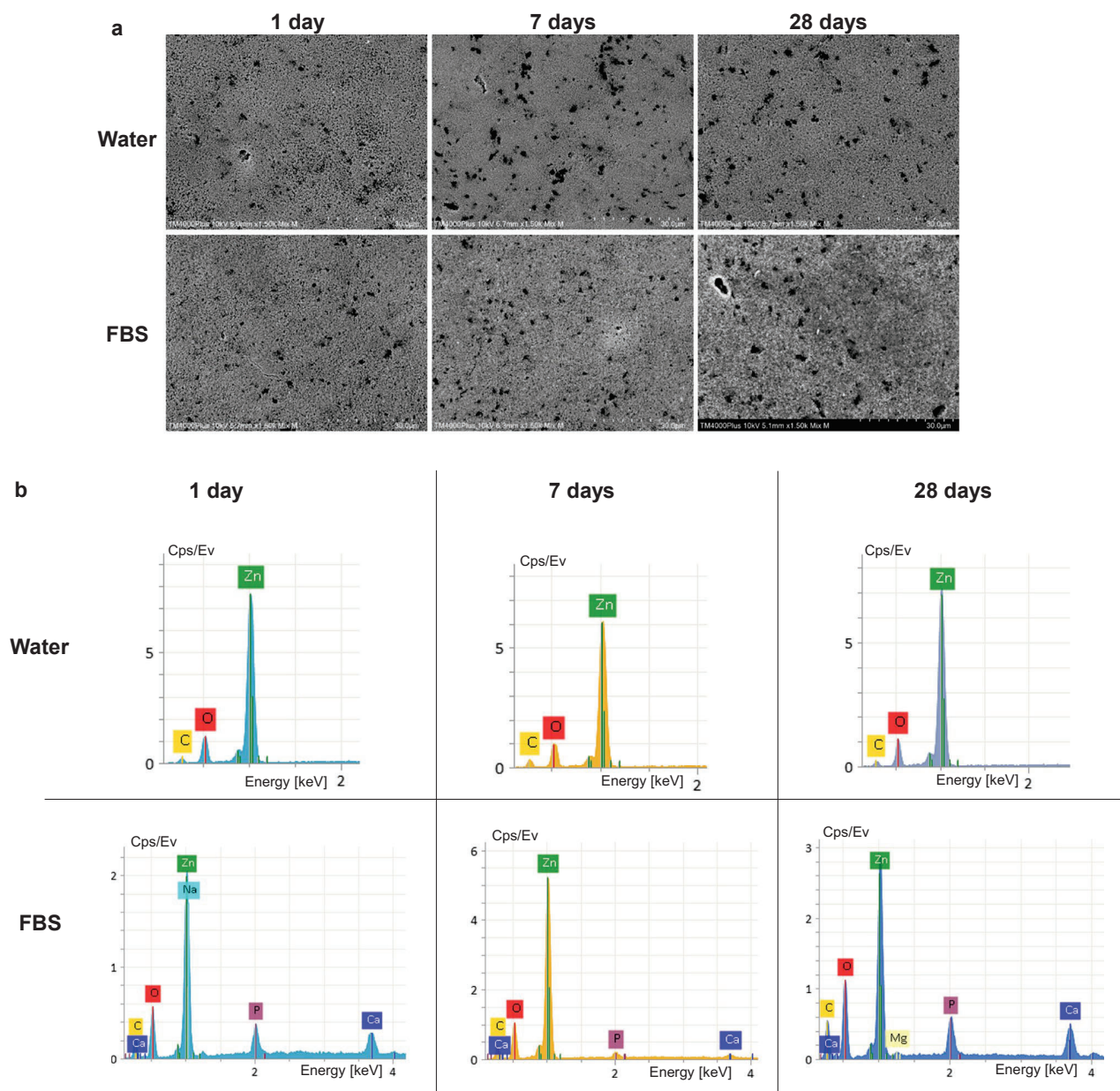


**Fig. 5** Representative scanning electron micrographs of IRM acquired with a mix of back-scatter and secondary electron signal detectors (1500×magnification) after exposure to ultrapure water (water) or

fetal bovine serum (FBS) (1500×magnification) for 1, 7, or 28 days (**a**). Representative energy-dispersive spectroscopic scans of selected spectrums (**b**)

material of completely different chemical composition from the tested hydraulic cements, but similar clinical application. IRM is used for root-end filling procedures and has reported similar clinical success to MTA [46, 47].

Root-repair and root-end filling materials are placed in a challenging biological environment, where they interact with tissue fluids, blood, and residual bacteria that might have survived the attempts of disinfection [48]. The materials can therefore be crucial in preventing bacteria from

getting access to nutrients that can enable them to proliferate and cause a re-infection. The role of their morphological characteristics in this dynamic environment defines their antibacterial profile to a significant extent together with the potentially leachable components [49]. Only few studies have assessed antimicrobial properties of hydraulic cements from the perspective of their use for root-end filling or perforation repair procedures [50]. At the same time, introducing chemical compounds to the formulation of TCS cements for

**Table 3** Mean and standard deviation of surface microhardness of test materials after 1, 7, or 28 days immersion in water or FBS. Read horizontally, the same small superscript letter indicates no statistically significant differences between different aging periods and immersion solutions within the same material ( $p > 0.05$ ). Read vertically, the same capital letter shows non-statistically significant differ-

ence among materials for the exact same conditions of testing (aging period and immersion solution) ( $p > 0.05$ ). Prototype cements' microhardness was not affected by SNP- or BG-incorporation ( $p > 0.05$ ). Biodentine had the highest values in all test conditions, while the microhardness of 28-day FBS-immersed Biodentine was higher than the respective water-exposed ( $p < 0.05$ )

Material	1 day		7 days		28 days	
	Water	FBS	Water	FBS	Water	FBS
<b>TZ-base</b>	8.05 (1.79) <sup>A-a,b</sup>	7.08 (1.79) <sup>A-a</sup>	10.59 (2.23) <sup>A-b</sup>	6.34 (1.13) <sup>A-a</sup>	8.25 (0.87) <sup>A-a,b</sup>	8.75 (2.38) <sup>A-a,b</sup>
<b>TZ-bg10</b>	7.64 (1.18) <sup>A-a</sup>	7.18 (1.08) <sup>A-a</sup>	7.83 (1.47) <sup>A-a</sup>	6.85 (1.83) <sup>A-a</sup>	8.1 (1.26) <sup>A-a</sup>	8.6 (2.4) <sup>A-a</sup>
<b>TZ-bg20</b>	6.23 (1.38) <sup>A-a,b</sup>	6.77 (1.41) <sup>A-a,b</sup>	8.07 (1.42) <sup>A-a</sup>	5.47 (1.25) <sup>A-b</sup>	7.63 (1.59) <sup>A-a,b</sup>	8.5 (2.63) <sup>A-a</sup>
<b>TZ-Ag0.5</b>	7.11 (2.22) <sup>A-a</sup>	6.59 (1.3) <sup>A-a</sup>	9.74 (1.96) <sup>A-b</sup>	7.31 (2.23) <sup>A-a,b</sup>	8.26 (1.45) <sup>A-a,b</sup>	7.99 (1.4) <sup>A-a,b</sup>
<b>TZ-Ag1</b>	7.46 (1.72) <sup>A-a</sup>	7.06 (1.37) <sup>A-a</sup>	8.98 (1.96) <sup>A-a</sup>	7.38 (2.02) <sup>A-a</sup>	8.3 (1.43) <sup>A-a</sup>	8.67 (2.43) <sup>A-a</sup>
<b>TZ-Ag2</b>	6.55 (1.3) <sup>A-a</sup>	7.56 (1.62) <sup>A-a,b</sup>	10.28 (1.32) <sup>A-c</sup>	7.54 (1.39) <sup>A-a,b</sup>	9.98 (2.74) <sup>A-b,c</sup>	8.96 (1.59) <sup>A-a,c</sup>
<b>Biodentine</b>	55.23 (6.87) <sup>B-a,b</sup>	53.8 (11.77) <sup>B-a,b</sup>	49.51 (2.6) <sup>B-a,c</sup>	47.88 (2.74) <sup>B-a,c</sup>	35.53 (4.89) <sup>B-c</sup>	67.56 (22.31) <sup>B-b</sup>
<b>IRM</b>	19.14 (3.2) <sup>C-a,b</sup>	23.3 (4.24) <sup>C-a,d</sup>	14.3 (2.03) <sup>C-b,c</sup>	28.51 (3.31) <sup>C-d</sup>	8.23 (1.05) <sup>A-c</sup>	44.21 (8.74) <sup>C-e</sup>

**Table 4** Median and interquartile range of contact angle measurements of test materials after 1, 7, or 28 days immersion in water or FBS. Read horizontally, same small superscript letters indicate no statistically significant differences between different aging periods and immersion solutions within the same material ( $p > 0.05$ ). Read vertically, same capital letters show non-statistically significant differ-

ences among materials for the exact same conditions of testing (aging period and immersion solution) ( $p > 0.05$ ). FBS-immersed prototype materials showed lower hydrophilicity than the respective water samples, particularly after 1 day ( $p < 0.05$ ), which was, however, gradually re-established through time

Material	1 day		7 days		28 days	
	Water	FBS	Water	FBS	Water	FBS
<b>TZ-base</b>	0 <sup>A-a</sup>	77 (13) <sup>A,B-b</sup>	0 <sup>A-a</sup>	0 (82) <sup>A-a,b</sup>	0 <sup>A-a</sup>	0 <sup>A-a</sup>
<b>TZ-bg10</b>	0 <sup>A-a</sup>	91 (27) <sup>B-b</sup>	0 <sup>A-a</sup>	46 (65) <sup>A-a</sup>	0 <sup>A-a</sup>	0 <sup>A-a</sup>
<b>TZ-bg20</b>	0 <sup>A-a</sup>	66 (16) <sup>A,B-b</sup>	0 <sup>A-a</sup>	0 (27) <sup>A-a,b</sup>	0 <sup>A-a</sup>	0 (63) <sup>A,B-a,b</sup>
<b>TZ-Ag0.5</b>	0 <sup>A-a</sup>	82 (47) <sup>A,B-b</sup>	0 <sup>A-a</sup>	0 (43) <sup>A-a</sup>	0 <sup>A-a</sup>	0 <sup>A-a</sup>
<b>TZ-Ag1</b>	0 <sup>A-a</sup>	63 (27) <sup>A,B-b</sup>	0 <sup>A-a</sup>	24 (57) <sup>A-a</sup>	0 <sup>A-a</sup>	0 <sup>A-a</sup>
<b>TZ-Ag2</b>	0 <sup>A-b</sup>	80 (48) <sup>A,B-b</sup>	0 <sup>A-a</sup>	34 (89) <sup>A-a,b</sup>	0 <sup>A-a</sup>	0 <sup>A-a</sup>
<b>Biodentine</b>	45 (26) <sup>B-a</sup>	70 (30) <sup>A,B-a</sup>	38 (63) <sup>B-a</sup>	90 (26) <sup>A-a</sup>	45 (45) <sup>B-a</sup>	38 (59) <sup>B-a</sup>
<b>IRM</b>	88 (25) <sup>C-a,b</sup>	40 (25) <sup>A-a,b</sup>	90 (20) <sup>C-a</sup>	35 (11) <sup>A-b</sup>	81 (14) <sup>C-a</sup>	37 (35) <sup>B-a,b</sup>

enhancement of antibacterial or biological properties should not compromise any of their existing physical properties.

A thorough characterization of materials' surface characteristics was performed after aging in different environmental conditions and time periods. Exposing the materials to a protein-rich medium (FBS) sought to resemble the interactions that take place between materials and host tissue fluids [51]. The results may be compared with results obtained under the more controlled in vitro environment in the absence of any organic or inorganic compounds. Little research has been conducted on the antibacterial properties after contact with clinically relevant fluids, but one previous study indicated a reduction in activity of MTA following

contact with blood and heparin [13]. To the best of our knowledge, this is the first study to evaluate antibacterial properties of Biodentine following exposure to a serum-containing environment. Testing was performed after three different incubation periods to follow changes in material properties as the hydration of cements was progressing until it was largely completed [3].

In the adhesion assay, direct bactericidal activity as well as anti-adherence surface characteristics may co-exist. Including longer incubation periods in our investigation enabled us to render these two roles more discrete, as the bactericidal effect might be decreased through time. The fluorescence assay for adhesion was compared in preliminary

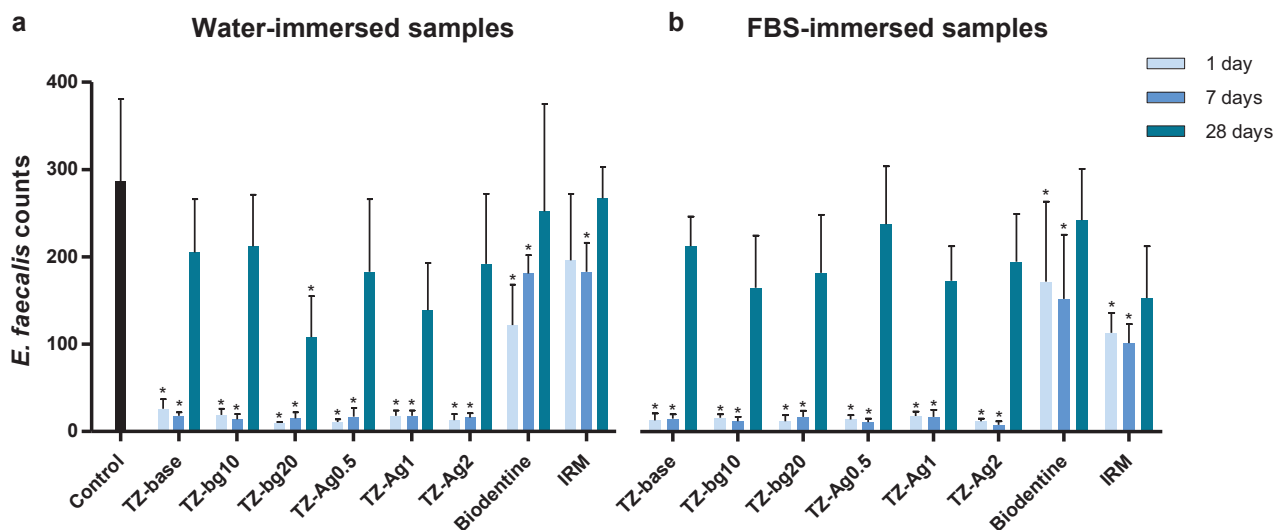


**Fig. 6** Mean and standard deviation of bacterial adhesion upon the surface of materials after a 1-h agitation period at 37 °C in an *Enterococcus faecalis* inoculum. Materials were previously aged in ultrapure water (water) (a) or fetal bovine serum (FBS) (b) for 1, 7, or 28 days.

Control corresponds to sterile membrane filters cut to the same diameter (9 mm) as the material specimens. Asterisk indicates statistically significant difference from the control ( $p < 0.05$ )

experiments with cultural data and found to yield similar, reliable, and reproducible results (data not shown). While the use of *E. faecalis* may not reflect fully the clinical scenario since endodontic infection has a polymicrobial etiology [52], it has been commonly used for in vitro and ex vivo evaluations of the antibacterial effect of root-end filling materials [50], and the results with a single organism are easily quantifiable and reproducible. The selection of the specific strain of *E. faecalis* that expresses the green-fluorescent protein enabled us to avoid excessive sample manipulation and any potential stain interference in the imaging process. Further investigations under a biofilm model might be useful as they could provide information on materials' antibacterial potential under more extreme testing conditions.

Inclusion of BG altered the roughness profile of the cement along the hydration process. Even though all prototype cements that contained additives showed rougher surfaces at 28 days following water immersion comparing to the non-modified cement, the TZ-bg20 was the only material that increased in surface roughness eventually from day 1. This may be partially explained by the different hydration mechanisms for TCS and BG particles [3, 22]. A recent study showed that 20% incorporation of a different BG-type (Biosilicate) into prototype TCS achieved complete killing of planktonic *E. faecalis* in contrast to the non-modified cement [53]. Despite differences in the experimental design and the category of BG, the above findings are in line with ours: the 1-day prototype materials did not allow initial bacterial adhesion, possibly due to direct killing, while in the 28-day samples, TZ-bg20 had

the lowest *E. faecalis* adhesion, which was significantly different from the positive control.

Silver nano-particles increased the roughness profile of cements after 28 days but did not have any other effect on the properties studied. Even though SNP have been used previously to improve the antibacterial properties of PC-based materials with reported success, the effect was only investigated 2 days after setting [54]. We found no change in the bacterial adhesion pattern from the addition of SNP. SNP might demand a longer interaction period with the negatively charged bacterial cells to achieve bacterial killing [55] following the early stages of bacterial adhesion, and it might also result from loss of SNP from the surface to the medium, rendering the surfaces relatively unaltered.

Biodentine showed an overall smoother surface morphology particularly up to 7 days after immersion, a result of the inclusion of the water-soluble polymer reducing cement flocculation [56]. In addition, decrease of the water/powder ratio in Biodentine increases the material hardness [45, 57]. This was evidenced by comparisons with the non-modified cement in our results. Bacteria adhered in large numbers to Biodentine. The material is moderately active towards *E. faecalis* [58]. Differences in the antibacterial activity in comparison with prototype cements might reflect a diverse extent of solubility and therefore leaching. Additionally, exposure of the materials to lower pH environments such as the bacterial inoculum could have resulted in a greater dissolution effect in the prototype cements, in contrast to Biodentine, which can withstand acidic environments [59].

Interestingly, the microhardness of Biodentine was reduced after long-term incubation in water, possibly due to continued dissolution. Changing of the immersion medium weekly might have affected microhardness, as it tends to increase leaching by not allowing buffering of the solution. In prototype materials and particularly in TZ-base, some minor fluctuations in the hardness values particularly between 7 and 28 days might have a similar explanation.

Immersion in FBS altered significantly the surface properties of all TCS-based materials. However, their behavior in the adhesion assay was unaltered. Material surfaces were progressively covered by products of the reaction of the calcium hydroxide with serum components, with SEM images and EDX analysis indicating gradual formation of a layer of calcium phosphate and mainly calcium carbonate. This layer decreased the hydrophilicity to some extent, particularly in the short-term immersion periods, while it resulted in reinforcement of surface hardness of Biodentine in the long term in contrast to its behavior in water. Alterations in the hydration process upon exposure to serum-containing environments have been described before both in vitro [13, 60] and in clinical conditions [16].

In IRM, even though the surface morphology of the material was not altered after the various exposure periods in FBS, the EDX analysis showed a qualitative modification with deposition of elements from the serum. Surface microhardness was consequently increased in FBS. This could be a result of a shift in the equilibrium of dissolution and uptake possibly caused by the serum components. Interestingly, IRM immersed in FBS showed higher wettability in combination with a reduction in the adhesion of *E. faecalis*. As the surface roughness of IRM remained stable in both media, the chemical changes in the material surface would seem responsible for the reduced bacterial adhesion. Increased hydrophilicity has been linked with reduced biofilm formation on dental resins [61] and may warrant further studies of hydrophilicity also of materials used for endodontic surgical procedures.

## Conclusions

Inclusion of silver nano-particles or bioactive glass did not affect the adhesion of *E. faecalis* in comparison to the non-modified composition. Exposure to FBS caused surface reactions in TCS-based cements that altered significantly their surface characteristics but did not affect the adhesion pattern. The measured physical parameters did not appear to be related to the degree of bacterial adhesion. Further studies should focus on the effect of leaching properties to the anti-bacterial profile upon alterations in the cement composition under different aging conditions.

**Supplementary Information** The online version contains supplementary material available at <https://doi.org/10.1007/s00784-022-04655-y>.

**Acknowledgements** Dimitri Alkarra for his help in fabrication of calibration-specimens for surface roughness assays. Professor Jon Einar Dahl for his constructive comments on the manuscript. Dr Manuel Espinosa for providing the *Enterococcus faecalis* OG1RF strain. Dr Amund Ruud and Dr Ida Stenhagen for their valuable help and technical assistance in physico-chemical testing.

**Author contribution** Andreas Koutroulis: conceptualization; data curation; formal analysis; investigation; methodology; and writing—original draft. Håkon Valen: conceptualization; methodology; supervision; validation; and writing—review and editing. Dag Ørstavik: supervision; validation; and writing—review and editing. Vasileios Kapralos: methodology and writing—review and editing. Josette Camilleri: conceptualization; methodology; supervision; validation; and writing—review and editing. Pia Titterud Sunde: conceptualization; methodology; supervision; validation; and writing—review and editing.

**Funding** Open access funding provided by University of Oslo (incl Oslo University Hospital) This study was funded by University of Oslo and Nordic Institute of Dental Materials (NIOM).

## Declarations

**Ethics approval** Not applicable.

**Consent to participate** Not applicable.

**Conflict of interest** The authors declare no competing interests.

**Open Access** This article is licensed under a Creative Commons Attribution 4.0 International License, which permits use, sharing, adaptation, distribution and reproduction in any medium or format, as long as you give appropriate credit to the original author(s) and the source, provide a link to the Creative Commons licence, and indicate if changes were made. The images or other third party material in this article are included in the article's Creative Commons licence, unless indicated otherwise in a credit line to the material. If material is not included in the article's Creative Commons licence and your intended use is not permitted by statutory regulation or exceeds the permitted use, you will need to obtain permission directly from the copyright holder. To view a copy of this licence, visit <http://creativecommons.org/licenses/by/4.0/>.

## References

1. Ørstavik D (2014) Endodontic filling materials. Endod Top 31:53–67. <https://doi.org/10.1111/etp.12068>
2. Gopikrishna V (2014) Grossman's endodontic practice. Wolters Kluwer, Mumbai
3. Camilleri J (2014) Mineral trioxide aggregate in dentistry: from preparation to application. Springer, Berlin
4. Giraud T, Jeanneau C, Rombouts C, Bakhtiar H, Laurent P, About I (2019) Pulp capping materials modulate the balance between inflammation and regeneration. Dent Mater 35:24–35. <https://doi.org/10.1016/j.dental.2018.09.008>
5. Torabinejad M, White DJ (1995) Tooth filling material and method of use. United States Patent 5415547

6. Camilleri J (2020) Classification of hydraulic cements used in dentistry. *Front Dent Med*. <https://doi.org/10.3389/fdmed.2020.00009>
7. Koutroulis A, Kuehne SA, Cooper PR, Camilleri J (2019) The role of calcium ion release on biocompatibility and antimicrobial properties of hydraulic cements. *Sci Rep* 9:19019. <https://doi.org/10.1038/s41598-019-55288-3>
8. Grech L, Mallia B, Camilleri J (2013) Characterization of set intermediate restorative material, Biodentine, bioaggregate and a prototype calcium silicate cement for use as root-end filling materials. *Int Endod J* 46:632–641. <https://doi.org/10.1111/iej.12039>
9. Siqueira JF Jr, Rocas IN (2008) Clinical implications and microbiology of bacterial persistence after treatment procedures. *J Endod* 34:1291–1301.e3. <https://doi.org/10.1016/j.joen.2008.07.028>
10. AlShwaimi E, Bogari D, Ajaj R, Al-Shahrani S, Almas K, Majeed A (2016) In vitro antimicrobial effectiveness of root canal sealers against *Enterococcus faecalis*: a systematic review. *J Endod* 42:1588–1597. <https://doi.org/10.1016/j.joen.2016.08.001>
11. Hülsmann M, Tulus G (2016) Non-surgical retreatment of teeth with persisting apical periodontitis following apicoectomy: decision making, treatment strategies and problems, and case reports. *Endod Top* 34:64–89. <https://doi.org/10.1111/etp.12098>
12. Estrela C, Sydney GB, Bammann LL, Felipe Junior O (1995) Mechanism of action of calcium and hydroxyl ions of calcium hydroxide on tissue and bacteria. *Braz Dent J* 6:85–90
13. Farrugia C, Baca P, Camilleri J, Arias Moliz MT (2017) Antimicrobial activity of ProRoot MTA in contact with blood. *Sci Rep* 7:41359. <https://doi.org/10.1038/srep41359>
14. Kebudi Benezra M, Schembri Wismayer P, Camilleri J (2017) Influence of environment on testing of hydraulic sealers. *Sci Rep* 7:17927. <https://doi.org/10.1038/s41598-017-17280-7>
15. Meschi N, Li X, Van Gorp G, Camilleri J, Van Meerbeek B, Lambrechts P (2019) Bioactivity potential of Portland cement in regenerative endodontic procedures: from clinic to lab. *Dent Mater* 35:1342–1350. <https://doi.org/10.1016/j.dental.2019.07.004>
16. Moinzadeh AT, Aznar Portoles C, Schembri Wismayer P, Camilleri J (2016) Bioactivity potential of EndoSequence BC RRM Putty. *J Endod* 42:615–621. <https://doi.org/10.1016/j.joen.2015.12.004>
17. Farrugia C, Lung CYK, Schembri Wismayer P, Arias-Moliz MT, Camilleri J (2018) The relationship of surface characteristics and antimicrobial performance of pulp capping materials. *J Endod* 44:1115–1120. <https://doi.org/10.1016/j.joen.2018.04.002>
18. Fan W, Wu D, Tay FR, Ma T, Wu Y, Fan B (2014) Effects of adsorbed and templated nanosilver in mesoporous calcium-silicate nanoparticles on inhibition of bacteria colonization of dentin. *Int J Nanomed* 9:5217–5230. <https://doi.org/10.2147/IJN.S73144>
19. Hiraishi N, Yiu CK, King NM, Tagami J, Tay FR (2010) Antimicrobial efficacy of 3.8% silver diamine fluoride and its effect on root dentin. *J Endod* 36:1026–1029. <https://doi.org/10.1016/j.joen.2010.02.029>
20. Gandolfi MG, Siboni F, Prati C (2016) Properties of a novel polysiloxane-guttapercha calcium silicate-bioglass-containing root canal sealer. *Dent Mater* 32:e113–e1126. <https://doi.org/10.1016/j.dental.2016.03.001>
21. Simila HO, Karpukhina N, Hill RG (2018) Bioactivity and fluoride release of strontium and fluoride modified Biodentine. *Dent Mater* 34:e1–e7. <https://doi.org/10.1016/j.dental.2017.10.005>
22. Hench LL (2006) The story of bioglass. *J Mater Sci Mater Med* 17:967–978. <https://doi.org/10.1007/s10856-006-0432-z>
23. Begum S, Johnson WE, Worthington T, Martin RA (2016) The influence of pH and fluid dynamics on the antibacterial efficacy of 45S5 bioglass. *Biomed Mater* 11:015006. <https://doi.org/10.1088/1748-6041/11/1/015006>
24. Wang Z, Shen Y, Haapasalo M (2014) Dental materials with antibiofilm properties. *Dent Mater* 30:e1–e16. <https://doi.org/10.1016/j.dental.2013.12.001>
25. Jensen KA, Thieret N (2014) The NANOGENTOX dispersion protocol for NANoREG. National Research Centre for the Working Environment. <http://safenano.re.kr/download.do?SEQ=175>, 2014. Accessed 13 February 2022
26. I.S.O 6876:(2012) Dentistry—root canal sealing materials (2012) International Organization for Standardization, Geneva
27. Formosa LM, Mallia B, Camilleri J (2012) The effect of curing conditions on the physical properties of tricalcium silicate cement for use as a dental biomaterial. *Int Endod J* 45:326–336. <https://doi.org/10.1111/j.1365-2591.2011.01980.x>
28. Nieto C, Espinosa M (2003) Construction of the mobilizable plasmid pMV158GFP, a derivative of pMV158 that carries the gene encoding the green fluorescent protein. *Plasmid* 49:281–285. [https://doi.org/10.1016/S0147-619X\(03\)00020-9](https://doi.org/10.1016/S0147-619X(03)00020-9)
29. Marending M, Bubenhofer SB, Sener B, De-Deus G (2013) Primary assessment of a self-adhesive gutta-percha material. *Int Endod J* 46:317–322. <https://doi.org/10.1111/j.1365-2591.2012.02117.x>
30. Hench LL (1998) Bioceramics. *J Amer Ceram Soc* 81:1705–1728. <https://doi.org/10.1111/j.1151-2916.1998.tb02540.x>
31. Björkenheim R, Strömberg G, Ainola M, Uppstu P, Aalto-Setälä L, Hupa L, Pajarinen J, Lindfors NC (2019) Bone morphogenic protein expression and bone formation are induced by bioactive glass S53P4 scaffolds in vivo. *J Biomed Mater Res B Appl Biomater* 107:847–857. <https://doi.org/10.1002/jbm.b.34181>
32. Shrestha A, Kishen A (2016) Antibacterial nanoparticles in endodontics: a review. *J Endod* 42:1417–1426. <https://doi.org/10.1016/j.joen.2016.05.021>
33. Hoikkala NPJ, Siekkinen M, Hupa L, Vallittu PK (2021) Behaviour of different bioactive glasses incorporated in polydimethylsiloxane endodontic sealer. *Dent Mater* 37:321–327. <https://doi.org/10.1016/j.dental.2020.11.013>
34. Hoikkala NJ, Wang X, Hupa L, Smatt JH, Peltonen J, Vallittu PK (2018) Dissolution and mineralization characterization of bioactive glass ceramic containing endodontic sealer GuttaFlow bioseal. *Dent Mater J* 37:988–994. <https://doi.org/10.4012/dmj.2017-224>
35. Rodríguez-Lozano FJ, Collado-Gonzalez M, Tomas-Catala CJ, Garcia-Bernal D, Lopez S, Onate-Sanchez RE, Moraleta JM, Murcia L (2019) GuttaFlow bioseal promotes spontaneous differentiation of human periodontal ligament stem cells into cementoblast-like cells. *Dent Mater* 35:114–124. <https://doi.org/10.1016/j.dental.2018.11.003>
36. Bovenkamp GL, Zanzen U, Krishna KS, Hormes J, Prange A (2013) X-ray absorption near-edge structure (XANES) spectroscopy study of the interaction of silver ions with *Staphylococcus aureus*, *Listeria monocytogenes*, and *Escherichia coli*. *Appl Environ Microbiol* 79:6385–6390. <https://doi.org/10.1128/AEM.01688-13>
37. Noronha VT, Paula AJ, Duran G, Galembeck A, Cogo-Muller K, Franz-Montan M, Duran N (2017) Silver nanoparticles in dentistry. *Dent Mater* 33:1110–1126. <https://doi.org/10.1016/j.dental.2017.07.002>
38. Rodrigues MC, Rolim WR, Viana MM, Souza TR, Gonçalves F, Tanaka CJ, Bueno-Silva B, Seabra AB (2020) Biogenic synthesis and antimicrobial activity of silica-coated silver nanoparticles for esthetic dental applications. *J Dent* 96:103327. <https://doi.org/10.1016/j.jdent.2020.103327>
39. Li F, Weir MD, Chen J, Xu HH (2013) Comparison of quaternary ammonium-containing with nano-silver-containing adhesive in antibacterial properties and cytotoxicity. *Dent Mater* 29:450–461. <https://doi.org/10.1016/j.dental.2013.01.012>

40. Afkhami F, Pourhashemi SJ, Sadegh M, Salehi Y, Fard MJ (2015) Antibiofilm efficacy of silver nanoparticles as a vehicle for calcium hydroxide medicament against *Enterococcus faecalis*. *J Dent* 43:1573–1579. <https://doi.org/10.1016/j.jdent.2015.08.012>
41. Ioannidis K, Niazi S, Mylonas P, Mannocci F, Deb S (2019) The synthesis of nano silver-graphene oxide system and its efficacy against endodontic biofilms using a novel tooth model. *Dent Mater* 35:1614–1629. <https://doi.org/10.1016/j.dental.2019.08.105>
42. Afkhami F, Ahmadi P, Chiniforush N, Sooratgar A (2021) Effect of different activations of silver nanoparticle irrigants on the elimination of *Enterococcus faecalis*. *Clin Oral Invest* 25:6893–6899. <https://doi.org/10.1007/s00784-021-03979-5>
43. Natale LC, Alania Y, Rodrigues MC, Simoes A, de Souza DN, de Lima E, Arana-Chavez VE, Hewer TLR, Hiers R, Esteban-Florez FL, Brito GES, Khajotia S, Braga RR (2017) Synthesis and characterization of silver phosphate/calcium phosphate mixed particles capable of silver nanoparticle formation by photoreduction. *Mater Sci Eng C Mater Biol Appl* 76:464–471. <https://doi.org/10.1016/j.msec.2017.03.102>
44. Flores CY, Miñán AG, Grillo CA, Salvarezza RC, Vericat C, Schilardi PL (2013) Citrate-capped silver nanoparticles showing good bactericidal effect against both planktonic and sessile bacteria and a low cytotoxicity to osteoblastic cells. *ACS Appl Mater Interfaces* 24:3149–3159. <https://doi.org/10.1021/am400044e>
45. Camilleri J, Sorrentino F, Damidot D (2013) Investigation of the hydration and bioactivity of radiopacified tricalcium silicate cement, Biodentine and MTA Angelus. *Dent Mater* 29:580–593. <https://doi.org/10.1016/j.dental.2013.03.007>
46. Tawil PZ, Trope M, Curran AE, Caplan DJ, Kirakozova A, Duggan DJ, Teixeira FB (2009) Periapical microsurgery: an in vivo evaluation of endodontic root-end filling materials. *J Endod* 35:357–362. <https://doi.org/10.1016/j.joen.2008.12.001>
47. Chong BS, Pitt Ford TR, Hudson MB (2003) A prospective clinical study of mineral trioxide aggregate and IRM when used as root-end filling materials in endodontic surgery. *Int Endod J* 36:520–526. <https://doi.org/10.1046/j.1365-2591.2003.00682.x>
48. Figdor D, Gulabivala K (2008) Survival against the odds: microbiology of root canals associated with post-treatment disease. *Endod Top* 18:62–77. <https://doi.org/10.1111/j.1601-1546.2011.00259.x>
49. Camilleri J, Arias Moliz T, Bettencourt A, Costa J, Martins F, Rabadjeva D, Rodriguez D, Visai L, Combes C, Farrugia C, Koidis P, Neves C (2020) Standardization of antimicrobial testing of dental devices. *Dent Mater* 36:e59–e73. <https://doi.org/10.1016/j.dental.2019.12.006>
50. Camilleri J, Atmeh A, Li X, Meschi N (2022) Present status and future directions - hydraulic materials for endodontic use. *Int Endod J*. <https://doi.org/10.1111/iej.13709>
51. Tingey MC, Bush P, Levine MS (2008) Analysis of mineral trioxide aggregate surface when set in the presence of fetal bovine serum. *J Endod* 34:45–49. <https://doi.org/10.1016/j.joen.2007.09.013>
52. Siqueira JF Jr, Rôças IN (2009) Diversity of endodontic microbiota revisited. *J Dent Res* 88:969–981. <https://doi.org/10.1177/0022034509346549>
53. Queiroz MB, Torres FFE, Rodrigues EM, Viola KS, Bosso-Martelo R, Chavez-Andrade GM, Souza MT, Zanutto ED, Guerreiro-Tanomaru JM, Tanomaru-Filho M (2021) Development and evaluation of reparative tricalcium silicate-ZrO<sub>2</sub>-Biosilicate composites. *J Biomed Mater Res B Appl Biomater* 109:468–476. <https://doi.org/10.1002/jbm.b.34714>
54. Vazquez-Garcia F, Tanomaru-Filho M, Chávez-Andrade GM, Bosso-Martelo R, Basso-Bernardi MI, Guerreiro-Tanomaru JM (2016) Effect of silver nanoparticles on physicochemical and antibacterial properties of calcium silicate cements. *Braz Dent J* 27:508–514. <https://doi.org/10.1590/0103-6440201600689>
55. Wu D, Fan W, Kishen A, Gutmann JL, Fan B (2014) Evaluation of the antibacterial efficacy of silver nanoparticles against *Enterococcus faecalis* biofilm. *J Endod* 40:285–290. <https://doi.org/10.1016/j.joen.2013.08.022>
56. Paillere AM, Ben Bassat M, Akman S (1992) Applications of admixtures for concrete. RILEM Technical Committees, E & FN Spon, an imprint of Chapman & Hall, New York,.
57. Grech L, Mallia B, Camilleri J (2013) Investigation of the physical properties of tricalcium silicate cement-based root-end filling materials. *Dent Mater* 29:e20–e28. <https://doi.org/10.1016/j.dental.2012.11.007>
58. Pelepenko LE, Saavedra F, Antunes TBM, Bombarda GF, Gomes B, Zaia AA, Camilleri J, Marciano MA (2021) Physicochemical, antimicrobial, and biological properties of White-MTA-Flow. *Clin Oral Invest* 25:663–672. <https://doi.org/10.1007/s00784-020-03543-7>
59. Elnaghy AM (2014) Influence of acidic environment on properties of Biodentine and white mineral trioxide aggregate: a comparative study. *J Endod* 40:953–957. <https://doi.org/10.1016/j.joen.2013.11.007>
60. Nekoofar MH, Davies TE, Stone D, Basturk FB, Dummer PM (2011) Microstructure and chemical analysis of blood-contaminated mineral trioxide aggregate. *Int Endod J* 44:1011–1018. <https://doi.org/10.1111/j.1365-2591.2011.01909.x>
61. Brambilla E, Ionescu A, Mazzoni A, Cadenaro M, Gagliani M, Ferraroni M, Tay F, Pashley D, Breschi L (2014) Hydrophilicity of dentin bonding systems influences in vitro *Streptococcus mutans* biofilm formation. *Dent Mater* 30:926–935. <https://doi.org/10.1016/j.dental.2014.05.009>

**Publisher's note** Springer Nature remains neutral with regard to jurisdictional claims in published maps and institutional affiliations.

# **Supplementary Information**

## **Surface characteristics and bacterial adhesion of endodontic cements**

### **Clinical Oral Investigations**

A. Koutroulis, H.V. Rukke, D. Ørstavik, V. Kapralos, J. Camilleri, P.T. Sunde

Section of Endodontics, Institute of Clinical Dentistry, Faculty of Dentistry, University of Oslo, Oslo, Norway

e-mail address: [andreas.koutroulis@odont.uio.no](mailto:andreas.koutroulis@odont.uio.no)



**Online Resource 1** Representative scanning electron micrographs of prototype materials acquired with a mix of back-scatter and secondary electron signal detectors (1500× magnification) after exposure to ultrapure water (water) or Fetal Bovine Serum (FBS) for 1, 7 or 28 days

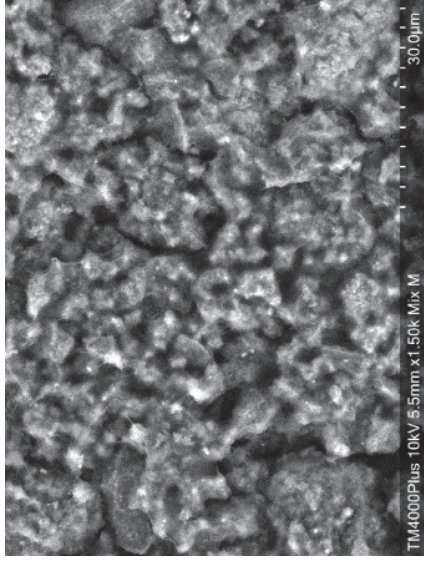
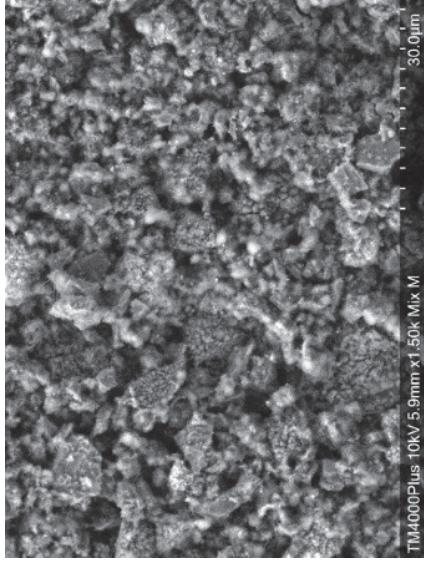
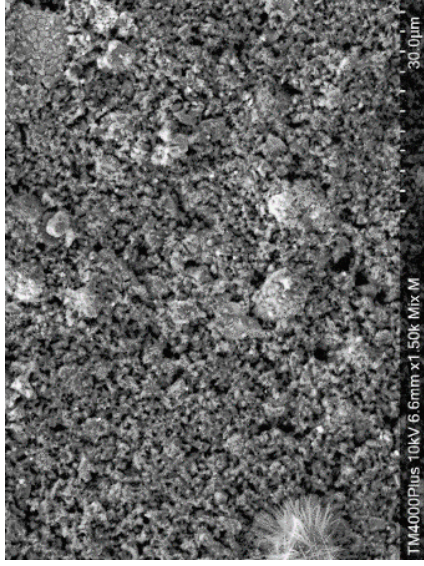
# TZ-base

1 Day

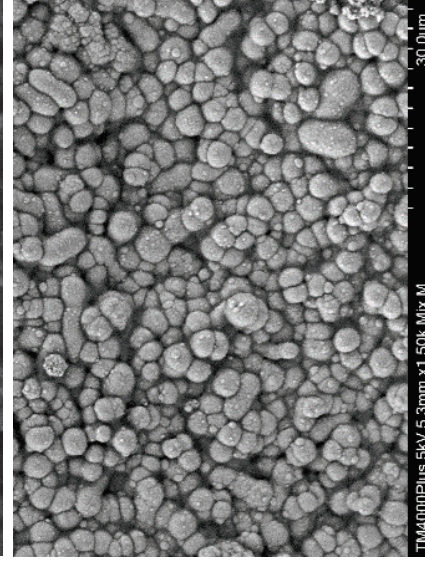
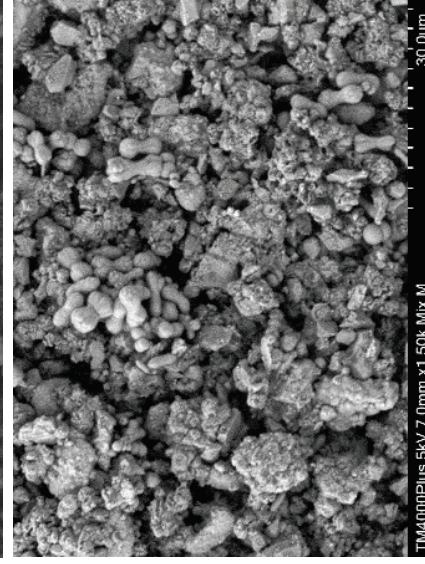
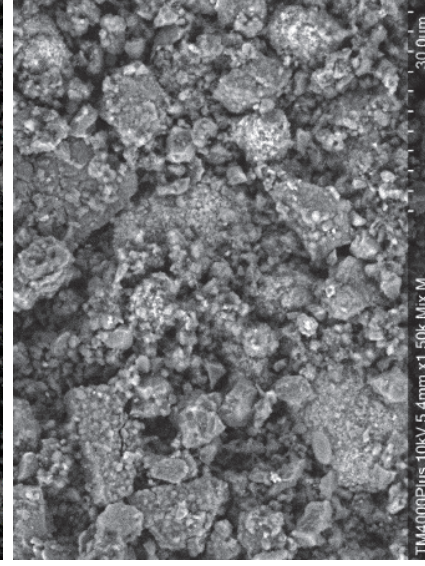
7 Days

28 Days

Water

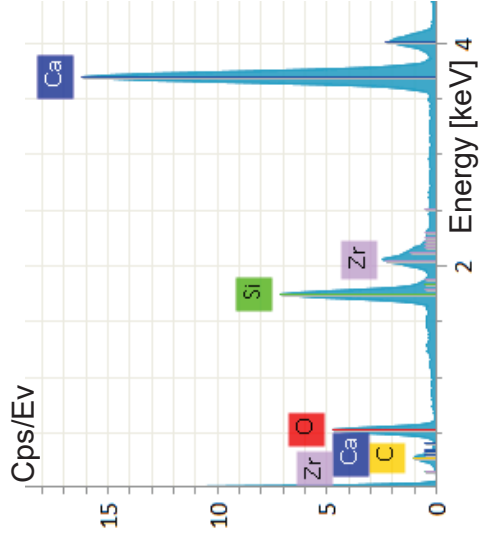


FBS

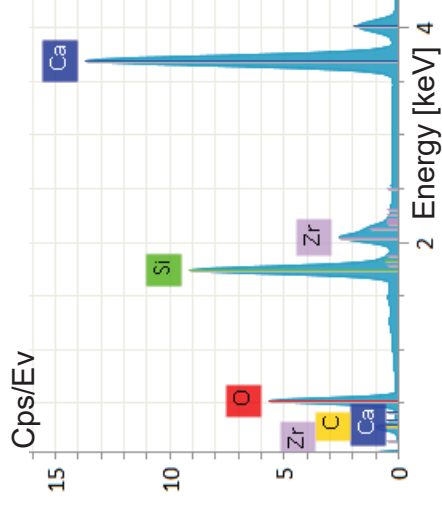


# TZ-base

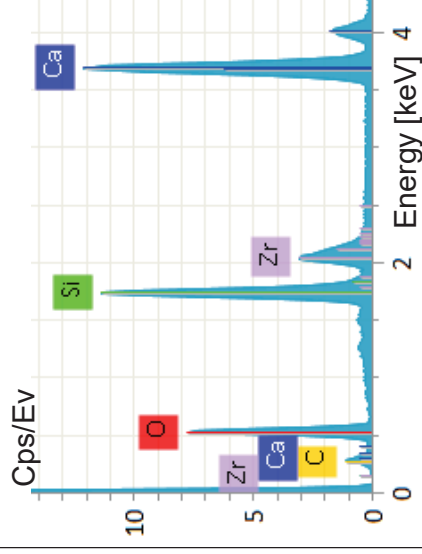
1 day



7 days

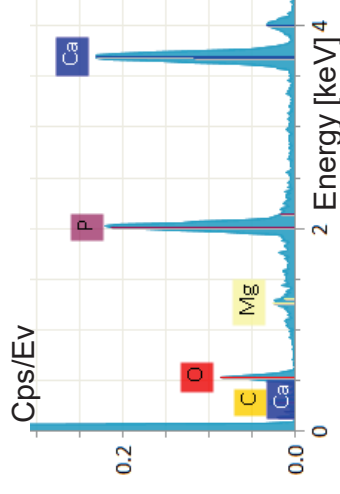
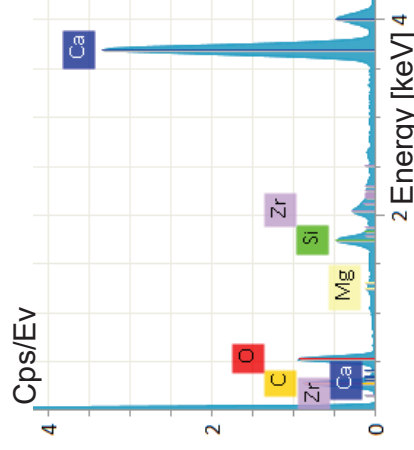
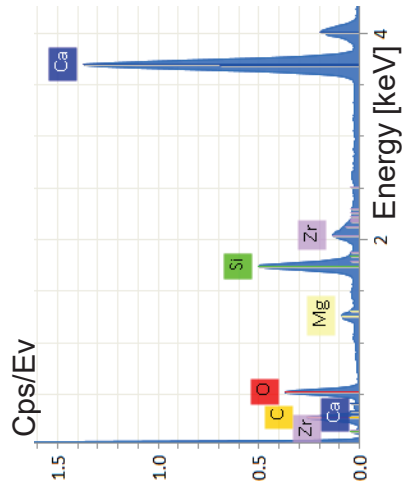


28 days



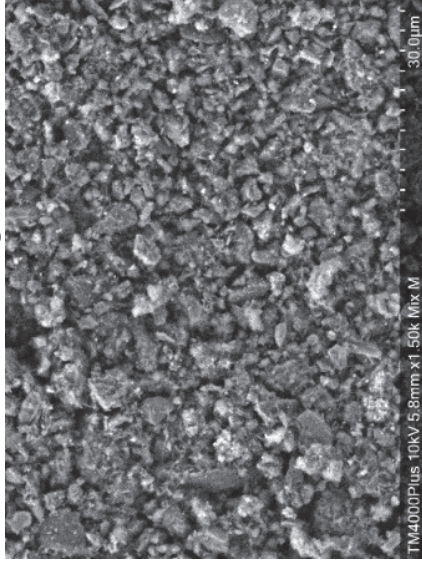
Water

FBS

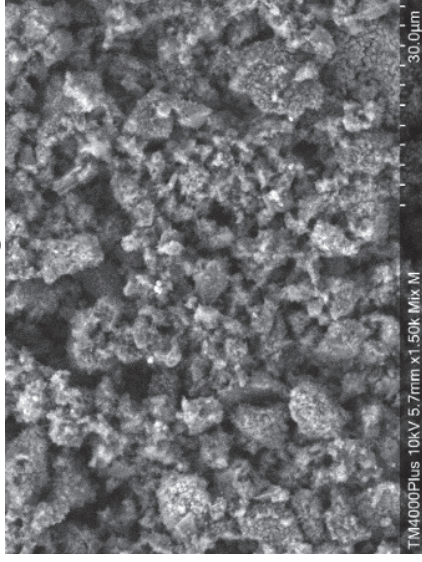


# TZ-bg10

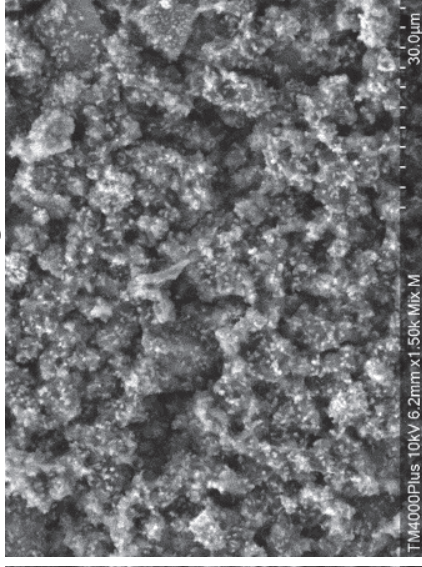
1 Day



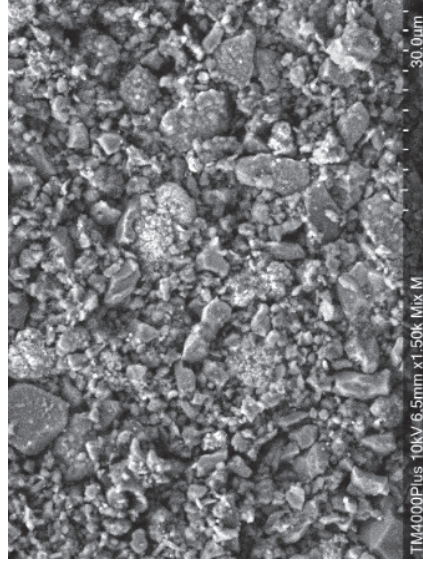
7 Days



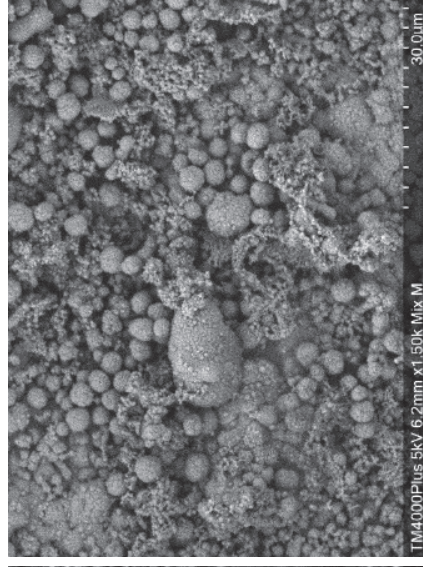
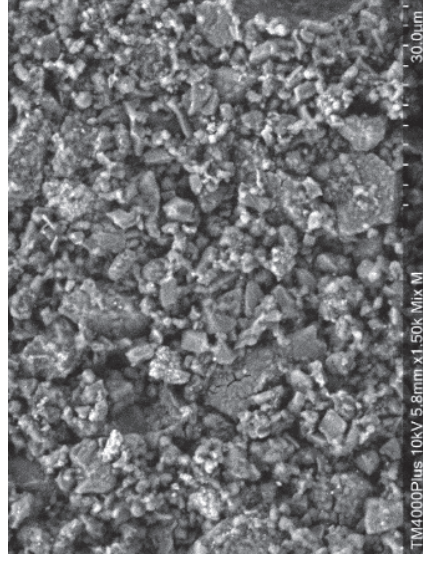
28 Days



Water



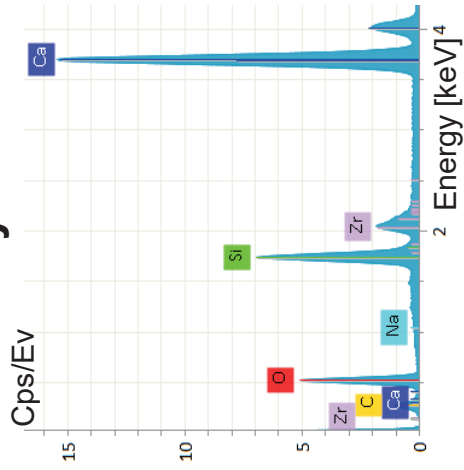
FBS



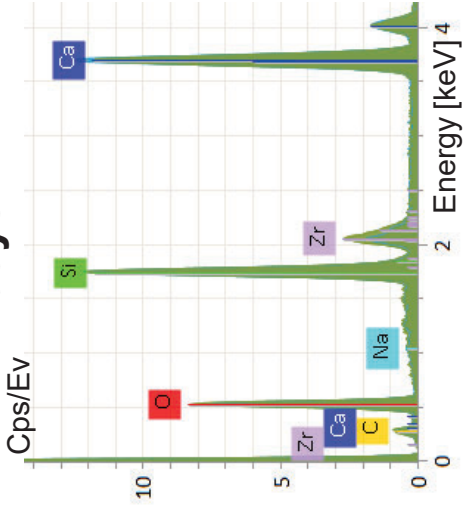
# TZ-bg10

**Water**

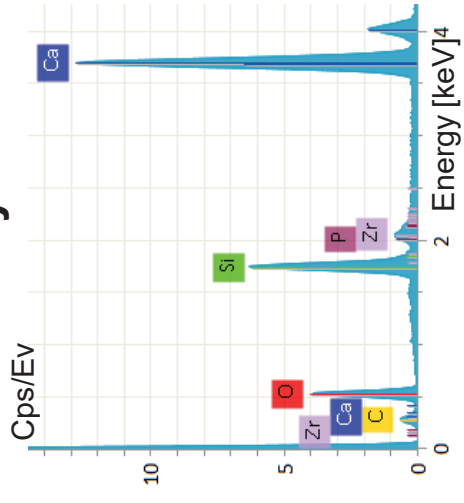
**1 day**



**7 days**

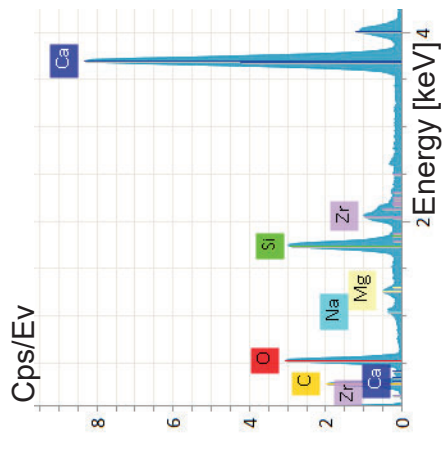


**28 days**

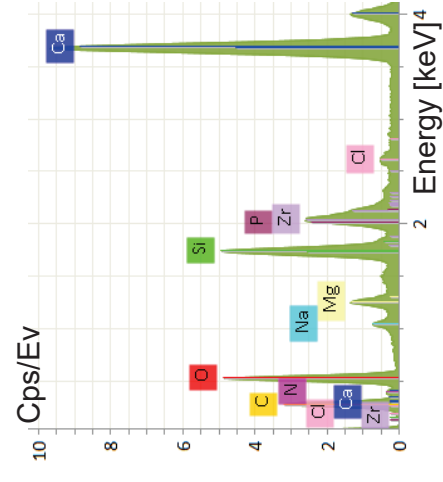


**FBS**

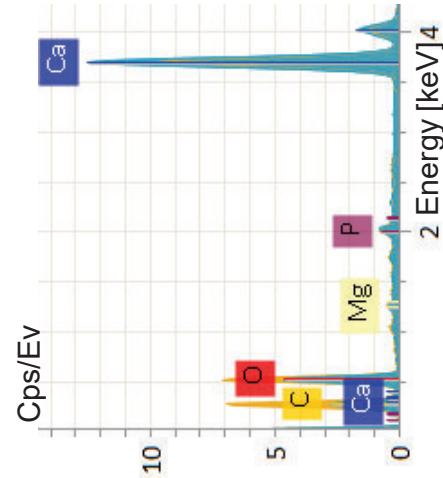
Cps/Ev



Cps/Ev

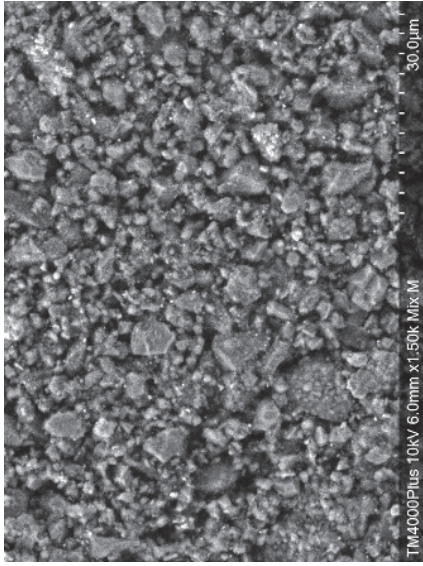


Cps/Ev

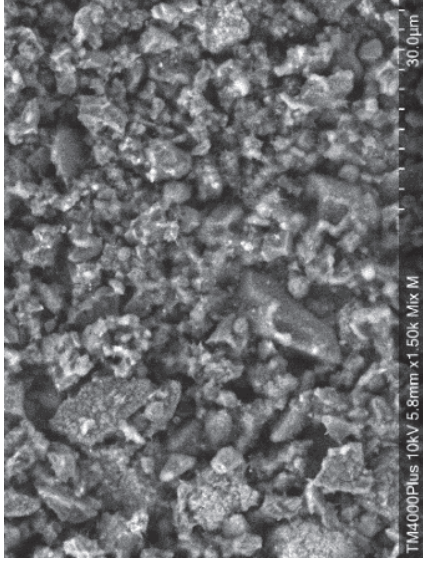


# TZ-bg20

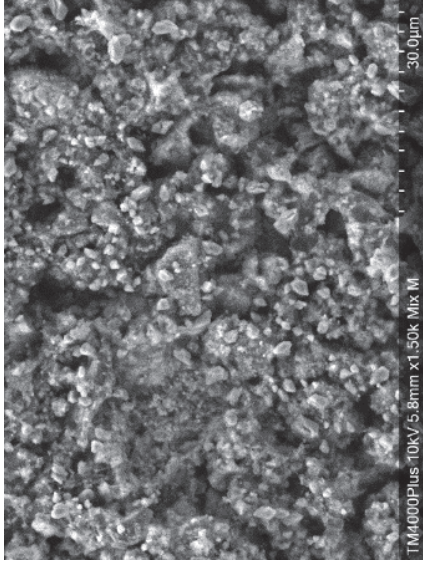
1 Day



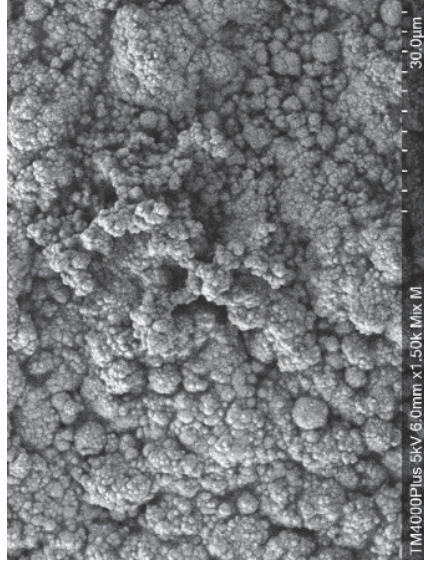
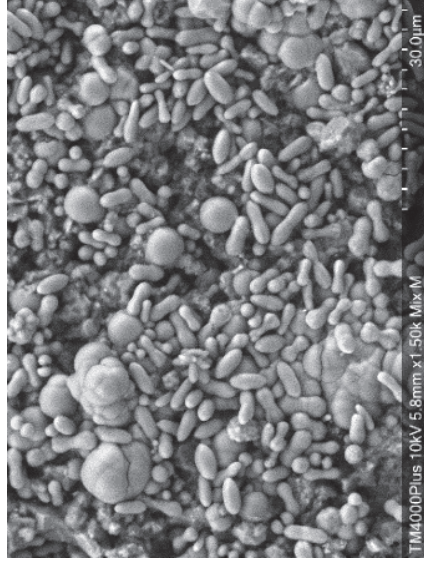
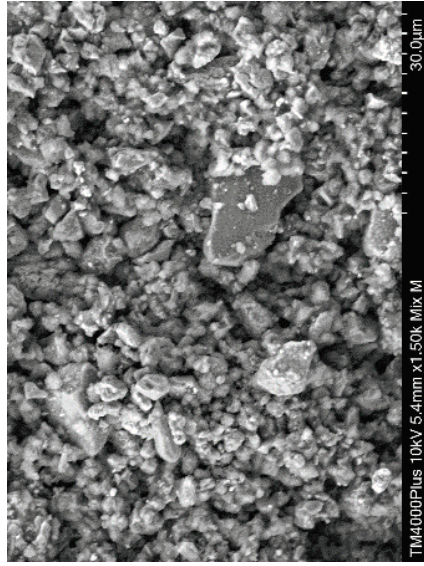
7 Days



28 Days



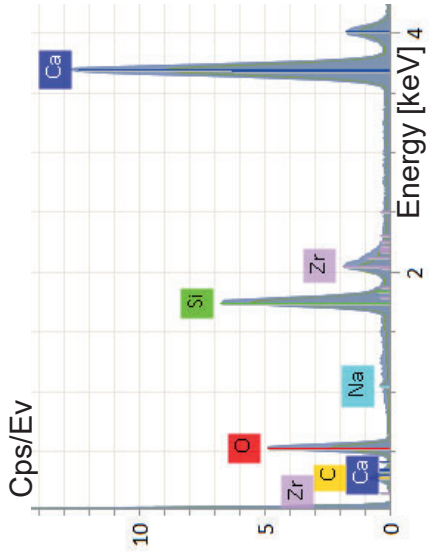
Water



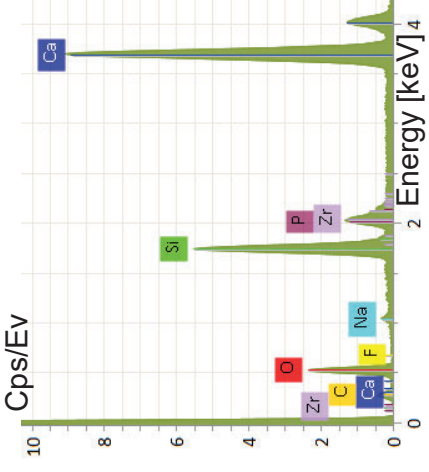
FBS

# TZ-bg20

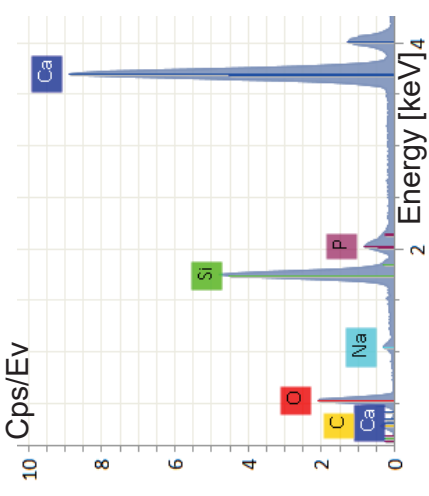
1 day



7 days

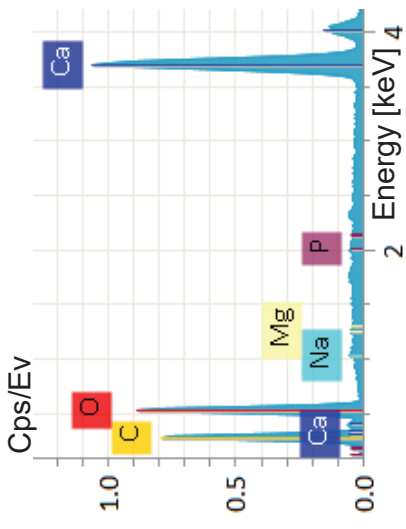
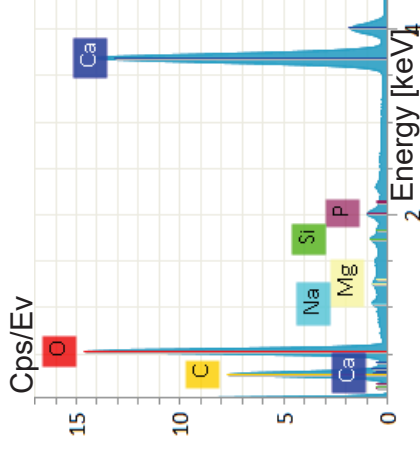
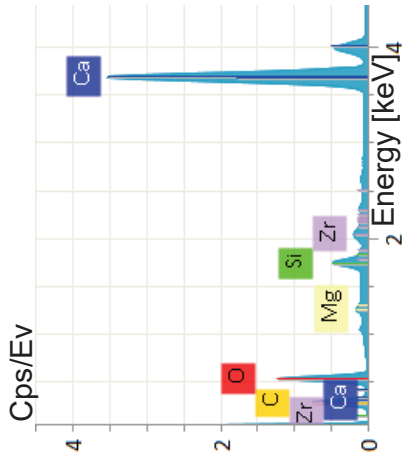


28 days



Water

FBS



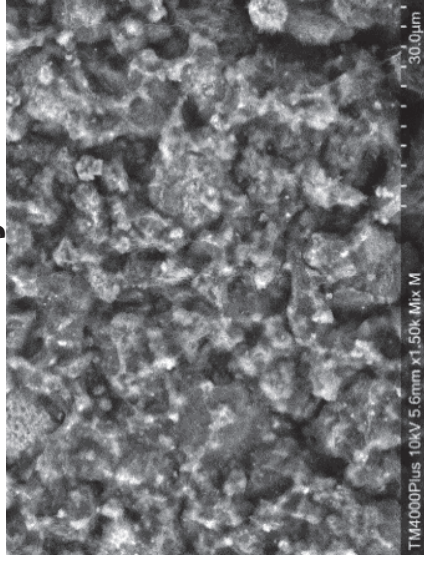
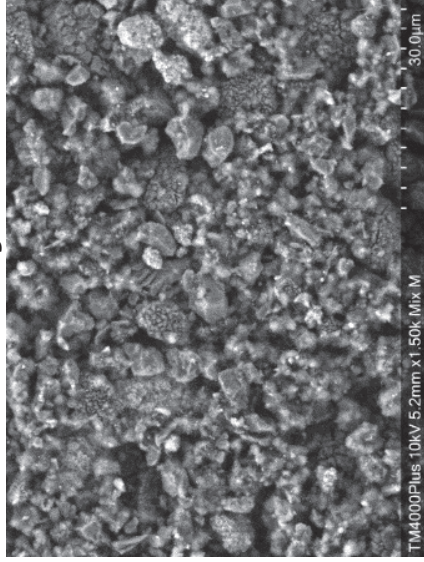
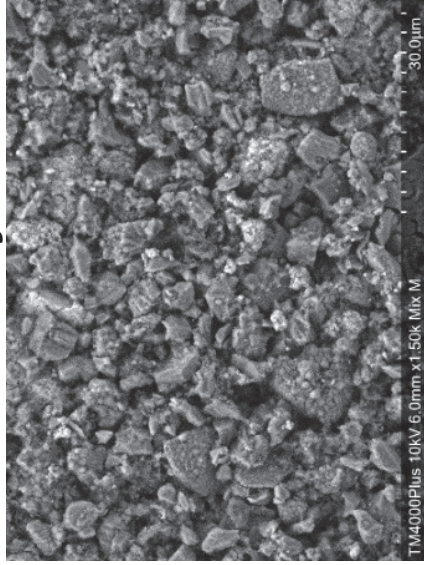
# TZ-Ag0.5

1 Day

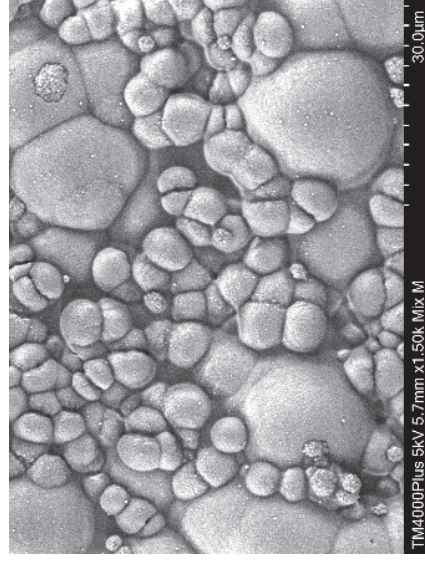
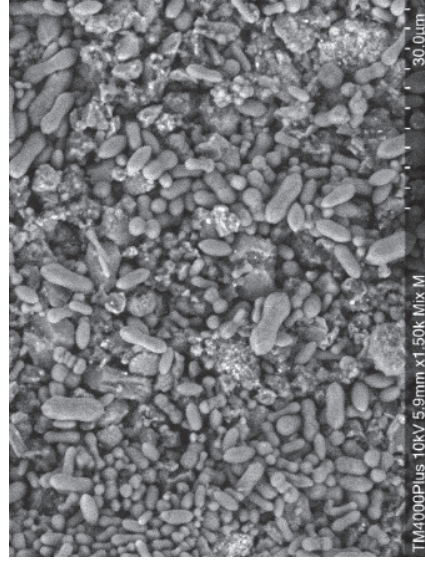
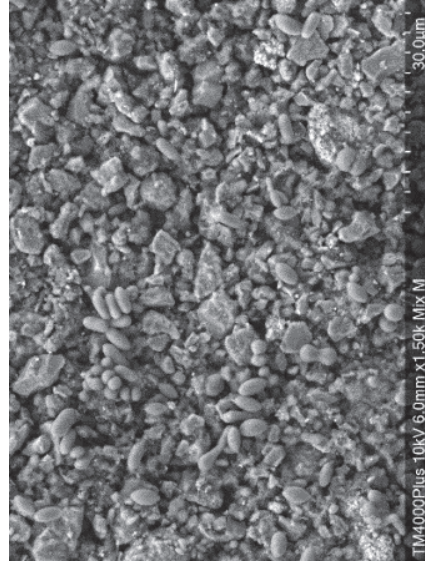
7 Days

28 Days

Water



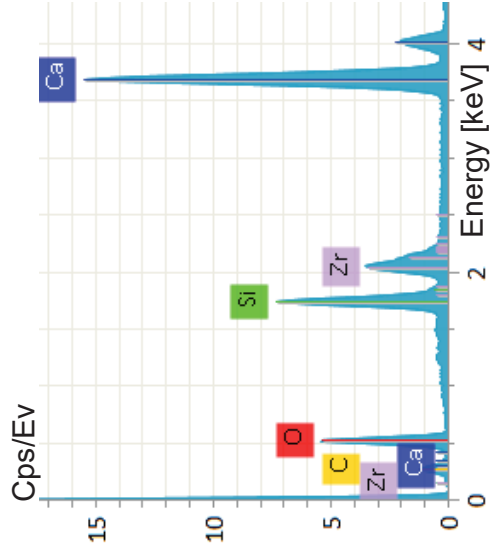
FBS





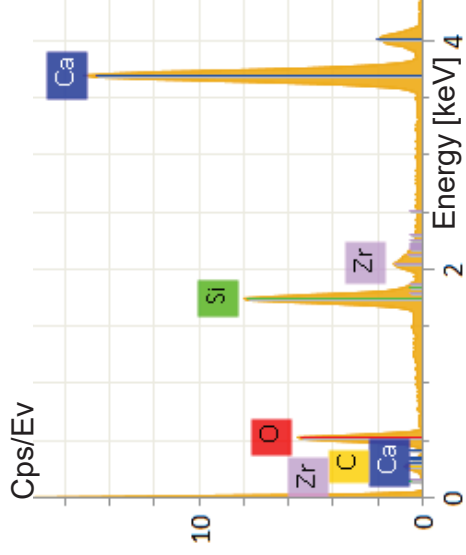
# TZ Ag0.5

1 day

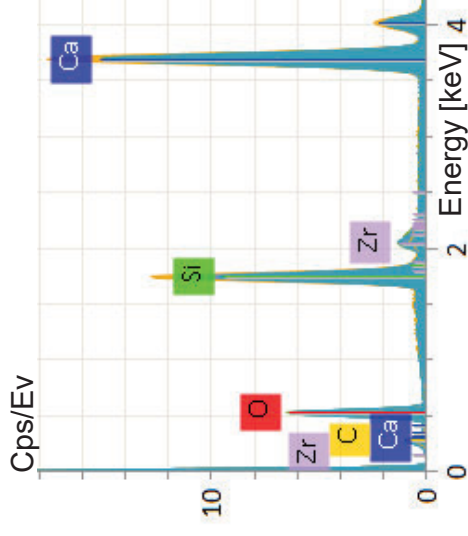


Water

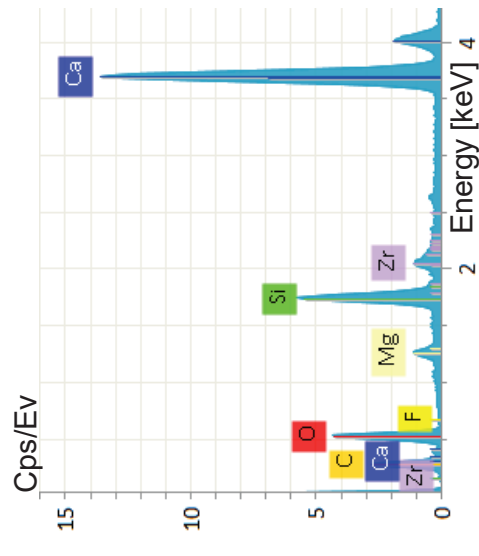
7 days



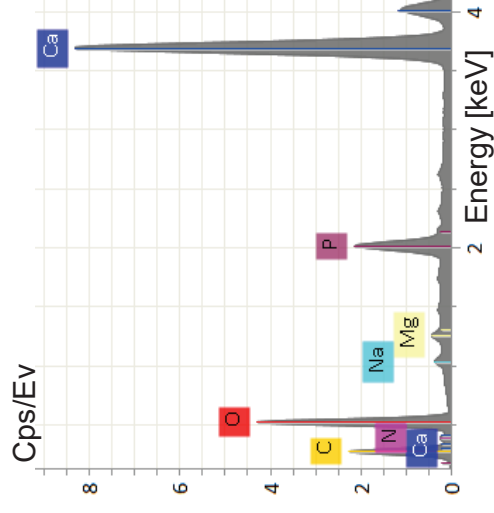
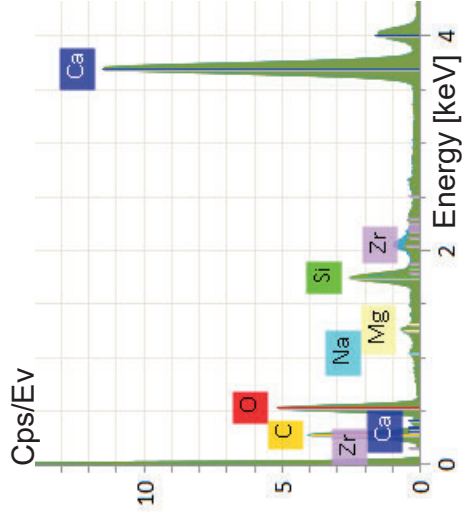
28 days



1 day

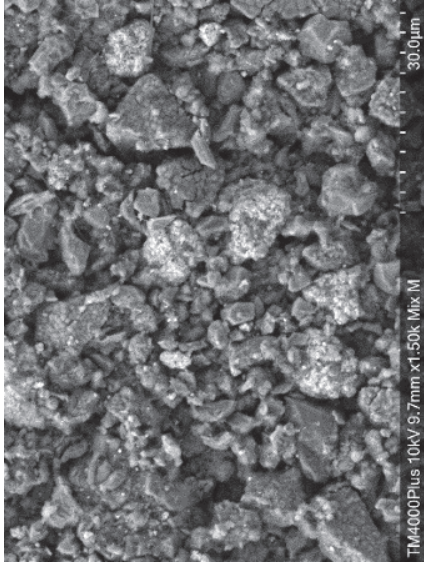


FBS

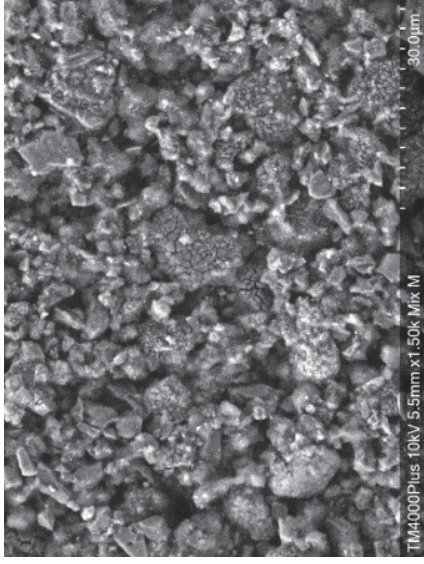


# TZ-Ag1

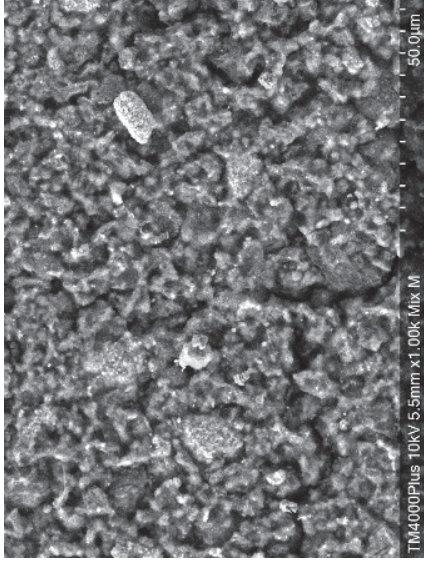
1 Day



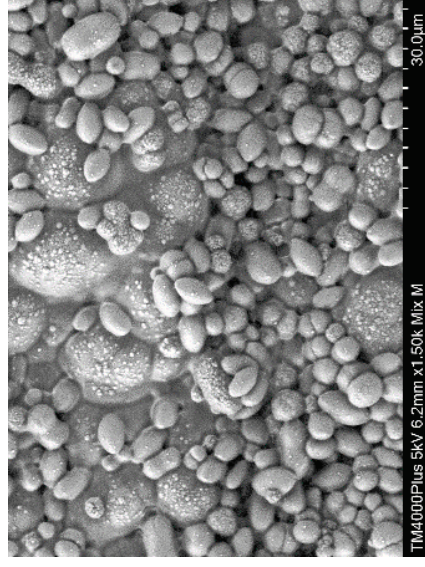
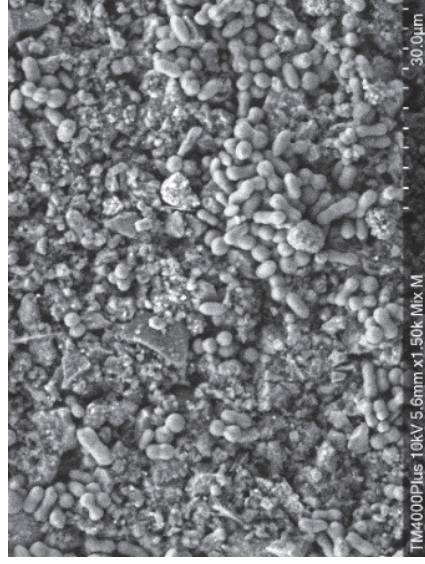
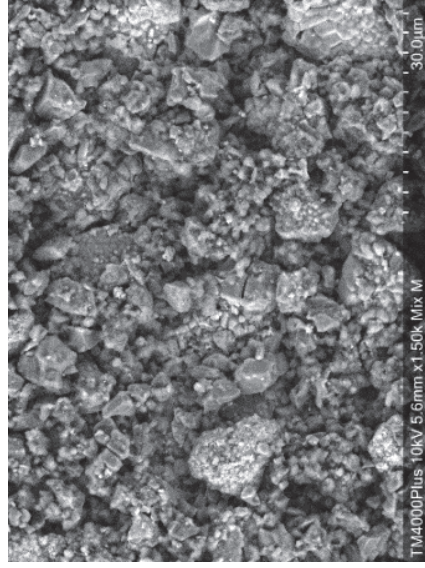
7 Days



28 Days



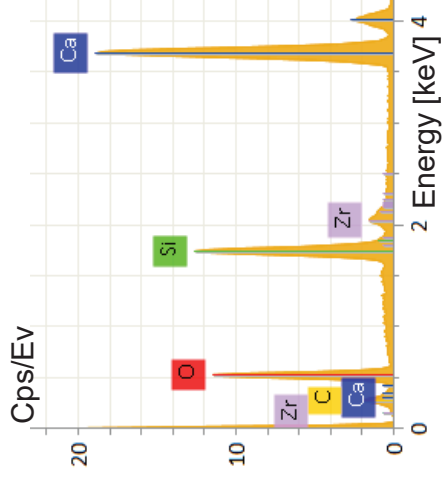
Water



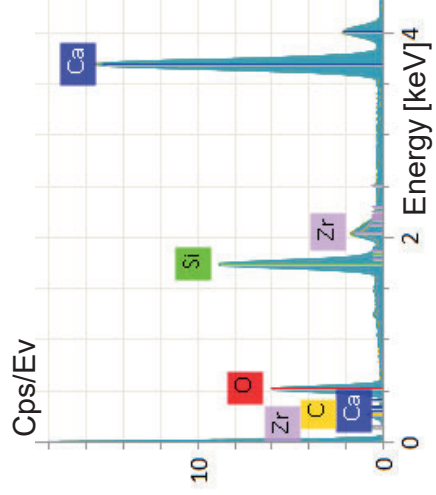
FBS

# TZ-Ag1

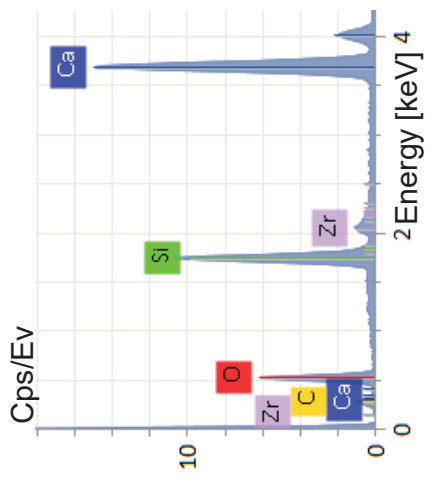
1 day



7 days

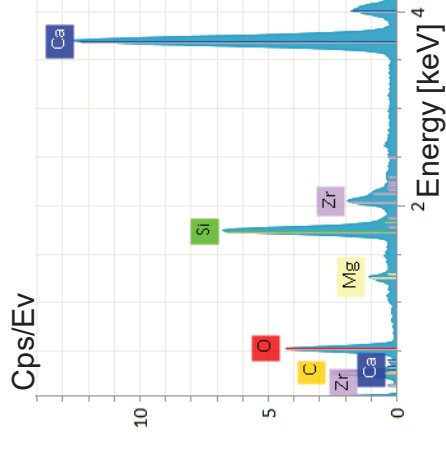


28 days

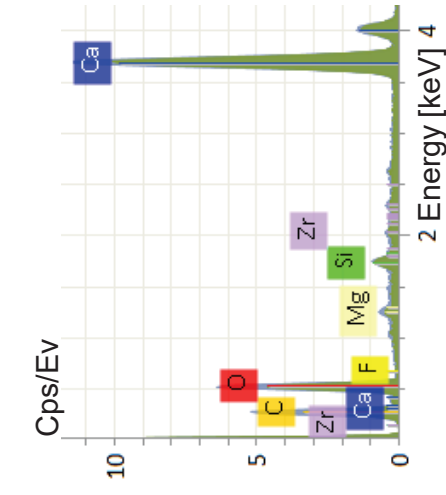


Water

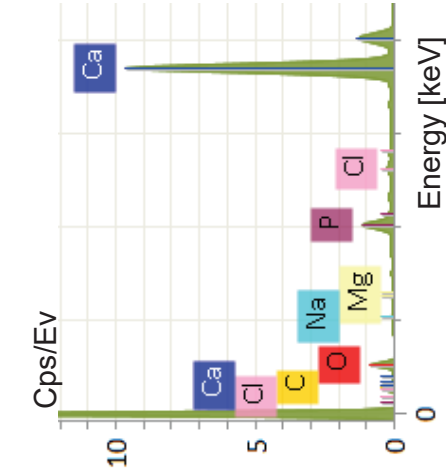
Cps/Ev



Cps/Ev

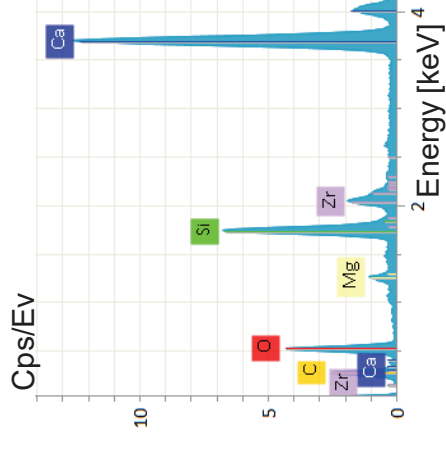


Cps/Ev

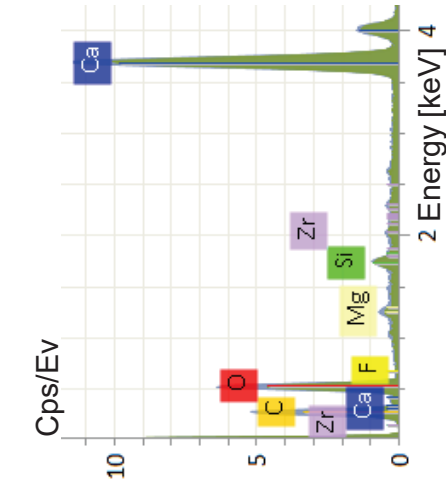


FBS

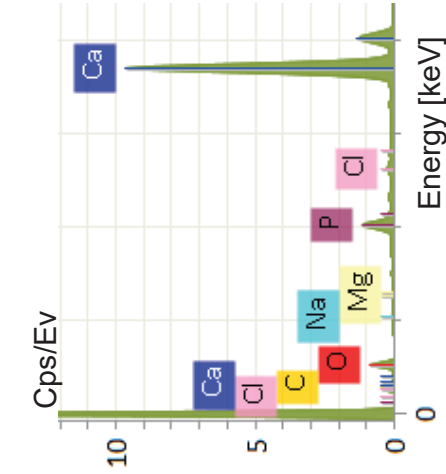
Cps/Ev



Cps/Ev



Cps/Ev



Energy [keV]

Energy [keV]

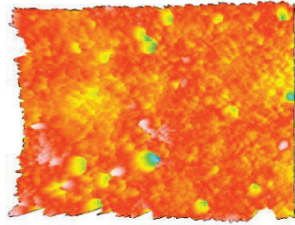
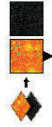
Energy [keV]

Energy [keV]

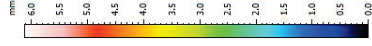
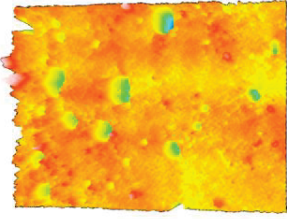
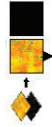
**Online Resource 2** Representative images acquired after stereoscopic reconstruction of scanning electron micrographs obtained with a quad-type backscatter electron detector at 200× magnification. Materials were exposure to ultrapure water (water) or Fetal Bovine Serum (FBS) for 1, 7 or 28 days prior to testing. Colours represent height (mm) as indicated in the scale bars on the right side of each image.

# TZ-base

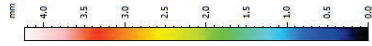
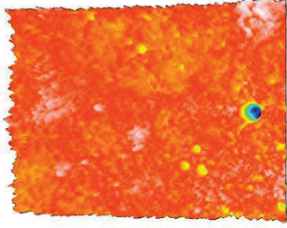
1 day



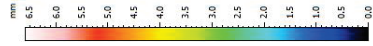
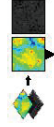
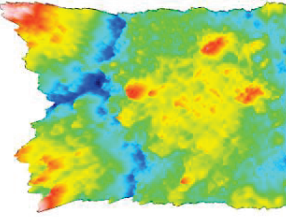
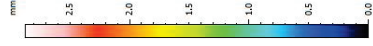
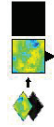
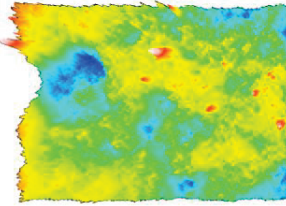
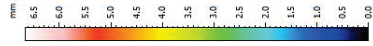
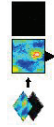
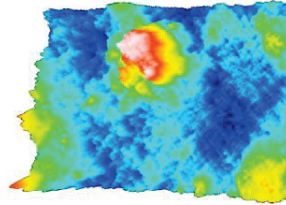
7 days



28 days



Water



FBS

# TZ-bg10

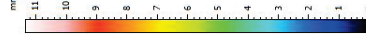
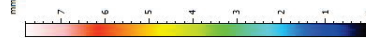
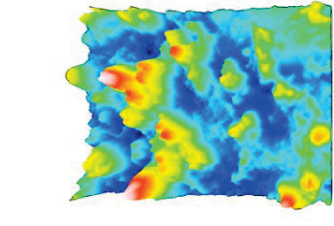
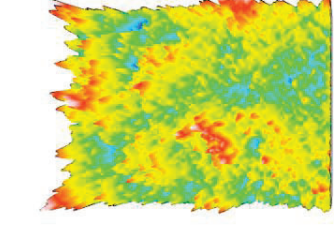
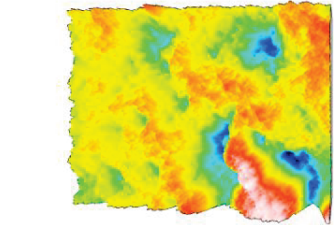
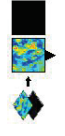
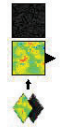
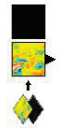
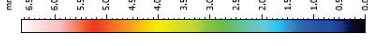
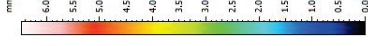
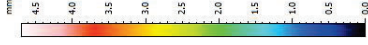
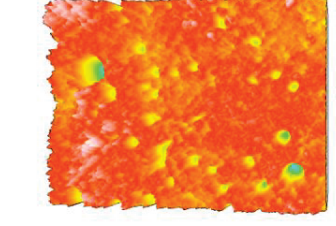
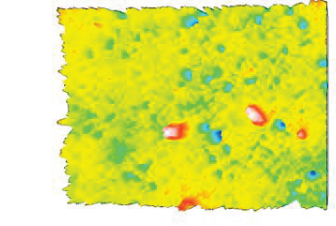
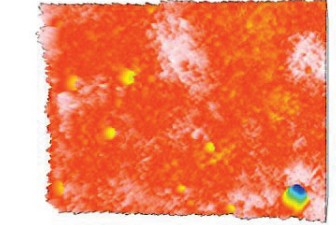
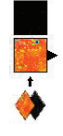
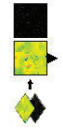
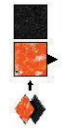
1 day

7 days

28 days

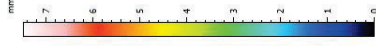
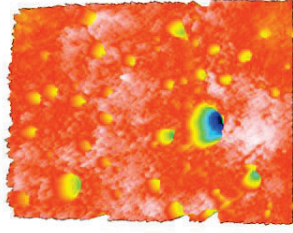
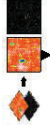
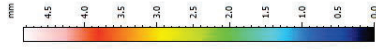
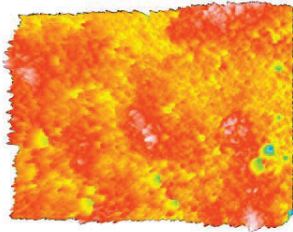
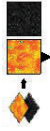
Water

FBS

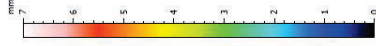
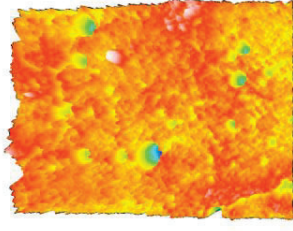
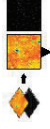


# TZ-bg20

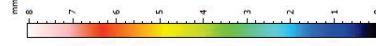
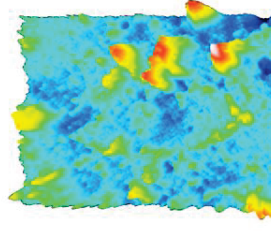
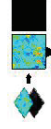
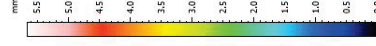
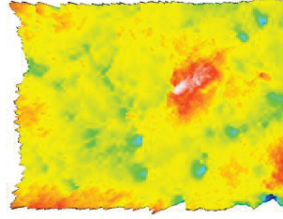
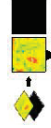
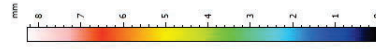
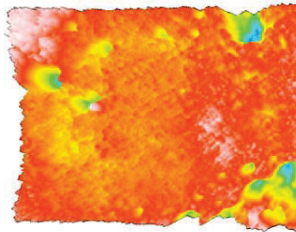
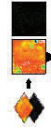
1 day



7 days



28 days

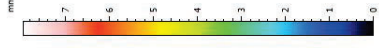
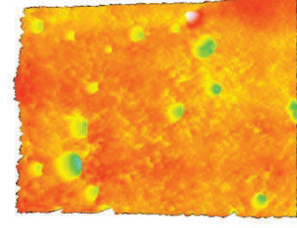
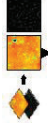
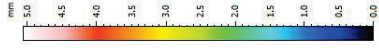
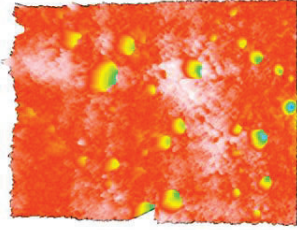
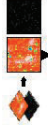


FBS

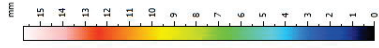
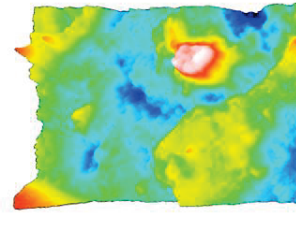
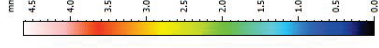
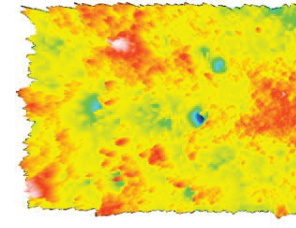
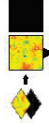
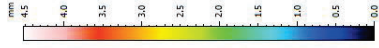
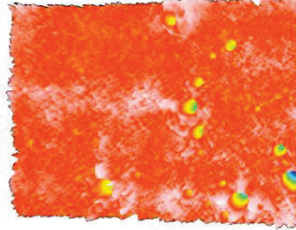
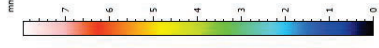
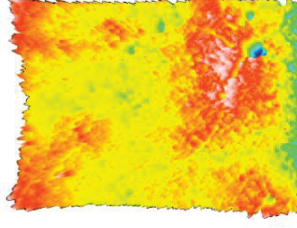
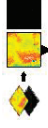
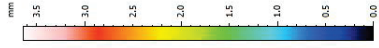
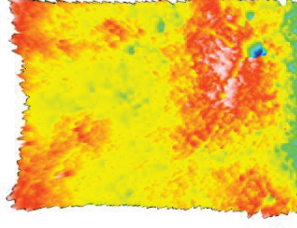
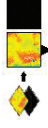
Water

# TZ-Ag0.5

1 day



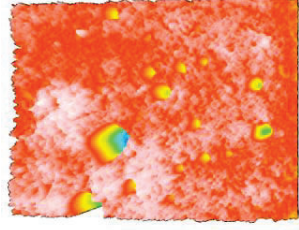
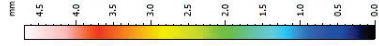
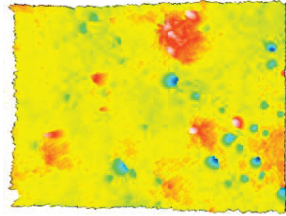
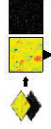
28 days



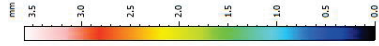
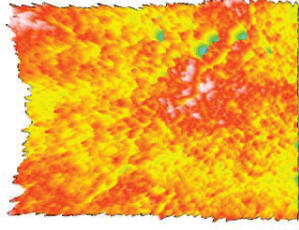
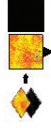


# TZ-Ag1

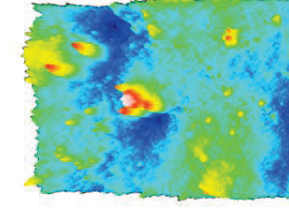
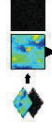
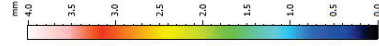
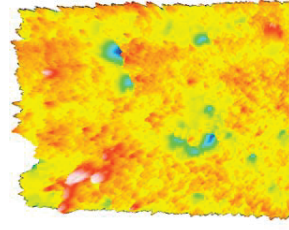
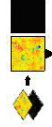
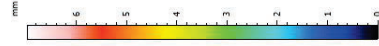
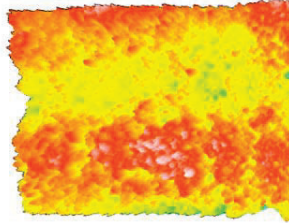
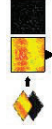
1 day



7 days



28 days

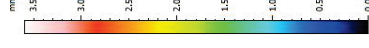
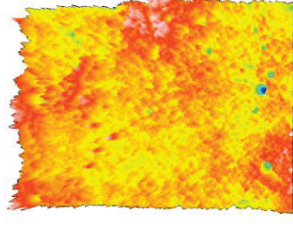
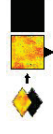
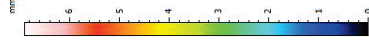
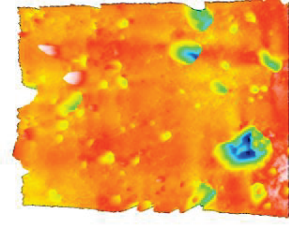
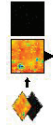
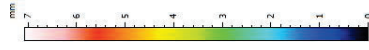
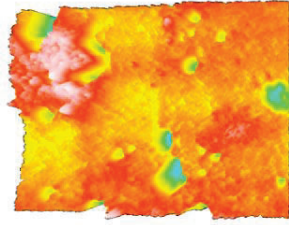
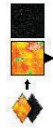


FBS

Water

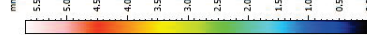
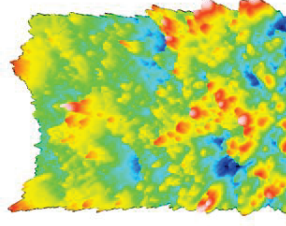
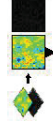
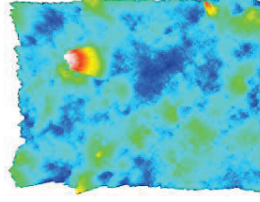
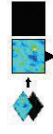
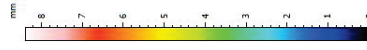
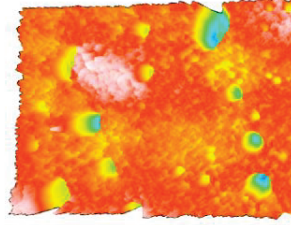
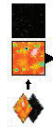
# TZ-Ag2

1 day



28 days

1 day

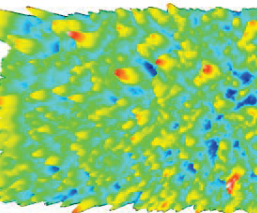
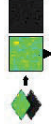
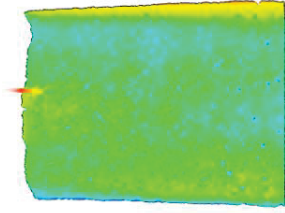


Water

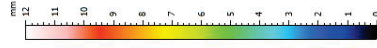
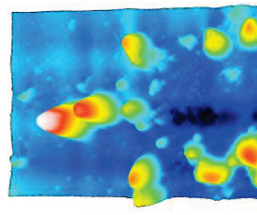
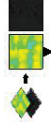
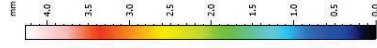
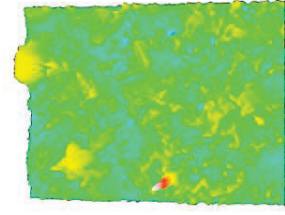
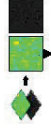
FBS

# Biodentine

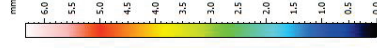
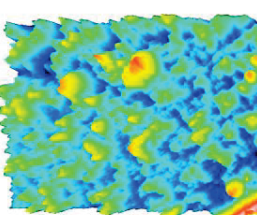
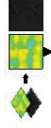
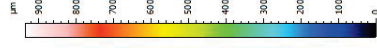
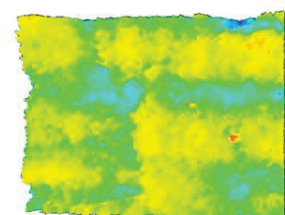
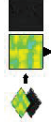
1 day



7 days



28 days

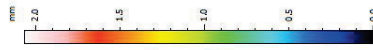
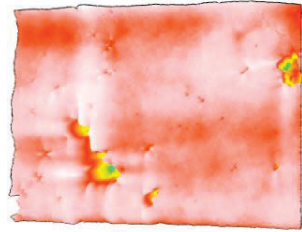


Water

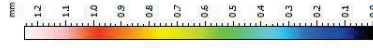
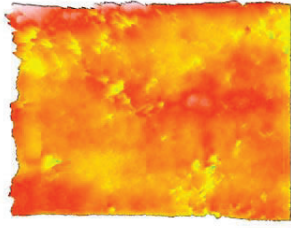
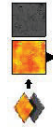
FBS

# IRM

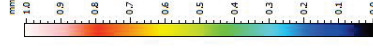
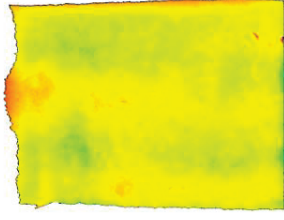
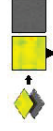
1 day



7 days

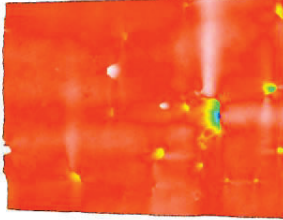
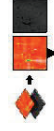
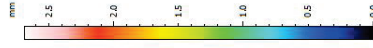
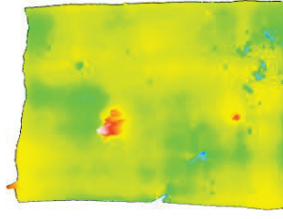
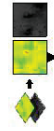
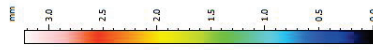
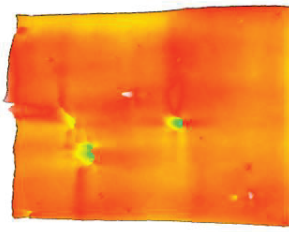
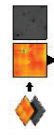


28 days



Water

FBS



**Online Resource 3** Mean and standard deviation of bacterial adhesion upon material surfaces after a 1 h-agitation period at 37 °C in an *Enterococcus faecalis* inoculum. Values are presented per material, immersion liquid (water or FBS) and immersion period (1, 7 or 28 days). Sterile membrane filters cut to the same diameter (9 mm) as the material specimens served as positive control. Read horizontally, different superscript letters indicate statistically significant differences between different aging periods and immersion solutions within the same material ( $p < 0.05$ ). Read vertically, different capital letters show statistically significant difference among materials for the exact same conditions of testing (aging period and immersion solution) ( $p < 0.05$ ). Asterisks indicate statically significant difference from the positive control ( $p < 0.05$ ) (a). Representative confocal microscope images of bacterial adhesion on TZ-base and Biodentine samples immersed in water for 1, 7 or 28 days before testing (b).

a

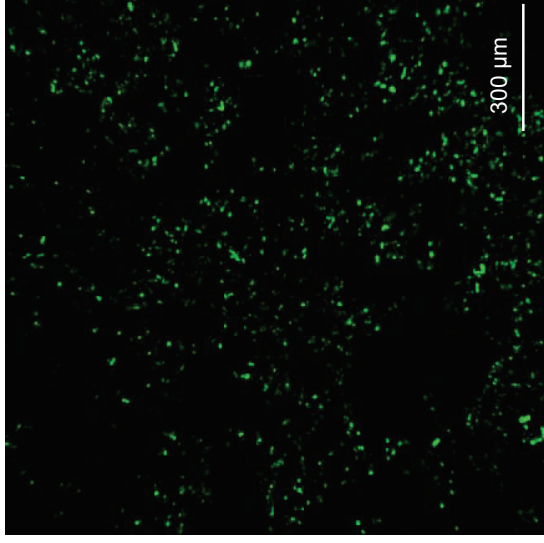
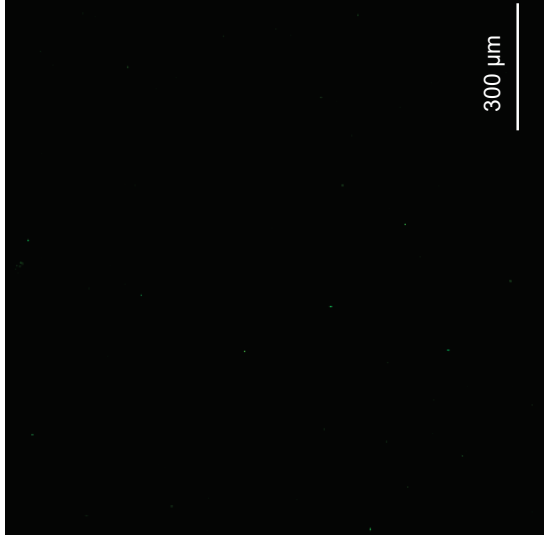
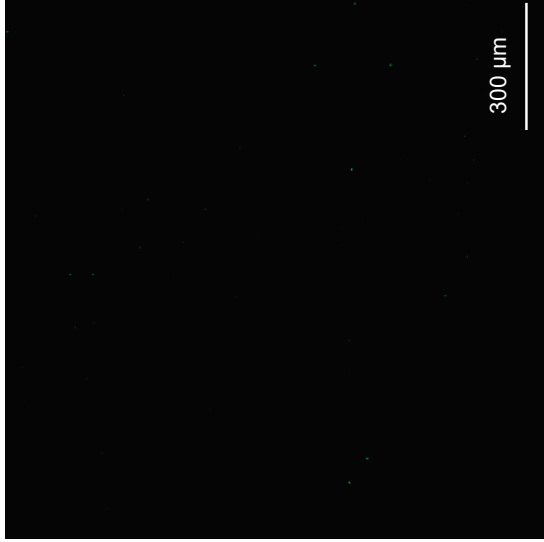
<i>E. faecalis</i> counts								
Material	1 days			7 days			28 days	
	Water	FBS	Water	FBS	Water	FBS	Water	FBS
<b>TZ-base</b>	26 (11) <sup>A-a*</sup>	13 (8) <sup>A-a*</sup>	18 (4) <sup>A-a*</sup>	15 (5) <sup>A-a*</sup>	205 (61) <sup>A-b</sup>	214 (34) <sup>A-b</sup>		
<b>TZ-bg10</b>	19 (7) <sup>A-a*</sup>	16 (4) <sup>A-a*</sup>	14 (6) <sup>A-a*</sup>	12 (5) <sup>A-a*</sup>	212 (59) <sup>A-b</sup>	166 (60) <sup>A-b</sup>		
<b>TZ-bg20</b>	10 (1) <sup>A-a*</sup>	12 (7) <sup>A-a*</sup>	15 (7) <sup>A-a*</sup>	17 (7) <sup>A-a*</sup>	108 (47) <sup>A-b*</sup>	183 (67) <sup>A-c</sup>		
<b>TZ-Ag0.5</b>	11 (3) <sup>A-a*</sup>	14 (5) <sup>A-a*</sup>	17 (10) <sup>A-a*</sup>	11 (4) <sup>A-a*</sup>	183 (83) <sup>A-b</sup>	239 (67) <sup>A-b</sup>		
<b>TZ-Ag1</b>	18 (6) <sup>A-a*</sup>	18 (5) <sup>A-a*</sup>	18 (6) <sup>A-a*</sup>	17 (8) <sup>A-a*</sup>	139 (54) <sup>A-b</sup>	174 (40) <sup>A-b</sup>		
<b>TZ-Ag2</b>	13 (7) <sup>A-a*</sup>	12 (3) <sup>A-a*</sup>	16 (5) <sup>A-a*</sup>	8 (4) <sup>A-a*</sup>	192 (80) <sup>A-b</sup>	196 (55) <sup>A-b</sup>		
<b>Biodentine</b>	122 (46) <sup>B-a*</sup>	173 (92) <sup>B-a*</sup>	181 (21) <sup>B-a*</sup>	153 (74) <sup>B-a*</sup>	252 (123) <sup>A-a</sup>	244 (59) <sup>A-a</sup>		
<b>IRM</b>	196 (76) <sup>B-a,b</sup>	114 (23) <sup>B-b*</sup>	183 (44) <sup>B-a,b*</sup>	102 (22) <sup>B-b*</sup>	267 (36) <sup>A-a</sup>	154 (60) <sup>A-b</sup>		
<b>Positive Control: 287 (94)</b>								

**b**

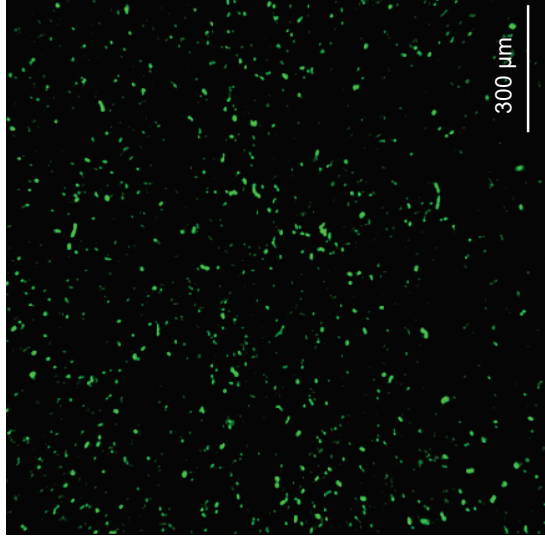
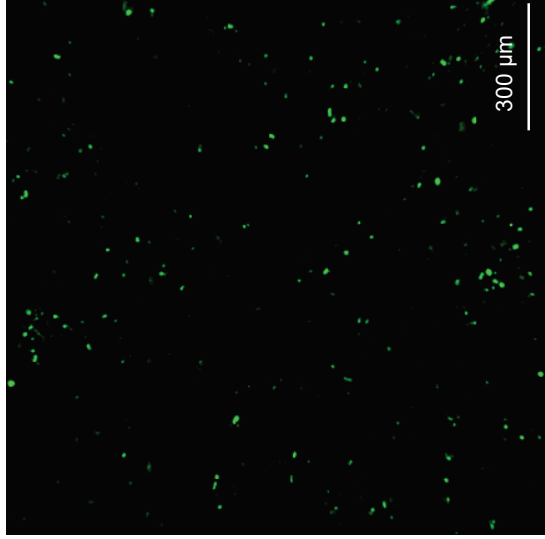
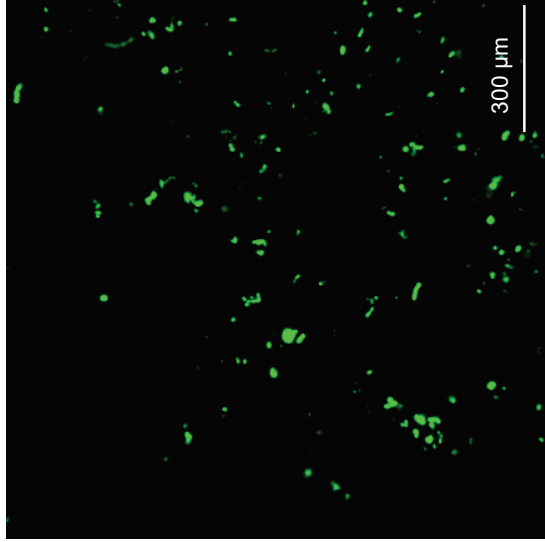
**1 day**

**7 days**

**28 days**



**TZ-base**



**Biodentine**





II



**ORIGINAL ARTICLE**

# Effect of exposure conditions on chemical properties of materials for surgical endodontic procedures

Andreas Koutroulis<sup>1</sup>  | Håkon Valen<sup>2</sup>  | Dag Ørstavik<sup>1</sup>  | Vasileios Kapralos<sup>1</sup>  |  
Josette Camilleri<sup>3</sup>  | Pia Titterud Sunde<sup>1</sup> 

<sup>1</sup>Section of Endodontics, Institute of Clinical Dentistry, Faculty of Dentistry, University of Oslo, Oslo, Norway

<sup>2</sup>Nordic Institute of Dental Materials (NIOM), Oslo, Norway

<sup>3</sup>School of Dentistry, Institute of Clinical Sciences, College of Medical and Dental Sciences, University of Birmingham, Birmingham, UK

**Correspondence**

Andreas Koutroulis, Section of Endodontics, Institute of Clinical Dentistry, Faculty of Dentistry, University of Oslo, P.O. Box 1109, Blindern, 0317 Oslo, Norway.  
Email: [andreas.koutroulis@odont.uio.no](mailto:andreas.koutroulis@odont.uio.no)

**Funding information**

UNIFOR, Grant/Award Number: 975503178/266; Universitetet i Oslo; Nordic Institute of Dental Materials

**Abstract**

This study investigated the role of aging and changes in environmental conditions on selected properties of a prototype radiopacified calcium silicate-based cement (TZ-base) with or without incorporation of silver nanoparticles or bioactive glass, and two commercial materials, Biodentine and intermediate restorative material. Materials were immersed in ultrapure water or fetal bovine serum for 28 days and were characterized with scanning electron microscopy and energy dispersive x-ray analysis. Immersion media were either replaced weekly or not replenished at all and were assessed for alkalinity and calcium release after 1, 7, 14, 21, and 28 days; antibacterial effect against 2-day monospecies biofilms; and cytotoxicity by the 3-(4,5-dimethylthiazolyl-2-yl)-2,5-diphenyl tetrazolium bromide assay after 1, 7, or 28 days. Alkalinity, calcium release, antibacterial activity, and cell cytotoxicity increased over time when the medium was not changed but decreased with medium replenishment. Immersion in fetal bovine serum resulted in lower alkalinity, less bactericidal properties, and lower cytotoxicity of prototype cements and Biodentine than did water immersion. Biodentine and 20% bioactive glass-containing cement had overall lower alkalinity, calcium release, and antibacterial activity than TZ-base, and Biodentine was less cytotoxic than TZ-base. In conclusion, exposure conditions and cement modifications significantly affected materials' leaching properties. Exposure conditions warrant consideration when evaluating cements' clinical properties.

**KEYWORDS**

anti-bacterial agents, bioactive glass 45S5, calcium silicate, chemical characterization

**INTRODUCTION**

Surgical endodontic procedures entail application and direct exposure of materials to host tissue fluids. Materials should remain physically stable but not necessarily inert, as stimulation of healing and antibacterial activity are desirable [1]. The

material may induce transient or more long-lasting changes in the local microenvironment; however, the microenvironment can also affect the material [2]. For hydraulic calcium silicate cements, *in vivo* conditions may alter their chemical reactivity through consumption of the released calcium hydroxide by the carbon dioxide present in the tissue fluid environment [3].

This is an open access article under the terms of the [Creative Commons Attribution-NonCommercial License](https://creativecommons.org/licenses/by-nc/4.0/), which permits use, distribution and reproduction in any medium, provided the original work is properly cited and is not used for commercial purposes.

© 2023 The Authors. *European Journal of Oral Sciences* published by John Wiley & Sons Ltd on behalf of Scandinavian Division of the International Association for Dental Research.

**TABLE 1** Presentation of test materials, their composition and handling procedure.

Material name	Composition	Handling
TZ-base	<u>Powder</u> : 80% w/w tricalcium silicate cement (CAS No: 12,168–85-3, American Elements), 20% w/w zirconium oxide (2–15 $\mu\text{m}$ particle size, Koch-Light Laboratories) <u>Liquid</u> : ultrapure water	Hand-mixed and spatulated at a 0.35 liquid/powder ratio
TZ-bg10, TZ-bg20	<u>Powder</u> : TZ-base with 10 or 20 % w/w bioactive glass 45S5 (Cas No: 65,997–17-3, Mo-Sci Corporation) replacement in the cementitious phase respectively <u>Liquid</u> : ultrapure water	
TZ-Ag0.5, TZ-Ag1, TZ-Ag2	<u>Powder</u> : TZ-base <u>Liquid</u> : 0.5, 1 or 2 mg/mL silver nanoparticle solution (CAS No: 7440–22-4, < 100 nm particle size, Sigma Aldrich) respectively, following dispersion of silver nanoparticles in ultrapure water [5]	
Biodentine (Septodont)	<u>Powder</u> : Calcium silicates, calcium carbonate, zirconium oxide <u>Liquid</u> : water, calcium chloride, water-soluble polymer	According to the manufacturer
Intermediate restorative material (IRM; Dentsply Sirona)	<u>Powder</u> : Zinc oxide, polymethylmethacrylate <u>Liquid</u> : eugenol, acetic acid	

The effect of environment on surface characteristics and corresponding antibacterial activity of hydraulic calcium silicate cements has been assessed *in vitro* [3–7]. However, despite the long known positive role of alkalinity on their antibacterial potential [8], the effect of clinical environment on antimicrobial properties associated with leaching is still not clear. Furthermore, studies on the antibacterial activity of endodontic cements for root-end filling and perforation repair *per se* are scarce [9].

Current formulations of commercial hydraulic calcium silicate cements appear to have limited antibacterial activity [10]. The bactericidal effect in hydraulic calcium silicate cements is mainly pH-dependent and is therefore considerably reduced over time as alkalinity is neutralized due to local interactions with host tissues [11]. Incorporation of silver nanoparticles could be explored to enhance their antibacterial profile [12]. Silver nanoparticles can damage bacterial cells by interfering with the permeability of the bacterial membrane as well as interacting with bacterial proteins and DNA [13]. Alternatively, bioactive glass formulations could promote release of calcium and phosphate ions and enhance the biological profile of cements [14]. Their incorporation in hydraulic calcium silicate cements could therefore be explored as well [15].

The aim of this study was to investigate the role of exposure conditions (immersion medium and aging period) on selected properties of endodontic cements used for surgical procedures. Furthermore, in order to assess the role of material composition on these properties, silver nanoparticles and bioactive glass were incorporated in prototype hydraulic calcium silicate cements. The null hypotheses were that aging period, immersion medium, and material composition do not affect the leaching characteristics of endodontic cements.

## MATERIAL AND METHODS

All chemicals and equipment were purchased from Merck unless stated otherwise. Table 1 presents the test materials.

Material discs (9 mm diameter, 1 mm thickness) were prepared and allowed to set for 24 h at 37°C, 100% relative humidity. Consequently, each material was immersed in tubes containing either 4 mL ultrapure water (water; Elix Essential 5 UV Water Purification System) or fetal bovine serum (F7524) and stored at 37°C. Testing of material leachates was conducted over a 28 day aging period, during which the immersion liquid was either replenished weekly or not changed at all (Figures 1A, 2A, 3A).

For biological assays, samples were additionally prepared inside cell culture inserts (pore size 0.4  $\mu\text{m}$ , 9 mm diameter) and placed immediately in 12-well plates containing 1.8 mL medium at 37°C for 24 h (Figure 2B).

Test conditions per assay are presented in Table 2 as well as in Figures 1–3. Leachates were sterile-filtered (Millex-GV, 0.22  $\mu\text{m}$ ) prior to testing.

## Chemical analysis

Alkalinity ( $n = 9$ /subgroup) was monitored with a pH meter (Sension+ PH3; Hach), and calcium ion release ( $n = 9$ /subgroup) with a calcium ion selective electrode connected to a laboratory meter (ION450; Radiometer analytical, Hach). Separate samples were assessed for pH and  $\text{Ca}^{2+}$  at the following periods: after 1, 7, or 28 days without changing the medium (independent samples); every 7 days for a total of 28 days upon replenishing the medium weekly

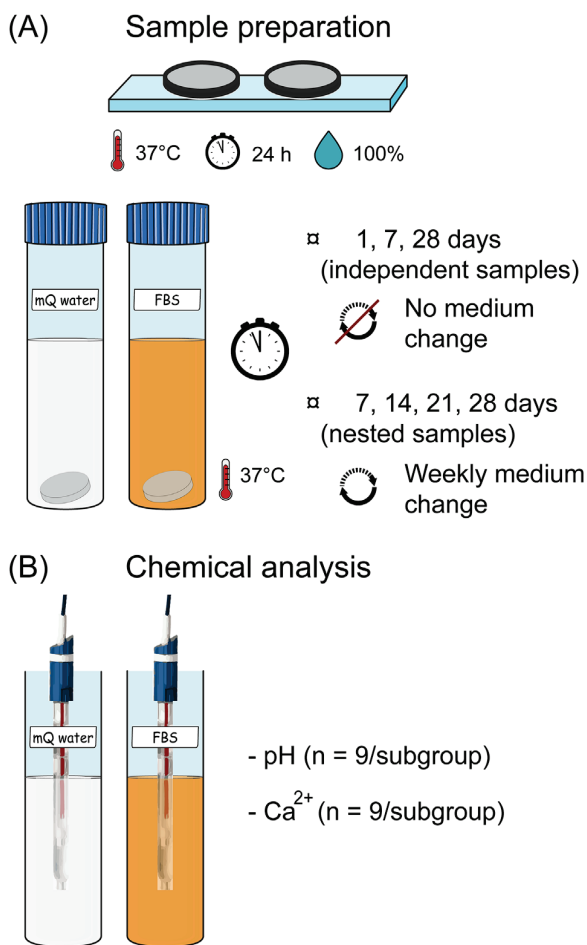


**FIGURE 1** Schematic representation of the chemical analysis. (A) Sample preparation for extract acquisition, and (B) testing of material extracts ( $n = 9/\text{subgroup}$ ). The analysis was performed separately for pH and  $\text{Ca}^{2+}$ . The figure was partially generated using Servier Medical Art, provided by Servier, licensed under a Creative Commons Attribution 3.0 unported license. FBS, fetal bovine serum; mQ, Milli-Q.

(nested specimens) (Figure 1, Table 2). For calibration purposes, three standard solutions were used in the alkalinity assessments (pH 4, 7, 10) and four standard solutions in the calcium release analysis (0.01, 0.1, 1, 10 mM Ca).

## Biological assays

All samples were incubated at 37°C, 5%  $\text{CO}_2$ , 100% relative humidity. Sterile water and fetal bovine serum served as negative controls. Testing of leachates was done after 1, 7, or 28 days for samples without any medium change (independent samples) and at 7 and 28 days for samples where the medium was refreshed weekly (nested samples) (Figure 2A). Material leachates were additionally obtained using an alternative

preparation method: Materials were placed into a cell culture insert system immediately after mixing for a 24 h aging period (0–24 h leachates) (Figure 2B, Table 2).

## Antibacterial activity

*Enterococcus faecalis* OG1RF ATCC 47077 and *Pseudomonas aeruginosa* ATCC 9027 from frozen stock cultures were incubated overnight in tryptic soy broth. Bacterial inocula ( $10^8$  CFU/mL) were prepared following centrifugation and resuspension of each culture in tryptic soy broth.

Two-day monospecies *E. faecalis* and *P. aeruginosa* biofilms were cultured upon membrane filters (MF-Millipore; 3 mm diameter), following a previously established protocol [16]. Briefly, membranes were placed upon tryptic soy broth agar plates and received 2  $\mu\text{L}$  bacterial inoculum. After 48 h incubation, membranes with biofilm were collected and immersed in 24-well plates containing 500  $\mu\text{L}$  test leachates ( $n = 9/\text{subgroup}$ ).

Following a 24 h overnight incubation, test membranes were retrieved and immersed in tubes containing 1 mL phosphate buffered saline, vortexed, and sonicated. Viable bacterial colonies were calculated upon serial dilution and plating on tryptic soy broth agar plates (Figure 2C).

## Cell viability

L929 murine fibroblast cells were cultured in 75  $\text{cm}^2$  flasks in Dulbecco's modified eagle's medium supplemented with 5% fetal bovine serum, 1% penicillin/streptomycin, 2 mM glutamine. At 70%–80% confluence, 10,000 cells were seeded in 96-well plates in 100  $\mu\text{L}$  medium. After 24 h incubation, the medium in the wells was replaced with 100  $\mu\text{L}$  fresh medium and 100  $\mu\text{L}$  test leachate ( $n = 9/\text{subgroup}$ ). Three dilutions of each leachate were also tested. The following day, solutions were aspirated and 100  $\mu\text{L}$  3-(4,5 dimethylthiazolyl-2-yl)-2,5-diphenyltetrazolium bromide (MTT; 0.5 mg/mL) was added to each well. After 3 h, MTT was replaced with 100  $\mu\text{L}$  dimethyl sulfoxide. The optical density of the wells was read in a microplate reader (Synergy H1; BioTek) at 570 nm (Figure 2D).

## Scanning electron microscopy (SEM) and energy dispersive X-ray (EDX) analysis

Following a 28 day incubation period in the two media without replenishment (Figure 3A), material specimens ( $n = 3/\text{subgroup}$ ) were retrieved, vacuum desiccated, embedded in epoxy resin, and ground and polished with a series of silicon carbide foils and polishing cloths (Struers).

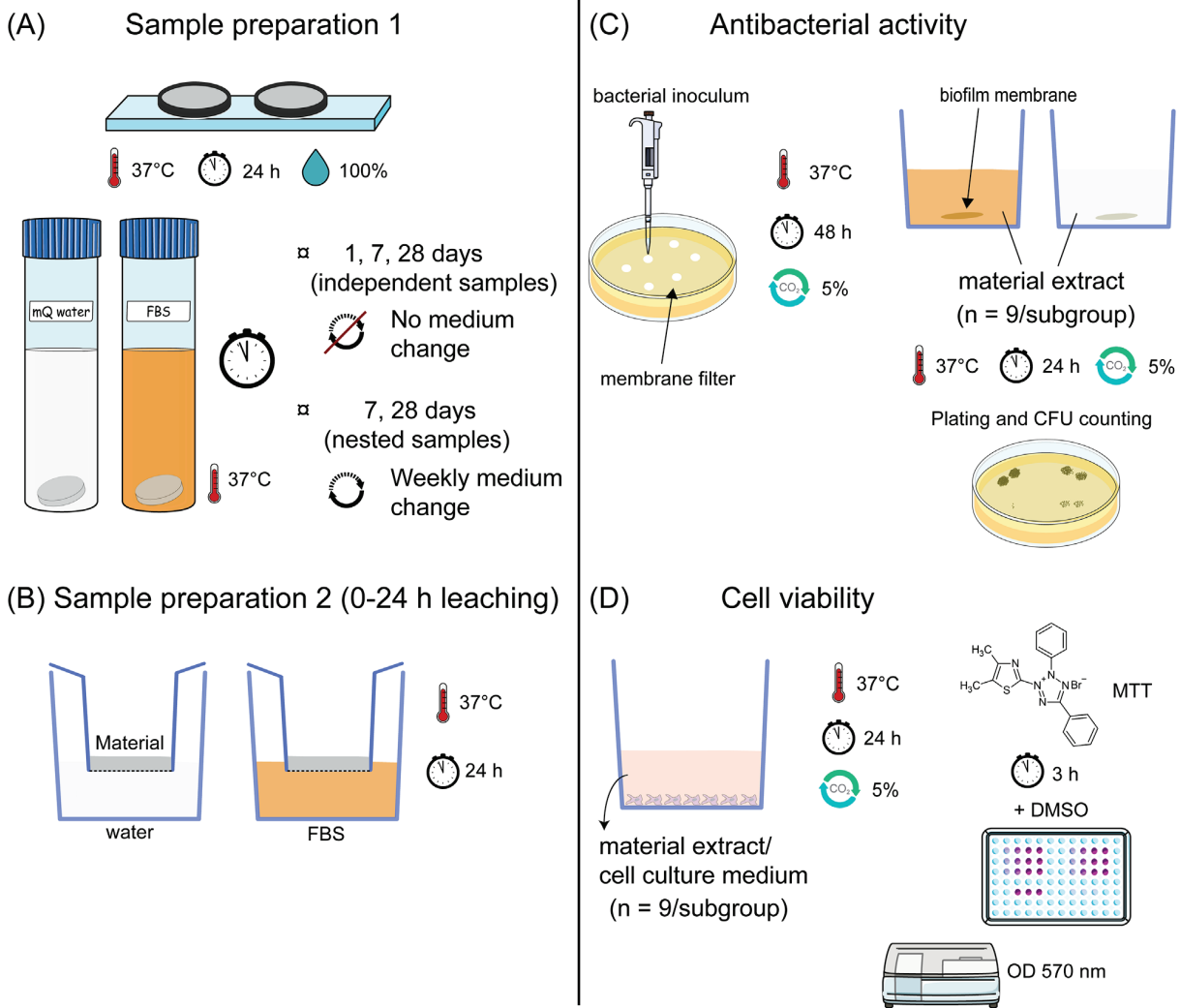


**FIGURE 2** Schematic representation of the biological assays. Material extracts were acquired using two different preparation methods. (A) In the first method, extracts were obtained after 1, 7, or 28 days with or without replenishing the medium weekly. (B) In the second method of extract preparation, materials were mixed and immediately placed in cell culture inserts positioned inside 12-well plates containing the respective extract medium for 24 h. (C) For antibacterial activity testing, membrane filters were placed on agar plates and received a bacterial inoculum to cultivate 2-day monospecies biofilms of *Enterococcus faecalis* and *Pseudomonas aeruginosa*. Subsequently, they were exposed to 500  $\mu$ L material extract for 24 h and bacterial viability was assessed by aliquots plated on agar plates. (D) For cell viability assessment, an MTT assay was performed using four different concentrations of each material extract. Parts of the figure were generated using Servier Medical Art, provided by Servier, licensed under a Creative Commons Attribution 3.0 unported license. DMSO, dimethylsulfoxide; FBS, fetal bovine serum; mQ, Milli-Q; MTT, 3-(4,5-dimethylthiazolyl-2-yl)-3,5-diphenyltetrazolium bromide; OD, optical density.

Finally, they were imaged in backscatter mode with scanning electron microscopy (SEM) (TM4000Plus II; Hitachi). Energy dispersive X-ray (EDX) analyses in random cement areas were also performed (Figure 3B).

## Statistical analysis

Power calculations were initially conducted considering a factorial analysis of variance and the sample size used in the

assays accounted overall for an effect size of  $f = 0.20$ – $0.28$  ( $\alpha$  error probability = 0.05, power = 0.95) upon estimations with G\*Power 3.1 (Heinrich Heine University).

Regression analyses were performed using Stata/SE 17.0 (StataCorp) to assess the effect of material, immersion medium, and aging period to pH, calcium release, bacterial survival, and cell viability. As data consisted of both repeated measurements within the 28 day period (nested samples) and independent ones, two different models were explored. Additionally, subgroup analyses were conducted, either for

**TABLE 2** Exposure conditions of materials per assay prior to testing.

Assay	Aging period prior to testing	Immersion medium
Chemical	<ul style="list-style-type: none"> <li>1, 7, 28 days without medium replenishment (independent samples)</li> <li>7, 14, 21, 28 days upon weekly medium change (nested samples)</li> </ul>	<ul style="list-style-type: none"> <li>Ultrapure water</li> <li>Fetal bovine serum</li> </ul>
Biological	<ul style="list-style-type: none"> <li>1, 7, 28 days without medium change (independent samples)</li> <li>7, 28 days upon weekly medium change (nested samples)</li> <li>24 h ("0–24 h") for samples prepared inside cell culture inserts</li> </ul>	
Characterization	28 days without changing medium	
<ul style="list-style-type: none"> <li>Scanning electron microscopy</li> <li>Energy dispersive X-ray analysis</li> </ul>		

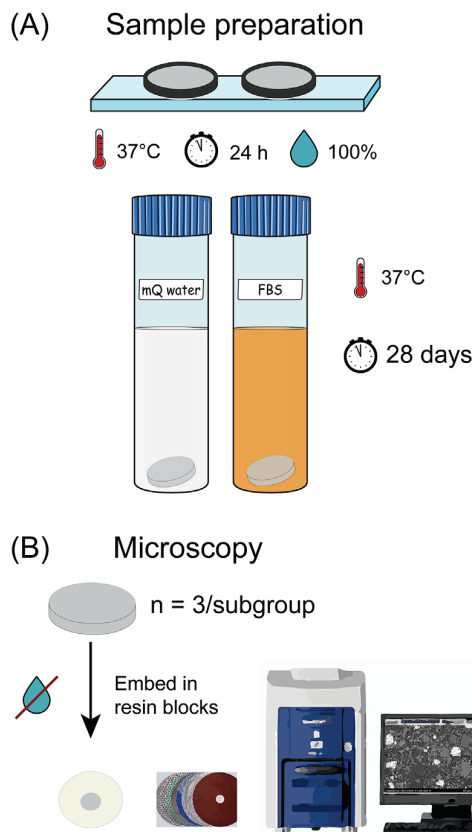


**FIGURE 3** Illustrative representation of sample preparation for scanning electron microscopy (SEM) and energy dispersive X-ray analysis. (A) Samples ( $n = 3$ /subgroup) underwent a 28-day immersion period in ultrapure water or fetal bovine serum (FBS). (B) Subsequently, they were retrieved, desiccated, embedded in epoxy resin and imaged in the SEM after grinding and polishing. Figure 3A was partially generated by using pictures from Servier Medical Art, provided by Servier, licensed under a Creative Commons Attribution 3.0 unported license. mQ, Milli-Q.

independent assessment of the effect of exposure conditions on properties of material leachates, or for comparison of the effect of material in the same immersion medium. Specifically for each assay, the following were performed:

- In the chemical analysis, multiple linear regression models were fitted for the independent leachate samples of pH and  $\text{Ca}^{2+}$  for material specimens where the medium was not refreshed (at 1, 7, 28 days;  $n = 378$ ). In addition, mixed-effects linear regression models were fitted to examine pH or calcium release as outcome variables for the weekly investigation of leachates of nested specimens following medium refreshment (at 7, 14, 21, and 28 days;  $n = 126$ ). For calcium release, subgroup analyses were also conducted for Biodentine ( $n = 54$ ) or for the prototype hydraulic calcium silicate cements ( $n = 324$ ), to assess the effect of the immersion medium in the accumulative leaching conditions separately. The intermediate restorative material (IRM) was not included in any of these analyses due to its different chemical composition.
- In the biological assays, the data from the antibacterial activity assays were logarithmically transformed and expressed as  $\log(\text{CFU}+1)/\text{mL}$ ; the data from cell viability were normalized to the respective negative control values and expressed as relative MTT activity (%). Multiple linear regressions were conducted for the independent leachate measurements, where the medium was not refreshed (at 1, 7, 28 days;  $n = 864$  for antibacterial activity and  $n = 432$  for cell viability), as well as for the 0–24 h leachates ( $n = 288$  for antibacterial activity;  $n = 144$  for cell viability). Additionally, mixed-effects linear regression models were fitted for data from nested material specimens (testing after 7 and 28 days upon weekly medium replenishment) for bacterial survival ( $n = 288$ ) and cell viability ( $n = 144$ ) as outcome variables. In all the above regression models for antibacterial assays, the factor “bacterium” was also included as

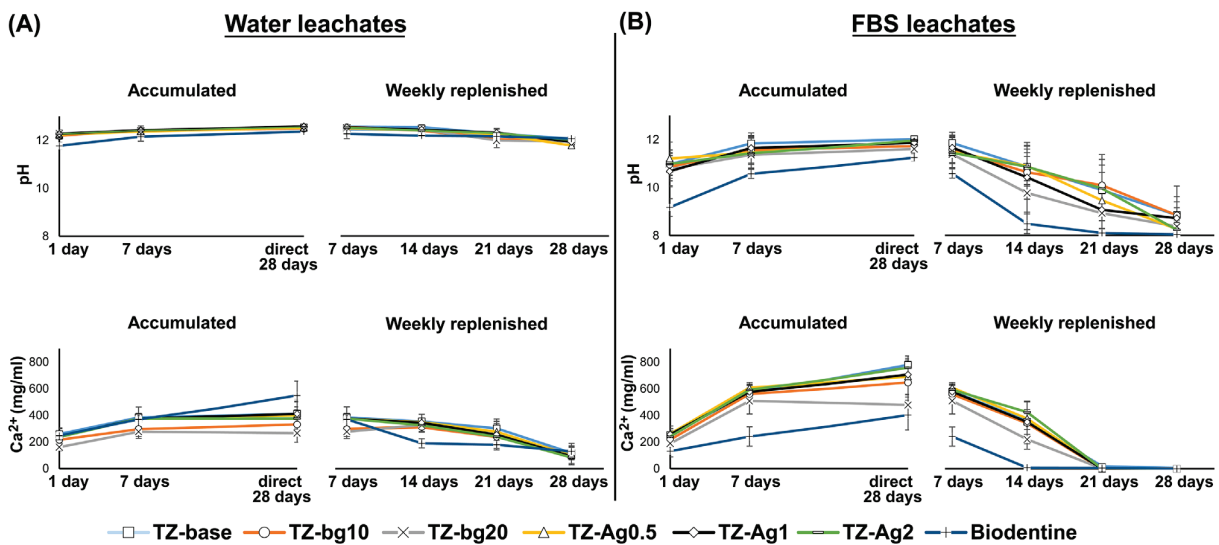


**FIGURE 4** Mean pH and calcium release (mg/mL) of materials immersed in (A) water or (B) fetal bovine serum (FBS) over a 28-day evaluation period. Line charts are organized on whether medium was replenished weekly or not (“accumulated”). An overlap in pH values of prototype cements is evident, particularly in water leachates. Test results for  $\text{Ca}^{2+}$  release were expressed following subtraction of the respective background measurements for pure water and neat fetal bovine solution (FBS). Error bars indicate standard deviation. TZ-base, prototype calcium silicate-based cement; TZ-bg10, TZ-base with 10% bioactive glass; TZ-bg20, TZ-base with 20% bioactive glass; TZ-Ag0.5, TZ-base with 0.5 mg/mL silver nanoparticle solution; TZ-Ag1, TZ-base with 1 mg/mL silver nanoparticle solution; TZ-Ag2, TZ-base with 2 mg/mL silver nanoparticle solution.

a predictor variable. Finally, for antibacterial activity, subgroup analyses were also conducted to compare the effect of each material within the same immersion medium and against the same bacterial species.

Evaluation of assumptions was conducted and in cases where heteroscedasticity of standardized residuals was observed, regressions were performed using robust standard errors. Additionally, the models were further validated by inspecting the QQ-plots of standardized residuals.

## RESULTS

### Chemical analysis

The data for pH and calcium ion leaching are shown in Figure 4A for water samples and in Figure 4B for fetal bovine serum-immersed materials. Results from the overall regression models are presented in Tables 3 and 4 for independent and nested leachate measurements, respectively.

Aging had a significant effect on pH; alkalinity was increased with aging when the medium was not replenished (Table 3; 7–28 days: mean increase = 0.25, 95% CI [0.16; 0.34]). Alternatively, the alkalinity decreased upon medium replenishment (Table 4; 14–21 days: mean decrease =  $-0.52$ , 95% CI [ $-0.73$ ;  $-0.31$ ]; 21–28 days: mean decrease =  $-0.53$ ,

95% CI [ $-0.72$ ;  $-0.33$ ]). Exposure to fetal bovine serum statistically significantly reduced the pH of hydraulic calcium silicate cements (Figure 2B). The prototype calcium silicate-based cement (TZ-base; i.e., without inclusions of silver nanoparticles or bioactive glass) had overall higher alkalinity compared to Biodentine and TZ-base with 20% bioactive glass (TZ-bg20).

Aging had a significant effect on calcium release as well, with a similar pattern as seen for alkalinity. The bioactive glass-containing materials and Biodentine leached overall significantly less  $\text{Ca}^{2+}$  than TZ-base, except for TZ-base with 10% bioactive glass (TZ-bg10) when the medium was changed weekly (Table 4). The immersion medium had a varied effect on the calcium leaching. In the nested samples model, fetal bovine serum immersion led to a decrease in calcium release compared to water. In the accumulative leaching model of independent measurements, subgroup analyses per material revealed that prototype cements leached more calcium ions when immersed in fetal bovine serum than in water. However, for Biodentine, fetal bovine serum significantly reduced the leaching of  $\text{Ca}^{2+}$  (Table 5; Figure 2).

### Antibacterial activity

Results from antibacterial assays are presented in Figure 5A and B for water and fetal bovine serum material leachates,



**TABLE 3** Multiple linear regression analyses for independent leachate samples for pH (model 1a) and calcium release (model 2a), with estimated change in pH and calcium release in comparison to the reference group of the predictor variables and their 95% confidence intervals provided.

Variable	Model 1a: pH. Independent samples of accumulative leaching ( <i>n</i> = 378)	Model 2a: Calcium release (mg/mL). Independent samples of accumulative leaching ( <i>n</i> = 378)
	Coefficient [95% CI]	Coefficient [95% CI]
Material (Ref. TZ-base)	–	–
TZ-bg10	–0.12 [–0.25; 0.01]	–64.47 [–101.65; –27.29]**
TZ-bg20	–0.17 [–0.32; –0.03]*	–132.28 [–167.03; –97.54]***
TZ-Ag0.5	–0.04 [–0.18; 0.10]	–13.8 [–50.42; 22.83]
TZ-Ag1	–0.09 [–0.23; 0.05]	–14.4 [–49.78; 20.98]
TZ-Ag2	–0.06 [–0.2; 0.08]	–13.86 [–51.29; 23.57]
Biodentine	–0.78 [–0.96; 0.60]***	–119.62 [–170.81; –68.43]***
Immersion medium (Ref. Water)	–	–
FBS	–1.07 [–1.15; 0.98]***	136.8 [115.18; 158.43]***
Aging period (Ref. 1 day)	–	–
7 days	0.47 [0.35; 0.59]***	211.83 [190.03; 233.64]***
Direct 28 days	0.72 [0.61; 0.83]***	289.68 [261.25; 318.12]***

TZ-base, prototype calcium silicate-based cement; TZ-bg10, TZ-base with 10% bioactive glass; TZ-bg20, TZ-base with 20% bioactive glass; TZ-Ag0.5, TZ-base with 0.5 mg/mL silver nanoparticle solution; TZ-Ag1, TZ-base with 1 mg/mL silver nanoparticle solution; TZ-Ag2, TZ-base with 2 mg/mL silver nanoparticle solution; FBS, fetal bovine serum.

\**P* < 0.05.

\*\**P* < 0.01.

\*\*\**P* < 0.001.

**TABLE 4** Mixed-effects linear regression analyses for nested data for pH (model 1b) and calcium release (model 2b), with coefficients and 95% confidence intervals (CIs).

Variable	Model 1b: pH. Repeated measurements upon weekly medium change ( <i>n</i> = 126)	Model 2b: Calcium release (mg/mL). Repeated measurements upon weekly medium change ( <i>n</i> = 126)
	Coefficient [95% CI]	Coefficient [95% CI]
Material (Ref. TZ-base)	–	–
TZ-bg10	–0.07 [–0.34; 0.2]	–28.44 [–62.77; 5.89]
TZ-bg20	–0.40 [–0.68; –0.13]**	–51.35 [–85.68; –17.02]**
TZ-Ag0.5	–0.21 [–0.49; 0.06]	–1.74 [–36.07; 32.59]
TZ-Ag1	–0.19 [–0.46; 0.08]	–12.96 [–47.29; 21.37]
TZ-Ag2	–0.25 [–0.52; 0.03]	–6.07 [–40.4; 28.26]
Biodentine	–0.82 [–1.09; –0.54]***	–125.16 [–159.49; –90.83]***
Immersion medium (Ref. Water)	–	–
FBS	–2.25 [–2.4; –2.1]***	–40.78 [–59.23; –22.42]***
Aging period (Ref. 7 days)	–	–
14 days	–0.68 [–0.88; –0.47]***	–131.38 [–156.73; –106.03]***
21 days	–1.20 [–1.40; –1.00]***	–307.97 [–334.71; –281.24]***
28 days	–1.73 [–1.92; –1.54]***	–383.06 [–408.41; –357.71]***

TZ-base, prototype calcium silicate-based cement; TZ-bg10, TZ-base with 10% bioactive glass; TZ-bg20, TZ-base with 20% bioactive glass; TZ-Ag0.5, TZ-base with 0.5 mg/mL silver nanoparticle solution; TZ-Ag1, TZ-base with 1 mg/mL silver nanoparticle solution; TZ-Ag2, TZ-base with 2 mg/mL silver nanoparticle solution; FBS, fetal bovine serum.

\**P* < 0.05.

\*\**P* < 0.01.

\*\*\**P* < 0.001.

**TABLE 5** Subgroup multiple linear regression analyses assessing separately the effect of prototype cements and Biodentine in calcium release (outcome variable) for the independent leachate measurements, with linear regression coefficients and confidence intervals as the estimates provided.

Variable	Model 2c: Calcium release (mg/mL). Independent samples of accumulative leaching-subgroup analysis for prototype cements (n = 324)	Model 2d: Calcium release (mg/mL). Independent samples of accumulative leaching-subgroup analysis for Biodentine (n = 54)
	Coefficient [95% CI]	Coefficient [95% CI]
Material (Ref. TZ-base)	–	Na.
TZ-bg10	–64.47 [–100.55; –28.39]**	Na.
TZ-bg20	–132.28 [–166.25; –98.31]***	Na.
TZ-Ag0.5	–13.8 [–49.46; 21.86]	Na.
TZ-Ag1	–14.4 [–49.17; 20.37]	Na.
TZ-Ag2	–13.86 [–50.01; 22.28]	Na.
Immersion medium (Ref. Water)	–	–
FBS	181.29 [161.38; 201.2]***	–130.12 [–175.52; –84.72]***
Aging period (Ref. 1 day)	–	–
7 days	227.82 [207.2; 248.44]***	115.9 [60.3; 171.5]***
Direct 28 days	290.25 [262.26; 318.23]***	286.31 [230.71; 341.91]***

TZ-base, prototype calcium silicate-based cement; TZ-bg10, TZ-base with 10% bioactive glass; TZ-bg20, TZ-base with 20% bioactive glass; TZ-Ag0.5, TZ-base with 0.5 mg/mL silver nanoparticle solution; TZ-Ag1, TZ-base with 1 mg/mL silver nanoparticle solution; TZ-Ag2, TZ-base with 2 mg/mL silver nanoparticle solution; FBS, fetal bovine serum.

\* $P < 0.05$ .

\*\* $P < 0.01$ .

\*\*\* $P < 0.001$ .

respectively, as well as in Figure 6 for test leachates extracted in the cell culture inserts (0–24 h). Results from the overall regression analyses are presented Tables 6–8 for independent, nested, and 0–24 h leachate samples, respectively.

Bacterial killing increased throughout time when the medium was not changed (Table 6; 7–28 days: mean decrease  $\log(\text{CFU}+1)/\text{mL} = -0.40$ , 95% CI [–0.62; –0.18]) and decreased when the medium was refreshed (Table 7). The immersion medium had a significant effect in bacterial survival; fetal bovine serum leachates showed reduced antibacterial activity compared with water leachates. TZ-base was overall significantly more antibacterial than Biodentine in all tested models; TZ-bg10 and TZ-bg20 except for when the medium was replenished; and IRM except for the 0–24 h aging condition (Table 8, Figure 6). Overall, silver nanoparticle-containing prototype cements exhibited similar antimicrobial activity to TZ-base. Subgroup analyses for water samples against *E. faecalis* showed a higher bacterial reduction induced by leachates of TZ-base with 2 mg/mL silver nanoparticle solution (TZ-Ag2) than the other cements investigated, except for the 0–24 h leaching period (Table 9, Figure 6); *E. faecalis* biofilms were overall more resistant to material leachates than *P. aeruginosa* biofilms, except for the 0–24 h leaching period (Table 8).

## Cell viability

Data for cell viability are presented in Figure 7A and B for water and fetal bovine serum material leachates respectively; Figure 8 shows normalized data from the MTT assay for the 0–24 h leachates. The outcomes from the overall regression analyses can be found in Tables 6–8. Results from diluted test leachates can be found in Figures S1 and S2.

Cell viability was decreased when the medium was not changed from 1 day onwards (Table 6), until it was eliminated at the direct 28 day period (7–28 days: mean decrease in relative MTT activity =  $-7.62$ , 95% CI [–9.76; –5.47]); refreshing the medium resulted in reduced cytotoxicity at 28 days (Table 7, Figure 7). The immersion medium significantly affected cell viability; fetal bovine serum leachates displayed diminished cytotoxicity values compared to the water leachates, particularly at 28 days upon medium change (Figure 7), but not in the 0–24 h leaching period (Table 8, Figure 8).

Biodentine and IRM had overall a less cytotoxic profile than TZ-base. Modifications in prototype cements did not significantly change the cell viability values compared to TZ-base. In prototype materials, only the 28 day fetal bovine serum leachates upon changing medium weekly reported higher cell viability than the cytotoxicity threshold (70%)

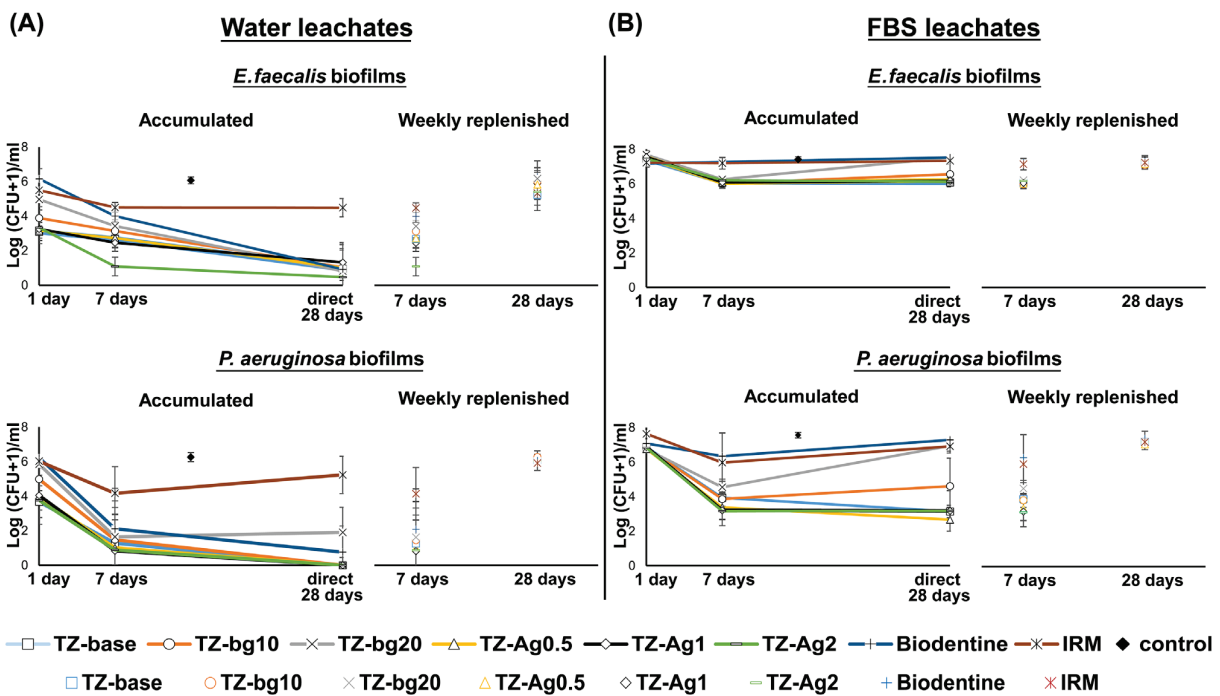


**FIGURE 5** Mean bacterial survival with standard deviation following overnight exposure of monospecies biofilms of *Enterococcus faecalis* or *Pseudomonas aeruginosa* to (A) water or (B) fetal bovine serum (FBS) material leachates aged for 1, 7, or 28 days with or without changing the medium weekly. Control corresponds to neat water or FBS respectively in each graph. Line charts correspond to groups without medium replenishment (“accumulated”) and graphs with markers and standard deviation are for groups with weekly medium replenishment. TZ-base, prototype calcium silicate-based cement; TZ-bg10, TZ-base with 10% bioactive glass; TZ-bg20, TZ-base with 20% bioactive glass; TZ-Ag0.5, TZ-base with 0.5 mg/mL silver nanoparticle solution; TZ-Ag1, TZ-base with 1 mg/mL silver nanoparticle solution; TZ-Ag2, TZ-base with 2 mg/mL silver nanoparticle solution; IRM, intermediate restorative material.

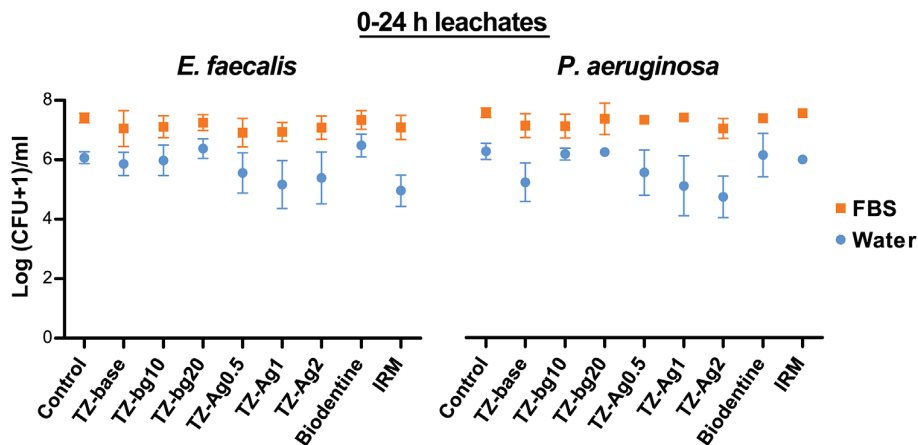


**FIGURE 6** Mean log(CFU+1)/mL and standard deviation of *Enterococcus faecalis* or *Pseudomonas aeruginosa* following exposure to water or fetal bovine serum (FBS) material leachates. Leaching of samples prior to testing was performed immediately after material mixing and placement in cell cultures inserts in the presence of medium for 24 h (0–24 h leachates). Antibacterial activity in leachates of FBS was overall significantly reduced in comparison to those of water. TZ-base, prototype calcium silicate-based cement; TZ-bg10, TZ-base with 10% bioactive glass; TZ-bg20, TZ-base with 20% bioactive glass; TZ-Ag0.5, TZ-base with 0.5 mg/mL silver nanoparticle solution; TZ-Ag1, TZ-base with 1 mg/mL silver nanoparticle solution; TZ-Ag2, TZ-base with 2 mg/mL silver nanoparticle solution; IRM, intermediate restorative material.

**TABLE 6** Multiple linear regression analyses for independent leachate samples for bacterial survival (LogCFU+1/mL) (model 3a) and cell viability (%) (model 4a), with the factor “Bacterium” only applicable to the model for bacterial survival.

Variable	Model 3a: Bacterial survival (LogCFU+1/mL). Independent samples of accumulative leaching (n = 864) Coefficient [95% CI]	Model 4a: Relative MTT activity (%). Independent samples of accumulative leaching (n = 432) Coefficient [95% CI]
Material (Ref. TZ-base)	–	–
TZ-bg10	0.39 [0.08; 0.7]*	0.27 [–2.51; 3.05]
TZ-bg20	1.09 [0.75; 1.43]***	0.97 [–2.80; 4.74]
TZ-Ag0.5	–0.06 [–0.36; 0.24]	–1.11 [–3.89; 1.67]
TZ-Ag1	–0.02 [–0.3; 0.25]	1.3 [–1.48; 4.07]
TZ-Ag2	–0.23 [–0.52; 0.06]	0.41 [–2.3; 3.11]
Biodentine	1.47 [1.11; 1.83]***	23.9 [16.5; 31.29]***
IRM	2.25 [1.91; 2.58]***	5.43 [0.19; 10.67]*
Immersion medium (Ref. Water)	–	–
FBS	3.42 [3.25; 3.58]***	2.95 [0.49; 5.4]*
Aging period (Ref. 1 day)	–	–
7 days	–2.00 [–2.19; –1.81]***	–18.19 [–21.72; –14.66]***
Direct 28 days	–2.40 [–2.60; –2.20]***	–25.81 [–28.98; –22.64]***
Bacterium (Ref: <i>Enterococcus faecalis</i> )	–	Na.
<i>Pseudomonas aeruginosa</i>	–0.94 [–1.10; –0.77]***	Na.

TZ-base, prototype calcium silicate-based cement; TZ-bg10, TZ-base with 10% bioactive glass; TZ-bg20, TZ-base with 20% bioactive glass; TZ-Ag0.5, TZ-base with 0.5 mg/mL silver nanoparticle solution; TZ-Ag1, TZ-base with 1 mg/mL silver nanoparticle solution; TZ-Ag2, TZ-base with 2 mg/mL silver nanoparticle solution; IRM, intermediate restorative material; FBS, fetal bovine serum.

\* $P < 0.05$ .

\*\*\* $P < 0.001$ .

**TABLE 7** Mixed-effects linear regression analyses for nested data for antibacterial activity (LogCFU+1/mL) (model 3b) and cell viability (%) (model 4b), with the predictor variable “Bacterium” applicable only to the model for bacterial survival.

Variable	Model 3b: Bacterial survival (LogCFU+1/mL). Repeated measurements upon weekly medium change (n = 288) Coefficient [95% CI]	Model 4b: Relative MTT activity (%). Repeated measurements upon weekly medium change (n = 144) Coefficient [95% CI]
Material (Ref. TZ-base)	–	–
TZ-bg10	0.16 [–0.21; 0.54]	–0.02 [–1.82; 1.78]
TZ-bg20	0.33 [–0.05; 0.70]	3.27 [–1.35; 7.88]
TZ-Ag0.5	–0.05 [–0.42; 0.33]	–0.28 [–2.07; 1.52]
TZ-Ag1	–0.09 [–0.47; 0.29]	0.47 [–1.74; 2.67]
TZ-Ag2	–0.3 [–0.68; 0.07]	0.54 [–1.82; 2.91]
Biodentine	0.88 [0.5; 1.25]***	5.82 [0.97; 10.67]*
IRM	0.97 [0.59; 1.34]***	11.75 [3.14; 20.36]**
Immersion medium (Ref. Water)	–	–
FBS	2.16 [1.97; 2.35]***	5.28 [2.47; 8.10]***
Aging period (Ref. 7 days)	–	–
28 days	2.77 [2.58; 2.96]***	64.71 [58.86; 70.55]***
Bacterium (Ref: <i>Enterococcus faecalis</i> )	–	Na.
<i>Pseudomonas aeruginosa</i>	–0.79 [–0.97; –0.60]***	Na.

TZ-base, prototype calcium silicate-based cement; TZ-bg10, TZ-base with 10% bioactive glass; TZ-bg20, TZ-base with 20% bioactive glass; TZ-Ag0.5, TZ-base with 0.5 mg/mL silver nanoparticle solution; TZ-Ag1, TZ-base with 1 mg/mL silver nanoparticle solution; TZ-Ag2, TZ-base with 2 mg/mL silver nanoparticle solution; IRM, intermediate restorative material; FBS, fetal bovine serum.

\* $P < 0.05$ .

\*\* $P < 0.01$ .

\*\*\* $P < 0.001$ .

**TABLE 8** Multiple linear regression analyses for leachate measurements for bacterial survival (LogCFU+1/mL) (model 3c) and cell viability (%) (model 4c) at the 0–24 h leaching period, with the factor “Bacterium” only applicable to the model for bacterial survival.

Variable	Model 3c: Bacterial survival (LogCFU+1/mL). 0–24 h leaching period (n = 288) Coefficient [95% CI]	Model 4c: Relative MTT activity (%). 0–24 h leaching period (n = 144) Coefficient [95% CI]
Material (Ref. TZ-base)	–	–
TZ-bg10	0.28 [0.04; 0.51]*	–7.46 [–16.01; 1.1]
TZ-bg20	0.49 [0.26; 0.72]***	–5.3 [–13.86; 3.26]
TZ-Ag0.5	0.03 [–0.23; 0.29]	0.27 [–8.28; 8.83]
TZ-Ag1	–0.17 [–0.46; 0.13]	–3.51 [–12.07; 5.05]
TZ-Ag2	–0.26 [–0.55; 0.04]	–1.76 [–10.32; 6.80]
Biodentine	0.51 [0.26; 0.76]***	16.22 [7.66; 24.78]***
IRM	0.08 [–0.17; 0.34]	45.28 [36.72; 53.83]***
Immersion medium (Ref. Water)	–	–
FBS	1.51 [1.38; 1.64]***	–2 [–6.28; 2.28]
Bacterium (Ref. <i>Enterococcus faecalis</i> )	–	Na.
<i>Pseudomonas aeruginosa</i>	0.05 [–0.08; 0.18]	Na.

TZ-base, prototype calcium silicate-based cement; TZ-bg10, TZ-base with 10% bioactive glass; TZ-bg20, TZ-base with 20% bioactive glass; TZ-Ag0.5, TZ-base with 0.5 mg/mL silver nanoparticle solution; TZ-Ag1, TZ-base with 1 mg/mL silver nanoparticle solution; TZ-Ag2, TZ-base with 2 mg/mL silver nanoparticle solution; IRM, intermediate restorative material; FBS, fetal bovine serum.

\* $P < 0.05$ .

\*\* $P < 0.01$ .

\*\*\* $P < 0.001$ .

**TABLE 9** Subgroup analyses assessing the effect of material and aging period only in water leachates against *Enterococcus faecalis* (LogCFU+1/mL), with multiple linear regression analyses for independent samples of accumulative leaching (model 3d) or for the 0–24 h leaching period (model 3f), and mixed-effects linear regression analysis for nested data (model 3e).

Variable	Model 3d: Bacterial survival (LogCFU+1/mL). Subgroup analyses for water leachates against <i>E. faecalis</i> biofilms—Independent samples of accumulative leaching (n = 216) Coefficient [95% CI]	Model 3e: Bacterial survival (LogCFU+1/mL). Subgroup analyses for water leachates against <i>E. faecalis</i> biofilms—Repeated measurements upon weekly medium change (n = 72) Coefficient [95% CI]	Model 3f: Bacterial survival (LogCFU+1/mL). Subgroup analyses for water leachates against <i>E. faecalis</i> biofilms—0–24 h leaching period (n = 72) Coefficient [95% CI]
Material (Ref. TZ-Ag2)	–	–	–
TZ-base	0.61 [0.1; 1.12]*	1.32 [0.92; 1.71]***	0.47 [–0.16; 1.11]
TZ-bg10	1.06 [0.61; 1.50]***	1.82 [1.42; 2.21]***	0.60 [–0.08; 1.27]
TZ-bg20	1.44 [0.91; 1.97]***	2.09 [1.69; 2.48]***	0.99 [0.37; 1.61]**
TZ-Ag0.5	0.68 [0.25; 1.11]***	1.45 [1.05; 1.85]***	0.17 [–0.56; 0.91]
TZ-Ag1	0.71 [0.27; 1.15]**	1.23 [0.84; 1.63]***	–0.22 [–1.01; 0.56]
Biodentine	2.07 [1.49; 2.64]***	2.59 [2.20; 2.99]***	1.09 [0.46; 1.72]**
IRM	3.20 [2.72; 3.67]***	2.86 [2.46; 3.25]***	–0.44 [–1.1; 0.23]
Aging period	(Ref. 1 day)		Na.
7 days	–1.17 [–1.4; –0.94]***	(Ref. 7 days)	Na.
28 days <sup>#</sup>	–2.79 [–3.16; –2.43]***	2.79 [2.52; 3.06]***	Na.

TZ-base, prototype calcium silicate-based cement; TZ-bg10, TZ-base with 10% bioactive glass; TZ-bg20, TZ-base with 20% bioactive glass; TZ-Ag0.5, TZ-base with 0.5 mg/mL silver nanoparticle solution; TZ-Ag1, TZ-base with 1 mg/mL silver nanoparticle solution; TZ-Ag2, TZ-base with 2 mg/mL silver nanoparticle solution; IRM, intermediate restorative material.

<sup>#</sup>Model 3d: 28 days of accumulative leaching; Model 3e: 28 days upon weekly medium change.

\* $P < 0.05$ .

\*\* $P < 0.01$ .

\*\*\* $P < 0.001$ .

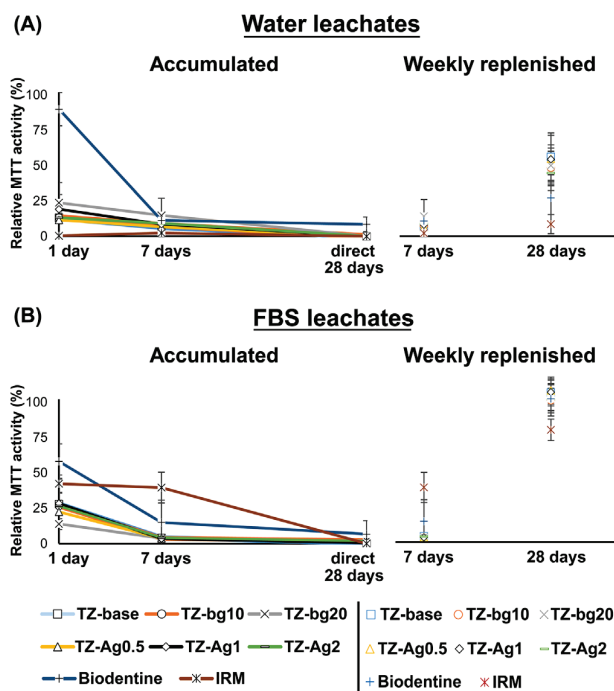


**FIGURE 7** Mean relative 3-(4,5 dimethylthiazolyl-2-yl)32,5-diphenyltetrazolium bromide (MTT) activity with standard deviation of L929 cell cultures following a 24 h exposure period to (A) water and (B) fetal bovine serum (FBS) material leachates from different aging periods. Graphs are separated depending on whether the medium was replenished weekly or not (accumulated). TZ-base, prototype calcium silicate-based cement; TZ-bg10, TZ-base with 10% bioactive glass; TZ-bg20, TZ-base with 20% bioactive glass; TZ-Ag0.5, TZ-base with 0.5 mg/mL silver nanoparticle solution; TZ-Ag1, TZ-base with 1 mg/mL silver nanoparticle solution; TZ-Ag2, TZ-base with 2 mg/mL silver nanoparticle solution; IRM, intermediate restorative material.

of ISO 10993-5:2009 [17]. Biodentine had values indicating absence of cytotoxicity in 1 day water leachates.

## Microscopy

SEM images of prototype cements and Biodentine revealed a hydrated matrix interrupted by particles consisting of calcium, silicon, and oxygen as well as particles rich in zirconium (Figure 9, Figure S3). In the bioactive glass-containing materials, particles rich in silicon, calcium, sodium, phosphate, and oxygen were also observed. Silver was occasionally demonstrated in the EDX scans of silver nanoparticle-containing materials. IRM had a dense matrix interrupted by pores and particles consisting mainly of zinc. In the fetal bovine serum-immersed materials, magnesium, fluorine, and sodium were additionally detected in the EDX scans.

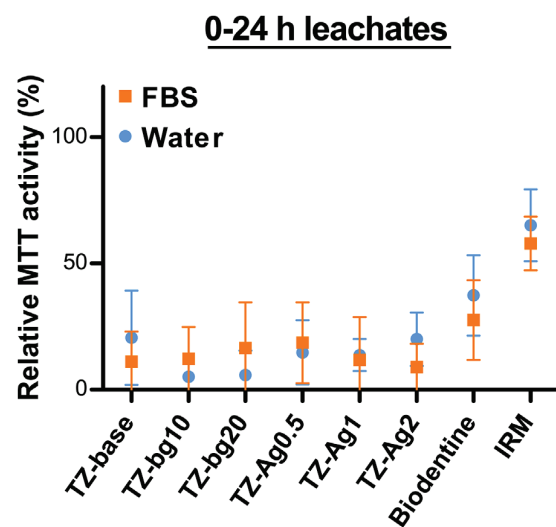


**FIGURE 8** Mean relative 3-(4,5 dimethylthiazolyl-2-yl)32,5-diphenyltetrazolium bromide (MTT) activity and standard deviation of L929 cell cultures after 24 h exposure to water or fetal bovine serum (FBS) leachates. Test leachates derived from a 24 h extract process from materials placed in cell culture inserts and immersed in well-plates containing the respective medium (0–24 h leachates). No significant differences were observed overall in cell viability between water and FBS leachates. TZ-base, prototype calcium silicate-based cement; TZ-bg10, TZ-base with 10% bioactive glass; TZ-bg20, TZ-base with 20% bioactive glass; TZ-Ag0.5, TZ-base with 0.5 mg/mL silver nanoparticle solution; TZ-Ag1, TZ-base with 1 mg/mL silver nanoparticle solution; TZ-Ag2, TZ-base with 2 mg/mL silver nanoparticle solution; IRM, intermediate restorative material.

## DISCUSSION

Hydraulic calcium silicate cements are used for a variety of endodontic procedures, each of which represents different clinical environments [10]. The present study investigated whether exposure conditions as well as material modifications affect selected properties of cements used for surgical endodontic procedures. Our results suggest that fetal bovine serum considerably reduced the antimicrobial potential of the leachable components. The effect of aging depended on the replenishment of the extract medium, having a cumulative effect in leachate reactivity when it was not refreshed or diminishing upon medium change. Biodentine and TZ-bg20 showed attenuated leaching properties compared to TZ-base, which consequently reduced their antibacterial activity and for Biodentine also the cytotoxic potential. The null hypothesis that exposure conditions and material composition do not affect the leaching characteristics of endodontic cements were therefore rejected.

Calcium hydroxide is a by-product of the reaction of tricalcium silicate cement with water; dispersion and consequent release of hydroxyl and calcium ions in the environment may

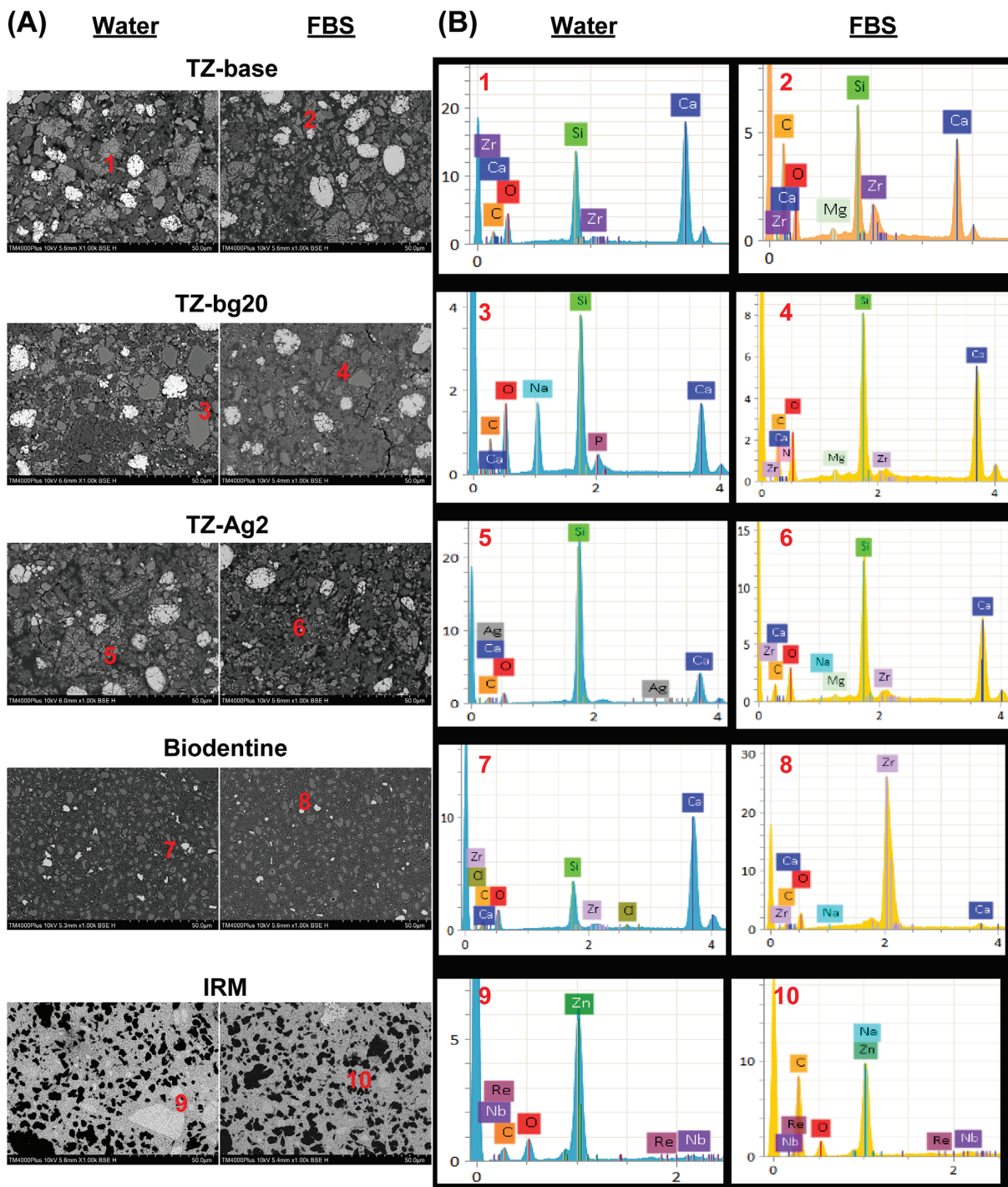


**FIGURE 9** (A) Indicative back-scatter scanning electron micrographs of polished sections of five test materials (1000× magnification) after a 28 day exposure period to water or fetal bovine serum (FBS), with (B) accompanying energy-dispersive X-ray (EDX) scans of areas with Arabic numbers in the micrographs. Unhydrated tricalcium silicate cement particles (1), zirconium oxide particles—depicted white in micrographs, as well as bioactive glass particles for TZ-bg20 (3) are spread in a hydrated matrix in prototype cements. Particles of smaller size are observed in Biodentine. Elemental analysis reveals the presence of sodium and magnesium in the material bulk of cements that were immersed in FBS. A universal color coding for elements in the EDX scans is used: C = orange; Ca = blue; Si = light green; Zr = purple; Na = light blue; O = red; P = plum; Mg = turquoise; Ag = grey; Zn = dark green. TZ-base, prototype calcium silicate-based cement; TZ-bg20, TZ-base with 20% bioactive glass; TZ-Ag2, TZ-base with 2 mg/mL silver nanoparticle solution; IRM, intermediate restorative material.

contribute to tissue healing and bacterial elimination [18, 19]. Indirect assays were therefore selected to evaluate leaching characteristics. Water and fetal bovine serum were used to explore the effect of extract medium in these assessments. Water is commonly employed in investigations of hydraulic calcium silicate cements [20] offering an easily standardized environment. Yet it does not represent the clinical situation as host tissue fluids comprise a complex environment rich in ions and proteins [21]. In that perspective, fetal bovine serum may be more clinically relevant [7].

Different incubation periods enabled monitoring a potential plateau in calcium hydroxide release and its relation to the biological activity of the cements. An additional testing period of leaching during the first hours immediately after placement was assessed in biological assays maintaining the same surface area/medium volume ratio. In clinical conditions, blood circulation and tissue fluid drainage may refresh the leachate micro-environment; thus, investigating cement extracts in a closed environment might provide an over-estimation of their effect due to cumulative leaching throughout time [10]. However, the *in vitro* extract refreshment conditions also fail to resemble the clinical case as constant blood supply [22] creates a continuous renewal of tissue fluid, unlike the periodic one-off medium change *in vitro*. As *in vivo* conditions are more complicated, outcomes from laboratory studies such as the present one on long-term material activity can only be extrapolated in respect to the relevant test conditions applied. This was highlighted by implementing the two different protocols of leaching conditions: weekly replenishment of the extract medium and a closed system, both of which were maintained throughout the 28 day evaluation period.

The study was mainly conducted on prototype hydraulic calcium silicate cements with or without incorporation of silver nanoparticles or bioactive glass. Two commercial materials were included for control purposes. Biodentine is a Type 4 hydraulic calcium silicate cement [23], a conventional tricalcium silicate cement with additives to its cementitious (calcium carbonate) and its liquid phase (calcium chloride) [24]. IRM was also tested as a material with different chemistry but similar clinical application [25].

Calcium leaching of prototype cements and Biodentine was affected differently by fetal bovine serum exposure. Prototype cements leached more  $\text{Ca}^{2+}$  in fetal bovine serum than water in the accumulative leaching model. Increased leaching has been previously reported in contact with blood [26] or in a serum-supplemented physiologic solution [21]. Contrarily, Biodentine released overall less  $\text{Ca}^{2+}$  in fetal bovine serum. A similar effect has been observed for Biodentine leachates in bicarbonate solution [27] but not in a serum-supplemented physiologic solution [21], possibly due to differences in the extract media. Carbon dioxide present in tissues can facilitate the consumption of leached  $\text{Ca}^{2+}$  towards carbonation [28]. Additionally, calcium carbonate precipitates upon the

material surface, blocking the pore channels through which calcium is leached [29, 30]. The latter scenario might be more relevant for describing the overall decreased leaching of Biodentine in fetal bovine serum, as observations from prototype hydraulic calcium silicate cements suggest that there is incomplete consumption of calcium via carbonation. Biodentine's hydration is less affected by environmental conditions [31] due to the presence of additives that accelerate the reaction, resulting in a higher percentage of amorphous phase [32] and thus rendering it more stable. This is evidenced also by the sharp reduction in the amount of  $\text{Ca}^{2+}$  after changing the extract medium.

The decreased leaching of calcium and hydroxyl ions of Biodentine compared to prototype hydraulic calcium silicate cements in fetal bovine serum was also demonstrated by its diminished antibacterial activity. Fetal bovine serum has a buffering capacity, containing proteins that act as weak acids [33]; as leachate alkalinity decreased, so did the bactericidal activity of hydraulic calcium silicate cements. At the same time, serum components may provide better conditions for bacteria to survive. In water, even though hydraulic calcium silicate cements showed relatively high—yet reduced—pH values after 28 days upon changing the medium, the bactericidal potential diminished. It could therefore be postulated that the antibacterial activity is determined by a relatively high alkalization potential. Biodentine showed a lower degree of alkalization particularly after the first day, which was accompanied by reduced bactericidal activity and cytotoxicity. These findings are in accordance with a previous study [19], despite differences with the current investigation in aging media and test methods employed.

The antibacterial effect of hydraulic calcium silicate cements showed a cumulative increase in water leachates when the medium was not refreshed, particularly from 1 to 7 days. In fetal bovine serum, the bactericidal activity peaked at 7 days and did not exhibit further improvement at the 28 day accumulative leaching period. Furthermore, for the bioactive glass-containing materials and Biodentine, the bactericidal activity was even further reduced beyond that time point. The latter findings indicate the dynamics of a constant buffering effect of fetal bovine serum in the antibacterial potential even in static conditions. High concentration of silver nanoparticles (2 mg/mL) induced enhanced antibacterial efficacy in water leachates against *E. faecalis*. *P. aeruginosa* was more susceptible than *E. faecalis* and a potential enhancement of the bactericidal activity from silver nanoparticles after 7 days could therefore not be distinguished. Silver nanoparticles have been previously incorporated in varying concentrations in hydraulic calcium silicate cements [34, 35]. As the reactivity of silver nanoparticles appears to depend on the specific physicochemical characteristics of each formulation [36], different concentrations employed in the literature cannot be directly compared. The silver nanoparticle



concentrations used in the current study were selected with the rationale to enable dispersion of silver nanoparticles to the liquid vehicle of prototype cements [37].

Silver nanoparticles did not increase the antibacterial activity of hydraulic calcium silicate cements in fetal bovine serum leachates. At the same time, the antibacterial effect of IRM was also affected negatively by exposure to fetal bovine serum, despite its different mechanism, namely eugenol released by progressive hydrolysis of the material surface in the presence of aqueous medium [38, 39]. Therefore, it seems that the clinical environment is capable not only of depressing the alkalinity-mediated bactericidal effect of hydraulic calcium silicate cements, but also neutralizing the antibacterial effect of other released constituents.

A recent study showed that the incorporation of 10% or 20% bioactive glass in tricalcium silicate cement does not have a negative impact on bacterial adhesion to the material surface. In fact, TZ-bg20 aged in water enhanced the cement's antibacterial characteristics [5]. Further evaluation of the independent antibacterial leaching of these cements was therefore deemed necessary. Bioactive glass 45S5 has been demonstrated to exhibit more favorable physicochemical characteristics compared to other bioactive glass formulations [40]. It also serves as a filler in a commercial endodontic material [40]. Bioactive glass altered the hydration profile of the tricalcium silicate cement; a more gradual  $\text{Ca}^{2+}$  release was observed that was overall lower than the unmodified cement. Calcium from bioactive glass particles might not be available in the environment and stay deposited in the cement instead [41]. This may explain the impaired antibacterial potential, which is described to mainly be pH-dependent as in tricalcium silicate cement [13]. Measurement of alkalinity might not serve as a sensitive indicator of the chemical reactivity and the calcium hydroxide release, due to possible saturation of the material leachates. However, this could be better reflected in results from calcium release experiments.

Within the limitations of the current study, it can be concluded that exposure conditions (immersion medium and aging period) significantly affected the materials' leaching properties. Aging of hydraulic calcium silicate cements in a more complex medium than water had a negative effect on their antibacterial properties. Laboratory studies should therefore incorporate such experimental parameters in order to better represent the clinical situation. Modifications in hydraulic calcium silicate cement composition altered the chemical properties of the cements. Biodentine showed reduced antibacterial capacity and cytotoxicity than TZ-base, as a consequence of its modifications from the standard cement/radio-opacifier composition. Addition of 2 mg/mL silver nanoparticles to hydraulic calcium silicate cement improved the bactericidal effect in water leachates, but not in a serum-containing environment.

## AUTHOR CONTRIBUTIONS

**Conceptualization:** Andreas Koutroulis, Håkon Valen, Josette Camilleri, Pia Titterud Sunde; **Methodology:** Andreas Koutroulis, Håkon Valen, Vasileios Kapralos, Josette Camilleri, Pia Titterud Sunde; **Validation:** Andreas Koutroulis, Håkon Valen, Dag Ørstavik, Josette Camilleri, Pia Titterud Sunde; **Formal analysis:** Andreas Koutroulis; **Investigation:** Andreas Koutroulis; **Writing – original draft preparation:** Andreas Koutroulis; **Writing – review and editing:** Håkon Valen, Dag Ørstavik, Vasileios Kapralos, Josette Camilleri, Pia Titterud Sunde; **Supervision:** Håkon Valen, Dag Ørstavik, Josette Camilleri, Pia Titterud Sunde; **Project administration:** Andreas Koutroulis, Håkon Valen, Josette Camilleri, Pia Titterud Sunde; **Funding acquisition:** Andreas Koutroulis, Håkon Valen, Pia Titterud Sunde.

## ACKNOWLEDGEMENTS

Else Morisbak and Dr. Ida Stenhagen for their technical assistance on the cytotoxicity assays and calcium release experiments, respectively. Naomi Azulay and Lambrini Veneti for their help with the statistical analysis. This work was supported by the University of Oslo, Nordic Institute of Dental Materials (NIOM) and Foundation for Dental Research UNIFOR (Stiftelsen til tannlegevitenskapens fremme, Oslo, Norway) Grant/Award Number: 975 503 178/266.

## CONFLICT OF INTEREST STATEMENT

The authors declare no potential conflicts of interest related to this study.

## DATA AVAILABILITY STATEMENT

The data that support the findings of this study are available from the corresponding author upon reasonable request.

## ORCID


Andreas Koutroulis  <https://orcid.org/0000-0002-7427-9978>

Håkon Valen  <https://orcid.org/0000-0002-9038-4153>

Dag Ørstavik  <https://orcid.org/0000-0003-0161-7857>

Vasileios Kapralos  <https://orcid.org/0000-0003-2234-7817>

Josette Camilleri  <https://orcid.org/0000-0003-3556-6365>

Pia Titterud Sunde  <https://orcid.org/0000-0002-6012-297X>

## REFERENCES

- Ørstavik D. Endodontic treatment of apical periodontitis. In: Ørstavik D, editor. *Essential endodontology: prevention and treatment of apical periodontitis*, 3rd ed. Hoboken: Wiley-Blackwell; 2020. 313-44.
- Darvell BW, Smith AJ. Inert to bioactive – a multidimensional spectrum. *Dent Mater*. 2022;38:2-6
- Moynadeh AT, Aznar Portoles C, Schembri Wismayer P, Camilleri J. Bioactivity potential of EndoSequence BC RRM putty. *J Endod*. 2016;42:615-21.

4. Farrugia C, Baca P, Camilleri J, Arias Moliz MT. Antimicrobial activity of ProRoot MTA in contact with blood. *Sci Rep.* 2017;7:41359. <https://doi.org/10.1038/srep41359>
5. Koutroulis A, Valen H, Ørstavik D, Kapralos V, Camilleri J, Sunde PT. Surface characteristics and bacterial adhesion of endodontic cements. *Clin Oral Investig.* 2022;26:6995-7009
6. Nekoofar MH, Oloomi K, Sheykhrezae MS, Tabor R, Stone DF, Dummer PM. An evaluation of the effect of blood and human serum on the surface microhardness and surface microstructure of mineral trioxide aggregate. *Int Endod J.* 2010;43:849-58.
7. Tingey MC, Bush P, Levine MS. Analysis of mineral trioxide aggregate surface when set in the presence of fetal bovine serum. *J Endod.* 2008;34:45-9.
8. Torabinejad M, Hong CU, McDonald F, Pitt Ford TR. Physical and chemical properties of a new root-end filling material. *J Endod.* 1995;21:349-53.
9. Camilleri J, Arias Moliz T, Bettencourt A, Costa J, Martins F, Rabadjeva D, et al. Standardization of antimicrobial testing of dental devices. *Dent Mater.* 2020;36:e59-73.
10. Camilleri J, Atmeh A, Li X, Meschi N. Present status and future directions – hydraulic materials for endodontic use. *Int Endod J.* 2022;55(Suppl 3):710-77.
11. Ji M, Chi Y, Wang Y, Xiong K, Chen X, Zou L. An in vitro evaluation of antimicrobial activity of a fast-setting endodontic material. *Sci Rep.* 2022;12:16021. <https://doi.org/10.1038/s41598-022-20454-7>
12. Kishen A. Advanced therapeutic options for endodontic biofilms. *Endod Top.* 2010;22:99-123.
13. Shrestha A, Kishen A. Antibacterial nanoparticles in endodontics: a review. *J Endod.* 2016;42:1417-26.
14. Hoikkala NPJ, Wang X, Hupa L, Smått JH, Peltonen J, Vallittu PK. Dissolution and mineralization characterization of bioactive glass ceramic containing endodontic sealer Guttaflow Bioseal. *Dent Mater J.* 2018;37:988-94.
15. Simila HO, Karpukhina N, Hill RG. Bioactivity and fluoride release of strontium and fluoride modified Biodentine. *Dent Mater.* 2018;34:e1-7.
16. Kapralos V, Rukke HV, Ørstavik D, Koutroulis A, Camilleri J, Sunde PT. Antimicrobial and physicochemical characterization of endodontic sealers after exposure to chlorhexidine digluconate. *Dent Mater.* 2021;37:249-63.
17. International Organization for Standardization. Biological evaluation of medical devices – part 5: tests for in vitro cytotoxicity. ISO 10993–5 2009. Accessed December 13 2022. <https://www.iso.org/standard/36406.html>
18. Atmeh AR, Watson TF. Biodentine™ physico-chemical properties: from interactions with dental tissues to ageing. In: I About, editor. *Biodentine™: properties and clinical applications.* New York: Springer; 2022. 11-30.
19. Koutroulis A, Kuehne SA, Cooper PR, Camilleri J. The role of calcium ion release on biocompatibility and antimicrobial properties of hydraulic cements. *Sci Rep.* 2019;9:19019. <https://doi.org/10.1038/s41598-019-55288-3>
20. Parirokh M, Torabinejad M. Mineral trioxide aggregate: a comprehensive literature review–Part I: chemical, physical, and antibacterial properties. *J Endod.* 2010;36:16-27.
21. Camilleri J, Wang C, Kandhari S, Heran J, Shelton RM. Methods for testing solubility of hydraulic calcium silicate cements for root-end filling. *Sci Rep.* 2022;12:7100. <https://doi.org/10.1038/s41598-022-11031-z>
22. Lakha T, Kheur M, Mühlemann S, Kheur S, Le B. Ultrasound and CBCT analysis of blood flow and dimensions of the lingual vascular canal: a case control study. *J Oral Biol Craniofac Res.* 2021;11:40-6.
23. Camilleri J. Classification of hydraulic cements used in dentistry. *Front Dent Med.* 2020;1:9. <https://doi.org/10.3389/fdmed.2020.00009>
24. Camilleri J. Biodentine™ microstructure and composition. In: I About, editor. *Biodentine™: properties and clinical applications.* New York: Springer; 2022. 1-10.
25. Tawil PZ, Trope M, Curran AE, Caplan DJ, Kirakozova A, Duggan DJ, et al. Periapical microsurgery: an in vivo evaluation of endodontic root-end filling materials. *J Endod.* 2009;35:357-62.
26. Schembri Wismayer P, Lung CY, Rappa F, Cappello F, Camilleri J. Assessment of the interaction of Portland cement-based materials with blood and tissue fluids using an animal model. *Sci Rep.* 2016;6:34547. <https://doi.org/10.1038/srep34547>
27. Atmeh AR. Investigating the effect of bicarbonate ion on the structure and strength of calcium silicate-based dental restorative material-Biodentine. *Clin Oral Investig.* 2020;24:4597-606.
28. Morandea A, Thiéry M, Dangla P. Investigation of the carbonation mechanism of CH and C-S-H in terms of kinetics, microstructure changes and moisture properties. *Cem Concr Res.* 2014;56:153-70.
29. Gervais C, Garrabrants AC, Sanchez F, Barna R, Moszkowicz P, Kosson DS. The effects of carbonation and drying during intermittent leaching on the release of inorganic constituents from a cement-based matrix. *Cem Concr Res.* 2004;34:119-31.
30. Gandolfi MG, Iacono F, Agee K, Siboni F, Tay F, Pashley DH, et al. Setting time and expansion in different soaking media of experimental accelerated calcium-silicate cements and Pro-Root MTA. *Oral Surg Oral Med Oral Pathol Oral Radiol Endod.* 2009;108:e39-45.
31. Ashofteh Yazdi K, Ghabraei S, Bolhari B, Kafili M, Meraji N, Nekoofar MH, et al. Microstructure and chemical analysis of four calcium silicate-based cements in different environmental conditions. *Clin Oral Investig.* 2019;23:43-52.
32. Grazziotin-Soares R, Nekoofar MH, Davies T, Hübler R, Meraji N, Dummer PMH. Crystalline phases involved in the hydration of calcium silicate-based cements: Semi-quantitative Rietveld X-ray diffraction analysis. *Aust Endod J.* 2019;45:26-32.
33. Figge J, Rossing TH, Fencel V. The role of serum proteins in acid-base equilibria. *J Lab Clin Med.* 1991;117:453-67.
34. Bahador A, Pourakbari B, Bolhari B, Hashemi FB. In vitro evaluation of the antimicrobial activity of nanosilver-mineral trioxide aggregate against frequent anaerobic oral pathogens by a membrane-enclosed immersion test. *Biomed J.* 2015;38:77-83.
35. Vazquez-Garcia F, Tanomaru-Filho M, Chávez-Andrade GM, Bosso-Martelo R, Basso-Bernardi MI, Guerreiro-Tanomaru JM. Effect of silver nanoparticles on physicochemical and antibacterial properties of calcium silicate cements. *Braz Dent J.* 2016;27:508-14.
36. Flores CY, Miñán AG, Grillo CA, Salvarezza RC, Vericat C, Schilardi PL. Citrate-capped silver nanoparticles showing good

- bactericidal effect against both planktonic and sessile bacteria and a low cytotoxicity to osteoblastic cells. *ACS Appl Mater Interfaces*. 2013;5:3149-59.
37. Jensen KA, Thieret N. The NANOGENOTOX dispersion protocol for NANoREG. National Research Centre for the Working Environment. 2014. Accessed 11 December 2022. <http://safenano.re.kr/download.do?SEQ=175>
38. Hume WR. In vitro studies on the local pharmacodynamics, pharmacology and toxicology of eugenol and zinc oxide-eugenol. *Int Endod J*. 1988;21:130-4.
39. Markowitz K, Moynihan M, Liu M, Kim S. Biologic properties of eugenol and zinc oxide-eugenol. A clinically oriented review. *Oral Surg Oral Med Oral Pathol Oral Radiol Endod*. 1992;73:729-37.
40. Hoikkala NPJ, Siekkinen M, Hupa L, Vallittu PK. Behaviour of different bioactive glasses incorporated in polydimethylsiloxane endodontic sealer. *Dent Mater*. 2021;37:321-7.
41. Jung MK, Park SC, Kim YJ, Park JT, Knowles JC, Park JH, et al. Premixed calcium silicate-based root canal sealer rein-

forced with bioactive glass nanoparticles to improve biological properties. *Pharmaceutics*. 2022;14:1903. <https://doi.org/10.3390/pharmaceutics14091903>

## SUPPORTING INFORMATION

Additional supporting information can be found online in the Supporting Information section at the end of this article.

**How to cite this article:** Koutroulis A, Valen H, Ørstavik D, Kapralos V, Camilleri J, Sunde PT. Effect of exposure conditions on chemical properties of materials for surgical endodontic procedures. *Eur J Oral Sci*. 2023;e12943. <https://doi.org/10.1111/eos.12943>

## SUPPORTING INFORMATION

### **Effect of exposure conditions on chemical properties of materials for surgical endodontic procedures**

**KOUTROULIS A, VALENH, ØRSTAVIK D, KAPRALOS V, CAMILLERI J, SUNDE PT.**

Faculty of Dentistry, University of Oslo, Oslo, Norway

Nordic Institute of Dental Materials (NIOM), Oslo, Norway

College of Medical and Dental Sciences, University of Birmingham, Birmingham, United Kingdom

**FIGURE S1** Mean and standard deviation of relative MTT activity of L929 cell cultures following a 24-h exposure period to water neat material leachates or three two-fold serial dilutions of them. Each graph presents results for material leachates aged under the exact same conditions prior to testing. Different letters upon bars indicate a significant difference between groups ( $P < 0.05$ ). Statistical analysis has been performed only for neat (1:1) leachate groups. BD: Biodentine.

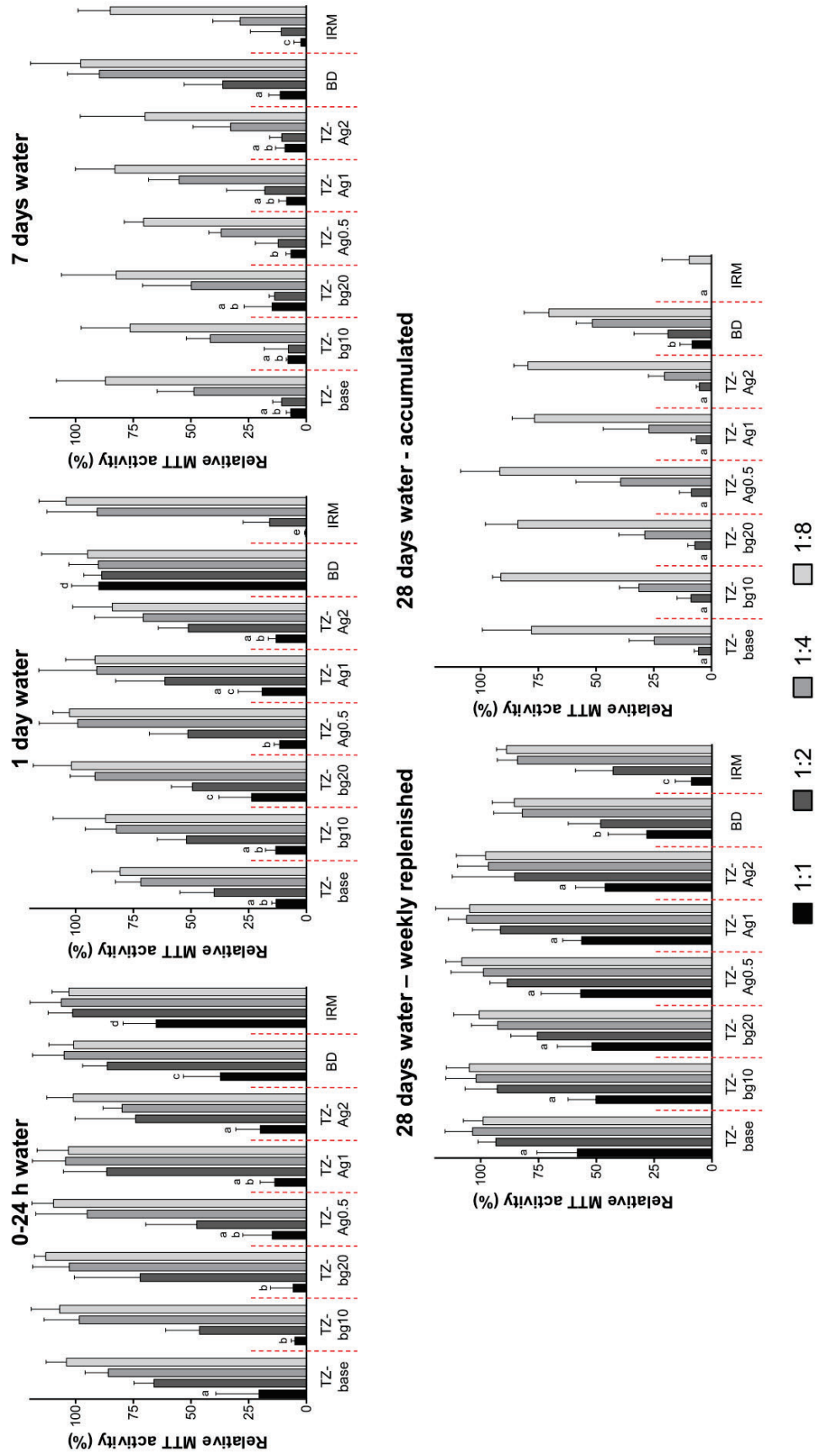


**FIGURE S2** Mean and standard deviation of relative MTT activity of L929 cell cultures following a 24-h exposure period to FBS neat material leachates or three two-fold serial dilutions of them. Each graph presents results for material leachates aged under the exact same conditions prior to testing. Different letters upon bars indicate a significant difference between groups ( $P < 0.05$ ). Statistical analysis has been performed only for neat (1:1) leachate groups. BD: Biodentine.

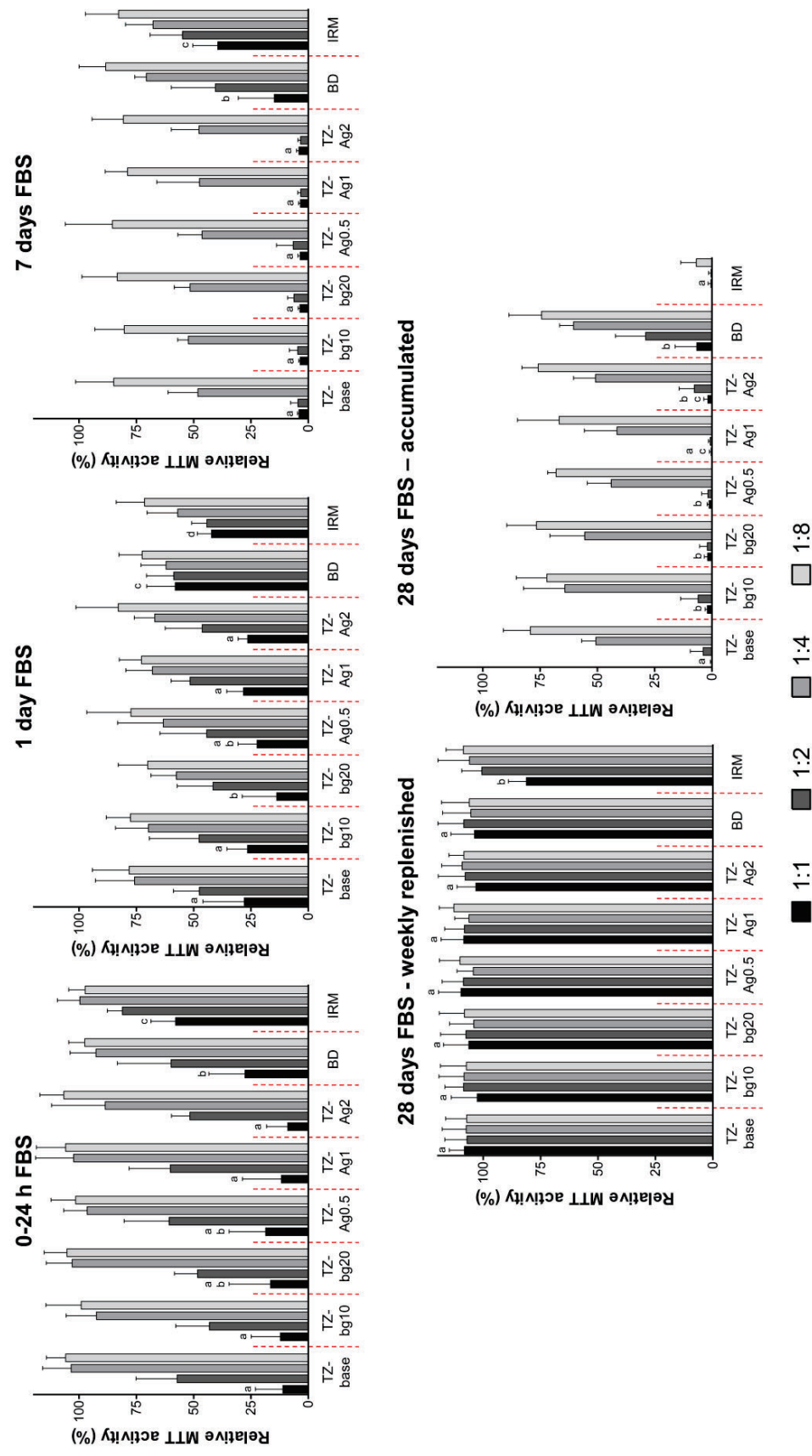
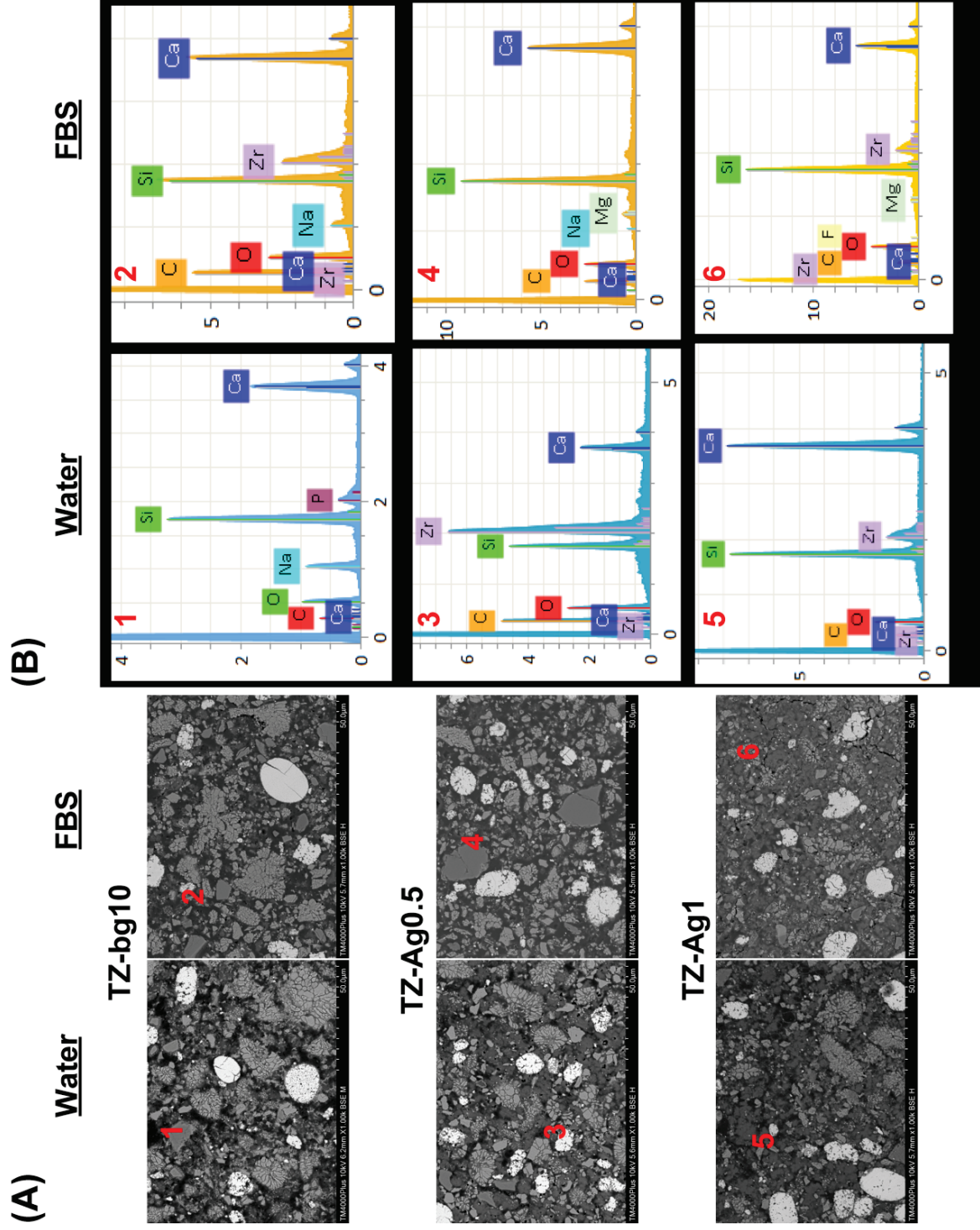


**FIGURE S3** (A) Back-scatter scanning electron micrographs of polished sections of TZ-bg10, TZ-Ag0.5 and TZ-Ag1 (1000 × magnification) after a 28-day immersion period in water or FBS. (B) Indicative energy-dispersive spectroscopic scans of areas with arabic numbers in the micrographs from (A). A universal color coding for elements in the EDX scans is used: C = orange; Ca = blue; O = red; Si = light green; Zr = purple; Na = light blue; P = plum; Mg = turquoise; Ag = grey; Zn = dark green.







III



## Article

# Antibacterial Activity of Root Repair Cements in Contact with Dentin—An Ex Vivo Study

Andreas Koutroulis <sup>1,\*</sup> , Håkon Valen <sup>2</sup>, Dag Ørstavik <sup>1</sup>, Vasileios Kapralos <sup>1</sup>, Josette Camilleri <sup>3</sup>   
and Pia Titterud Sunde <sup>1,\*</sup>

<sup>1</sup> Section of Endodontics, Institute of Clinical Dentistry, Faculty of Dentistry, University of Oslo, 0317 Oslo, Norway; d.s.orstavik@odont.uio.no (D.Ø.); vasileios.kapralos@odont.uio.no (V.K.)

<sup>2</sup> Nordic Institute of Dental Materials (NIOM), 0855 Oslo, Norway; hakon.valen@niom.no

<sup>3</sup> School of Dentistry, Institute of Clinical Sciences, College of Medical and Dental Sciences, University of Birmingham, Birmingham B15 2TT, UK; j.camilleri@bham.ac.uk

\* Correspondence: andreas.koutroulis@odont.uio.no (A.K.); p.t.sunde@odont.uio.no (P.T.S.)

**Abstract:** This study assessed the antibacterial characteristics of the dentin/material interface and dentin surfaces exposed to experimental hydraulic calcium silicate cement (HCSC) with or without bioactive glass (BG) replacement (20% or 40%) or mixed with a silver nanoparticle (SNP) solution (1 or 2 mg/mL), and Biodentine, TotalFill BC RRM putty and Intermediate Restorative Material (IRM). Human root dentin segments with test materials were assessed at 1 or 28 days. In one series, the specimens were split to expose the dentin and material surfaces. A 24 h direct contact test was conducted against three-day established *Enterococcus faecalis* and *Pseudomonas aeruginosa* monospecies biofilms. In another series, the dentin/material interface of intact specimens was exposed to biofilm membranes for 3 days and the antibacterial activity was assessed via confocal microscopy. The interface was additionally characterised. All one-day material and dentin surfaces were antibacterial. Dentin surfaces exposed to HCSC with 40% BG-replacement, Biodentine and IRM had decreased antibacterial properties compared to those of the other cements. The HCSC mixed with a 2 mg/mL SNP solution had the highest antimicrobial effect in the confocal assay. The interfacial characteristics of HCSCs were similar. The test materials conferred antibacterial activity onto the adjacent dentin. The BG reduced the antibacterial effect of dentin exposed to HCSC; a 2 mg/mL SNP solution increased the antibacterial potential for longer interaction periods (three-day exposure).

**Keywords:** bacterial viability; characterisation; endodontic cement; perforation repair; root-end filling material; tricalcium silicate



**Citation:** Koutroulis, A.; Valen, H.; Ørstavik, D.; Kapralos, V.; Camilleri, J.; Sunde, P.T. Antibacterial Activity of Root Repair Cements in Contact with Dentin—An Ex Vivo Study. *J. Funct. Biomater.* **2023**, *14*, 511. <https://doi.org/10.3390/jfb14100511>

Academic Editor: Huiliang Cao

Received: 28 August 2023

Revised: 18 September 2023

Accepted: 8 October 2023

Published: 11 October 2023



**Copyright:** © 2023 by the authors. Licensee MDPI, Basel, Switzerland. This article is an open access article distributed under the terms and conditions of the Creative Commons Attribution (CC BY) license (<https://creativecommons.org/licenses/by/4.0/>).

## 1. Introduction

Hydraulic calcium silicate-based cements (HCSCs) are a material category with applications in many clinical endodontic procedures [1–3]. The hydration reaction of calcium silicate, forming calcium silicate hydrate gel and calcium hydroxide, is the principal chemical reaction in these materials [4]. Their main beneficial properties are the hydraulic nature and the release of calcium hydroxide; the former may enable them to withstand exposure to the wet clinical environment, while the latter's potential role in providing an alkaline-mediated antimicrobial effect has been described [5]. Ionic leaching has also been linked to the materials' osteogenic potential in contact with bone tissue [6].

Several formulations have been launched since the introduction of the first commercialised HCSC in the 1990s, Mineral Trioxide Aggregate (MTA) [7]. Biodentine (Septodont, Saint Maur-des-Fosses, France) and TotalFill formulations (FKG Dentaire Sar, La Chaux-de-Fonds, Switzerland) are representative materials of the newer generations of HCSCs. These materials consist mainly of pure calcium silicates, inert fillers as radio-opacifiers, and other additives. Biodentine contains a plasticiser for the improvement of the handling properties, and calcium chloride and calcium carbonate to accelerate the setting time and control

the hydration reaction, respectively [8]. TotalFill products are applied without previous mixing with a liquid component, needing the moisture available in the application field for hydration instead. They also contain calcium sulphate as a moderator of the hydration reaction, as well as calcium phosphate cement [9].

The interactions of HCSCs with the clinical environment vary depending on the specific procedure for which the materials are applied [4]. When used for retrograde filling or perforation repair, the materials should establish a barrier between the periradicular tissues and the root canal system to prevent infections [10]. Bacteria that have survived insufficient root canal disinfection procedures may create pathways towards the extraradicular area [11]. The role of dentin in this process is also important since bacteria can colonise dentinal tubules [12], especially when a root resection is performed and the tubules are exposed to the periradicular area [1]. The interactions between the material and dentin at the interfacial area are therefore crucial for the establishment of a physically adequate seal, and the release of antibacterial constituents that may aid in reducing the risk of reinfection.

The incorporation of compounds that could enhance the adaptation of HCSC to dentin would be beneficial in securing a physical barrier. Bioactive glass (BG) formulations are calcium sodium phosphosilicates with a re-mineralisation capacity; in contact with the phosphate-containing host tissue, the BG reacts by releasing calcium and sodium ions, with the subsequent formation of a silica-rich layer, which serves as a substrate for hydroxyapatite formation [13]. Their apatite-forming ability has been exploited upon incorporation into resin composites [14], endodontic sealers [15], HCSCs, and, particularly, Biodentine [16,17]. At the same time, modifications towards the enhancement of target cement properties may negatively affect other basic material characteristics [18].

From a different angle, enhancing the bactericidal potential of HCSCs through the addition of antibacterial constituents could be beneficial given that reports on their current efficacy seem somewhat inconclusive [4]. Candidates for such additions include silver nanoparticles (SNPs), which can impair the bacterial cell membrane, disrupt protein synthesis, inhibit DNA replication and eventually cause cell death [19,20]. In fact, their use has been explored in several aspects of root canal disinfection as irrigation solutions, medicaments, and for incorporation in endodontic cements [21].

The aim of the current study was to assess the antibacterial characteristics of the dentin/material interface of prototype HCSCs with or without addition of silver nanoparticles or bioactive glass in comparison with the commercial materials Biodentine, TotalFill BC RRM Putty and Intermediate Restorative Material. The null hypotheses tested were that the antibacterial properties of cements upon the dentin/material interface will not differ for modified HCSCs and that contact with cements will not contribute to any dentin antibacterial effect.

## 2. Materials and Methods

### 2.1. Test Materials

The following chemicals were used to make up the prototype cements: tricalcium silicate cement (TCS; American Elements, Los Angeles, CA, USA); zirconium oxide (ZO; Koch-Light Laboratories, Colnbrook, Bucks, UK); ultrapure water (water; Elix Essential 5 UV Water Purification System, Merck KGaA, Darmstadt, Germany); bioactive glass 45S5 (BG; Cas No: 65997-17-3, 10 µm particle size, Mo-Sci Corporation, Rolla, MO, USA); and silver nanopowder (100 nm particle size, Sigma-Aldrich, Gillingham, UK) dispersed in water at a concentration of 1 mg/mL or 2 mg/mL SNP-concentration [22].

The tested materials were as follows:

- TZ-base: 80% *w/w* TCS and 20% *w/w* ZO mixed with water;
- TZ-bg20: TZ-base with 20% *w/w* BG replacement of TCS mixed with water;
- TZ-Bg40: TZ-base with 40% *w/w* BG replacement of TCS mixed with water;
- TZ-Ag1: TZ-base mixed with 1 mg/mL SNP solution (0.35 mg SNP addition per 1 g of TZ-base powder);

- TZ-Ag2: TZ-base mixed with 2 mg/mL SNP solution (0.7 mg SNP addition per 1 g of TZ-base powder);
- Biodentine (Septodont, Saint Maur-des-Fosses, France);
- TotalFill Root Repair Material—BC RRM Putty (TotalFill; FKG Dentaire, La Chaux-de-Fonds, Switzerland);
- Intermediate Restorative Material (IRM; Dentsply Sirona, Charlotte, NC, USA).

Before placement, the prototype materials were hand-spatulated at a 0.35 liquid/powder ratio and the commercial materials were handled according to the manufacturers' instructions.

## 2.2. Preparation of Root Segments

The Regional Committee for Medical and Health Research Ethics evaluated the project and deemed that no approval was required to conduct the study (REC Ref. 283811). Extracted human teeth were collected from a tooth biobank (REC Ref. 2013/413). The teeth's coronal parts and apical 2 mm were sectioned with a precision cutting machine (IsoMet Low Speed; Buehler, Lake Bluff, IL, USA). Two forms of root segments preparations were acquired:

1. 3 mm length (Figure 1a);
2. 1.5 mm thickness (Figure 2a).

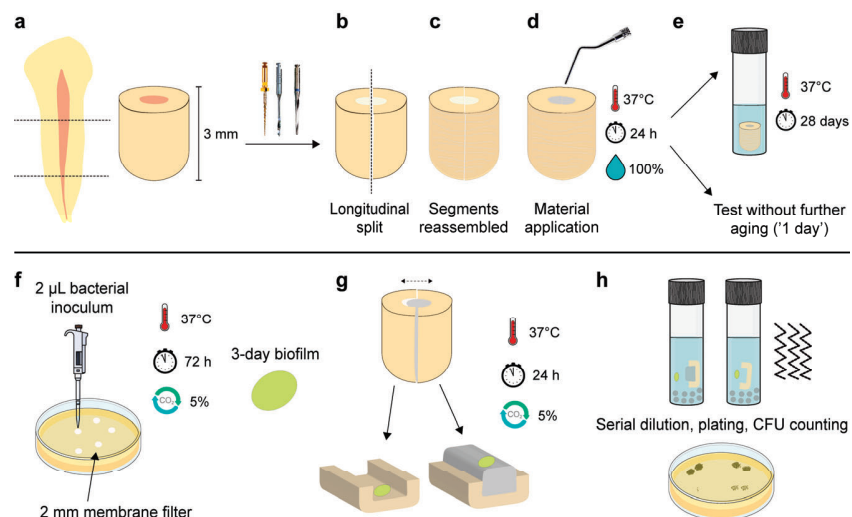


**Figure 1.** Schematic representation of the antibacterial assay described by Kapralos et al. [23]. (a) Root segments (3 mm length) were obtained and the canal spaces were enlarged with a series of rotary instruments and post drills. Subsequently, (b) the root segments were longitudinally split with a cut-off instrument and (c) were reassembled and held tightly with plastic membrane. (d) The materials were applied inside the clamped segments and were allowed to set for 24 h. (e) They were then either used directly for antibacterial testing or immersed in Hank's balanced salt solution for 28 days prior to testing. (f) For antibacterial testing, three-day monospecies biofilms of *Enterococcus faecalis* and *Pseudomonas aeruginosa* were formed upon membrane filters. (g) The two parts of the root segments were carefully separated and the biofilm membranes were placed in direct contact with the material surface and the dentin surface. (h) Following a 24 h contact period, each part of the segment with the respective biofilm membrane was immersed in tubes containing phosphate-buffered saline and glass beads, vigorously vortexed and plated after serial dilutions. Colony-forming units (CFUs) were counted the next day. Figure 1e,f,h was partly generated using Servier Medical Art (Servier, Suresnes, France), licensed under a Creative Commons Attribution 3.0 unported license.

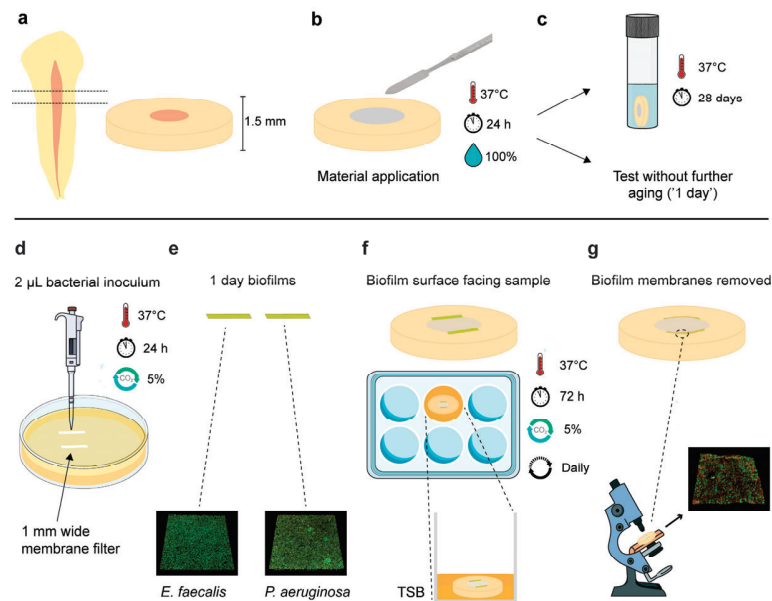


**Figure 2.** Schematic representation of the 3-day biofilm assay upon the dentin/material interface. (a) Root segments (1.5 mm thick) were acquired. (b) Upon preparation of the root segments, the materials were compacted in the root canal space. (c) The specimens were allowed to set for 24 h, and, consequently, they were either immediately tested (1 day), or immersed in Hank's balanced salt solution for a total period of 28 days prior to testing. (d) Membrane filters positioned upon agar plates were inoculated with *Enterococcus faecalis* or *Pseudomonas aeruginosa*. (e) One-day monospecies biofilms were obtained. (f) Biofilm membranes were positioned along the dentin/material interface, with the biofilm surface in direct contact with the sample. The samples were incubated with tryptic soya broth (TSB) for 3 days and transferred to new wells with a fresh medium daily. (g) The biofilm membranes were removed and the dentin/material interface area below was stained with a bacterial viability kit and imaged with confocal laser scanning microscopy. Figure 2c,d,f,g was partly generated using Servier Medical Art (Servier, Suresnes, France), licensed under a Creative Commons Attribution 3.0 unported license.

The 3 mm long root segments were instrumented with ProTaper rotary files (Dentsply Maillefer, Tulsa, OK, USA) and fibre post drills (3M, St. Paul, MN, USA) up to size 5. A saline solution was used for irrigation. Subsequently, they were carefully longitudinally split using the cutting machine (Figure 1b).

The 1.5 mm thick root segments were carefully enlarged with the fibre post drills to ensure that the samples had similar internal diameters in the root canal area.

The internal surfaces of all root segments were treated with 17% ethylenediaminetetraacetic acid (Pulpdent, Watertown, MA, USA) for 5 min and subsequently with saline solution. The specimens that were used for antibacterial assays were autoclaved in vials with water at 121 °C for 21 min. Finally, the split root segments were reassembled and clamped with Parafilm M (Bemis; Thermo Fisher Scientific, Waltham, MA, USA) wrapped around them (Figure 1c).

### 2.3. Assessment of Antibacterial Effect

Sterile equipment was used for all the procedures.

#### 2.3.1. Material Application and Testing Periods

The materials were compacted in root segments (Figures 1d and 2b) and were allowed to set for 24 h at 37 °C, wrapped with a wet gauze. The next day, they were either tested ('1-day samples') or immersed in 1 mL of Hank's balanced salt solution (HBSS; H6648,

Sigma-Aldrich, Gillingham, UK) and stored for a total of 28 days at 37 °C before they were retrieved and tested ('28-day samples') (Figures 1e and 2c). Twelve specimens per subgroup (n = 12) were used in each experiment (f = 0.25;  $\alpha$  = 0.05; power = 95%), as indicated by an a priori power analysis estimation using G\*power 3.1.9.2 (Heinrich Heine University, Düsseldorf, Germany).

### 2.3.2. Test Bacteria

*Enterococcus faecalis* OG1RF American Type Cell Culture Collection (ATCC; Manassas, VA, US) 47077 and *Pseudomonas aeruginosa* ATCC 9027 were grown overnight in tryptic soya broth (TSB; Sigma-Aldrich, Gillingham, UK) at 37 °C in a 5% CO<sub>2</sub>-supplemented atmosphere. A bacterial inoculum ( $\approx 10^8$  colony forming units (CFUs)/mL) for each species was prepared the next day following centrifugation of the overnight culture and resuspension in TSB.

### 2.3.3. Antibacterial Effect against Three-Day Established Biofilms

A previously described protocol was employed to investigate the direct antimicrobial efficacy of materials after contact with dentin and any potential residual antibacterial activity in the dentin surfaces [23]. Three-day monospecies *E. faecalis* and *P. aeruginosa* biofilms were cultured on circular membrane filters cut to a 2 mm diameter (MF-Millipore; 0.45  $\mu$ m pore size, Merck KGaA, Darmstadt, Germany). The membranes were positioned upon TSB agar plates and received a 2  $\mu$ L bacterial inoculum. After 72 h of incubation at 37 °C and in a 5% CO<sub>2</sub>-supplemented atmosphere, the membranes were retrieved (Figure 1f).

The root segments were unwrapped from the parafilm and carefully separated, resulting in a dentin/material segment, referred to as 'material surface', and a material-free dentin segment, referred to as 'dentin surface'. Scanning electron microscopy (TM4000Plus II, Hitachi, Tokyo, Japan) with accompanying energy dispersive X-ray analysis was performed at this point in two additional root segments from each material to confirm that the dentin surfaces were not covered with material remnants (Figure S1).

The biofilm membranes were carefully positioned in direct contact with the material and dentin surfaces (Figure 1g). They were additionally positioned upon dentin surfaces that had not come into contact with any material, serving as negative control (n = 12/bacterium). The samples were incubated for 24 h at 37 °C in a 5% CO<sub>2</sub>-supplemented atmosphere. Subsequently, they were transferred to tubes containing glass beads and 2 mL of phosphate-buffered saline and vortexed. After 10-fold serial dilutions, the samples from the liquid were plated on TSB agar plates, and the bacterial counts were assessed the following day (Figure 1h).

### 2.3.4. Biofilm Assay at the Dentin/Material Interface

Following the specified ageing periods of 1 or 28 days, the intact root segments (1.5 mm thick) were carefully ground with silicon carbide paper discs (Grit 500; Struers, Rotherham, UK) to ensure a flat surface, and subsequently rinsed with sterile water. They were then dried with filter paper and sterilised for 20 min on each side under UV light.

One-day monospecies *E. faecalis* and *P. aeruginosa* biofilms were cultured on rectangular membrane filters (1 mm wide) with the same method described for the three-day circular biofilm membranes above (Figure 2d,e). Consequently, the rectangular biofilm membranes were carefully positioned along the length of the dentin/material interface of each sample (two membranes per root disc), with the biofilm surface facing towards the sample. The specimens were transferred into 24-well plates and inoculated with 800  $\mu$ L TSB (Figure 2f). They were incubated at 37 °C in a 5% CO<sub>2</sub>-supplemented atmosphere for 72 h. Every 24 h, the samples were transferred into a new well with fresh TSB.

After this period, the samples were retrieved and gently immersed in sterile pure water. The biofilm membranes were carefully removed, and the samples were then stained with a 50  $\mu$ L dye solution of LIVE/DEAD BacLight Bacterial Viability Kit (Invitrogen,

Eugene, OR, USA) for 20 min in a dark room. Subsequently, they were immersed in water to remove the excess of stain and imaged using a confocal laser scanning microscope (CLSM; Olympus FluoView FV1200, Olympus, Tokyo, Japan). Three microscopic confocal volumes from random areas upon the dentin/material interface where the biofilm membranes were previously positioned were acquired from each sample using a 60× water immersion lens, 1 μm step-size and a format of 480 × 480 pixels (Figure 2g). For a better orientation in the area of interest and threshold application in the CLSM, samples that were not subjected to a biofilm challenge were additionally imaged (Figure S2). Polyester coverslip discs (13 mm, Thermanox Coverslips, Thermo Fisher Scientific, Waltham, MA, USA) were used as additional negative control substrates to confirm biofilm formation upon the areas where the rectangular biofilm membranes were applied. The percentage of injured/dead cells and the total biofilm volume (μm<sup>3</sup>) were assessed with Bioimage\_L software (v.3.0, Department of Oral Biology, Malmo University, Sweden) [24].

#### 2.4. Microstructural and Chemical Analysis of the Interface

The materials (n = 3/group) were compacted in the root segments (1.5 mm thick) as specified in the section above (Figure 2b) and were stored in HBSS at 37 °C for 28 days (Figure 2c). Subsequently, the samples were retrieved, dried in filter paper, vacuum-desiccated and embedded in auto-polymerising epoxy resin (Epoxyfix; Struers, Rotherham, UK). They were then ground in water and polished with a series of silicon carbide papers and a polishing cloth (Struers, Rotherham, UK). A diamond suspension (DP-1 μm; Struers, Rotherham, UK) was used for the polishing procedure. The material to dentin interface was imaged with a scanning electron microscope (SEM; TM4000Plus II, Hitachi, Tokyo, Japan) under backscatter mode following the sputter-coating of specimens with gold (Agar Scientific, Essex, UK). Energy dispersive X-ray (EDX) analysis was performed and elemental maps across the interfaces were created.

#### 2.5. Data Analysis

The data were assessed for normality with the Shapiro–Wilk test as well as histogram and q-q plot evaluation. Due to the absence of normal distribution, the data from confocal microscopy were subjected to square root transformation, while the data from the CFU-based direct contact experiments were log-transformed and expressed as log(CFU + 1)/mL.

For data from the CFU-based experiment of dentin surfaces and those from confocal microscopy, univariate general linear models were fitted for the following factors: ‘Materials’, ‘Ageing period’, and ‘Bacterium’. The normality of residuals following each analysis was assessed with q-q plots. Pairwise comparisons were conducted with the Bonferroni correction. Additionally, a Student’s t-test was conducted for the comparison of dentin surfaces with the negative control.

For data from the CFU-based experiment of material surfaces, an analysis was conducted with non-parametric tests as, despite the log-transformation of the data and due to the presence of many zero values within groups, none of the applied generalised linear models could provide an adequate fit. We therefore decided to perform analyses for materials within the same ageing period and for the same test bacterium with the Kruskal–Wallis test and post hoc methods adjusted using the Bonferroni correction. Mann–Whitney U tests were used in the case of comparing the effect of the ageing period within the same material and test bacterium, as well as for comparisons with the negative control.

All analyses were conducted with SPSS software 29.0 (IBM, Armonk, NY, USA). The significance level was set as  $\alpha = 0.05$ .

### 3. Results

#### 3.1. Antibacterial Investigation

##### 3.1.1. Independent Assessment of Material and Dentin Surfaces

Figure 3 presents the results from the antibacterial testing of dentin and material surfaces.



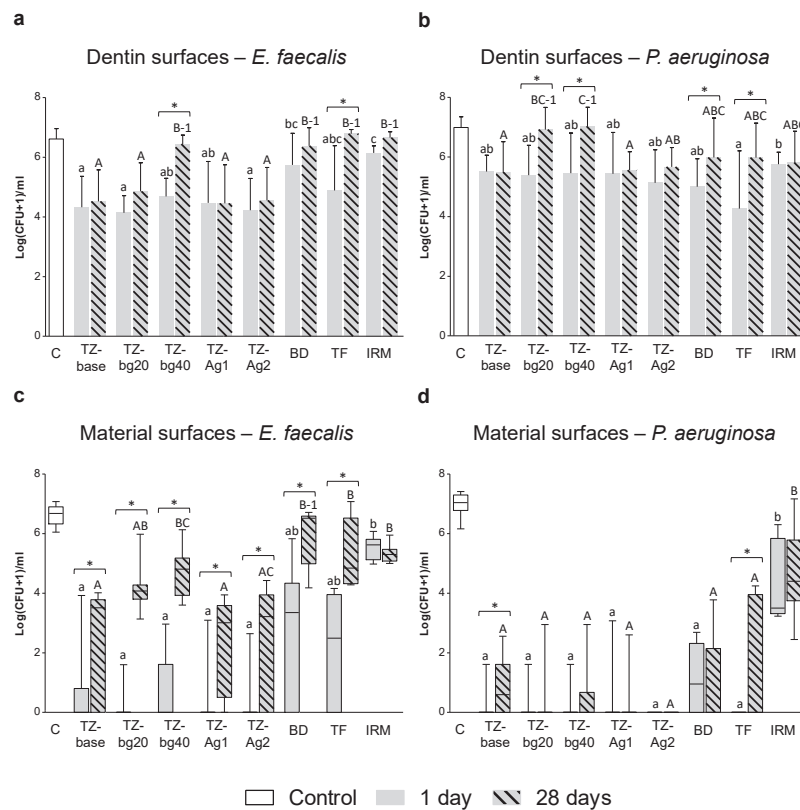


**Figure 3.** Antibacterial activity of dentin and material surfaces from split root segments. (a,b) Mean log(CFU + 1)/mL and standard deviation of *Enterococcus faecalis* or *Pseudomonas aeruginosa*, respectively, following direct exposure of 3-day monospecies biofilms with dentin surfaces. (c,d) Box and whiskers plots (minimum value, lower quartile, median value, upper quartile and maximum value) for bacterial survival following exposure to material surfaces from the root segments. Different lowercase letters per graph indicate statistically significant differences among the 1-day samples. Different capital letters indicate statistically significant differences among the 28-day samples. Brackets with asterisks above bars or boxes indicate a significant difference between 1- and 28-day samples within the same material. Groups with the number ‘1’ did not show any statistical reduction in bacterial counts compared to the control ( $p < 0.05$ ). Abbreviations: C, negative control; BD, Biodentine; TF, TotalFill.

### Dentin Surfaces

Upon accounting for the effect of the ‘Ageing period’ and ‘Bacterium’, the overall antibacterial activity of the dentin surfaces following contact with TZ-bg40, Biodentine and IRM was significantly lower than that of the respective specimens from TZ-base, TZ-Ag1 and TZ-Ag2 ( $p < 0.001$  for comparisons with TZ-bg40 and IRM;  $p < 0.05$  for comparisons with Biodentine).

More specifically, the dentin surfaces that had been in contact with the prototype HCSC for 1 or 28 days presented significantly reduced *E. faecalis* colonies compared to the control ( $p < 0.05$ ), except for those in contact with TZ-bg40 for 28 days. The dentin surfaces exposed to Biodentine, TotalFill and IRM presented reduced *E. faecalis* colonies only after 1 day of application ( $p < 0.05$ ) (Figure 3a).

All samples caused a reduction in bacterial counts against *P. aeruginosa* compared to the control ( $p < 0.05$ ), except for those in 28-day contact with TZ-bg20 or TZ-bg40 (Figure 3b).

Material Surfaces

All prototype HCSCs significantly reduced the colonies of both bacterial species after 1 and 28 days of material ageing ( $p < 0.05$ ). TZ-base, TZ-Ag1 and TZ-Ag2 caused a higher logCFU-reduction in *E. faecalis* biofilms than that of the commercial cements in the 28-day test period ( $p < 0.01$ ). The bactericidal effect of both the prototype and the commercial HCSCs against *E. faecalis* was reduced between the 1 and 28 days samples ( $p < 0.05$ ). A decline in antibacterial effectiveness against *P. aeruginosa* over time was observed for TZ-base and TotalFill (Figure 3c,d).

3.1.2. Biofilm Assay upon the Dentin/Material Interface

Figure 4 shows the results of the percentage of dead/injured bacteria, and Table 1 presents the total biofilm volume for *E. faecalis* and *P. aeruginosa*. Figure 5 shows representative confocal laser scanning microscope images from the test samples.

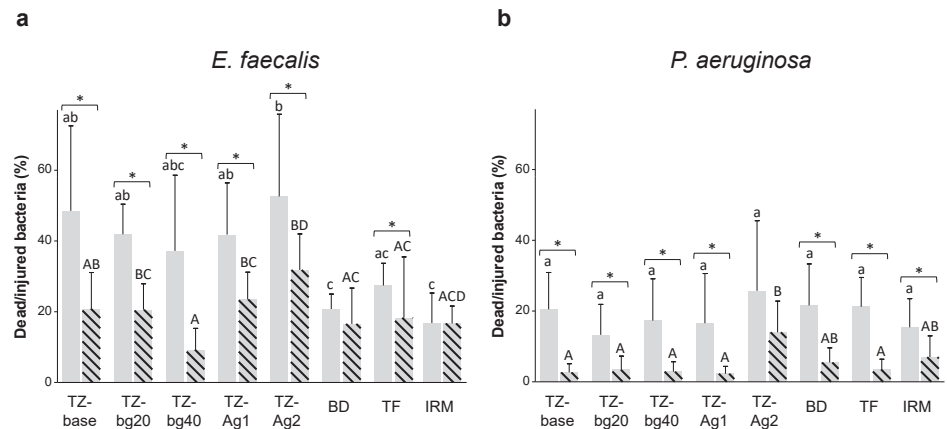


**Figure 4.** Mean and standard deviation of dead/injured (a) *Enterococcus faecalis* or (b) *Pseudomonas aeruginosa* cells (%) prior to root square transformation of the data. Different lowercase letters indicate statistically significant differences among the 1-day samples. Different capital letters indicate statistically significant differences among the 28-day samples. Brackets with asterisks above bars in the graphs indicate a significant difference between the 1- and 28-day samples within the same material ( $p < 0.05$ ).

**Table 1.** Mean and standard deviation of *Enterococcus faecalis* or *Pseudomonas aeruginosa* biofilm volume ( $\mu\text{m}^3$ ) (%) prior root square transformation of the data. Different lowercase letters indicate statistically significant differences among the 1-day samples. Different capital letters indicate statistically significant differences among the 28-day samples. Different numbers indicate a statistically significant difference within the same material and test bacterium between the two ageing periods ( $p < 0.05$ ). Abbreviations: BD, Biodentine; TF, TotalFill.

		Total Biofilm Volume ( $\mu\text{m}^3$ )							
		TZ-Base	TZ-bg20	TZ-bg40	TZ-Ag1	TZ-Ag2	BD	TF	IRM
<i>E. faec.</i>	1 day	59,931 (42,448) a-1	35,408 (16,886) a-1	51,258 (46,555) a-1	43,023 (25,834) a-1	45,676 (47,451) a-1	38,514 (33,513) a-1	71,417 (32,892) a-1	59,927 (65,753) a-1
	28 days	78,597 (38,789) A,B-1	64,425 (35,105) A,B-1	125,866 (13,320) B-2	66,004 (45,395) A,B-1	55,959 (42,533) A,B-1	30,916 (9190) A-1	94,330 (67,094) B-1	58,524 (45,241) A-1

Table 1. Cont.

		Total Biofilm Volume ( $\mu\text{m}^3$ )							
		TZ-Base	TZ-bg20	TZ-bg40	TZ-Ag1	TZ-Ag2	BD	TF	IRM
<i>P. aerug.</i>	1 day	21,419 (18,042) a-1	31,569 (21,395) a-1	36,863 (29,436) a-1	44,020 (40,201) a-1	37,925 (40,419) a-1	41,428 (22,880) a-1	47,609 (26,390) a-1	41,750 (30,932) a-1
	28 days	52,284 (29,498) A-2	37,383 (41,044) A-1	30,143 (23,320) A-1	40,528 (24,824) A-1	53,708 (22,489) A-1	44,770 (23,916) A-1	44,612 (28,209) A-1	31,252 (15,382) A-1

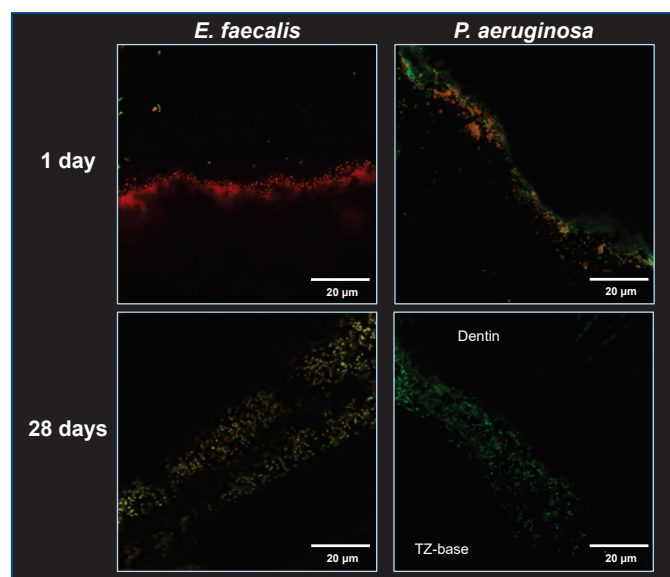


Figure 5. Representative confocal laser scanning microscope images from z stack series of biofilms upon the dentin/material interface for TZ-base following staining with bacterial viability kit. Dead-injured bacteria were stained red, and live ones appear as green. All images had the same magnification (60 $\times$ ) and pixel format (512  $\times$  512) and each image represents an area of 88  $\times$  88  $\mu\text{m}$ .

A significantly lower proportion of dead/injured bacteria was overall observed in the 28-day samples compared to the 1-day specimens ( $p < 0.001$ ). TZ-Ag2 had an overall significantly higher antibacterial effect than the other tested materials ( $p < 0.05$ ; Figure 4). The *P. aeruginosa* specimens were less susceptible to the antibacterial effect of materials than *E. faecalis* ( $p < 0.001$ ).

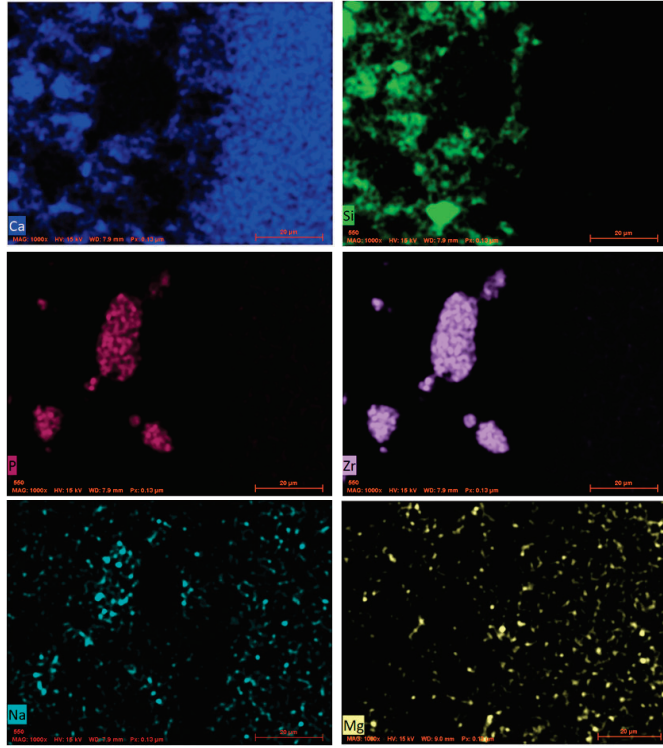
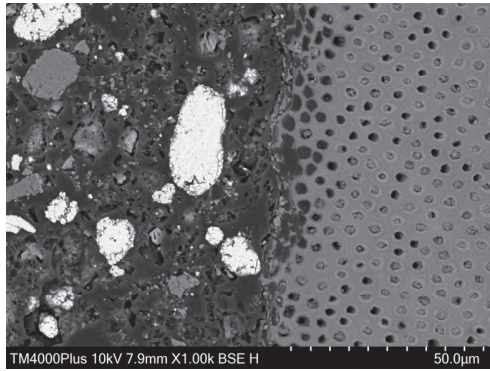
The *E. faecalis* biofilms upon the dentin/material interface were significantly thicker compared to *P. aeruginosa* ( $p < 0.001$ ). Taking into account the factors ‘Ageing period’ and ‘Bacterium’, the biofilm volume was not affected by the material type ( $p > 0.05$ ). It was, nevertheless, overall larger in the 28-day test root segments than in the 1-day ones ( $p < 0.001$ ).

### 3.2. Characterisation of the Dentin/Material Interface

Indicative microscopic images with accompanying elemental maps of the dentin/material interfacial zones are presented in Figure 6. Silicon was the most prevalent element in the interface of calcium silicate cements, especially for TZ-bg40, followed by Biodentine and TotalFill. Calcium was also evident in all HCSCs. The migration of silver into dentin was evident in the SNP-containing cements, especially in TZ-Ag2. Gaps of varying width between the material and dentin surface occurred in all samples.

**a**

**TZ-base**



**TZ-bg20**

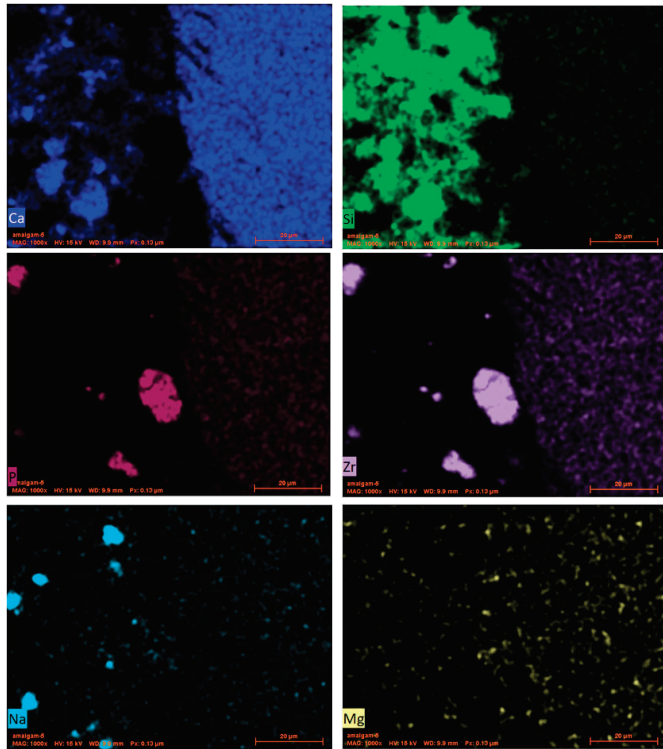
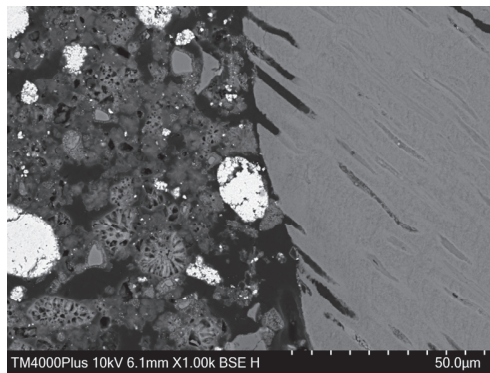


Figure 6. Cont.

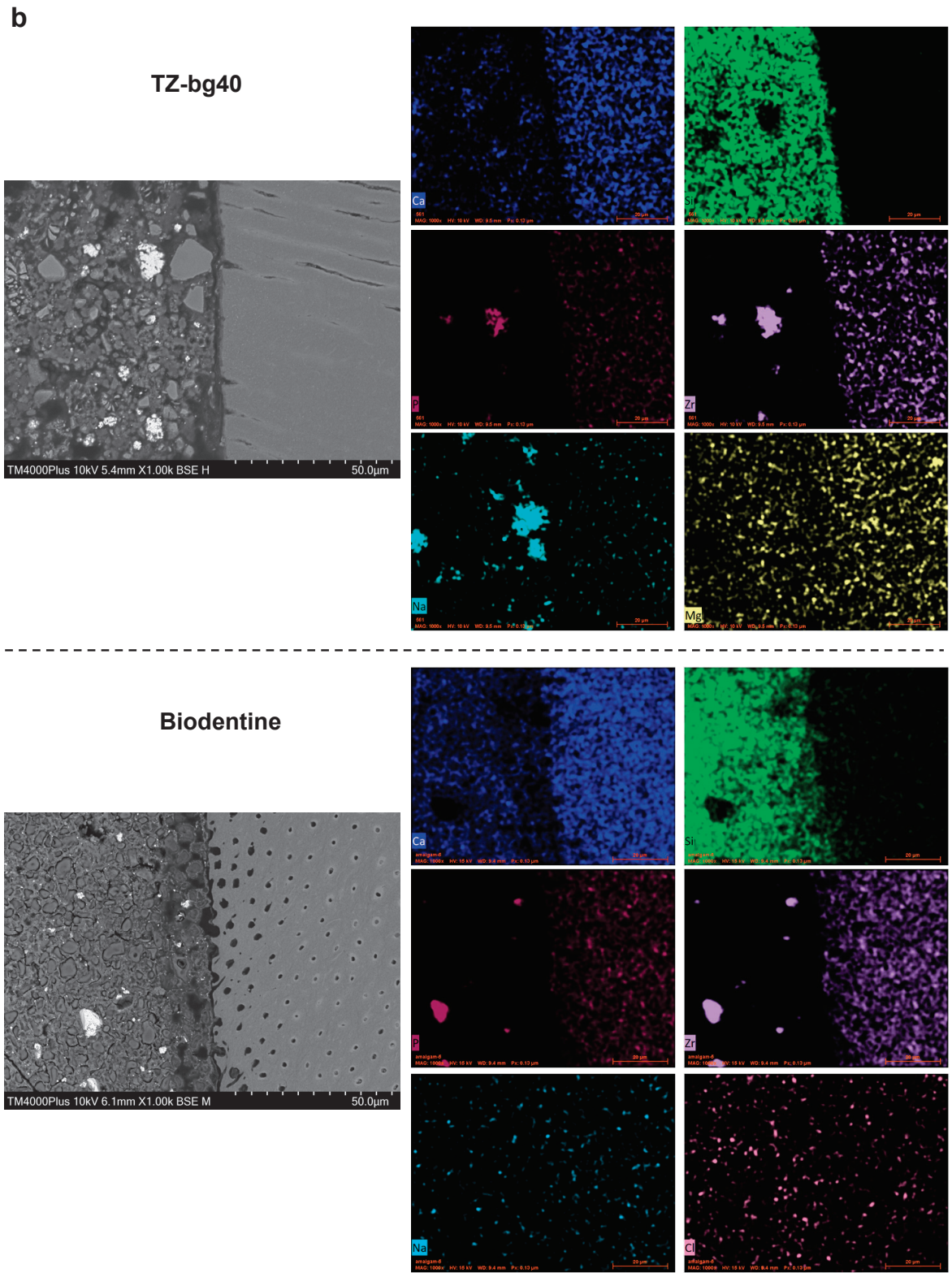
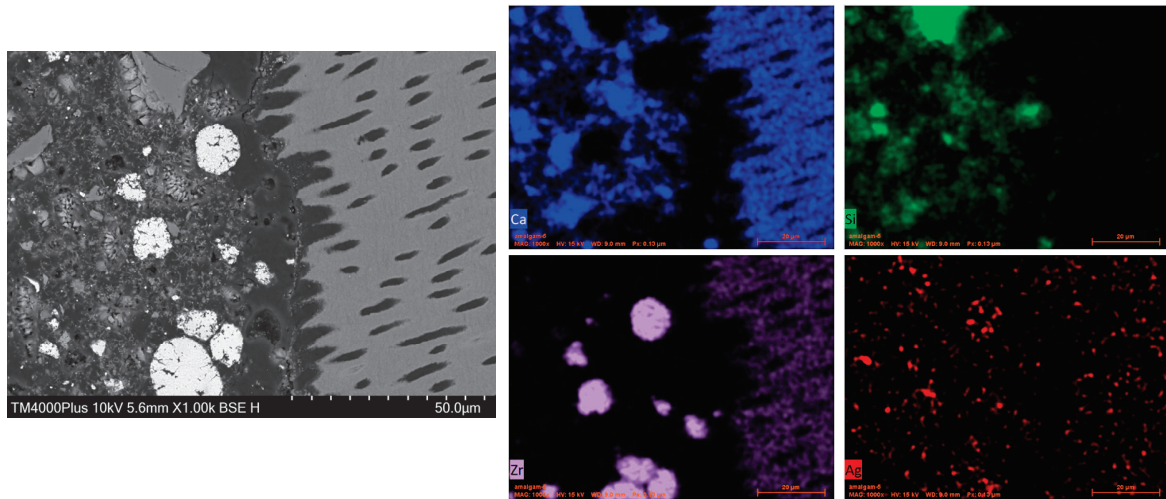


Figure 6. Cont.

C

TZ-Ag1



TZ-Ag2

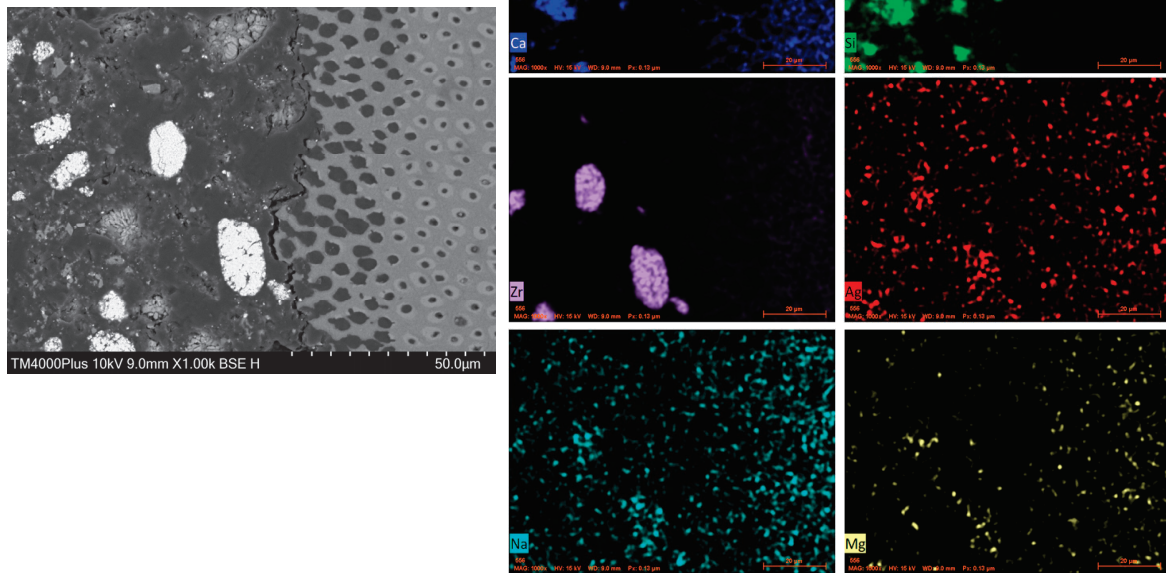
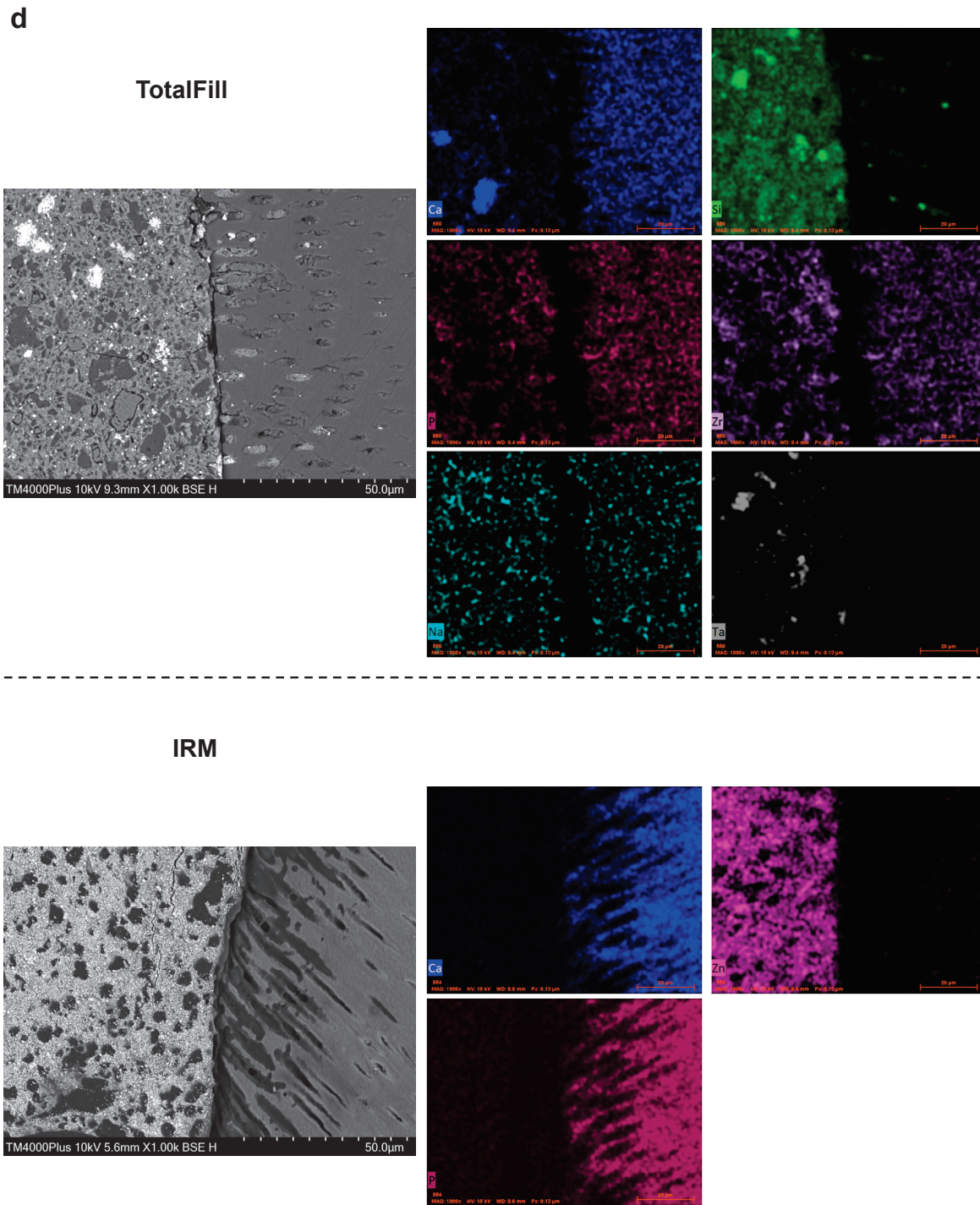


Figure 6. Cont.



**Figure 6.** Backscatter scanning electron micrographs of the dentin/material interface (1000×) accompanied by elemental maps mainly of calcium (blue), silicon (green), and zirconium (purple), as well as sodium (light blue), phosphate (plum), magnesium (yellow), chlorine (lilla), silver (red), tantalum (grey) or zinc (Tyrian purple) for (a) TZ-base and TZ-bg20, (b) TZ-bg40 and Biodentine, (c) TZ-Ag1 and TZ-Ag2, (d) TotalFill and IRM. An overlap in the peaks of phosphate and zirconium exists.

#### 4. Discussion

The current study assessed the antibacterial properties of prototype and commercial HCSCs at the dentin/material interface. All tested cements conferred an antibacterial activity to the adjacent dentin tested 1 day following material application. Changes in the antibacterial efficiency were observed with material modifications across the different assays such as a reduction upon replacement of TCS with 40% BG, or enhancement after the incorporation of 2 mg/mL SNP into the liquid component. The null hypotheses that the antibacterial characteristics of cements would be similar and that dentin exposed to materials would not present any antibacterial potential were therefore rejected.

Reinfection by persisting or newly established microorganisms in the root canal system may occur following retrograde treatment or perforation repair [11]. This makes the antibacterial properties of root repair materials worth investigating [25]. Common commercial HCSCs exhibit varying antibacterial efficacy [4], which is mainly ascribed to the creation of an alkaline microenvironment. Yet, alkalinity may be buffered by tissue fluids, particularly in an acidic inflamed environment [26]. Furthermore, the role of dentin appears to be intricate. From one perspective, dentin also has a buffering capacity [26,27], which can be detrimental to the antibacterial effect [28]. At the same time, due to its complex anatomy, it can act as a reservoir of the ions released by the adjacent cements and mediate an antibacterial effect to the microenvironment through this ionic flow [29].

Considering these aspects, we used SNPs because they may diffuse into dentinal tubules and be subsequently released to enhance the antibacterial activity [30]. Bioactive glass was employed to assess whether it could alter the antibacterial characteristics of HCSC at the interface. The original BG formulation—BG 45S5—was used in the current study [13].

By evaluating the properties of commercial and prototype HCSCs in the same study, a more comprehensive understanding of the effects of incorporating chemical compounds into them can be achieved. HCSCs were assessed in the context of their use for root-end filling and perforation repair procedures, where the materials should provide an adequate seal between the root canal system and the periradicular area [10]. Biodentine and TotalFill are indicated for such applications [31,32]. Finally, the properties of the zinc oxide eugenol-based IRM were also examined as a comparative reference. IRM is an extensively studied cement that is widely employed in retrograde procedures, presenting a success rate similar to that of MTA [33,34].

Two studies have previously used a dentin substrate to evaluate the antibacterial properties of Biodentine [35,36], while, to the best of our knowledge, the antibacterial properties of the putty version of TotalFill have not been tested on a dentin model before. The lack of standardised test protocols for antibacterial testing [37] and limited data from *ex vivo* models for root repair materials [4] suggest a knowledge gap regarding the essential properties of the most widely used HCSCs. Two distinct dentin models were therefore utilised here to investigate the antibacterial properties at the dentin/material interface.

The materials were tested either 1 or 28 days after placement. It is anticipated that the elution of antimicrobial compounds by HCSCs, specifically hydroxyl ions, would decrease in the long term [38].

The split tooth model, originally designed to assess the residual antimicrobial effect of irrigation solutions and sealers [23], was used here to independently evaluate the antibacterial potential of both the material and the dentin surface at the interface following the designated application periods. Even though dentin does not serve as a substrate for biofilm cultivation in the model, it enables the investigation of the indirect antibacterial potential from the test materials. Our results did in fact demonstrate the transfer of an antimicrobial effect to dentin. However, replacing BG in HCSC resulted in a reduction in this effect after 28 days, especially upon 40% replacement of TCS. Prior studies have demonstrated that the antibacterial properties of a different form of BG were enhanced upon contact with powdered dentin or bone; mineralised tissues appear to facilitate the dissolution of BG, resulting in an increased release of silica and elevated pH levels [39–41].



Even though the bactericidal potential of BG is mainly alkaline-related, the current study showed that its effect appeared to be insufficient to compensate for the antibacterial activity lost due to the replacement of tricalcium silicate. This inferior antibacterial potential is also evident in studies where BG undergoes ageing under physiological conditions, as the buffering capacity of the host's fluids can moderate the alkalisation effect [42,43]. Thus, the beneficial characteristics of BG could be further explored as additions in the cementitious phase of HCSC instead of replacing a portion of the TCS. The potential of BG to enhance the remineralisation process on dentin [44] could be further explored in conjunction with its antibacterial characteristics. Even though the evaluation of the former was not in the scope of the current study, no consistent pattern of coverage of dentinal tubules was observed as being carried out by the BG-containing HCSCs compared to the unmodified cement. Upon assessing model reproducibility, the SEM/EDX observations of the split segments showed the occasional presence of cement particles on the dentin surface, with some of them also penetrating inside the dentinal tubules. The materials affected the elemental composition of dentin segments as evidenced by the spectroscopical scans, yet these findings were not exclusive to the BG-containing cements.

In order to further assess the antibacterial effect of this area under different conditions, an assay of biofilm growth upon the intact dentin/material interface was conducted. The colonisation of this area could lead to reinfection following treatment [45]. Previous studies have investigated this aspect for endodontic sealers [46,47] but it has not been explored for root repair cements. In the current model, biofilms were initially cultured for one day on membrane filters before being exposed to samples. This approach aided in better localising the specific area of interest. The results showed that the addition of 2 mg/mL SNP to prototype HCSC enhanced its antibacterial performance. The release of SNPs in the neighbouring dentin was confirmed with elemental mapping. However, no enhancement of the antibacterial properties was evident in the split tooth model. The combination of the findings from the two ex vivo models in this study suggests that more extended interaction periods might be required for SNPs to fully exert their antibacterial potential, as has been previously indicated [48]. At the same time, the current results complement the previous research on early bacterial adhesion upon the TZ-Ag2 surface, where no significant changes were observed after 1 h of exposure to an *E. faecalis* inoculum [38]. From another perspective, SNP concentrations higher than the ones used in the current study could be explored in order to achieve potentially more efficient bacterial killing. Here, we selected the 2 mg/mL SNP-concentration based on a protocol for sufficient particle dispersion [22]. Attaining an optimal concentration towards the potential clinical usage of SNPs should also be determined through a combined evaluation of their effect on host tissue cells. The discolouration potential is also a concern [21], particularly given the intended release of SNPs into the subsequent tissues, especially dentin.

The improved antibacterial performance of TZ-Ag2 was mainly evident against *P. aeruginosa*. Gram-negative bacteria are reportedly more susceptible to SNPs due to the thinner layer of peptidoglycan in their cell wall [49]. The Gram-positive *E. faecalis* that was tested here is the most frequently studied bacterium in endodontic literature [50]. Even though its direct causal relationship with post-treatment apical periodontitis has been questioned, it is indeed a commonly isolated bacterium from failed endodontic cases [51–53]. The Gram-negative *P. aeruginosa* has also been recovered from persistent endodontic infections [53]. Interestingly, the susceptibility of the two bacterial species differed in the experimental assays, indicating the importance of including variations in the methodological models and the test parameters. The cultivation of monospecies biofilms for antibacterial testing is, however, an undisputed limitation in the current study, as it does not replicate the complexity and resistance of multispecies biofilms that are apparent in clinical practice. On the other hand, the utilisation of simplified biofilm models could ensure better reproducibility in the initial assessment of antibacterial properties [50] and provide insights for subsequent testing.

Overall, in both dentin models studied, no significant differences in the antibacterial potential of the two commercial HCSCs, Biodentine and TotalFill, were observed. However, the indirect antibacterial effect of Biodentine on dentin surfaces appeared smaller than that on the unmodified prototype cement. In fact, the antimicrobial activity of dentin surfaces in contact with either TotalFill or Biodentine was reduced from 1 to 28 days. This observation can be attributed to a faster hydration reaction for both commercial HCSCs compared to the experimental formula (TZ-base), even though the reaction of TotalFill is dependent on the moisture available in the environment [9], which could slow down the process. The putty version, however, is reported to react faster than the paste form [9], possibly due to a difference in the particle size [54]. The faster hydration reaction of Biodentine compared to the radiopacified tricalcium silicate cement is mainly ascribed to the addition of calcium carbonate to the former and has been previously documented [8,55]. Once the most significant part of hydration has taken place, less calcium hydroxide is released. Therefore, the buffering capacity of dentin had a greater impact on the commercial materials, probably due to the earlier completion of diffusion of the hydroxyl ions. The antibacterial characteristics of Biodentine and TotalFill formulations have been found to be similar when tested against cariogenic bacteria with the rationale to use these as pulp capping agents [55,56]. The zinc oxide eugenol-based IRM showed an overall steadier yet inferior antibacterial potential in our experiments. Our findings are in accordance with those of Dragland et al. [57], who reported a stable and modest antibacterial behaviour of IRM over time against *E. faecalis*, as well as a gradual release of eugenol in long evaluation periods.

The dentin/material interface was additionally characterised by means of SEM, EDX and elemental mapping to gain a better understanding of the interactions occurring in that area. Sample dehydration, a step that is required prior to SEM observation, and sample-induced shrinkage caused by the constant vacuum environment during observation can both impair the adaptability of HCSCs to dentin [58]. However, a potential material detachment from the dentin surface does not seem to alter the elemental distribution in the two surfaces [59]. The observations of the interfaces did not reveal notable differences among the HCSCs. The SNPs migrated to dentin, while the BG particles were evident in the bulk of the respective BG-containing cements. Studies on the interfacial characteristics of HCSCs in contact with dentin report somewhat conflicting findings. Atmeh et al. [60] reported the formation of an intermediate mineralised layer at the interface, accompanied by tag-like structures within the dentinal tubules that are triggered by HCSC's rapid local calcium hydroxide release. This 'mineral infiltration zone' has been disputed in subsequent studies, which attribute its presence to an artefact induced by the fluorescent dyes used in confocal microscopy [58]. In contrast, one study reports conventional calcium phosphate precipitation in the interfacial gaps from the reaction of calcium from HCSC with phosphorus in the dentin component [59]. Therefore, the occasional tag-like structures within the dentinal tubules, as also sporadically evident in the current study, are regarded as the cement's gap-filling property rather than a consistent formation of a mineral layer [59].

## 5. Conclusions

This investigation of the antibacterial properties of HCSCs at the dentin/material interface showed residual antibacterial activity in the dentin surfaces. In the split tooth model, the replacement of TCS with 40% BG reduced the bactericidal activity. A 2 mg/mL SNP liquid component mixed with the prototype HCSC demonstrated an improved antibacterial potential during a three-day biofilm assay at the dentin/material interface, although the effect was relatively small.

**Supplementary Materials:** The following supporting information can be downloaded at: <https://www.mdpi.com/article/10.3390/jfb14100511/s1>, Figure S1: Indicative scanning electron microscope (SEM) images of dentin surfaces from the split tooth block model accompanied by energy dispersive X-ray analyses (EDX) of selected regions or elemental mapping. The images suggest that no complete coverage of the dentin surface by material remnants takes place following the separation of the two parts of the root segment. (a) Root surfaces treated with 17% ethylenediaminetetraacetic acid (EDTA)

and with no application of a material (control specimens) were assessed to detect the main elements as well as the trace ones depicted in dentin segments following EDTA pre-treatment. (b) SEM images and EDX analyses from dentin surfaces previously in contact with TZ-base, TZ-bg20 and TZ-bg40. Some zirconium oxide particles, as well as cement particles, can be sporadically depicted. (c) Dentin surfaces and elemental maps for TZ-Ag1 and TZ-Ag2. Some agglomerated silver nanoparticles could also be depicted (red arrow). (d) SEM images and EDX analyses from dentin surfaces previously in contact with Biodentine, TotalFill and IRM. Material residues are mainly depicted inside the dentin tubules; Figure S2: Representative confocal laser scanning microscope images (60×) for orientation upon the dentin/material surface and optimisation of threshold options. The specimens were not exposed to any bacteria. Biodentine was used for these internal controls.

**Author Contributions:** Conceptualisation, A.K., H.V., J.C. and P.T.S.; methodology, A.K., H.V., V.K., J.C. and P.T.S.; validation, A.K., H.V., D.Ø., V.K., J.C. and P.T.S.; formal analysis, A.K.; investigation, A.K.; data curation, A.K.; writing—original draft preparation, A.K.; writing—review and editing, H.V., D.Ø., V.K., J.C. and P.T.S.; supervision, H.V., J.C. and P.T.S.; project administration, H.V., J.C. and P.T.S.; funding acquisition, A.K., H.V., J.C. and P.T.S. All authors have read and agreed to the published version of the manuscript.

**Funding:** This work was supported by the University of Oslo, Nordic Institute of Dental Materials (NIOM) and UNIFOR 975503178/266 (Foundation: Stiftelsen til tannlegevitenskapens fremme).

**Institutional Review Board Statement:** The Regional Committee for Medical and Health Research Ethics that evaluated the project deemed that no approval was required to conduct the study (REC Ref. 283811). Extracted human teeth were collected from a tooth biobank (REC Ref. 2013/413).

**Informed Consent Statement:** Not applicable.

**Data Availability Statement:** The data that support the findings of this study are available from the corresponding author upon reasonable request.

**Acknowledgments:** Amund Ruud for the valuable technical assistance with specimen grinding and polishing.

**Conflicts of Interest:** The authors declare no conflict of interest.

## References

1. Camilleri, J.; Pertl, C. Root-end filling and perforation repair materials and techniques. In *Endodontic Materials in Clinical Practice*, 1st ed.; Camilleri, J., Ed.; Wiley-Blackwell: Hoboken, NJ, USA, 2021; pp. 219–261.
2. American Association of Endodontists. AAE Position Statement on Vital Pulp Therapy. Available online: <https://www.aae.org/specialty/clinical-resources/guidelines-position-statements/> (accessed on 12 May 2023).
3. Donnermeyer, D.; Bürklein, S.; Dammaschke, T.; Schäfer, E. Endodontic sealers based on calcium silicates: A systematic review. *Odontology* **2019**, *107*, 421–436. [[CrossRef](#)]
4. Camilleri, J.; Atmeh, A.; Li, X.; Meschi, N. Present status and future directions—Hydraulic materials for endodontic use. *Int. Endod. J.* **2022**, *55*, 710–777. [[CrossRef](#)]
5. Sfeir, G.; Zogheib, C.; Patel, S.; Giraud, T.; Nagendrababu, V.; Bukiet, F. Calcium silicate-based root canal sealers: A narrative review and clinical perspectives. *Materials* **2021**, *14*, 3965. [[CrossRef](#)]
6. Gandolfi, M.G.; Iezzi, G.; Piattelli, A.; Prati, C.; Scarano, A. Osteoinductive potential and bone-bonding ability of ProRoot MTA, MTA Plus and Biodentine in rabbit intramedullary model: Microchemical characterization and histological analysis. *Dent. Mater.* **2017**, *33*, e221–e238. [[CrossRef](#)]
7. Torabinejad, M.; White, D.J. Tooth Filling Material and Method of Use. U.S. Patent 5,769,638, 23 June 1998.
8. Camilleri, J.; Sorrentino, F.; Damidot, D. Investigation of the hydration and bioactivity of radiopacified tricalcium silicate cement, Biodentine and MTA Angelus. *Dent. Mater.* **2013**, *29*, 580–593. [[CrossRef](#)]
9. Zamparini, F.; Siboni, F.; Prati, C.; Taddei, P.; Gandolfi, M.G. Properties of calcium silicate-monobasic calcium phosphate materials for endodontics containing tantalum pentoxide and zirconium oxide. *Clin. Oral Investig.* **2019**, *23*, 445–457. [[CrossRef](#)]
10. Ørstavik, D. Endodontic filling materials. *Endod. Top.* **2014**, *31*, 53–67. [[CrossRef](#)]
11. Hülsmann, M.; Tulus, G. Non-surgical retreatment of teeth with persisting apical periodontitis following apicoectomy: Decision making, treatment strategies and problems, and case reports. *Endod. Top.* **2016**, *34*, 64–89. [[CrossRef](#)]
12. Siqueira, J.F., Jr.; Rôças, I.N.; Ricucci, D. Biofilms in endodontic infection. *Endod. Top.* **2010**, *22*, 33–49. [[CrossRef](#)]
13. Hench, L.L. The story of Bioglass. *J. Mater. Sci. Mater. Med.* **2006**, *17*, 967–978. [[CrossRef](#)]
14. Yun, J.; Burrow, M.F.; Matinlinna, J.P.; Wang, Y.; Tsoi, J.K.H. A narrative review of bioactive glass-loaded dental resin composites. *J. Funct. Biomater.* **2022**, *13*, 208. [[CrossRef](#)] [[PubMed](#)]

15. Hoikkala, N.J.; Wang, X.; Hupa, L.; Smått, J.H.; Peltonen, J.; Vallittu, P.K. Dissolution and mineralization characterization of bioactive glass ceramic containing endodontic sealer Guttaflow Bioseal. *Dent. Mater. J.* **2018**, *37*, 988–994. [CrossRef] [PubMed]
16. Corral Nunez, C.; Covarrubias, C.; Fernandez, E.; Oliveira, O.B.J. Enhanced bioactive properties of Biodentine™ modified with bioactive glass nanoparticles. *J. Appl. Oral Sci.* **2017**, *25*, 177–185. [CrossRef] [PubMed]
17. Simila, H.O.; Karpukhina, N.; Hill, R.G. Bioactivity and fluoride release of strontium and fluoride modified Biodentine. *Dent. Mater.* **2018**, *34*, e1–e7. [CrossRef] [PubMed]
18. Darvell, B.W. Introduction: Materials chemistry as a means to an end(o)—The invisible foundation. In *Endodontic Materials in Clinical Practice*, 1st ed.; Camilleri, J., Ed.; Wiley-Blackwell: Hoboken, NJ, USA, 2021; pp. 1–14.
19. Noronha, V.T.; Paula, A.J.; Duran, G.; Galembeck, A.; Cogo-Müller, K.; Franz-Montan, M.; Durán, N. Silver nanoparticles in dentistry. *Dent. Mater.* **2017**, *33*, 1110–1126. [CrossRef]
20. Shrestha, A.; Kishen, A. Antibacterial nanoparticles in endodontics: A review. *J. Endod.* **2016**, *42*, 1417–1426. [CrossRef]
21. Afkhami, F.; Forghan, P.; Gutmann, J.L.; Kishen, A. Silver nanoparticles and their therapeutic applications in endodontics: A narrative review. *Pharmaceutics* **2023**, *15*, 715. [CrossRef]
22. Jensen, K.A. *The NANOGENOTOX Dispersion Protocol for NANoREG*; National Research Centre for the Working Environment: Copenhagen, Denmark, 2014. Available online: <http://safenano.re.kr/download.do?SEQ=175> (accessed on 9 June 2023).
23. Kapralos, V.; Valen, H.; Koutroulis, A.; Camilleri, J.; Ørstavik, D.; Sunde, P.T. The dentine-sealer interface: Modulation of antimicrobial effects by irrigation. *Int. Endod. J.* **2022**, *55*, 544–560. [CrossRef]
24. Chávez de Paz, L.E. Image analysis software based on color segmentation for characterization of viability and physiological activity of biofilms. *Appl. Environ. Microbiol.* **2009**, *75*, 1734–1739. [CrossRef]
25. Torabinejad, M.; Hong, C.U.; Ford, T.R.P.; Kettering, J.D. Antibacterial effects of some root end filling materials. *J. Endod.* **1995**, *21*, 403–406. [CrossRef]
26. Bosaid, F.; Aksel, H.; Azim, A.A. Influence of acidic pH on antimicrobial activity of different calcium silicate based–endodontic sealers. *Clin. Oral Investig.* **2022**, *26*, 5369–5376. [CrossRef] [PubMed]
27. Wang, J.D.; Hume, W.R. Diffusion of hydrogen ion and hydroxyl ion from various sources through dentine. *Int. Endod. J.* **1988**, *21*, 17–26. [CrossRef] [PubMed]
28. Haapasalo, H.K.; Siren, E.K.; Waltimo, T.M.; Ørstavik, D.; Haapasalo, M.P. Inactivation of local root canal medicaments by dentine: An in vitro study. *Int. Endod. J.* **2000**, *33*, 126–131. [CrossRef] [PubMed]
29. Du, T.; Wang, Z.; Shen, Y.; Ma, J.; Cao, Y.; Haapasalo, M. Combined antibacterial effect of sodium hypochlorite and root canal sealers against *Enterococcus faecalis* biofilms in dentin canals. *J. Endod.* **2015**, *41*, 1294–1298. [CrossRef] [PubMed]
30. Fan, W.; Wu, D.; Tay, F.R.; Ma, T.; Wu, Y.; Fan, B. Effects of adsorbed and templated nanosilver in mesoporous calcium-silicate nanoparticles on inhibition of bacteria colonization of dentin. *Int. J. Nanomed.* **2014**, *9*, 5217–5230. [CrossRef]
31. Septodont. Biodentine Instructions for Use File. Available online: <https://www.septodontusa.com/wp-content/uploads/2022/11/Biodentine-IFU.pdf?x92757> (accessed on 6 July 2023).
32. FKG Dentaire. Totalfill Bioceramic Root Repair Material Instructions for Use File. Available online: [https://www.fkg.ch/sites/default/files/201801\\_B\\_4940A\\_TotalFill%20RRM%20IFU\\_REV%201\\_EN\\_CS\\_DA\\_DE\\_ES\\_0.pdf](https://www.fkg.ch/sites/default/files/201801_B_4940A_TotalFill%20RRM%20IFU_REV%201_EN_CS_DA_DE_ES_0.pdf) (accessed on 25 June 2023).
33. Chong, B.S.; Pitt Ford, T.R.; Hudson, M.B. A prospective clinical study of Mineral Trioxide Aggregate and IRM when used as root-end filling materials in endodontic surgery. *Int. Endod. J.* **2003**, *36*, 520–526. [CrossRef]
34. Lindeboom, J.A.H.; Frenken, J.W.; Kroon, F.H.; van den Akker, H.P. A comparative prospective randomized clinical study of MTA and IRM as root-end filling materials in single-rooted teeth in endodontic surgery. *Oral Surg. Oral Med. Oral Pathol. Oral Radiol. Endodontology.* **2005**, *100*, 495–500. [CrossRef]
35. Marggraf, T.; Ganas, P.; Paris, S.; Schwendicke, F. Bacterial reduction in sealed caries lesions is strain- and material-specific. *Sci. Rep.* **2018**, *8*, 3767. [CrossRef]
36. Jardine, A.P.; Montagner, F.; Quintana, R.M.; Zaccara, I.M.; Kopper, P.M.P. Antimicrobial effect of bioceramic cements on multispecies microcosm biofilm: A confocal laser microscopy study. *Clin. Oral Investig.* **2019**, *23*, 1367–1372. [CrossRef]
37. Camilleri, J.; Arias Moliz, T.; Bettencourt, A.; Costa, J.; Martins, F.; Rabadijeva, D.; Rodriguez, D.; Visai, L.; Combes, C.; Farrugia, C.; et al. Standardization of antimicrobial testing of dental devices. *Dent. Mater.* **2020**, *36*, e59–e73. [CrossRef]
38. Koutroulis, A.; Valen, H.; Ørstavik, D.; Kapralos, V.; Camilleri, J.; Sunde, P.T. Surface characteristics and bacterial adhesion of endodontic cements. *Clin. Oral Investig.* **2022**, *26*, 6995–7009. [CrossRef]
39. Zehnder, M.; Soderling, E.; Salonen, J.; Waltimo, T. Preliminary evaluation of bioactive glass S53P4 as an endodontic medication in vitro. *J. Endod.* **2004**, *30*, 220–224. [CrossRef] [PubMed]
40. Zehnder, M.; Waltimo, T.; Sener, B.; Soderling, E. Dentin enhances the effectiveness of bioactive glass S53P4 against a strain of *Enterococcus faecalis*. *Oral Surg. Oral Med. Oral Pathol. Oral Radiol. Endodontology.* **2006**, *101*, 530–535. [CrossRef]
41. Waltimo, T.; Zehnder, M.; Soderling, E. Bone powder enhances the effectiveness of bioactive glass S53P4 against strains of *Porphyromonas gingivalis* and *Actinobacillus actinomycetemcomitans* in suspension. *Acta Odontol. Scand.* **2006**, *64*, 183–186. [CrossRef] [PubMed]
42. Allan, I.; Newman, H.; Wilson, M. Antibacterial activity of particulate bioglass against supra- and subgingival bacteria. *Biomaterials* **2001**, *22*, 1683–1687. [CrossRef] [PubMed]
43. Xie, Z.P.; Zhang, C.Q.; Yi, C.Q.; Qiu, J.J.; Wang, J.Q.; Zhou, J. In vivo study effect of particulate Bioglass in the prevention of infection in open fracture fixation. *J. Biomed. Mater. Res. B Appl. Biomater.* **2009**, *90*, 195–201. [CrossRef]

44. Wang, Z.; Jiang, T.; Sauro, S.; Wang, Y.; Thompson, I.; Watson, T.F.; Sa, Y.; Xing, W.; Shen, Y.; Haapasalo, M. Dentine remineralization induced by two bioactive glasses developed for air abrasion purposes. *J. Dent.* **2011**, *39*, 746–756. [[CrossRef](#)]
45. Williamson, A.E.; Dawson, D.V.; Drake, D.R.; Walton, R.E.; Rivera, E.M. Effect of root canal filling/sealer systems on apical endotoxin penetration: A coronal leakage evaluation. *J. Endod.* **2005**, *31*, 599–604. [[CrossRef](#)]
46. DaSilva, L.; Finer, Y.; Friedman, S.; Basrani, B.; Kishen, A. Biofilm formation within the interface of bovine root dentin treated with conjugated chitosan and sealer containing chitosan nanoparticles. *J. Endod.* **2013**, *39*, 249–253. [[CrossRef](#)]
47. Del Carpio-Perochena, A.; Kishen, A.; Shrestha, A.; Bramante, C.M. Antibacterial properties associated with chitosan nanoparticle treatment on root dentin and 2 types of endodontic sealers. *J. Endod.* **2015**, *41*, 1353–1358. [[CrossRef](#)]
48. Wu, D.; Fan, W.; Kishen, A.; Gutmann, J.L.; Fan, B. Evaluation of the antibacterial efficacy of silver nanoparticles against *Enterococcus faecalis* biofilm. *J. Endod.* **2014**, *40*, 285–290. [[CrossRef](#)]
49. Abbaszadegan, A.; Ghahramani, Y.; Gholami, A.; Hemmateenejad, B.; Dorostkar, S.; Nabavizadeh, M.; Sharghi, H. The effect of charge at the surface of silver nanoparticles on antimicrobial activity against gram-positive and gram-negative bacteria: A preliminary study. *J. Nanomater.* **2015**, *16*, 720654. [[CrossRef](#)]
50. Swimberghe, R.C.D.; Coenye, T.; De Moor, R.J.G.; Meire, M.A. Biofilm model systems for root canal disinfection: A literature review. *Int. Endod. J.* **2019**, *52*, 604–628. [[CrossRef](#)] [[PubMed](#)]
51. Pinheiro, E.T.; Gomes, B.P.; Ferraz, C.C.; Sousa, E.L.; Teixeira, F.B.; Souza-Filho, F.J. Microorganisms from canals of root-filled teeth with periapical lesions. *Int. Endod. J.* **2003**, *36*, 1–11. [[CrossRef](#)] [[PubMed](#)]
52. Rôças, I.N.; Hülsmann, M.; Siqueira, J.F., Jr. Microorganisms in root canal-treated teeth from a German population. *J. Endod.* **2008**, *34*, 926–931. [[CrossRef](#)] [[PubMed](#)]
53. Rôças, I.N.; Siqueira, J.F., Jr. Characterization of microbiota of root canal-treated teeth with posttreatment disease. *J. Clin. Microbiol.* **2012**, *50*, 1721–1724. [[CrossRef](#)] [[PubMed](#)]
54. Setzer, F.C.; Kratchman, S.I. Present status and future directions: Surgical endodontics. *Int. Endod. J.* **2022**, *55*, 1020–1058. [[CrossRef](#)]
55. Koutroulis, A.; Kuehne, S.A.; Cooper, P.R.; Camilleri, J. The role of calcium ion release on biocompatibility and antimicrobial properties of hydraulic cements. *Sci. Rep.* **2019**, *9*, 19019. [[CrossRef](#)]
56. Kato, G.; Gomes, P.S.; Neppelenbroek, K.H.; Rodrigues, C.; Fernandes, M.H.; Grenho, L. Fast-setting calcium silicate-based pulp capping cements-integrated antibacterial, irritation and cytocompatibility assessment. *Materials* **2023**, *16*, 450. [[CrossRef](#)]
57. Dragland, I.S.; Wellendorf, H.; Kopperud, H.; Stenhagen, I.; Valen, H. Investigation on the antimicrobial activity of chitosan-modified zinc oxide-eugenol cement. *Biomater. Investig. Dent.* **2019**, *6*, 99–106. [[CrossRef](#)]
58. Hadis, M.; Wang, J.; Zhang, Z.J.; Di Maio, A.; Camilleri, J. Interaction of hydraulic calcium silicate and glass ionomer cements with dentine. *Materialia* **2020**, *9*, 100515. [[CrossRef](#)]
59. Li, X.; Pongprueksa, P.; Van Landuyt, K.; Chen, Z.; Pedano, M.; Van Meerbeek, B.; De Munck, J. Correlative micro-Raman/EPMA analysis of the hydraulic calcium silicate cement interface with dentin. *Clin. Oral Investig.* **2016**, *20*, 1663–1673. [[CrossRef](#)] [[PubMed](#)]
60. Atmeh, A.R.; Chong, E.Z.; Richard, G.; Festy, F.; Watson, T.F. Dentin-cement interfacial interaction: Calcium silicates and polyalkenoates. *J. Dent. Res.* **2012**, *91*, 454–459. [[CrossRef](#)] [[PubMed](#)]

**Disclaimer/Publisher’s Note:** The statements, opinions and data contained in all publications are solely those of the individual author(s) and contributor(s) and not of MDPI and/or the editor(s). MDPI and/or the editor(s) disclaim responsibility for any injury to people or property resulting from any ideas, methods, instructions or products referred to in the content.

Supplementary Materials

# Antibacterial Activity of Root Repair Cements in Contact with Dentin – An Ex Vivo Study

Andreas Koutroulis <sup>1,\*</sup>, Håkon Valen <sup>2</sup>, Dag Ørstavik <sup>1</sup>, Vasileios Kapralos <sup>1</sup>, Josette Camilleri <sup>3</sup> and Pia Titterud Sunde <sup>1,\*</sup>

<sup>1</sup> Section of Endodontics, Institute of Clinical Dentistry, Faculty of Dentistry, University of Oslo, P.O. Box 1109, Blindern, 0317 Oslo, Norway; d.s.orstavik@odont.uio.no (D.Ø.); vasileios.kapralos@odont.uio.no (V.K.)

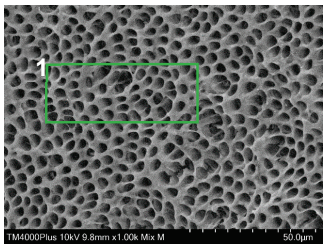
<sup>2</sup> Nordic Institute of Dental Materials (NIOM), 0855 Oslo, Norway; hakon.valen@niom.no

<sup>3</sup> School of Dentistry, Institute of Clinical Sciences, College of Medical and Dental Sciences, University of Birmingham, Birmingham B15 2TT, UK; j.camilleri@bham.ac.uk

\* Correspondence: andreas.koutroulis@odont.uio.no (A.K.); p.t.sunde@odont.uio.no (P.T.S.)

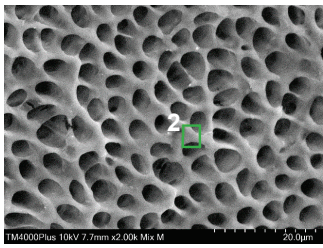
## a Dentin segments treated with 17% EDTA – No material application

1



Element	At No.	Netto	Mass [%]	Mass Norm. [%]	Atom [%]	abs. error [%] (1 sigma)	rel. error [%] (1 sigma)
C	6	31173	34.50	42.10	56.78	4.26	12.34
N	7	1911	8.99	10.98	12.69	1.75	19.43
O	8	6843	13.82	16.87	17.08	2.08	15.02
Na	11	1558	0.84	1.02	0.72	0.09	10.39
P	15	39419	6.91	8.43	4.41	0.29	4.21
Ca	20	64207	16.87	20.60	8.32	0.53	3.15
Sum				81.93	100.00	100.00	

2

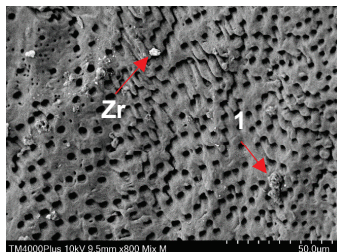


Element	At No.	Netto	Mass [%]	Mass Norm. [%]	Atom [%]	abs. error [%] (1 sigma)	rel. error [%] (1 sigma)
C	6	2214	6.72	7.58	13.64	1.18	18.90
O	8	11293	30.52	34.44	49.68	4.23	13.85
Mg	12	742	0.27	0.31	0.29	0.05	16.59
Al	13	1705	0.51	0.57	0.49	0.05	10.68
Si	14	1082	0.28	0.32	0.26	0.04	14.57
P	15	54450	14.21	16.04	11.95	0.57	4.01
Ca	20	80746	35.76	40.36	23.24	1.10	3.07
Sum				88.12	100.00	100.00	

b

**TZ-base**

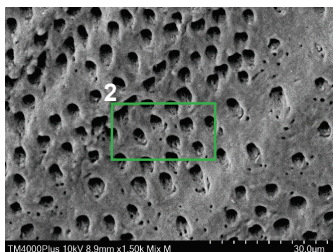
1



Element	At No.	Netto	Mass [%]	Mass Norm. [%]	Atom [%]	abs. error [%] (1 sigma)	rel. error [%] (1 sigma)
C	6	10184	20.37	17.35	27.04	2.87	14.09
N	7	1710	8.07	6.87	9.18	1.61	19.98
O	8	23229	47.07	40.09	46.90	5.97	12.68
Mg	12	3068	0.71	0.61	0.47	0.07	9.48
Si	14	4104	0.76	0.65	0.43	0.06	7.97
P	15	39382	7.77	6.62	4.00	0.32	4.17
Ca	20	64591	28.14	23.97	11.19	0.87	3.09
Zr	40	13815	4.52	3.85	0.79	0.20	4.44
Sum				117.42	100.00	100.00	

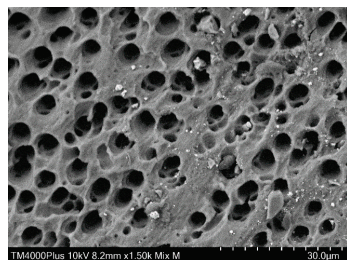
**TZ-bg20**

2



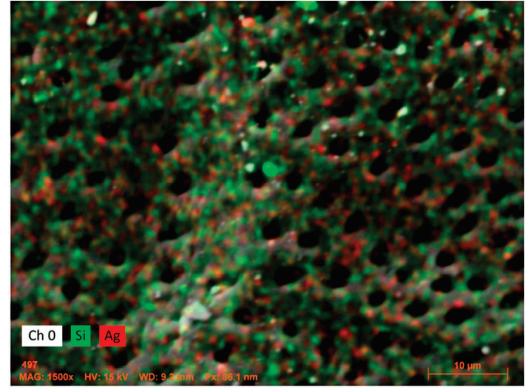
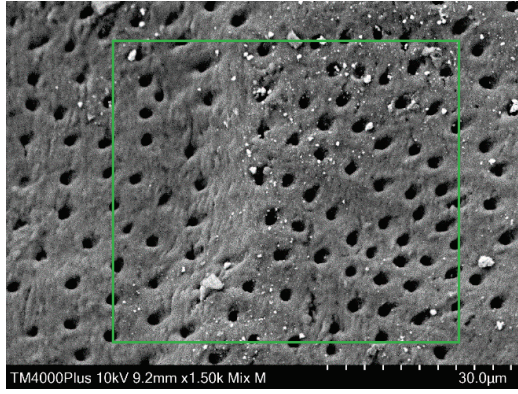
Element	At No.	Netto	Mass [%]	Mass Norm. [%]	Atom [%]	abs. error [%] (1 sigma)	rel. error [%] (1 sigma)
C	6	11534	22.33	18.27	28.25	3.09	13.84
N	7	1607	8.09	6.62	8.78	1.64	20.29
O	8	22757	48.92	40.03	46.48	6.21	12.70
Na	11	881	0.30	0.24	0.20	0.05	16.45
Mg	12	2049	0.50	0.41	0.31	0.06	11.27
P	15	37190	8.30	6.79	4.07	0.34	4.15
Ca	20	69916	29.54	24.17	11.20	0.91	3.09
Zr	40	11538	4.24	3.47	0.71	0.19	4.51
Sum				122.22	100.00	100.00	

**TZ-bg40**

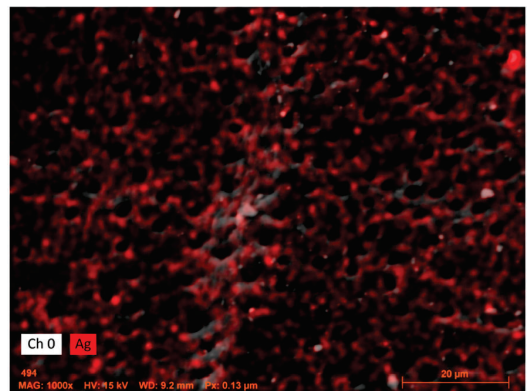
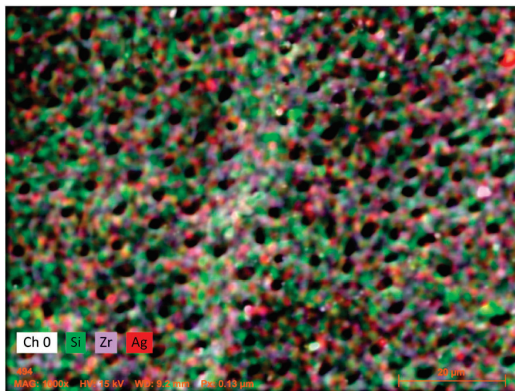
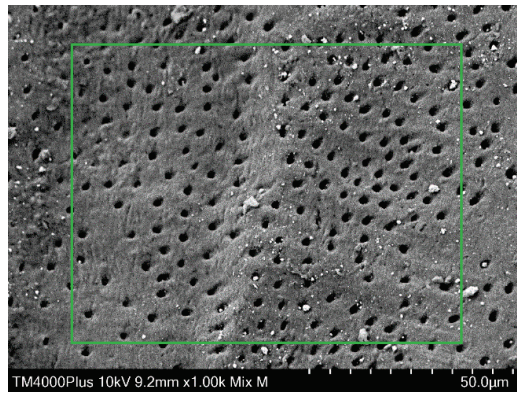


c

TZ-Ag1



TZ-Ag2

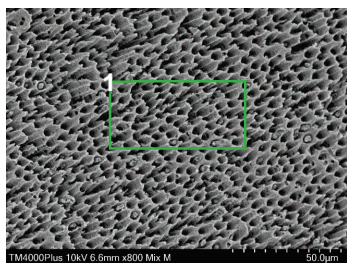




d

**Biodentine**

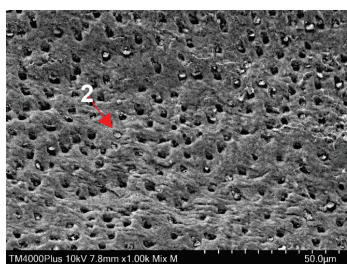
1



Element	At No.	Netto	Mass [%]	Mass Norm. [%]	Atom [%]	abs. error [%] (1 sigma)	rel. error [%] (1 sigma)
C	6	3112	7.65	8.37	14.93	1.34	17.50
O	8	17139	38.34	41.97	56.20	5.03	13.12
Mg	12	1306	0.37	0.40	0.35	0.05	13.48
Al	13	4762	1.12	1.22	0.97	0.08	7.33
Si	14	2307	0.50	0.54	0.41	0.05	10.07
P	15	44148	9.76	10.69	7.39	0.40	4.10
Cl	17	2530	0.73	0.80	0.48	0.06	7.56
Ca	20	77337	32.90	36.01	19.25	1.01	3.07
Sum				91.36	100.00	100.00	

**TotalFill**

2



Element	At No.	Netto	Mass [%]	Mass Norm. [%]	Atom [%]	abs. error [%] (1 sigma)	rel. error [%] (1 sigma)
C	6	2414	7.36	7.62	15.03	1.36	18.48
O	8	17087	36.62	37.93	56.18	4.81	13.13
Mg	12	4119	1.42	1.47	1.43	0.11	7.57
Si	14	19289	5.04	5.23	4.41	0.24	4.77
P	15	16885	4.55	4.71	3.61	0.20	4.48
Ca	20	49816	23.78	24.63	14.56	0.74	3.12
Zr	40	40062	17.77	18.41	4.78	0.70	3.92
Sum				91.36	100.00	100.00	

**IRM**

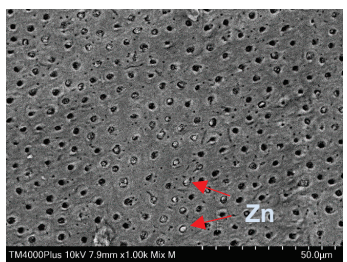


**Figure S1.** Indicative scanning electron microscope (SEM) images of dentin surfaces from the split tooth block model accompanied by energy dispersive x-ray analyses (EDX) of selected regions or elemental mapping. Images suggest that no complete coverage of the dentin surface by material remnants takes place following separation of the two parts of the root segment. (a) Root surfaces treated with 17% ethylenediaminetetraacetic acid (EDTA) and no application of material (control specimens) were assessed to detect the main elements as well as trace ones depicted in dentin segments following EDTA pretreatment. (b) SEM images and EDX analyses from dentin surfaces previously in contact with TZ-base, TZ-bg20 and TZ-bg40. Some zirconium oxide particles as well as cement particles can be sporadically depicted. (c) Dentin surfaces and elemental maps for TZ-Ag1 and TZ-Ag2. Some aggregated silver nanoparticles could also be depicted (red arrow). (d) SEM images and EDX analyses from dentin surfaces previously in contact with Biodentine, TotalFill and IRM. Material residues are mainly depicted inside the dentin tubules.

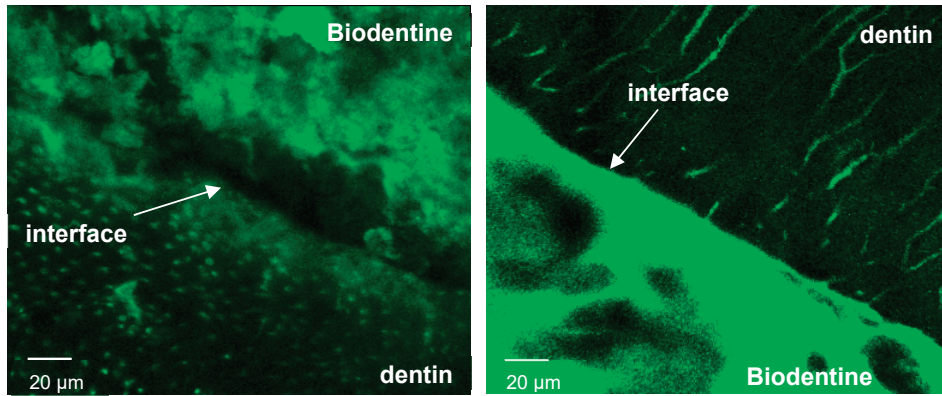


**Figure S2.** Representative confocal laser scanning microscope images (60×) for orientation upon the dentin/material surface and optimization of threshold options. Specimens were not exposed to any bacteria. Biodentine was used for these internal controls.